INVESTIGATING THE MOLECULAR REGULATION OF ANGIOGENESIS IN THE HEART

Matthew Scott Dukinfield

Submitted in partial fulfilment of the requirements of the
Degree of Doctor of Philosophy
September 2018

Adhesion and Angiogenesis Laboratory
Centre for Tumour Biology
Bart's Cancer Institute
School of Medicine and Dentistry
Queen Mary University of London
Charterhouse Square
London EC1M 6BQ
United Kingdom

I, Matthew Scott Dukinfield, confirm that the research included within this thesis is my own work or that where it has been carried out in collaboration with, or supported by others, that this is duly acknowledged below, and my contribution indicated. Previously published material is also acknowledged below.

I attest that I have exercised reasonable care to ensure that the work is original and does not to the best of my knowledge break any UK law, infringe any third party's copyright or other Intellectual Property Right, or contain any confidential material.

I accept that the College has the right to use plagiarism detection software to check the electronic version of the thesis.

I confirm that this thesis has not been previously submitted for the award of a degree by this or any other university.

Signature:

Date: 19/09/18

Details of collaboration:

Human Heart tissue was obtained with help from Kenneth Marguiles and Ken Bedi. RNA-Seq data was analysed by Prof. Jun Wang and Eleni Maniati of the Bart's Cancer Institute. A previous Post-Doc, Dr. Delphine Lees, worked with me on figures 39 and 43 of Chapter 7.

Details of relevant publications:

Alexopoulou, A.N., Lees, D.M., Bodrug. N., Lechertier, T., Fernandez I., D'Amico, G., **Dukinfield, M.,** Batista, S., Serrels, B., Hodivala-Dilke, K. *Focal Adhesion Kinase (FAK) tyrosine 397E mutation restores the vascular leakage defect in endothelium-specific FAK-kinase dead mice*, J Pathol. (2017)

Baliga, R.S. and Preedy, M.E.J., **Dukinfield, M.S.,** Chu, S.M., Aubdool, A.A., Bubb, K.J., Moyes, A.J., Tones, M.A., Hobbs, A.J. *Phosphodiesterase 2 inhibition preferentially promotes NO/guanylyl cyclase/cGMP signaling to reverse the development of heart failure,* PNAS (2018).

Moyes, A.J. and Chu, S.M., Aubdool, A.A., **Dukinfield, M.S.,** Marguiles, K.B., Bedi, K.C., Hodivala-Dilke, K., Baliga, R.S., Hobbs, A.J. *C-type natriuretic peptide coordinates cardiac structure and function,* Eur Heart J (2019).

Dukinfield M., Maniati E., Reynolds L., Aubdool A., Wang J., Bedi K., Marguiles K., Hobbs A., Hodivala-Dilke K. *Repurposing the utility of an anti-cancer drug for the treatment of hypertrophic heart disease.* (under review – Journal of Pathology)

ABSTRACT

Angiogenesis is the formation of new blood vessels from pre-existing ones, and is an essential process during tissue regeneration, growth, reproduction and development. It is a highly regulated event that involves the interplay of multiple different signalling networks, and if dysregulated, can contribute to several different pathological conditions, including arthritis, diabetic retinopathy, heart disease and cancer. The signalling networks that mediate angiogenesis consist of a complex balance between many stimulatory or inhibitory factors. Those same key factors can regulate the proliferation, migration and remodelling of endothelial cells that form the basis of an organised vasculature. Thus, the regulation of angiogenesis is a common thread between seemingly unrelated diseases, like heart disease and cancer. My PhD acts as a bridge between the molecular regulation of cardiac and cancer blood vessels – learning from the latter to apply to cardiac disease. Herein we have investigated two questions: (1) The utility of low dose Cilengitide in the treatment of heart failure. (2) The role of endothelial cell focal adhesion kinase and angiocrine signalling in cancer.

We demonstrate that treatment with low dose Cilengitide reduces or even reverses the pathogenesis of heart failure within a murine model of pressure-overload induced heart failure. We go on to show that low dose Cilengitide enhances myocardial angiogenesis and may also beneficially target the cardiomyocyte itself directly. Furthermore, we show that targeting the kinase domain of focal adhesion kinase within the endothelium is crucial for tumour cell sensitisation to the DNA-damaging therapy, doxorubicin.

ACKNOWLEDGEMENTS

I'd like to take this opportunity to thank my fantastic supervisor, Kebs. Your advice, direction and input have been absolutely invaluable throughout. I hope you enjoyed your brief foray into the world of heart failure.

I've had the opportunity to work with some really outstanding scientists and people in my time here. A HUGE thanks have to go to Louise, Gabi, Delphine, Bruce and Julie. Louise and Gabi, you've been there to answer the million questions (and then some) that I've had over the years and for that I can't thank you enough. Bruce and Julie, you've kept my mice alive (literally). Both I and the mice thank you for that. I really couldn't have done any of this work without any of you. A big thanks must go to everyone else in the lab too – you've all made my time here really special.

It's been a massive pleasure to work alongside members of the Hobbs lab, too. I can't thank you guys enough. Reshma especially made all of this work possible.

Thank you to Louise for not dumping me when I coughed in your face that one time. Thank you for your support.

Finally, thank you to all my friends and family.

TABLE OF CONTENTS

LIST OF FIGURES

Figure 16: Cilengitide functions as a dose dependent regulator of cardiac inotropy in pressure-overload-induced heart failure.

Figure 17: Transverse aortic constriction (TAC) surgery in mice causes a reduction in cardiac contractility and an increase in left ventricular dilatation by 3 weeks.

Figure 18: Pressure overload induced cardiac pathobiology is suppressed with delayed low dose Cilengitide treatment.

Figure 19: Pressure overload induced cardiac hypertrophy is ameliorated with delayed low dose Cilengitide treatment.

Figure 20: Pressure overload induced cardiac gene changes are ameliorated with delayed low dose Cilengitide treatment.

Figure 21: Low dose Cilengitide's cardioprotective effects may continue, even after cessation of treatment.

Figure 22: Cardiac blood vessel number does not differ temporally after TAC surgery

Figure 23: Treatment with low dose Cilengitide enhances cardiac angiogenesis *in vivo.*

Figure 24: Isolated cardiomyocytes and cardiac endothelial cells express β3 and β5 integrin receptor subunits in differing relative quantities.

Figure 25: Principle component analysis (PCA) demonstrates good clustering between cardiac endothelial cells treated with low dose Cilengitide.

Figure 26: Low dose Cilengitide stimulates DNA-replication, mitosis and cell-cycle transition in cardiac endothelial cells *in vitro* within 24 hours*.*

Figure 27: Low dose Cilengitide stimulates DNA-replication, mitosis and cell-cycle transition in cardiac endothelial cells *in vitro* within 48 hours*.*

Figure 28: Angiotensin II induces cardiac hypertrophy *in vitro*.

Figure 29: Principle component analysis (PCA) demonstrates poor clustering between cardiomyocytes treated with vehicle, low dose Cilengitide, angiotensin II or angiotensin II-low dose Cilengitide combined.

Figure 30: Low dose Cilengitide will dysregulate several enriched pathways in angiotensin II treated cardiomyocytes.

LIST OF TABLES

LIST OF ABBREVIATIONS

α-SMA – alpha-smooth muscle actin
μl – micro litre
ABI – Ankle Brachial Index
ANOVA – Analysis of Variance
ANP – Atrial Natriuretic Peptide
APS – Ammonium Persulphate
ARRIVE – Animal Research: Reporting of *In Vivo* Experiments
B16F0 – Melanoma cell line
B2M – Beta 2 Microglobulin
BM – MNC – Bone Marrow Mononuclear Cell
BNP – Brain Natriuretic Peptide
BSA – Bovine Serum Albumin
cDNA – complementary DNA
cTnT – Cardiac Troponin T
DCM – Dilated Cardiomyopathy
Dil. – Dilated
DLL4 – Delta-like 4
DMEM – Dulbecco's Modified Eagle Media
DMSO – Dimethyl sulfoxide
DNA – Deoxyribonucleic acid
E (number) – Embryonic day
EC – Endothelial cell
ECG – Electrocardiogram
ECL – Ehanced chemiluminescence
ECM – Extracellular matrix
EDTA – Ethylenediaminetetraacetic acid
EF – Ejection Fraction
EPC – Endothelial progenitor cell
EPDC – Epicardium derived cell
FAM-tagged – Fluorescein adidite
FAK – Focal adhesion kinase
FBS – Foetal bovine serum
FGF – Fibroblast growth factor
FS – Fractional Shortening
GAPDH – Glyceraldehyde 3-phosphate dehydrogenase
HEPES – 4-(2-hydroxyethyl)-1-piperazineethanesulfonic acid
HF – Heart Failure
HFPEF – Heart Failure with Preserved Ejection Fraction

HFREF – Heart Failure with Reduced Ejection Fraction
HGF – Hepatocyte Growth Factor
HIF – Hypoxia Inducible Factor
HPRT-1 – Hypoxanthine Phosphoribosyltransferase 1
HRP – Horseradish peroxidase
IA – Intra-arterial
ICAM – Intercellular Adhesion Molecule
IGF – Insulin Growth Factor
IM – Intra-muscular
IP – Intra-peritoneal
Isc. – Ischemic
ISO – Isoprenaline
IV – Intra-venous
L – Length
LDCIL – Low dose Cilengitide
LV – Left Ventricular
LVEF – Left Ventricular Ejection Fraction
LVIDd – Left Ventricular Internal Diameter (diastole)
LVIDs – Left Ventricular Internal Diameter (systole)
MABP – Mean Arterial Blood Pressure
MATLAB – Matrix Laboratory
MI – Myocardial Infarction
MLEC – Mouse lung endothelial cell
ml – millilitre
mm – millimetre
mM – millimolar
MMP – Metallo-matrix protein
mRNA – messenger ribonucleic acid
MTT – (3-(4,5-Dimethylthiazol-2-yl)-2,5-Diphenyltetrazolium Bromide)
MYH6 – Myosin Heavy Chain 6
MYH7 – Myosin Heavy Chain 7
NH – Non-failing with Hypertrophy
NF – Non-failing
nM – nanomolar
PAD – Peripheral Artery Disease
PBS – Phosphobuffered saline
PBSC – Peripheral Blood Stem Cell
PCR – Polymerase Chain Reaction
Pdgfb – Platelet derived growth factor
PE – Phycoerythrin

PEO – Proepicardial organ
PI3K – Phosphatidylinositol-4,5-bisphosphate 3-kinase
PIGF – Placental growth factor
PMT – Polyoma Middle T
PVDF – Polyvinylidene difluoride
qPCR – Quantitative PCR
RIN – RNA integrity value
RNA – Ribonucleic acid
RNA-seq – RNA-sequencing
RPM – Revolutions per minute
RT-qPCR – Quantitative reverse transcriptase PCR
SDF-1 – Stromal cell derived factor-1
SV – Stroke Volume
TAC – Transverse Aortic Constriction
TCPO2 – Transcutaneous Oxygen
TGBβ-1 – Transforming Growth Factor Beta-1
VCAM -1 – Vascular Cellular Adhesion Molecule-1
VEGF – Vascular Endothelial Growth Factor
VEGF-R – Vascular Endothelial Growth Factor Receptor
W – Width
w/v – Weight/Volume
WGA – Wheat Germ Agglutinin

CHAPTER 1.0: GENERAL INTRODUCTION

Endothelial cells are a pivotal feature of the vasculature and play a variety of critical roles in the control of its function [1]. As such, as our understanding of endothelial cells have grown, so has their list of functions. Indeed, endothelial cells have gone from being passive conduits for delivering blood, to multifunctional cells that can establish tissue-specific vascular niches which deploy specific sets of growth factors, known as angiocrine factors [2]. Central to their new-found responsibility, is the fact that endothelial cells form the interface between blood and the surrounding tissue. In this fashion, the endothelium connects circulating cells within the vessel lumen itself to those cells present in the vascular wall. It is this feature that allows them to respond to changes in blood composition and blood flow and effect physiological changes in the surrounding tissue to achieve vascular homeostasis {Rubanyi, 1993 #532}. As such, dysfunction of the endothelium can result in the development of a multitude of vascular disorders; chief amongst these, angiogenic disorders.

Herein we examine the endothelium as both a tissue-specific angiocrine secretion factory, and also as a pivotal element of myocardial angiogenesis. we aim to uncover chief mechanisms that will govern these functions in order to achieve functional improvement in either cancer or heart failure, respectively.

CHAPTER 2.0: MATERIALS AND METHODS

2.1 Animal care and procedures

This project has been approved by the UK Home Office and all procedures were carried out according to the ARRIVE guidelines (Animal Research: Reporting of *In Vivo* Experiments).

Note: All surgical procedures were conducted under 2% isoflurane anaesthesia. Confirmation of anaesthesia was assessed using the pedal reflex.

2.1.1 Abdominal transverse aortic constriction (TAC)

Abdominal TAC is a common experimental procedure used to elicit pressure overload-induced heart failure (HF) in murine models. TAC provides a time-dependent, reproducible model of HF characterized by a significant rise in left ventricular weight, deleterious myocardial dilation, and a reduction in cardiac inotropy, and rise in myocardial fibrosis. Physiologically this mimics many of the clinical features of human aortic stenosis.

Male C57BL6 mice (Charles River) underwent TAC surgery at 4-5 weeks of age (body weight between 20 and 22g). Mice were anaesthetised with isoflurane anaesthesia, placed in a supine position on the procedure table, and an incision made along the ventral underbelly using scissors, extending from the xiphoid process of the sternum, down to the groin to reveal the abdominal muscle. The abdominal muscle was then cut the same distance along the linea alba to allow

easy reattachment of the two halves. The two sides of the abdominal muscles were clipped back to reveal the abdominal gastrointestinal organs, and these were carefully moved to expose the underlying abdominal aorta. The aorta was cleaned of visceral fat using blunt dissection, and carefully separated from parallel vasculature, whilst avoiding any spinal nerves. The abdominal aorta was then constricted using a 6-0 silk suture tied to the width of a 27-gauge needle at a position rostral to the renal artery bifurcation. Great care was taken to ensure the knot remained taut after tying. This was to ensure minimal variability amongst aortic lumen occlusion between animals, and therefore minimize differences in the degree of aortic stenosis. The skin and abdominal muscles were closed with a 6-0 silk suture thread. SHAM operated mice underwent the same operation with the exception of aortic constriction. In an effort to ensure reproducibility amongst TAC surgeries only male mice weighing between 20 and 22g (correlating to 4 – 5 weeks of age) were used, although it may be more pertinent to in future classify mice according to abdominal aortic size, rather than body weight. Echocardiography was performed up to 3 days prior to surgery, 3 weeks following surgery, and then at 6 (and/or 12 weeks) following surgery. At the experimental end-point, mice were sacrificed and their lungs, kidneys and hearts excised. Hearts were halved longitudinally (at roughly the atrioventricular valves) and either snap frozen in liquid nitrogen (for immunohistochemistry) or stored in an RNAlater stabilization solution (for RT-qPCR).

2.1.2 Isoprenaline-induced heart failure

Isoprenaline (ISO) is a synthetic catecholamine that stimulates beta-adrenoreceptors in the heart resulting in a marked elevation of heart rate and cardiac contractility. Chronic administration of ISO in experimental modes causes cardiac hypertrophy, ECG abnormalities, myocardial apoptosis and changes to cardiac inotropy [3]. Chronically, this can lead to HF. These effects are both time and concentration dependent. Thus, isoprenaline-infusion is an excellent model of heart failure associated with pathological hypertrophy and contractile failure.

Mini-pumps were filled with an ISO solution of 100µl in a vehicle containing saline and 0.05% ascorbic acid, and then left in a sterile incubator at 37°C for ~24 hours prior to implantation. Surgery was completed under sterile conditions and subcutaneous implant was made at the dorsal aspect of the scruff of the neck. Male C57BL6 mice (Charles River) underwent mini-pump implantation neck at 4-5 weeks of age. All mice were infused subcutaneously with ISO at a rate of 20mg/kg/day for 2 weeks via an Alzet osmotic minipump (model 1002, Alzet osmotic minipumps, Cupertino, CA, USA). Echocardiography was performed up to 3 days prior to surgery, 7 days following surgery and then at 14 days following surgery. At the experimental end-point, mice were sacrificed, and their lungs, kidneys, hearts, and aorta excised.

2.1.3 Cilengitide

Cilengitide (Bachem) was stored as a 2M solution in saline at -20°C prior to use, before thawing and serial diluting to an appropriate concentration with sterile saline for use.

Cilengitide treatment began in mice in tandem to TAC surgery, or after heart failure had already been established (at 3-4 weeks post-TAC). Injections were administered 3 times per week at doses of 50ug/kg and 500ug/kg via the peritoneum (IP). The doses of Cilengitide used here were obtained from previous publications by the Hodivala-Dilke lab [4] [5]. Low dose Cilengitide (LDCIL) is classified as 50ug/kg according to these same papers.

2.1.4 Echocardiography

Cardiac function was assessed by transthoracic echocardiography using a VisualSonics Vevo 770 30-MHz transduction probe. Mice were anaesthetised with isoflurane anaesthesia (1.5% in O_2), hair removed from their chest with hair removal cream, and then were placed in a supine position onto a warmed pad (46°C). The chest was covered in ultrasound gel, and the transduction probe was positioned adjacent to the mitral valve, at the tips of the papillary muscles, and images were taken just below this to ensure positional reproducibility. Left ventricular internal diameter (LVID) and LV posterior wall thicknesses at diastole (d) and systole (s) were measured from short-axis M-mode images. LV ejection fraction (EF%) was calculated as follows: $LVEF\% = [(LVIDd)^3 - (LVIDs)^3]/(LVIDd)^3 \times 100$; LV fractional shortening (FS%) was calculated as follows: $LVFS\% = (LVIDd - LVIDs)/LVIDd \times 100$. Values were averaged between

3 distinct images, meaning a single mouse underwent 3 echocardiograms per assessment to improve reproducibility and accuracy.

Echocardiography was completed at 0 (i.e. 1-3 days prior to surgery), 3 and 6 (and/or 12) weeks post-TAC surgery in the majority of cases.

All efforts were made to ensure consistency between mouse echocardiographs, including: pad temperature to be maintained at 46°C, isoflurane anaesthesia at 1.5%, oxygen flow at 1.5L/M, and cardiac function to be measured in the same anatomical location throughout.

2.1.5 Mean arterial blood pressure (MABP)

Blood pressure was recorded in anaesthetised mice via intra-arterial cannulation of a carotid artery 6 weeks post-TAC surgery, using a Microtip pressure catheter (Millar instruments). Mice were placed in a supine position on a pre-warmed heating mat (46°C), and a midline incision made extending the length of the neck with surgical scissors. The large salivary glands were gently moved laterally, and a single carotid artery was located for cannulation. The carotid artery was blunt dissected to remove visceral fats, and then ligated with surgical suture at its most rostral and caudal ends, leaving a space of roughly 2mm in between (**figure 2**). A small incision was made between the two ties using fine dissection spring-tip scissors, and a microtip pressure catheter was inserted into the artery (**figure 2**). The region of the artery housing the catheter was tied in place, and the caudal tie loosened to allow blood flow into the pressure catheter. Mice were allowed to recover for 5 minutes, or until the blood pressure trace steadied. MABP was then averaged across a 30 second period using MATLAB analysis. All efforts were

made to ensure mouse body temperature, and levels of anaesthesia in particular, remained constant between animals.

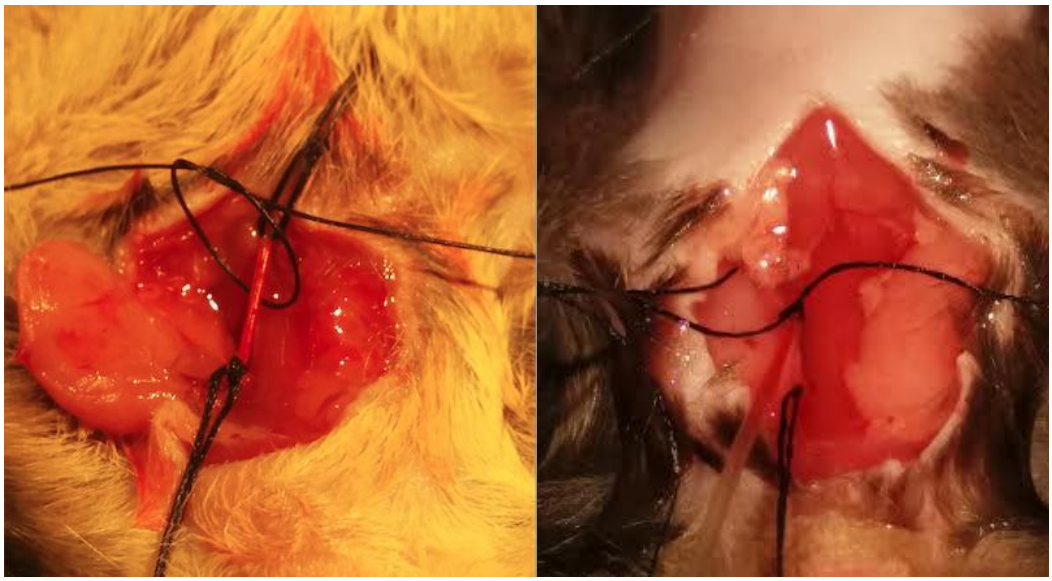

Figure 1: Isolation of carotid artery followed by intra-carotid cannulation to measure MABP.

2.1.6 Subcutaneous tumour growth models

B16F0 cells (derived from a C57BL6 melanoma cell line) were used to perform subcutaneous tumour growth experiments. Pdgfb-iCre^{ER};R26FAK$^{KD/KD;}$FAK$^{fl/fl}$ mice were anaesthetised, and 1x10^{6} cells (B16F0) resuspended in 100μl of PBS were injected subcutaneously into the flank. Tumours were allowed to grow for 10 days, or until tumours reached a volume of 100mm^{3} (as assessed by digital callipers), before mice being IP injected with 100μl tamoxifen (50mg/ml) for 3 consecutive days to induce cre-recombination. After the third tamoxifen injection, mice were solely fed a diet consisting of tamoxifen pellets or tamoxifen mash to sustain cre-mediated genetic alterations. In tandem to the final tamoxifen injection,

mice were injected with Doxorubicin (6mgkg^{-1}) for 3 days, or with PBS, via IP. Tumour volume was measured using digital callipers at pre-determined days throughout, and animals were culled and tumours excised 18-20 days post-injection, or before tumours reached a volume of 1500mm^3. Tumours were weighed, and longitudinally halved, before either being fixed in 4% formaldehyde or snap-frozen in liquid nitrogen in chilled isopentane.

2.1.7 Tumour progression assessment

Tumours were measured at defined time points using callipers. The end tumour volume was calculated as LxW^{2}x0.52, where L is length and W is width.

2.2 Cell culture

All procedures were carried out under sterile conditions in a tissue culture hood.

2.2.1 Cell culture media and other cell culture reagents

2.2.1a Cardiomyocyte cell growth media

Primary mouse cardiomyocytes (derived from C57/BL6) were grown in primary D-MEM (Dullbeco's Modified Eagle's Medium) (Sigma), supplemented with 10% FBS (Fetal Bovine Serum) (Sigma), 1% Penicillin Streptomycin (Sigma) and 1:1000 cardiomyocyte growth isolate (Pierce cardiomyocyte isolation kit, Thermo scientific). Media was stored at 4°C. Cells were incubated at 37°C and 5% CO_2. 2ml media was used per well.

2.2.1b Endothelial cell growth media (MLEC – mouse lung endothelium cell

culture)

Primary mouse endothelial cells (derived from C57/BL6) were cultured in low-glucose D-MEM (Sigma) and Ham's F12 (Gibco) medium supplemented with 0.1mg/ml Heparin (sigma), 100µg/ml Penicillin Streptomycin, 6mM l-glutamine (Sigma), 20% FBS and 50µg/ml endothelial mitogen (BioRad). Media was sterile filtered before use and kept at 4°C. Cells were incubated at 37°C and 5% CO_2. 10ml media was used per T75 flask, and 5ml per T25 flask.

2.2.1c B16F0 cell growth media

B16F0 mouse melanoma cells (derived from C57/BL6) were cultured in high-glucose DMEM (Sigma), supplemented with 10% FBS. Media was stored at 4°C. Cells were incubated at 37°C and 5% CO_2. 15ml media was used per T175 flask. Media was changed every other day.

2.2.1d Collagenase solution

0.1% (w/v) collagenase solution was prepared by dissolving 0.05g type I collagenase (Gibco) in 25ml of PBS (plus calcium and magnesium) at 37°C for 1 hour. A further 25ml PBS (plus calcium and magnesium) was then added, and the solution was sterile filtered using a 0.2mm filter (BD Falcon). Collagenase solution was always prepared fresh prior to use.

2.2.1e Flask coating solution

For mouse primary cardiomyocyte cell culture, a 6-well plate was pre-coated with 0.1% gelatin (Porcine skin type A – Sigma) at 37°C for 1 hour. For primary mouse

endothelial cell culture, a T25 plate was pre-coated with 0.1% gelatin (Porcine skin type A – Sigma), 30µg/ml bovine collagen (Nutacon), and 1µg/ml fibronectin (Millipore) at 37°C for 1 hour. B16F0 mouse melanoma cells were cultured in uncoated T175 flasks. Gelatin, collagen and fibronectin were stored at 4°C.

2.2.1f Antibody and magnetic bead solution for cell sorting

For magnetic bead mediated endothelial cell sorting, 50µl bead solution (Invitrogen) was washed 3 – 4 times in rounds of 1ml DPBS, before overnight incubation with 10µl anti-CD31 (BD BioScience) at 4°C.

2.2.2 Endothelial cell isolation (from hearts)

Primary mouse endothelial cells were isolated from the whole hearts of C57BL6 3-7-day old mice. Hearts were removed, mechanically minced with scissors, and digested in pre-heated (37°C) 10ml 0.1% collagenase type I solution (Gibco Invitrogen) for 1 hour. Usually 3 hearts were minced together for a single prep. The collagenase reaction was stopped by adding equal parts MLEC media to solution, and the digested tissue was homogenized in a dish by syringing up to 30 times with a 19 and 21-gauge needle, and then passed through a 70um pore-size cell strainer. Cells were centrifuged at 1500rpm for 3 minutes, and the resulting cell-suspension was incubated in a solution containing 1-2µl magnetic beads conjugated to a CD31 antibody (BD BioScience) to separate cardiac endothelial cells from the total cell population. Sorted cells were plated in T25 flasks coated with 0.1% gelatin, 1µg/ml fibronectin and 30µg/ml bovine collagen, suspended in mouse lung endothelial cell culture (MLEC) media and incubated at 37°C, 5% CO_2.

Cells were washed 3-4 times in PBS the next day to remove excess red blood cells and other cell-debris.

2.2.3 Endothelial cell isolation (from lungs)

Primary endothelial cells were isolated from the lungs of Pdgfb-iCre^{ER};R26FAK$^{KD/KD}$;FAK$^{fl/fl}$ mice, at ages of 2 months or older (maximum 4 months). After culling by cervical dislocation, lungs were removed from the thoracic cavity, and cleaned of visceral fats, clotted blood and fibrous tissue, followed by a 10 second immersion in 70% ethanol and then in Ham's F12 medium. Usually, the lungs of 3 mice were minced together using fine scissors. The minced lungs were then transferred to a tube with 10ml of 0.2% type 1 collagenase (Gibco Invitrogen), diluted in PBS, and incubated in a pre-heated water bath at 37°C. The collagenase reaction was stopped by adding equal parts MLEC media to solution, and the digested tissue was homogenized in a dish by syringing up to 30 times with a 19 and 21-gauge needle, and then passed through a 70μm pore-size cell strainer. Cells were centrifuged at 1500rpm for 3 minutes, and the resulting cell pellet resuspended in 10ml of MLEC media and plated in a T75 tissue culture flask. The next day, cells were washed 3-4 times in PBS to removed excess red blood cells and other cell-debris.

Endothelial cell colonies were selected by magnetic immunosorting with ICAM-2 antibodies (Abd Serotec). The antibody solution for sorting consisted of 5μl anti ICAM-2 stock solution diluted in 3ml of PBS, and magnetic beads were prepared by diluting 3μl stock Dynabead solution (Dyna-Invitrogen Bead separation) in 3ml MLEC media. Cells were first chilled at 4°C for 30 minutes in PBS, and then

incubated for a further 30 minutes at 4°C in antibody solution. After this, the antibody solution was replaced with the magnetic bead mixture and incubated for 30 minutes at 4°C. Next, cells were trypsinised, resuspended in 10ml MLEC media and transferred to a 15ml falcon tube that was placed in a magnetic bead sorter. Here, bead-bound cells were immuno-magnetically sorted, and were resuspended in MLEC media and plated in pre-coated T25 flasks.

2.2.4 Passaging endothelial cells (cardiac and lung)

Endothelial cells from both the lungs and heart were split into new flasks when they reached 80% confluence. Here, media was removed and cells were washed 3-4 times with PBS. Trypsin (25% trypsin-EDTA from Gibco, Invitrogen) was added to cells (2ml per T25, 4ml per T75 flask), and incubated for 3 minutes at 37°C. Cell detachment was confirmed and equal parts MLEC media was added to cell solutions, before transfer to pre-coated flasks. Mouse lung endothelial cells were usually split at a 1:3 ratio, whilst mouse cardiac endothelial cells were split at a 1:2 ratio. Primary endothelial cells were passage no more than 1 (cardiac) or 2 (lung) times before immortalization.

2.2.5 Transfection of mouse lung endothelial cells (for immortalization)

Mouse lung endothelial cells were transfected with PyMT (Polyoma middle T) virus to induce cell immortalisation for subsequent assays.

Sub confluent (70-80%) endothelial cells were trypsinised and plated onto pre-coated T25 flasks at a density of 1 million cells per flask. The next day, cells were trypsinised, counted and spun for 10 minutes at 1200 rpm. Cells were resuspended

in 100ul of transfection solution (200mM HEPES, 137mM NaCl, 5mM KCl, 6mM D-glucose, 7mM Na_2HPO_4) containing PyMT, and then electroporated. Cells were left to recover in MLEC media for 15 minutes and finally decanted into a pre-coated T25 flask. Immortalised cells hereafter will be illustrated with the presence of a PMT suffix.

2.2.6 Cardiomyocyte cell isolation

Primary mouse cardiomyocyte cells were isolated from the whole hearts of 1 – 3-day old C57BL6 wild-type mice. Hearts were dissected and removed from the thoracic cavity, mechanically minced with scissors and digested in cardiomyocyte isolation enzyme 1 (200µl per heart) and cardiomyocyte isolation enzyme 2 (10µl per heart) (Pierce primary cardiomyocyte isolation kit, Thermo Scientific). Digested hearts were then homogenized by gently pipetting up to 30 times with a 1ml pipette, and the resulting single cell suspension added to complete D-MEM solution (D-MEM, 10% FBS, 1% Penicillin Streptomycin). After combination of all cell suspensions, the total number of viable cells were counted, and plated at approximately 1 million cells per well of a 6 well plate. The following day, wells were washed with PBS (without calcium and magnesium), and complete cardiomyocyte growth medium added. Complete cardiomyocyte media thereafter was replaced every other day.

2.2.7 *In vitro* cardiomyocyte hypertrophy studies

Following 5 days incubation at 37°C, 5% CO_2, primary mouse cardiomyocytes were serum starved for 24 hours in a 0.5% FBS-DMEM media. Cells were then

washed and recoated with complete cardiomyocyte growth media. For cardiomyocyte hypertrophy assessment 1uM angiotensin II (Alfa Aesar) was added to cardiomyocyte growth media post serum starvation (i.e. day 6 post-culture), and this was repeated the next day. Images of cardiomyocytes were captured using a bright field microscope at 40x magnification at 0, 24 and 48-hour post-angiotensin II treatment (i.e. day 6, 7 and 8 post-culture) and analysed using image J software. In tandem to angiotensin II treatment, cells were either treated with vehicle, low dose Cilengitide (20nM) (Bachem), or PI3k inhibitor (1μM).

After 8-day culture and treatment, cardiomyocytes were either lysed for RNA or Western-analysis (see details given below).

2.2.8 Doxorubicin stimulation of endothelial Pdgfb-iCre^{ER}; R26FAK$^{KD/KD}$; FAK$^{fl/fl}$ PMT cells

Immortalized endothelial cells were treated with either vehicle or fresh doxorubicin (Tevaguard) (125μM) in full MLEC media for 44 hours, before being serum starved in Optimem (supplemented with vehicle or doxorubicin as above) for a further 4 hours**.**

2.2.9 Cytokine arrays

Pdgfb-iCre^{ER};R26FAK$^{KD/KD}$;FAK$^{fl/fl}$ PMT cells were grown in normal full MLEC media and treated with either vehicle, or fresh doxorubicin (125μM) for 44 hours once confluent, before being serum starved in Optimem (supplemented with vehicle or doxorubicin as above) for a further 4 hours. Whole cell lysates were

extracted in high SDS buffer and mouse XL cytokine arrays (proteome profiler ARY028, R&D systems) were performed according to the manufacturer's instructions using 120μg of lysates per membrane. Pixel analysis was used for quantification with ImageJ software.

2.2.10 MTT assay

Pdgfb-iCre^{ER};R26FAK$^{KD/KD}$;FAK$^{fl/fl}$ KD PMT cells were grown in normal full MLEC media until confluence. Cells were then treated with 7.5μg/ml Mitomyocin C for 2 hours at 37°C to correct for proliferative differences between samples. Next, 1 million cells were seeded in a T25 flask, and left to recover for 24 hours. Cells were treated with either vehicle, or doxorubicin (125μM) for 48 hours. Next, conditioned cell media was collected from these treated cells and passed through a 70μm filter to remove debris. In tandem B16F0 melanoma cells were plated (500 cells per 96 well) and grown in full media. After 2 days, B16F0 full media was removed, and replaced with MLEC conditioned media. After 2-3 days, MTT was added to B16F0 wells and incubated at 37°C for an appropriate time. Media was removed, 50μl DMSO added to each well, and samples were measured via spectrophotometry at an absorbance of 570nm.

2.3 RNA analysis by RT-qPCR and RNA-seq

2.3.1 RNA extraction

Medium was removed and cells were washed 3 times in PBS. 350μl RLT lysis buffer (Qiagen) (plus 1:100 beta-mercaptoethanol) was added to each well to disrupt and lyse the cells. Cell lysate samples were then combined with an equal

volume of 70% ethanol, before being transferred into a RNeasy spin column, and centrifuged for 15 seconds at full speed in an Eppendorf Microcentrifuge. The flow through was discarded. Next, 350µl of Buffer RW1 was added to each column and spun for 15 seconds at max peed. The flow through was discarded and 80µl of DNase solution in Buffer RDD (70ul RDD:10ul DNase) was added directly to the RNeasy spin column membrane and left at room temperature for 15 minutes. 350µl of Buffer RW1 was then added to the RNeasy spin column and spun for 15 seconds at max speed, and the flow through discarded. 500µl Buffer RPE was added to the RNeasy spin column and spun for 15 seconds at max speed, and the flow through discarded. This step was repeated, and then columns were spun for 2 minutes to dry the RNeasy spin column membrane, and the flow through discarded. The RNeasy spin column was placed in a new 2ml collection tube and spun for a further 1minute at full speed without the addition of buffers to ensure there was no ethanol carry over. The RNeasy spin column was then carefully removed and placed in a fresh collection tube. Between 15µl and 30µl (depending on the expected yield of RNA) of RNase-free water was added directly to the column and spun for 1 minute at max speed to elute the RNA. The flow through was collected in a labelled 1.5ml collection tube and stored at -80°C until required.

For whole hearts, less than 100mg of tissue was lysed with 700ul RLT lysis buffer (Qiagen) (supplemented 1:100 beta-mercaptoethanol) in a QIAshredder (Qiagen) for 10 minutes. Tissues were then processed as above with the RNeasy mini kit as above.

2.3.2 RNA purity assessment

The purity and quantity of RNA was analysed using a Spectophotometer, which read absorbance at 260/280 and 260/230nm (NanoDrop, Wilmington, US). All samples were expected to exhibit a 260/280 ratio of approximately >2.0, indicating that the RNA was pure and free of nucleic acid contaminants, and a 260/230 ratio of >1.8, which was used as a secondary measure of nucleic acid purity. For RNA-Seq, RNA integrity (RIN) was assessed using gel electrophoresis to evaluate the ratio of 28s to 18s rRNA.

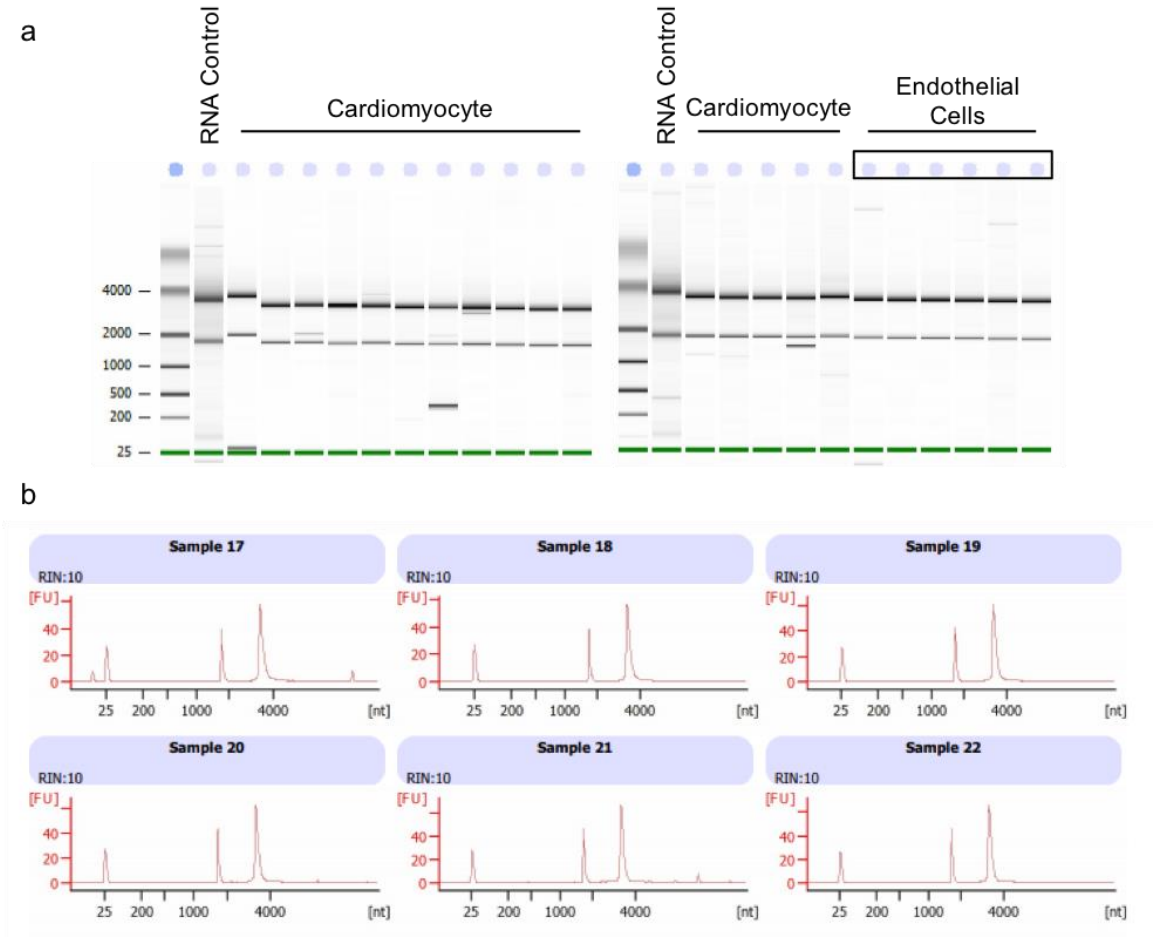

Figure 2: RNA integrity (RIN) assessment of samples sent for RNA-Seq. (**a**) Gel electrophoresis of samples sent for RNA-Seq. (**b**) Representative RIN values of cardiac endothelial samples (17-22). Conducted with help from QMUL genomics centre.

2.3.3 Reverse transcription

Complimentary DNA (cDNA) synthesis was carried out using the Applied Biosystems High Capacity cDNA Reverse Transcription (RT) Kit on a thermal cycler as per the manufacturer's instructions.

High capacity cDNA reverse transcription recipe:

Component	**Volume (μl)**
10x RT buffer	2.0
25x dNTP mix	0.8
10x RT random primers	2.0
Multiverse reverse transcriptase	1.0

Table 1: High capacity cDNA reverse transcription recipe.

cDNA was made up to a total quantity of either 600 (most mouse tissue and/or cells), or 1000ng (human heart tissue).

Thermal cycle conditions:

	Step 1	**Step 2**	**Step 3**	**Step 4**
Temperature (°C)	25°C	37°C	85°C	4°C
Time (minutes)	10 minutes	120 minutes	5 minutes	Infinite

Table 2: Thermal cycle conditions – cDNA synthesis.

2.3.4 Quantitative PCR (qPCR)

Analyses were performed using the ABI Prism 7500 Sequence Detection system Instrument and software (PE Applied Biosystems). RT-qPCR was performed using sample cDNA, an internal control GAPDH (VIC-tagged) and specific TaqMan probes (FAM-tagged).

RT-qPCR was carried out using the TaqMan Universal PCR Master Mix (PE Applied Biosystems) in a 96 well plate. 160ng of cDNA from each sample was amplified using qPCR across 40 cycles.

	Step 1	Step 2	Step 3 – 4: 40x cycles	
Temperature (°C)	60°C	95°C	95°C	60°C
Time (minutes)	10 minutes	10 minutes	15 seconds	60 seconds

Table 3: Thermal cycle conditions - RTqPCR.

Target mRNA was normalised to GAPDH (HPRT-1 if human), and the expression level of each gene determined relative to the initial experimental controls using 2^{-ddCT} method.

The following primers were used (with associated primer codes):

Note - All primers are Taqman unless otherwise stated. For Taqman assays, all housekeeping primers are VIC-tagged, and genes of interest are FAM-tagged.

Primer	**Assay ID (Thermofisher Taqman)**
ANP	Mm01255747_g1
BNP	Mm01255770_g1
Myh7	Mm00600555_m1
Myh6	Mm00440359_m1
β3 Integrin (mouse)	Mm00443980_m1
β5 Integrin (mouse)	Mm00439825_m1
β3 Integrin (human)	Hs01001469_m1
β5 Integrin (human)	Hs00174435_m1
GAPDH (mouse)	Mm99999915_g1
HPRT-1 (human)	Hs02800695_m1
FAK (mouse)	Forward: GGCGTTGCCATCAATACCA Probe: AAGGCATGCGGACACA Reverse: GGTGTATGTGTCTTCCTCATCGAT
FAK (chicken)	Forward: CAACAGCAAGAGATGGAAGAAG ATC Probe: ACGATTCCTGGTAATGAA Reverse: 5′-CCGTCCTCCCGTTCAATG-3′
Primer	**Primer sequence 5'-3' (SYBR)**
RLP-19 (SYBR)	Forward: GCTTGCCTCTAGTGTCCTCC Reverse: TTGGCGATTTCATTGGTCTCA
β-actin (SYBR)	Forward: CACAGCTTCTTTGCAGCTCCTT Reverse: TCAGGATACCTCTCTTGCTCT
CTGF (SYBR)	Forward: GGGCCTCTTCTGCGATTC Reverse: ATCCAGGCAAGTGCATTGGT

Table 4: Primer codes for RT-qPCR.

2.3.5 RNA-Seq

Cells were harvested 48 hours after treatment and total RNA was extracted as above using the RNeasy Mini kit with DNase treatment (Qiagen). The quality of RNA was assessed and only RNAs with an RNA integrity value (RIN) of greater than 7 was used for sequencing, with a minimum input of 1μg of RNA. Poly-A library preparation was performed at the Queen Mary University of London Genome Centre according to manufacturer's instructions (Illumina). Briefly, first-strand cDNA was generated using random hexamer-primed reverse transcription, followed by second-strand cDNA synthesis using RNase H and DNA polymerase, and ligation of sequencing adapters using the TruSeq RNA Sample Preparation Kit (Illumina). Per sample, 20 million reads were generated, with a read length of 75 base pairs. The prepared libraries were sequenced using the Illumina sequencing platform NextSeq 500 high output run (150 cycles). Data was received in a FASTQ format and analysed by Prof. Jun Wang and Eleni Maniati of the Bart's Cancer Institute.

Human RNA-Seq and microarray data were obtained from [6], and contained 6 RNA-Seq, and 313 microarray data sets.

2.5 Protein analysis by Western Blotting

2.5.1 Cell lysis

For all western blot procedures, cells were grown to 70-90% confluence and lysed with either RIPA buffer (Millipore – 50mM Tris-HCl pH 7.4, 1% NP-40, 0.5% sodium deoxycholate, 0.1% SDS, 150mM NaCl, 2mM EDTA, 50mM NaF), or high SDS

buffer (3% SDS, 60mM sucrose. 65mM Tris pH 6.8), both supplemented with protease inhibitor (1:100, CalbioChem – 100mM AEBSF hydrochloride, 60μM Aprotinin, 5mM Bestatin, 1.5mM E-64 protease inhibitor, 2mM Leupeptin hemisulfate and 1mM pepstatin). 80μl lysis buffer was used for 6 well plates and T25 flasks, and 180μl for T75 flasks. Cells were scraped on ice if RIPA-lysed, or at room temperature if high-SDS lysed.

For whole hearts, less than 100mg of tissue was lysed with 200-500μl high-SDS buffer (supplemented with 1:100 protease inhibitor) (size dependent) in a QIAshredder (Qiagen) for 10 minutes.

RIPA-lysed cells were transferred to an Eppendorf and centrifuged at 12000rpm for 10 minutes at 4°C, and the supernatant transferred to a fresh Eppendorf for storage. High-SDS lysed cells/tissue were transferred to an Eppendorf and sonicated for 10 seconds, before being vortexed at max speed for a further 10 seconds. Aliquots were stored at -20°C in all cases.

2.5.2 Protein quantification

Protein concentrations were calculated using the colorimetric DC Bio-Rad assay (Bio-Rad laboratories). Protein standards were obtained by preparing an increasing gradient of bovine serum albumin (BSA) in RIPA or high-SDS buffer, from 0-2000μg/ml. In order to quantify protein concentrations 5μl of the protein of interest was sampled in triplicate in a 96 well plate, to which 25μl of Reagent A' (prepared by mixing 1ml Reagent A with 20ul Reagent S), and 200μl of Reagent B was added. Solutions were incubated at room temperature for 15 minutes, before optical reading using an absorbance microplate reader set at 620nm

wavelength. Further analysis was completed using Magellan software.

2.5.3 SDS-polyacrylamide gele electrophoresis

8% (p-Akt, total Akt) or 10% (FAK, β3/β5 integrin) polyacrylamide gels (1.5mm thick) were used for resolving protein lysates.

10% Acrylamide gel recipe (10ml per gel):

Reagent	**Volume**
30% Acrylamide	3.3ml
1.5M Tris (pH 8.8)	3.8ml
Distilled water	5.9ml
10% SDS	0.1ml
Ammonium persulphate (APS) 10%	0.1ml
TEMED	0.006ml

Table 5: 10% Acrylamide gel recipe.

Resolving gel was poured into cassettes (Invitrogen), and a thin layer of water was added onto the gel to prevent air-gel contact, which can impair successful polymerization.

Stacking gel recipe (2ml per gel):

Reagent	**Volume**
30% Acrylamide	0.33ml
Distilled water	1.4ml
1M Tris (pH 6.8)	0.25ml
10% SDS	0.02ml
Ammonium persulphate (APS) 10%	0.02ml
TEMED	0.002ml

Table 6: Stacking gel recipe.

Following polymerization of the resolving gel excess water was removed and stacking gel was poured into the cassette. A 10-12 well comb was added, and stacking gel left to polymerize. Next, the gel-cassette was placed in a gel tank (Invitrogen) filled with running buffer (1x Tris-Glycine-SDS). Lysates were boiled at 100°C for 10 minutes and loaded into the gel, which was run at 110V for 30 minutes, followed by 140V for a further 1 hour at room temperature, or until the desired separation was achieved.

2.5.4 Transfer

Resolved proteins were transferred from gels to pre-wet Hybond nitrocellulose or PVDF membranes (GE). A ‘sandwich’ was assembled of sponges, Whatman paper, membrane and gel in transfer buffer (1x Tris-Glycine, 20% Ethanol) prior to transfer. To remove air bubbles here, a plastic pipette was rolled over the transfer

‘sandwich’. The assembly was placed in a transfer apparatus and this was placed in a gel tank filled with transfer buffer. Transfer was performed at 4°C at 30V for 75 minutes, and successful transfer was evaluated via the immersion of the membrane into a Ponceau S red (Sigma) solution for 1 minute. Membranes were then washed with distilled water and kept in washing buffer (PBS-0.1% Tween-20) prior to Western blotting.

2.5.5 Western Blotting

After protein transfer, membranes were blocked with 5% milk for 1 hour and probed with primary antibody (1:1000) overnight at 4°C in a 5% BSA blocking buffer. Blots were washed for 5 minutes 3 – 6 times in 0.1% PBS-Tween 20 and incubated with a relevant horseradish peroxidase (HRP) conjugated secondary antibody in 5% milk for 2 hours at room temperature. Once again, blots were washed for 5 minutes 3-6 times in 0.1% PBS-Tween 20. Reactive bands amongst the membrane were visualized using an enhanced chemiluminescent kit (Millipore), and exposed using either auto radiographic film, or the Chemidoc.

The following housekeeping antibodies were used:

Antibody	Company	Dilution	Host	Reactivity
GAPDH	Millipore	1:5000	Mouse (monoclonal)	Mouse
GAPDH	Santa-cruz	1:2000	Mouse	Human
Hsc-70	Santa-cruz	1:5000	Mouse (monoclonal)	Mouse

Table 7: Housekeeping antibody list.

The following primary antibodies were used:

Antibody	Company	Dilution	Host	Reactivity
FAK	Millipore	1:1000	Mouse	Mouse
β3 integrin	Cell signalling	1:1000	Rabbit	Human
β5 integrin	Cell signalling	1:1000	Rabbit	Human
p-Akt	Cell signalling	1:1000	Rabbit	Mouse
Total Akt	Cell signalling	1:1000	Mouse	Mouse

Table 8: Primary antibody list.

2.5.6 Enhanced chemiluminescence (ECL)

ECL (ThermoFisher) is a light emitting and non-radioactive method used to detect immobilized specific antigens that are conjugated to HRP-labelled antibodies. Following incubation with luminescent reagents for 1 minutes, membranes were exposed on either autoradiographic film, or using the Chemidoc system.

2.5.7 Densitometry

ImageJ software was used for densitometric analysis of western blotting bands.

2.6 Genotyping and PCR

2.6.1 Generation of mice

To study the effect of inducible endothelial-specific FAK kinase deletion *in vivo*, we used a knockout/knockin system whereby endogenous mouse FAK was deleted and myc-tagged chicken FAK [wild-type (WT) or mutant] was expressed under control of the R26 promoter upon tamoxifen induction. To this end, we used what I will refer to as a Pdgfb-iCre^{ER}; R26FAK$^{KD/KD}$;FAK$^{fl/fl}$; mouse (EC FAK^{KD}). The mouse model has been used successfully in a recent publication [7]. The validation of chicken FAK, as well as its characterisation and generation were described elsewhere by *Tavora et al.* [8]. Those mice without cre were used as controls (EC FAK^{WT}).

2.6.2 Reagents

2.6.2a Tail lysis buffer

Tail lysis buffer consisted of 10mM Tris-HCL (pH 8.5), 10mM EDTA, 100mM NaCl and 0.2% SDS. 0.1mg/ml proteinase-K was thawed and added immediately before addition to ear clips.

2.6.2b TE buffer

TE buffer consists of 10mM Tris-HCL (pH 7.5) and 1mM EDTA.

2.6.3 DNA extraction from ear snips

Tissue samples were digested over night at 56°C in 100µl tail lysis buffer (plus 0.1mg/ml proteinase K). The following morning, 100µl isopropanol was added, plates were centrifuged at 2600rpm for 30 minutes, and the supernatant was removed by inverting the plate. The DNA pellet was dried at 56°C for 1 – 2 hours, and this was then re-suspended in 200µl TE buffer and left at RT for 1-2 hours before use.

2.6.4 Polymerase chain reaction (PCR)

PCR was performed to genotype all mice. I was responsible for maintaining all the breeding programs and genotyping of all the mice used during my PhD.

All primers (Invitrogen) were stored as a stock solution of 100µM in nuclease free water at 4°C.

2.6.4a FAK$^{fl/fl}$ (LP2) PCR

PCR for LP2 genotyping (**figure 4**) was performed using the following oligonucleotide primers:

Primer	**Primer sequence 5'-3'**
LP2as	5'-TTAATAAGACCAGAGGACTCAGC-3'
LP2h	5'-GGAAGAAGCTTGTATACTGTATG-3'
LP2s	5'-ATTGTGCTATACTCACATTTGGA-3'

Table 9: LP2 primer sequence.

For all LP2 reactions 1.5µl DNA was added to 24µl total MasterMix (MegaMix-Blue

(Microzone)), and 0.3μl total primer mix (LP2as, LP2h, LP2s 1:1:1).

	Step 1	**Step 2 – 4: 36x cycles**			**Step 5**	**Step 6**
Temperature (°C)	94°C	94°C	56°C	72°C	70°C	18°C
Time (minutes)	3 minutes	1 minute	45 seconds	60 seconds	5 minutes	Infinite

Table 10: LP2 PCR thermocycler cycle.

Product size: LP2 697 bp and wild-type 429 bp.

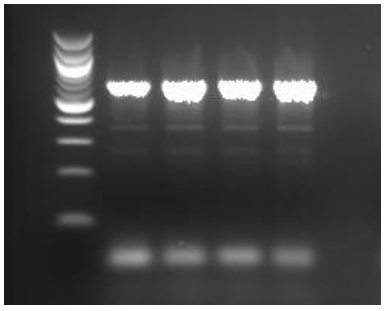

Figure 3: LP2 example PCR. Note: all samples here are LP2 positive where LP2 is 697bp.

2.6.4b Pdgfb-iCre^{ER} PCR

PCR for Pdgf*b*-iCre^{ER} genotyping was performed using the following primer sequences:

Primer	**Primer sequence 5'-3'**
Cre Fwd	5'-GCCGCCGGGATCACTCTC-3'
Cre Bwd	5'-CCAGCCGCCGTCGCAACT-3'
B2M Fwd	5'-CACCGGAGAATGGGAAGCCGAA-3'
B2M Bwd	5'-TCCACACAGATGGAGCGTCCAG-3'

Table 11: *Pdgfb*-iCreER primer sequence.

For all Pdgf*b*-iCre^{ER} genotyping (**figure 5**) 1.5µl DNA was added to 24µl total MasterMix (12µl DreamTaq Green PCR (2x) (LifeTechnologies), 12µl nuclease free water), and 0.3µl total primer mix (Cre Fwd, Cre Bwd, B2M Fwd, B2M Bwd 1:1:1:1).

	Step 1	**Step 2 – 4: 34x cycles**			**Step 5**	**Step 6**
Temperature (°C)	94°C	94°C	65°C	72°C	70°C	18°C
Time	4 mins	30 seconds	80 seconds	60 seconds	10 mins	Infinite

Table 12: *Pdgfb*-iCreER thermocycler cycle.

Product size: Cre 443 bp, B2M 295 bp.

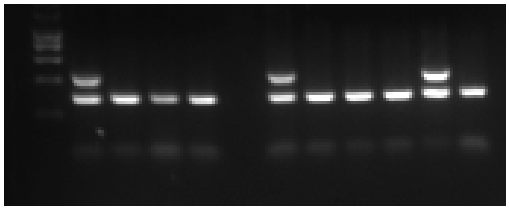

Figure 4: *Pdgfb*-iCreER example PCR. Note: Cre 443bp, B2M 295bp.

2.7 Immunohistochemistry (mouse)

2.7.1 Immunohistochemistry on paraffin sections

Myocardium was fixed in 10% neutral buffered formalin for 24 hours at room temperature, before being transferred to 70% ethanol. Tissues were paraffin embedded, sectioned to 5µm and dewaxed in xylene, then rehydrated in a decreasing ethanol gradient for 3-5 minutes per condition (100, 100, 80, 70, 50, distilled water). Antigen retrieval was performed by boiling slides in 10mM citrate buffer (pH 6.0) for 13 minutes. Sections were left to cool for 10 minutes in PBS, before proceeding with the intended staining procedure.

2.7.1a Picrosirius Red staining

For collagen fibre staining, heart sections were dewaxed (as above) and then were incubated in phoshomolybdic acid for 2 minutes, before being transferred to picrosirius red for 60 minutes, and finally immersed in acidified water (5ml acetic acid per 1ml water) for a further 2 minutes on a shaker. For best results, sections were then immediately transferred to 100% ethanol without being dehydrated in

multiple rounds of increasing ethanol concentrations. Tissues were then immersed in xylene for 10 minutes before being mounted in DPX and finally cover-slipped. The positive fraction of percentage area of red staining of an entire section was quantified after setting an appropriate threshold with ImageJ.

2.7.2 Immunohistochemistry on frozen sections

Myocardium was snap frozen in liquid nitrogen and stored at -80°C before being transferred to an OCT-containing mould. Cryosections were cut to 5um and transferred to slides, and then fixed in 100% acetone at -20°C.

2.7.2a Wheat Germ Agglutinin (WGA) staining

To quantify cell area size (of cardiomyocytes), tissues were blocked in 5% normal goat serum for 1 hour and incubated with WGA Alexa Fluor 488 (Invitrogen) conjugate antibody (1:100) in blocking buffer (5% normal goat serum) for 2 hours at room temperature. Sections were washed 3 times in PBS and mounted in anti-fade gold with DAPI (Molecular Probes). Images were taken on a Zeiss axioplan microscope, and the cardiomyocyte size was analysed with ImageJ (NIH). The cardiomyocyte size was estimated as an average of ~100-200 cells per heart.

2.7.2b Masson's Trichrome staining

Masson's trichrome staining was used to detect the abundance of collagen fibers amongst mouse heart tissue sections. Tissues were fixed in Bouin's solution for 1 hour at 56°C, before being rinsed in tap water for 5-10 minutes. Tissues were then immersed in Weigert's iron hematoxylin (mixed equal parts A and B) for 10

minutes, and rinsed in tap water, followed by staining in Beibrich scarlet-acid fuchsin for 15 minutes. Samples were washed in distilled water and left in phospolybdic-phosphotungstic acid solution for 15 minutes, and then transferred without washing to aniline blue solution for a further 10 minutes. Sections were rinsed briefly in distilled water, and immersed in 1% acetic acid for 5 minutes, before being washed again in water, and then transferred to 100% ethanol and cleared in xylene. Samples were finally mounted in DPX. The positive fraction of percentage area of red staining of an entire section was quantified after setting an appropriate threshold with ImageJ.

2.7.2c CD31 staining and quantification of blood vessel density

For anti-CD31 (BD Bioscience) stains, tissues were blocked in 5% normal goat serum for 1 hour, followed by incubation with anti-CD31 primary antibody (1:100) in blocking buffer (5% normal goat serum) for 2 hours at room temperature. Next, sections were incubated for 1 hour at room temperature with an appropriate secondary antibody, conjugated to a green (usually 488) fluorophore, before being washed 3 times in PBS and then mounted in anti-fade gold with DAPI.

Images were taken with an Axioplan Zeiss microscope. To quantify cardiac blood vessel density, the number of CD31-positive blood vessels present across an entire area of transversely-orientated cardiac tissue was counted within a field of view taken at 40x magnification. 3 of these fields were used per heart and an average taken across fields.

2.8 Immunohistochemistry (human)

Procurement of human myocardial tissue was performed under protocols approved by Institutional Review Boards at the University of Pennsylvania (Pennsylvania, USA), Johns Hopkins University (Maryland, USA) and VU University Medical Center, (Amsterdam, The Netherlands) and its coordinated affiliated centres. Thank you to Kenneth Marguiles and Ken Bedi. Failing human hearts were procured at the time of orthotopic heart transplantation at the Hospital of University of Pennsylvania. Non-failing hearts were obtained at the time of organ donation from cadaveric donors. In all cases, hearts were arrested *in situ* using ice-cold cardioplegia solution, transported on wet ice, and flash frozen in liquid nitrogen within 4 hours of explantation. All samples were full-thickness biopsies obtained from the free wall of the left ventricle. Heart failure with preserved ejection fraction (HFPEF) patients were referred for cardiac catheterization and left ventricular endomyocardial biopsy because of clinical suspicion of restrictive cardiomyopathy. Left ventricular biopsies were obtained using femoral artery access and a long bioptome. Control samples for these studies were obtained from explanted unused donor hearts.

Donated myocardium was pre-sectioned onto slides, and thus could be immediately processed. Tissues were dewaxed in xylene, then rehydrated in a decreasing ethanol gradient (100, 100, 80, 70, 50, distilled water). Antigen retrieval was performed by boiling slides in 10mM citrate buffer (pH 6.0) for 13 minutes. Sections were left to cool for 10 minutes in PBS, before proceeding with the intended staining procedure.

2.8.1 β3 and β5 immunostaining (co-staining with Cardiac Troponin T, CD31 or α-SMA)

For anti-β3 (Invitrogen) and anti-β5 (Millipore) stains, tissues were blocked in 10% normal goat serum and 1% BSA for 1 hour, followed by incubation with anti-β3 or anti-β5 primary antibody (1:200) in blocking buffer (10% normal goat serum, 1% BSA) overnight. Sections were co-incubated with cardiac troponin T (cTnT) (1:200), CD31 (Santa Cruz) (1:200) or PE-α-SMA (Invitrogen) (1:200) also overnight. Next, sections were incubated for 2 hours at room temperature with an appropriate secondary antibody in blocking buffer (10% normal goat serum, 1% BSA), conjugated to a 488 (β3/β5) or 546 (cTnT, CD31) fluorophore, before being immersed in Sudan black for 15 minutes to reduce autofluorescence. α-smooth muscle actin (α-SMA) was pre-conjugated to PE (phycoerythrin). Sections were washed thoroughly in tap water for 5 minutes, and washed 3-6 times in PBS for 3 minutes, and finally mounted in prolong gold with DAPI. β3 and β5 stained sections were imaged on either the Zeis Axioplan, or Zeis 710 confocal microscope, and processed using Image J software.

2.9 Statistical analysis

All results are presented as mean ± SEM for at least 3 biological replicates, unless otherwise stated. Sample sizes were based upon previous power calculations performed by former investigators. Unless otherwise stated P values were calculated using one-way ANOVA with Tukey's post-hoc analysis. $P<0.05$ was considered statistically significant.

2.10 Ethical regulations

All procedures were approved by our local animal ethics committee at the Queen Mary University of London and were executed in accordance with UK Home Office regulations.

CHAPTER 3.0: INTRODUCTION

HEART FAILURE AND ANGIOGENESIS

3.1 General Introduction: Vascular System

3.1.1 Organisation and function of the cardiovascular system

The survival, reproduction and growth of living organisms rely on the delivery and recycling of metabolites to and from all cells in the body. Through evolution, as organisms grow in size and complexity, the simple diffusion of metabolites through cell membranes and across multiple cell layers was complemented with the development of specialised transport and exchange structures. As such, vertebrates developed highly complex and hierarchised blood vascular systems [9]. Additionally, these circuits co-developed as networks to facilitate movement of factors regulating whole organism homeostasis, including temperature regulation, hormonal communication, and the circulation of immune factors and cells.

The blood vascular system of vertebrates is organised in a closed network of accumulating (veins and venules) and distributing (arteries and arterioles) vessels connected to a central peristaltic pump known as the heart. In tissues, the exchange of gases and metabolites takes place through networks of fine capillaries, whose organisation throughout the body ascertains sufficient

distribution of resources to all organs. The efficiency and adaptability of the vertebrate's cardiovascular system lies in the structural specialisation and hierarchical organisation of the vessels within its network. Capillaries are made of a single layer of endothelial cells and are surrounded by a basement membrane and pericytes. Capillaries can locally adapt to the metabolic needs of the surrounding tissue, and deliver interchangeable levels of resources accordingly, by regulating their own permeability at various levels through fenestration, opening of cell junctions, partial digestion of the basement membrane, and/or detachment of pericytes. In contrast, larger vessels such as arteries and veins are surrounded by multiple layers of connective tissue and vascular smooth muscle cells (VSMCs), and as such can handle higher blood volumes and pressure levels and adapt their diameter to modulate flow between tissues [10].

3.1.2 Development of the vascular system – vasculogenesis and angiogenesis

Because of its critical role in nutrient and oxygen delivery, the cardiovascular system is the first organ system to reach a functional state during embryonic development [11]. In vertebrates, blood vessel formation starts soon after gastrulation [11]. Mice for example, will exhibit vessel formation at E7-8, whilst in humans, early vessels will form within 3 weeks [12, 13]. Central to early blood vessel formation is vasculogenesis, or the assembly of new blood vessels from individual precursor cells. In the embryo, blood vessels begin life as blood islands,

the earliest of which includes the yolk sac, connecting stalk and chorion. Blood islands are composed of pluripotent haemangioblasts, which are capable of differentiating into either angioblasts (i.e. vascular precursor cells), or haemocytoblasts (i.e. blood precursor cells) [14]. The differentiation of a haemangioblasts is determined by the spatiotemporal protein expression of fibroblast growth factor (FGF) – those cells on the inside of an island receive relatively less FGF and will form endothelial precursor cells, and those on the outside of an island will see relatively more FGF and form primitive haematopoietic cells [15].

Angioblasts are migratory cells that will coalesce into cords and aggregate to form a lumen. The progressive fusion and extension of many of these primitive luminated vessels together forms a primordial vascular plexus, which once established, will itself ramify and undergo a broad remodelling of extensive growth, migration, sprouting and branching to further generate new vessels, in a process called angiogenesis [16]. Angiogenesis refers to the formation of vessels from pre-existing vessels and occurs either through the splitting of existing vessels (intussusceptive angiogenesis i.e. non-sprouting), or the sprouting, and later fusion, of vessel branches from a parent vessel (sprouting angiogenesis). The overall process of angiogenesis constitutes a ‘second-wave’ of blood vessel formation that occurs after ‘first-wave’ developmental vasculogenesis. Angiogenesis generates a dense plexi of capillaries from which arteries and veins later develop and mature to generate a whole organism, fully functional vasculature [17].

3.1.3 Angiogenesis

Angiogenesis is an essential process during tissue regeneration, growth, reproduction and development. It is a highly regulated event that involves the interplay of multiple different signalling networks, and if dysregulated can contribute to several different pathological conditions, including arthritis, diabetic retinopathy, heart disease and cancer [17]. There are two main types of angiogenesis: sprouting and non-sprouting angiogenesis [17]. Sprouting angiogenesis refers to the formation of new blood vessels from pre-existing vasculature [18]. Initiation of sprouting requires the specification of endothelial cells into 'tip' and 'stalk' cells bearing different morphologies and functional properties [18]. Endothelial tip cells are minimally proliferative, polarized and migratory, whereas stalk cells are highly proliferative and will form the nascent vascular lumen cell [19].

Tip-cell selection

Tip cells express high levels of platelet derived growth factor-b (PDGF-b), vascular endothelial growth factor receptor-2 (VEGFR-2), VEGFR-3, UNC-5 homolog B (UNC5B), delta-like 4 (Dll-4) and have low levels of Notch signalling activity [20] [21]. In contrast, stalk cells exhibit high levels of Notch-1, which is activated by tip-cell Dll-4, and thus possess high Notch signalling activity [22] [21]. In this way, the interaction between Dll-4 and Notch-1 establishes lateral inhibition between cell types, leading to a positive feedback loop, which allows Notch activity to further determine differential cell fate [23] [20]. Consequently, pharmacologic blockade of

Notch signalling using γ-secretase inhibitors or inducible endothelial-specific deletion of the Notch-1 receptor both lead to the formation of excessive tip cell numbers, and a corresponding relative reduction in stalk cell number [24] [25] [26]. In addition, analysis of the retina of *DLL4*$^{+/-}$ mice shows that virtually every endothelial cell, with the exception of the main arteries, extends filopodia, and thus adopt a tip cell-like phenotype [26]. Previously it was thought that, once selected, cells will keep their fate and that the once selected tip cells will remain at the leading position of the sprout. However, it is now known that cells continually interchange their places - tip cells become stalk cells and vice versa [20].

Extracellular matrix (ECM)

Before endothelial cell migration can occur, the extracellular matrix (ECM) must be degraded. Tip cells do this by secreting several proteolytic enzymes, including, urokinase plasminogen activators (uPa), plasmin and metalloproteinases (MMPs). Growth factors liberated from the ECM after its degradation will further potentiate endothelial growth and migration [27].

Migration

Tip cells guide outgrowing capillaries across a concentration gradient of matrix-bound vascular endothelial growth factor (VEGF). Tip cells explore their environment by extending motile filopodia, which express VEGFR-2 and -3, and transduce the migratory signal initiated by VEGF binding, thus directing vessel growth [21]. Consequently, VEGFR-2 blockade results in sprouting defects [28], and VEGFR-3 inhibition with monoclonal antibodies results in decreased

sprouting, vascular density, vessel branching and endothelial cell proliferation in mouse angiogenesis models [29].

The migration of tip cell filipodia, and thus endothelial cells is a tightly regulated process. In theory, if all cells were to migrate, vessels should disintegrate and conversely, if all cells were to proliferate, vessels would likely only increase in diameter. When a chemotactic stimulus is present, such as VEGF, different signalling pathways converge to modify cytoskeletal remodelling. Firstly, endothelial cells polarize, resulting in the formation of a leading edge that contains thin, needle-like protrusions called filipodia. Cdc42 is a prerequisite for protrusion formation in most polarizing cells, including endothelial cells [30]. As such, the *in vivo* deletion of Cdc42 in embryonic endothelial cells results in blocked lumen formation and endothelial tearing, leading to lethality of mutant embryos by E9-10 due to failed blood circulation [30]. To transform protrusion formation into forward movement, cells will anchor to a substrate at focal complexes. Once attached, the continuous addition of G-actin at the barbed ends of actin filaments will push the plasma membrane and the extended leading edge forward, which then stabilizes through the formation of new adhesion sites. Focal complexes disassemble at the rear, and reassemble at the leading edge, thus perpetuating forward motion [31].

Adhesion

Focal adhesion complexes are composed of a large number of adhesion-related proteins including integrins and cadherins [32]. As will be discussed in further detail later, integrins belong to a family of heterodimeric transmembrane glycoproteins which mediate cell-ECM and cell-cell interactions. VEGF-induced angiogenic cell migration requires αvβ3, αvβ5 and β1 integrins [33]. Consequently, integrin β1-deficient endothelial cells are defective in cell adhesion and migration [34] [35]. However, mice lacking αvβ3 and αvβ5 integrins are viable and fertile and blood vessel development in these animals is not disturbed. Importantly, loss of β3-integrin enhances tumour angiogenesis [36]. A possible explanation for this is a compensatory response mediated by enhanced VEGF/VEGFR2 signalling [37].

Lumen formation and vessel stabilisation

To establish a properly patterned vascular tree, tip cells are followed by morphologically distinct stalk cells, which form a lumenised tube growing behind the tip cell. The lumen of a blood vessel is essential for providing blood to any given tissues, and only once it has been established can blood flow through a newly formed vessel. As a vessel elongates, stalk cells proliferate in response to VEGF and establish adherens junctions between neighbouring cells. In doing so, they are able to create a lumen, synthesize a basement membrane, associate with pericytes, and finally increase the mass and surface of the growing vessel [38] [17].

In order to be functional, the new vessels need to be stabilized. Active angiogenic sprouts progressively become quiescent as a result of decreased endothelial cell migration proliferation. Stabilisation of newly formed vessels is mainly a result of synthesis and deposition of new basement membrane and recruitment of perivascular cells, such as pericytes, if associated with capillaries and immature vessels, or vascular smooth muscle cells, if covering larger vessels such as arteries and veins. Interaction of pericytes and endothelial cells promotes a quiescent state by inhibiting endothelial migration and proliferation [39]. This may be partially controlled by pericyte-induced endothelial cell expression of plasminogen activator inhibitor type 1 (Pal-1), or endothelial cell Tie2 receptor expression [40] [41].

In summary, the sprouting angiogenic process (after the release of pro-angiogenic growth factors) can be summarized by: (1) Endothelial cell activation and basement membrane degradation by the production of matrix metalloproteinases (MMP), (2) sprout formation involving elevated endothelial cell proliferation and migration, and (3) lumen formation and (4) vessel stablisation and maturation by the production of new basement membrane and recruitment of pericytes (Figure 1) [17].

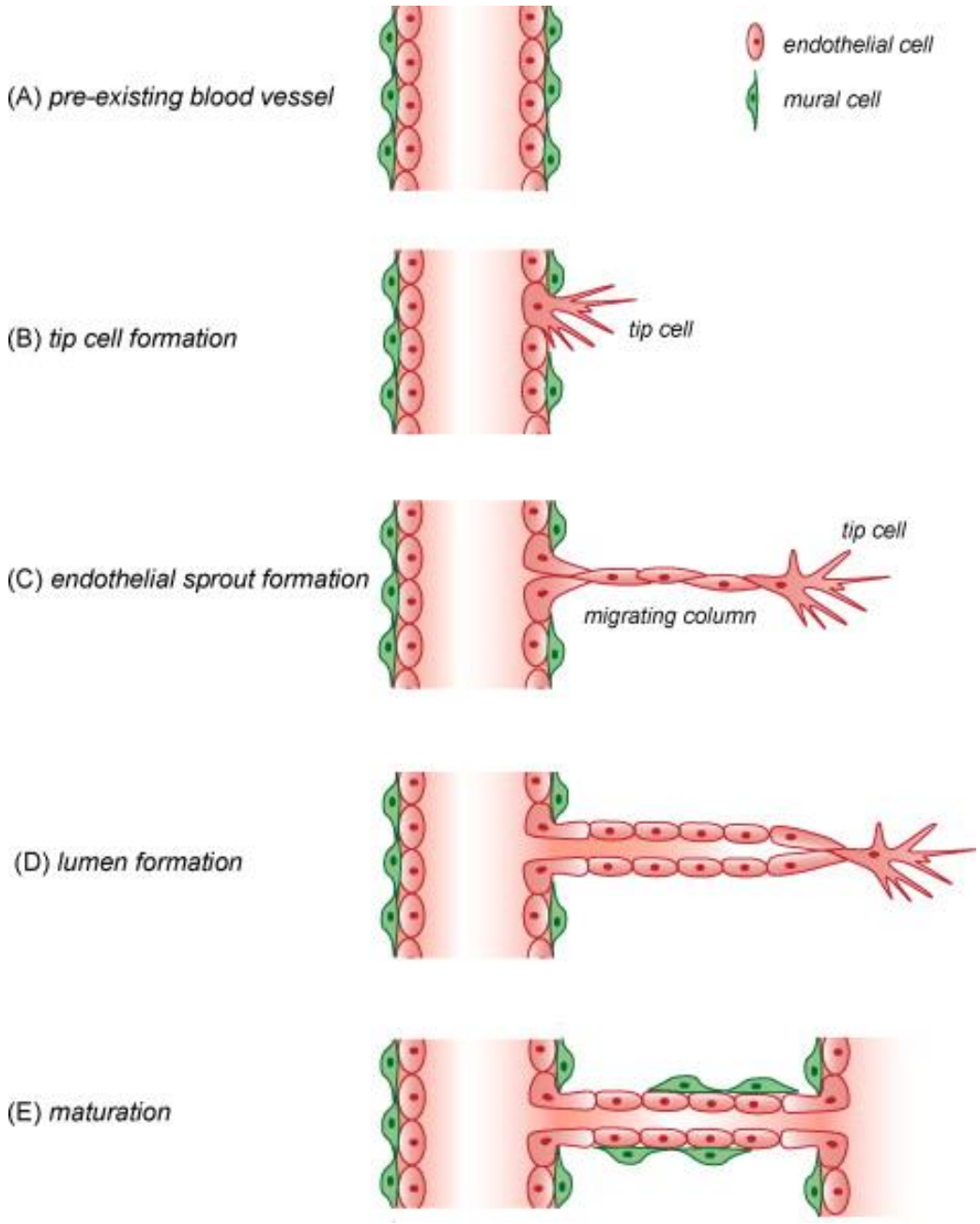

Figure 5: Schematic representation of the sprouting angiogenic process. (A) Angiogenesis begins from an existing vessel. (B) Tip cells are selected from quiescent endothelial cells, (C) a filipodia forms, and a migrating column of endothelial cells move according to a cocktail of signalling molecules. (D) During endothelial sprouting, vacuoles form which will eventually form the lumen of a blood vessel. (E) Vessels undergo stabilization mediated by intracellular adhesion, and the coverage of mural cells. Taken from [18].

Non-sprouting angiogenesis

As an alternative to sprouting angiogenesis, internal division of pre-existing capillaries through the insertion of trans-capillary pillars can also form new vessels [42]. This type of angiogenesis, known as intussusception, or non-sprouting angiogenesis, is known to occur during the development of different organs but has not yet been implicated in pathological situations, such as tumour angiogenesis [43].

Until recently it as thought that new blood vessels could arise only from sprouting and non-sprouting angiogenesis. However, in 1997 it was suggested that, for the first time, endothelial progenitor cells (EPCs) could also be implicated in angiogenesis [44]. The precise role of EPCs is still not well understood, however, it is generally thought EPCs may derive from a subpopulation of undifferentiated bone marrow peripheral mononuclear cells [45]. EPCs may be mobilized into the peripheral circulation, and then sites of neovascularization, in response to haematopoietic stimulators such as VEGF or stromal derived factor-1 (SDF-1) [46]. Once here, the contribution of EPCs towards neo-vessel formation may range from 5-25%, as indicated by EPC labelling experiments [47]. Therapeutic transplantation of human EPCs into nude mice following hindlimb ischemia will reduce the rate of limb loss dramatically, and also improve blood flow and capillary density in affected areas [48]. Dysfunctional EPCs, as in older patients or in diabetics, will reduce overall tissue neovascularization, thereby indicating their general contribution to angiogenesis [49].

3.1.4 Growth factor signalling pathways in angiogenesis - VEGF

The angiogenic process is dependent upon the fine regulation of several pro- and anti-angiogenic factors including FGF, angiopoietins, transforming growth factor β (TGF-β), endostatin, thrombospondin-1, Delta-Notch, Ephrin-Eph and perhaps most importantly, VEGF [38]. VEGF is considered to be the 'master regulator' of blood vessel formation, and as such this will be the main focus of my description here. VEGF is responsible for several responses in endothelial cells including: proliferation, migration, survival, differentiation, tube formation, permeability and vessel formation [50]. The VEGF family comprises seven members: VEGF-A, VEGF-B, VEGF-C, VEGF-D, PlGF VEGF-E and VEGF-F. With the exception of the latter 2 members, 5 genes of the VEGF family exist in mammalian genomes, including humans. All members have a common VEGF homology domain [38].

VEGF-A is the most well characterised gene of the VEGF family and has five alternative splicing isoforms: 121, 165, 183, 189 and 206 amino acids [50]. Different splice variants may display differential functions according to their distinct chemotactic properties, receptor specificity and tissue specific expression [51]. *VEGF-A* is unique amongst VEGF family members in that even if only a single copy of the *VEGF-A* gene is deficient (e.g. in heterozygotic *VEGF-A* gene knockout mice), the mutant embryo dies at early embryogenesis (E10-E12) due to immature formation and dysfunction of the circulatory system [52]. This indicates that the local concentration of VEGF-A in tissue is tightly regulated during embryogenesis, and half the level of the VEGF-A protein is insufficient to complete

the formation of the body's closed circulatory system. Homozygous VEGF-A knockout mice die earlier than heterozygous mice, at E9, and this is due to severe defects in the formation of blood islands, endothelial cells and angiogenic sprouting [53].

The expression of VEGF-A is ubiquitous – it is produced by several cell types including macrophages, keratinocytes, pancreatic cells, hepatocytes, vascular smooth muscle cells, embryonic fibroblasts, tumour cells and cardiomyocytes [54]. To this end, cell-specific VEGF-A null models exhibit a wide array of phenotypes. For example, VEGF-A knockout in cardiomyocytes results in hearts with: fewer coronary microvessels, thinned ventricular walls, depressed basal contractile function, induction of hypoxia-responsive genes involved in energy metabolism, and an abnormal response to β-adrenergic stimulation [55].

Among subtypes of VEGF-A, VEGF-A_{165} may be the most important, both qualitatively and quantitatively. Maes *et al*. reported that VEGF-A_{165} is essential and sufficient for angiogenesis because VEGF-A_{164} transgenic mice in a *VEGF-A*–null genetic background are alive and relatively healthy [56]. $VEGF_{120}$ on the other hand, is insufficient for normal vessel growth by itself. *Carmeliet et al.* demonstrated that homozygous $VEGF_{120}$ embryos (i.e. those lacking $VEGF_{164/188}$) died shortly after birth and the remainder gained less weight and died before postnatal day 14 of heart failure. $VEGF_{120}$ hearts exhibited depressed myocardial contractility and cardiac dilation associated with severe cardiac angiogenic defects [57]. More recently, another subtype of VEGF-A, VEGF-A_{xxxb}, was reported in humans. VEGF-A_{xxxb} activates VEGF-A receptors much more weakly than normal

VEGF-A, suggesting that VEGF-A_{xxxb} could be a physiological competitor against VEGF-A [58].

VEGF-A binds to and activates both VEGFR-1 and VEGFR-2, promoting angiogenesis, vascular permeability, cell migration, and gene expression. After activation an autocrine loop of VEGF-A and its receptor system develops within vascular endothelial cells, and this can further contribute to overall endothelial cell function [59].

VEGF-B and PlGF bind to and activate only VEGFR-1. VEGFR-1 will bind tightly to its ligands but has a weak tyrosine kinase activity, and thus generates signals weaker than VEGFR-2. Perhaps correspondingly, both *PlGF* null and *VEGF-B* null mice are alive at birth and display no significant defects related to angiogenesis, suggesting that these genes are dispensable at embryogenesis [60] [61]. However, in the adult, the knockout of PlGF impairs angiogenesis and arteriogenesis during pathological conditions such as tumour growth, heart, limb and ocular ischemia [61]. In addition, VEGF-B was recently reported to improve cardiac function after myocardial infarction in rats [62], and VEGF-B knockout mice display smaller than average hearts, atrial conduction defects, vascular dysfunction after coronary occlusion and impaired recovery from experimentally induced myocardial ischemia [63]. Other studies show that VEGF-B is required for efficient revascularization after myocardial infarction, but not for revascularization of the ischemic mouse hindlimb [64] [65]. VEGF-B is also not required for angiogenesis in tissues other than the myocardium, such as the skin, lung, or retina [65]. These results indicate that, although PlGF and VEGF-B are not

essential at embryogenesis, they have a variety of functions under pathological or stressed conditions across multiple cell types.

Unlike other members of the VEGF family, VEGF-C and VEGF-D are produced as immature forms and are cleaved by proteases such as furin in both the amino- and carboxyl-terminal portions [66] [67]. After processing, these molecules develop a higher affinity for VEGFR-3, but also have a weak affinity for VEGF-2 [68]. VEGF-C is expressed during embryogenesis, whereas VEGF-D is expressed after birth. *VEGF-C* null mice show severe accumulation of fluid in tissues due to poor development of lymph vessels, whereas VEGF-D null mice display no obvious vascular defects [69] [70] [71]. In addition, VEGF-D and VEGF-C double mutant mice are indistinguishable from VEGF-C mutants, suggesting that VEGF-D does not influence vascular development [72]. However, upregulation of VEGF-D will promote pathological tumour lymphangiogenesis and metastasis in mouse models [73] [74].

VEGFRs are tyrosine kinase receptors (TKRs) containing an extracellular domain for ligand binding, a transmembrane domain, and a cytoplasmic domain, including a tyrosine kinase domain. VEGFR-1 has a much weaker kinase activity than VEGFR-2, and the signalling cascade is not fully understood. Ligand binding to VEGFR-2 induces dimerization and autophosphorylation at multiple tyrosine residues within its intracellular domain. Two major autophosphorylation sites include Y-951 and Y-1175 [75] [76].

Both VEGFR-1 and -2 are mainly expressed on endothelial cells. However, VEGFR-1 is also expressed on trophoblast cells, monocytes, and renal mesangial cells, whilst VEGFR-2 has been detected on megakaryocyte. At later developmental stages, the blood vascular expression of VEGFR-2 decreases, and in adults, is upregulated under pathological conditions such as tumour angiogenesis [77] [78].

Deletion of VEGFR-2 in mice leads to embryonic lethality between E8.5 and E9.5 due to a lack of blood island formation in the yolk sac, an absence of vasculogenesis and severe defects in the development of endothelial and haematopoietic cells [79], indicating an essential role in developmental angiogenesis and haematopoiesis.

The primary function of VEGFR-1 appears to be that of a VEGF-trap, to fine tune the amount of VEGF-A acting on VEGFR-2. Evidence for this comes from VEGFR-1 knockouts. Mice here die at E8.5 because of increased proliferation of endothelial cells that fill and obstruct the vessel lumen [80]. The underlying mechanism is believed to involve excess stimulation of VEGFR2 by the higher availability of VEGF-A.

VEGFR-3 is almost exclusively expressed by lymphatic endothelium in the adult but is upregulated in blood vascular endothelium during certain pathologies, including chronic inflammation and tumour angiogenesis [81]. In early development, VEGFR-3 is expressed in both blood and lymphatic endothelial cells [82]. Furthermore, VEGFR-3 is expressed in non-endothelial cells, including

neuronal progenitors, macrophages and osteoblasts [82] [83]. After its activation by VEGF-C or -D, VEGFR-3 will either form homodimers or a heterodimer pair with VEGFR-2. The relative contribution of VEGFR-3 homodimers versus VEGFR-3/R-2 complexes to activation of various intracellular signalling pathways and cell biology has not yet been established.

Deletion of VEGFR-3 in mice results in embryonic lethality at E9.5 due to cardiovascular failure [84]. Vasculogenesis occurs in these embryos but remodelling of the primary vascular plexus is severely defective [84].

3.2 The Cardiac Vasculature

3.2.1 Cardiac vascular expansion during development and adulthood

Because of its critical role in nutrient and oxygen delivery, the heart is one of the first organs to develop in the embryo. Heart development begins with the formation of an avascular, primitive tube which consists of a thin layer of cardiomyocytes and is lined by endothelial cells. At this early stage, oxygen is delivered to cardiomyocytes via simple diffusion across the endothelium, but as the myocardium becomes thicker (through cellular proliferation), oxygen delivery via diffusion becomes insufficient, and a dedicated primitive vascular plexus forms. Soon after, the proepicardial organ (PEO) will attach to the heart, and proepicardial mesothelial cells will begin to migrate and envelop the surface of the developing heart, giving rise to the primitive epicardium and subepicardial space [11] [85]. Genetic ablation of PEO results in the absence of epicardium and abnormality of the coronary vascular system [86]. Next, a subpopulation of epicardial cells will

delaminate from the epicardial epithelium and undergo epithelial-mesenchymal transition, generating a number of migratory mesenchymal cells, (epicardium derived cells – EPDCs), that populate the subepicardial space and subsequently the myocardium. It is thought that EPDCs give rise to cardiomyocytes and a range of coronary vascular cells [87] [86]. Endothelial precursor cells within the subepicardial space migrate over the heart and coalesce into cords to form a primitive vascular plexus. This undergoes extensive remodelling, ramification and patterning to form a developed network that resembles the mature coronary artery tree. Vessel growth is then directed towards the aorta, where the two networks will eventually intersect and amalgamate [88]. Once perfused, these capillaries remodel into larger vessels, mesenchymal cells are recruited, and vessels are further subdivided into a more organized network of specialized vessels of varying size.

At birth, the majority of cardiomyocytes discontinue the cell cycle and become quiescent [89], although some will retain a very low proliferative capacity [90]. Subsequent growth of the heart is achieved through cardiac hypertrophy of individual myocytes, meaning embryonic myocardial tissue mass possesses only a fraction of the thickness that it will hold in later life [89]. As a cardiomyocyte hypertrophies, its oxygen and nutrient demands begin to rise. This is compensated for by a significant expansion of the myocardial vasculature [13]. Murine capillary density will increase three- to fourfold in the first 3 weeks of development and the number of smooth muscle cell-covered coronary vessels increases tenfold over

the same period [91]. Additionally, increasing cardiac vessel density in the absence of other stimuli can solely drive cardiac tissue growth. Transgenic overexpression of pro-angiogenic PR39 in mice will increase myocardial hypertrophy in tandem to increasing cardiac endothelial cell mass and capillary number [92].

In contrast to active vessel growth in the embryo and newborn, the adult myocardium remains in a quiescent state. Only when provoked by cardiac stressors or pathological conditions will vascular beds expand or contract. It is generally thought that adult vascular expansion can be generated by three relatively distinct, but complementary mechanisms, termed: collateral enlargement, angiogenesis and postnatal vasculogenesis [93].

Collateral enlargement describes the in-situ development of large collateral vessels from pre-existing arteriolar anastomoses, leading to neovascularization between the two areas. One of the most important initiators of collateral enlargement is shear stress [94], and not ischemia as in angiogenesis or vasculogenesis. Because of this, collaterals are usually located near to obstructions, or occlusions of major arteries, where they act as a conduit between anastomoses to restore blood flow. Collaterals have been shown to preserve myocardial function, limit infarct size, and positively influence post-infarct remodelling in the heart [95].

Vascular remodelling in the adult heart

Despite previously held dogma, it is now known that active vasculogenesis and angiogenesis will occur in the adult heart. The primary initiator is thought to be

hypoxia, and many of the angiogenic processes responsible are thought to be the same as in development. Although vascular beds are capable of a significant expansion through these mechanisms, its capacity to do so is limited, and this can result in relative local ischemia due to an imbalance in rates of oxygen supply and cellular metabolism. If ischemia becomes too severe, over time tissue will die and are replaced by a less compliant fibrotic tissue, instead of contractile cardiomyocytes [96].

3.2.2 The molecular regulation of cardiac blood vessel development

Relatively few factors have been described as specifically important for overall cardiac vessel development. During coronary vessel development, one such essential factor is the transcription factor GATA-4 and its co-factor FOG-2. GATA-4 is present in both the endocardium and myocardium of the developing atria and ventricles, and FOG-2 is expressed similarly. Both GATA-4 and FOG-2 null mice display an intact epicardium but lack any form of coronary vasculature or epicardial-derived cells [97] [98]. This suggests that FOG-2/GATA-4 interaction is essential for the initiation of EMT within the proepicardium, and thus the development of coronary vasculature. In addition, VCAM-1 and α4 integrin is also indispensable for coronary vessel development. VCAM-1 and α4 integrin null mice display very similar phenotypes. In both, the formation of the epicardium is severely inhibited and no subepicardial vessels develop [99] [100]. Cells from the PEO often fail to leave the PEO, and if they do, are unable to adhere to the heart or migrate out to form the epicardium. Collectively this demonstrates that VCAM-1

and α4 integrins are essential for migration of PEO cells and epicardial formation and migration thereafter.

Both VEGF-A homozygote and heterozygote knockout embryos are unable to survive to term due to general impairment of blood vessel formation in the early embryo [50]. This makes it difficult to assess VEGF-A function during postnatal angiogenic processes by conventional transgene technology. However, VEGF-A120 mice, where VEGF-A164/188 isoforms are absent, will survive to term and instead die postnatally due to cardiac failure associated with severe heart ischemia [57]. These mice almost totally lack any form of postnatal capillary or coronary vessel growth, and those cardiac vessels that were present were severely defective. Postnatal ablation of total VEGF-A function by administering soluble Flt-1 receptor antagonist is also lethal. In the heart this leads to cardiomyocyte necrosis and a massive reduction in cardiac capillary density [101]. Together these experiments illustrate the importance of VEGF-A in postnatal cardiac vessel expansion, and in particular the significance of VEGF-A 164 and 188 isoforms.

VEGF-B transcripts are expressed predominantly (but not exclusively) in the heart during murine embryogenesis and throughout adult life [102], thus it is likely that VEGF-B plays an important role in cardiac angiogenesis and vessel growth. In the developing heart, VEGF-B protein is first detected at E8.5 in mice [103]. This closely correlates to the commencement of coronary endothelial growth. Thereafter, it appears that capillary density follows VEGF-B expression levels, whereby the highest capillary density rates correlate to areas of highest VEGF-B expression, both before and after birth. By the time VEGF-B rates become

relatively even throughout the heart any regional disparities in capillary growth is lost.

VEGF-B null mice overall appear relatively healthy and normal and display no overall defects in vasculogenesis during embryogenesis. The hearts of these mice appear morphologically and functionally similar after birth but are significantly smaller than VEGF-B+/+ littermates at all postnatal time points [63]. Since postnatal heart growth appears to be mainly due to increases in the coronary microvasculature and associated vessels, you would expect that VEGF-B null mice would display defects in vessel density, but this was not the case. In fact, capillary and coronary vessel density appeared normal. This study demonstrates that VEGF-B likely plays an important but redundant role in postnatal and embryonic cardiac vessel growth. As VEGF-B can form stable heterodimers with VEGF-A, and the two are generally co-expressed it is likely that VEGF-B absence is compensated for by functional VEGF-A, and thus VEGF-A is a more potent driver of cardiac vessel growth. More recent studies show that VEGF-B is required for efficient revascularization after myocardial infarction, but not for revascularization of the ischemic mouse hindlimb [65]. The cardioprotective effect of exogenous VEGF-B has also been documented elsewhere by multiple groups [92] [62], further reinforcing the notion that VEGF-B is a vital element of pathological cardiac vessel formation, particularly after MI.

Findings obtained from mouse models and human diseases with FGF signalling disorders indicate that several FGFs are involved in myocardial vessel

development during embryogenesis, adulthood and disease. Chief amongst these are FGF-1 and -2. FGF-2 null mice are healthy and display relatively little overt defects in global vasculogenesis or angiogenesis. However, after cardiac stress, such as during aortic banding, mice exhibit reduced cardiomyocyte hypertrophy and interstitial fibrosis [104]. Furthermore, deletion of FGF-2 markedly worsened the process of myocardial infarct repair, whilst its over expression curbed infarct expansion and preserved LV function also after MI [105]. In the latter experiments, overexpression of FGF-2 increased endothelial cell proliferation and myocardial revascularization, whilst vascular density was reduced significantly in FGF-2 knockout hearts. Both FGF-1 and -2 expressions closely correlates to areas of myocardial revascularization after MI. Here, angiogenesis is initiated at the border zone between infarcted and non-infarcted myocardium and then extends into the infarcted myocardium. It is most evident in the first week post-MI and then begins to slow. Zhao et al. show that FGF-1 and -2 follow this pattern – FGF protein increased up until day 7 post MI and then declined, and expression moved from the border zone to the infract zone with time [106]. In addition, transgenic myocardial overexpression of FGF-1 increases coronary artery density and branching [107], which again reinforces the notion that FGF is an important mediator of cardiac vessel formation.

Overall, the roles of FGF and VEGF during early coronary angiogenesis may be subtly different. This was assessed in an informative study by Tomanek et al. Here, inhibitory antibodies were used to determine that both VEGF and bFGF modulate capillary growth, but only FGF will specifically facilitate arteriolar growth.

Additionally, both factors need to be present in order to properly establish the normal hierarchy of the arteriolar tree [108]. As a caveat to all of this it should be noted however that the antibodies used in this study did not specifically inhibit their own target – for example both anti-VEGF and anti-FGF antibodies decreased VEGF protein, and both demonstrate differential effects on mRNA quantities – this should be minded when analysing this data.

3.2.3 Vascular changes during cardiac disease

Heart failure occurs when the heart is unable to provide sufficient blood flow to the body's organs and is a final common pathway of various cardiovascular diseases, including sustained pressure overload (i.e hypertension), myocardial infarction or ischemia, volume overload (i.e. valvular disease), and inherited/acquired cardiomyopathies. Across many of these pathologies, it has been observed that the affected tissues may present with lower capillary number versus a healthy counterpart [109]. In addition, the transgenic knockout of pro-angiogenic molecules, in particular VEGF, can worsen cardiac pathology in animal disease models, including: pressure overload [110] and isoprenaline induced cardiac hypertrophy [55]. Similarly, the downregulation of pro-angiogenic factors (such as VEGF), as in old age, can itself worsen or initiation cardiac pathology [111]. By contrast, increasing angiogenesis has been proven to provide cardioprotective effects [112, 113].

The suppression of capillary density and angiogenesis in the myocardium may be specifically involved in the transition from compensated, to decompensated heart

failure and disease. For example, in a pressure overload induced model of heart failure, HIF-1, a key transcription factor involved in the cellular response to hypoxia and therefore angiogenesis, is first up regulated within 14 days post-surgery in conjunction with a rise the number of cardiac microvessels. However, over the course of a prolonged cardiomyopathy (i.e. 28 days post-surgery), HIF-1 and VEGF were down regulated despite a persisting hypoxia and myocardial ischemia, leading to a reduction in cardiac microvessel density relative to day 14 values (i.e. a more acute cardiomyopathy). Day 28 hearts, or those hearts with fewer cardiac microvessels, proved to perform worse relative to day 14 hearts, or those with more cardiac microvessels [114]. The paradoxical down regulation of HIF-1 in such hearts despite an ongoing hypoxia may be due to accumulating levels of the tumour suppressor gene p53 in hypertrophied cardiomyocytes. An indication for this comes from observations in other cell types. One notable experiment showed that the homozygous deletion of murine p53 in tumour engrafted nude mice will lead to augmented HIF-1α activity, and therefore increased tumour neovascularization, and increased tumour volume [115]. In addition, the expression of p53 is markedly up regulated in the myocardium following pressure overload induced heart failure, and this is associated with an increase in cardiac markers of dysfunction, as well as a reduction in myocardial HIF-1α and angiogenesis [114]. Similarly, *Shiojima L et al.* show that coronary angiogenesis is enhanced during the acute phase of adaptive cardiac growth but reduced as hearts underwent pathological remodelling [116]. Enhanced angiogenesis in this study was associated with rapamycin-dependent induction of myocardial VEGF and

angiopoietin-2 expression. As such, inhibition of angiogenesis with a decoy VEGF receptor in the acute phase of adaptive cardiac growth led to decreased capillary density, contractile dysfunction, and impaired cardiac growth.

Together the experiments outlined here illustrate that both heart size and cardiac function are angiogenesis dependent, and disruption of coordinated tissue growth and angiogenesis in the heart contributes to the progression from adaptive cardiac hypertrophy to heart failure.

In tandem to changes in total microvascular density there are also a number of changes to microvascular anatomy following cardiac disease. Most recently, 3D automated image analysis has used VE-Cadherin labelling of porcine cardiac sections to reconstruct a complete template of the microvasculature which has been used to analyse MI [117]. MI elicits intensive structural remodelling 7 days post MI which begins to deteriorate by 45 days post MI. In functional terms this led to low capacity for blood flow and long diffusion distances, leading to worse oxygenation in surrounding tissue. Furthermore, individual micro vessels were larger in diameter and had an increased number of endothelial cells per unit length, likely reflecting adaptation to persistent high flow in those remaining vessels. Interestingly, microvessels at day 3 post MI exhibit the most structural similarity to basal controls, whilst day 1 and 7 post MI vessels were very different in their densities and size to both basal, and day 3 microvessels. Vessels in the infarct region were most dilated at day 1, began to constrict at day 3 and then were pruned and arterialized by day 7. There was some increase in

microvasculature density at day 1 post MI, but overall the number of microvessels, and especially capillaries, declined by day 7 in the infarct zone. Finally, vessels outside the infarct and border zone remain minimally changed.

The latter end of vascular remodelling after injury in the heart is indicated by the recruitment of pericytes. Pericytes associating with newly formed blood vessels thus represents the final stage in vessel maturity and establishes a functional blood vessel proper. Prior to this, the endothelial plexus exists as a plastic structure which can be pruned or added to according to available oxygen as previously described. Pericytes prevent this and thus stabilize the vasculature [118]. In aortic banding models, pericytes associate with the vasculature as early as day 2 post-surgery, which coincides with the start of deleterious cardiac remodelling in this study. This indicates that there is a physiological attempt to stabilize vessels during a period where the number of vessels is in decline. By day 7, which is coincident with the end of deleterious cardiac remodelling here, pericyte coverage returns to normal levels as does microvessel density [119]. Collectively this illustrates the importance of not only vessel density during cardiac recovery, but also their structure and maturity.

3.2.4 The cardiac endothelial cell and Cilengitide

Endothelial cells are the theme that ties our projects together. Between organs and vascular beds, they are a highly specialized cell type that displays marked diversity. A recent interesting study aimed to assess their transcriptome by RNA-seq. Here, *Lother et al.* reveal that cardiac endothelial cells exhibit a distinct gene

expression profile versus renal, cerebral or pulmonary ECs. From a pathway perspective, enriched elements include: cytokine-cytokine receptor interactions, ECM-receptor interaction, fatty acid transport, PPAR (peroxisome proliferator-activated receptor) signalling and haematopoietic cell lineage pathways [120]. Overall, this study provides salient evidence of heterogeneity between organ-specific ECs, but what is of particular interest to me is the fact that ECM-receptor interactions are significantly upregulated here versus other ECs.

Our hypothesis hinges upon the fact that integrins within the cardiac endothelial cell are present and can be therapeutically modified by Cilengitide. Cilengitide is a cyclic pentapeptide [cyclo(RGDf-N(Me)V)] developed initially as an anti-angiogenic therapy. Versus (non-specific) linear peptides, cyclic RGD peptidomimetics show substantial specificity and activity (where RGD relates to the amino acid sequence - arginine, glycine, aspartame). Indeed, in comparison to the linear control peptide GRGDS, c(RGDfV) showed increased inhibition of A375 cell adhesion to laminin P1 (20-fold) and to Vitronectin (100-fold), and increased specificity for αvβ3 (versus αIIbβ3) [291]. The tripeptide sequence Arg-Gly-Asp is the main pharmacophoric feature that facilitates these properties. Arg and Asp residues promote ionic interactions with the receptor (with the carboxylate of Asp coordinating divalent cations) and the Gly imposes steric restrictions [291]. The N-methylation of c(RGDfV) to ‘make’ Cilengitide - c(RGDf-N(Me)V) increases the selectivity for αvβ3 versus c(RGDfV) alone and increases its affinity for αvβ5 [291]. More generally, N-methylation is used to enhance the biological activity and

selectivity profile of peptides and to overcome their pharmacokinetic limitations i.e. increasing their metabolic stability and bioavailability [291]. Figure 6 shows the chemical structure of Cilengitide (PubChem).

Cilengitide acts as a highly potent inhibitor of angiogenesis and induces apoptosis of growing endothelial cells via the inhibition of the interaction between integrins with their ECM ligands [290] [291]. Cilengitide has been shown to influence cellular adhesion to αvβ3 ligands, to induce increased apoptosis after detachment of αvβ3 and αvβ5 expressing cells *in vitro* and to block the growth of human xenografts in nude mice [291]. Additionally, at high doses Cilengitide displays anti-angiogenic and anti-tumour activity in various animal models through a significant reduction of functional vessel density and retardation of tumour growth and metastasis *in vivo* [290] [291].

Cilengitide has entered multiple clinical trials as an anti-cancer therapy, both as a single agent and in in combination with radio-chemotherapy treatment. Its administration in humans has proven to be safe, even when co-administered with cytotoxic agents [291]. However, it has been removed from recent clinical trials (most notably the CENTRIC trial [250]) due to not meeting its clinical end point (usually of overall survival). Because of this, the authors of the CENTRIC trial recommended not pursuing further testing of Cilengitide in future anticancer clinical trials [250]. Some authors have refuted this claim, citing that the CENTRIC trial should have instead given Cilengitide twice a week, as doses of once a week would restrict its anti-angiogenic properties [424]. In line with this rebuttal, we postulate that the reason for Cilengitide's failure to meet its clinical end points is that, in

contrast to a high dose Cilengitide treatment regimen, low dose Cilengitide paradoxically exerts a VEGF-mediated pro-angiogenic effect on the tumour vasculature [4]. Indeed, Reynolds *et al* demonstrated that, mechanistically, low dose Cilengitide does not act as an αvβ3-integrin antagonist and accordingly does not affect cell adhesion or migration, but instead alters αvβ3-signalling to enhance the activation and recycling of the major pro-angiogenic receptor VEGF-receptor 2 [4]. In addition, Reynolds *et al* implicate the Rab4a recycling pathway as part of this process. They find that the suppression of Rab4A clearly opposes the effects that low doses of αvβ3/αvβ5 inhibitors have on VEGFR2 and αvβ3 integrin recycling, VEGFR2 degradation, endothelial cell migration and angiogenesis [4]. This suggests that low doses of RGD-mimetic αvβ3/αvβ5 inhibitors promote endothelial cell migration to VEGF by promoting the Rab4A-mediated recycling of both αvβ3 integrin and VEGFR2.

Most recently, Wong *et al.* have exploited the features of low dose Cilengitide to improve chemotherapy efficacy in cancer models *in vivo* by increasing tumour blood vessel number and directly enhancing chemotherapy delivery and metabolism in malignant cells [5]. In combination with the Reynolds study this suggests that low dose Cilengitide treatment could be used as a strategy to affect αvβ3-integrin signalling without affecting cell adhesion and migration.

One must be cautious in translating the results of mouse studies to humans however, as the metabolism of Cilengitide is highly specific between species [425]. Here, Cilengitide proved to be minimally metabolised *in vivo* in animals and humans, but there was a significant difference in the excretion of Cilengitide [C^{14}]

between all species, both renally and via biliary routes [425].

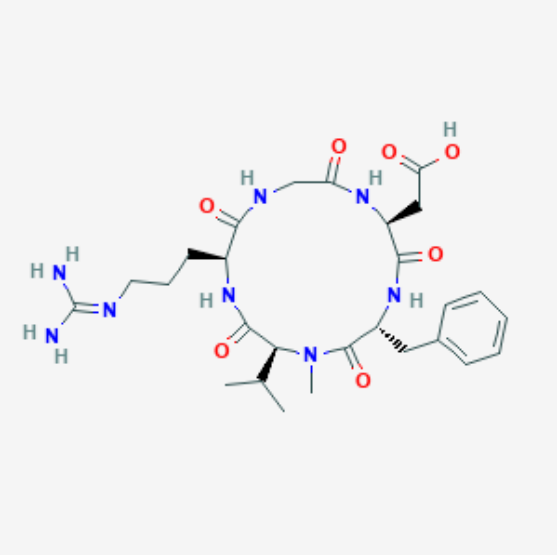

Figure 6: Chemical Structure of Cilengitide (PubChem).

3.3 Therapeutic Angiogenesis

3.3.1 Angiogenesis as a potential therapy

Therapeutic angiogenesis aims to induce, augment and regulate the host angiogenic response in order to re-vascularize ischemic tissues, and usually involves the delivery of growth factors and/or stem/progenitor cells. Growth factors may be delivered as whole proteins or more recently as genes encoding target proteins. Cells may be delivered in isolation, alongside other cells, as part of a bio-scaffold or in conjunction with pro-angiogenic growth factors. Despite intensive efforts and a wealth of positive pre-clinical data, clinical trials testing the pro-angiogenic potential of various molecules and cell-based therapies have not yet achieved the expected results. Although part of this failure may be attributable to suboptimal delivery strategies, stimulating the growth of durable and functional vessels is a more formidable challenge than was anticipated. Anti-angiogenic therapy similarly has faced problems, particularly in cancers. This may be, at least in part, due to acquired resistance to anti-angiogenic agents, or the potential for anti-angiogenics to minimize the effective delivery of co-delivered chemotherapies. Despite this, therapeutic angiogenesis remains a promising strategy. The following sections will outline current pro-vascular therapies in myocardial ischemia and discuss their relevance and mechanisms.

3.3.2 Growth factor therapy in heart disease

Various growth factors have been utilized for therapeutic angiogenesis including FGF, VEGF, PDGF, PlGF, hepatocyte growth factor (HGF), angiopoietin-1 and insulin-like growth factor (IGF-1). Among these, VEGF and FGF are arguably the most well-studied and have reached human clinical trials [121] [122]. As the probable master regulator of physiological angiogenesis, one would expect that VEGF would be the most potent and viable choice of pro-angiogenic growth factor. However, when delivered alone VEGF will actually lead to the formation of leaky, unstable and relatively sub-functional microvessels [123]. Co-delivery with angiopoietin-1 [124] or PDGF-B [125] can improve this by helping to stabilize newly formed nascent vessels with mesenchymal cells. Similarly, the microvasculature of VEGF-PlGF chimeric mice was significantly denser, less leaky, contained fewer local inflammatory factors and were more stable than VEGF-transgene controls [126]. Combining growth factors as a single adjunctive therapy will in future allow clinicians to 'match' synergistic growth factors to induce maximal clinical efficacy. A summary of growth-factor induced cardiac regeneration mechanisms is given below (**table 13**).

Factor	Mechanism	Reference
VEGF	Angiogenesis	[127] [121] [128]
FGF	Angiogenesis	[129] [130] [122]
HGF	Anti-apoptosis Cardiac stem cell chemotaxis and activation	[131] [132]
SDF-1	Hematopoietic stem cell mobilization and homing	[133]
IGF-1	Cardiac stem cell viability and differentiation	[134]
PDGF	Anti-apoptosis	[135]
G-CSF	Hematopoietic stem cell mobilization and homing Anti-apoptosis	[136]
Angiopoietin	Angiogenesis and vascular stabilization	[137]
Neuregulin	Cardiomyocyte proliferation	[138]
Erythropoietin	Anti-apoptosis	[139]

Table 13: A summary of growth-factor induced cardiac regeneration mechanisms.

To date, there have been a number of pre-clinical and clinical studies evaluating the safety and efficacy of growth factors for inducing angiogenesis in ischemic heart disease and peripheral arterial disease (PAD) [140] [141] [142]. Early phase I and II human clinical trials with VEGF and FGF were promising, but larger randomized placebo-controlled trials failed to demonstrate significant benefits in the approved clinical end-points. Preclinical data demonstrate that the delivery of FGF or VEGF eventually results in unstable vessel growth that resembles immature tumour vasculature. The limited clinical response to growth factor therapy is likely due to a number of factors. Growth factor therapy is generally limited by poor biostability, rapid diffusion high cost and short half-lives *in vivo*. Furthermore, such approaches often require supraphysiological doses or multiple injections to sustain long-term function. This could lead to excessive uncontrolled vascular formation in non-affected tissues, which may precipitate various pathologies and exacerbate existing disease conditions.

The growth factors delivered during gene transfer therapy are often the same as in protein therapy (VEGF, FGF etc) [143] [144]. Gene therapy currently utilizes three distinct mechanisms of delivery – naked DNA, virus or liposome. Of these, delivery of naked DNA is clearly the most simplistic (and cheapest) of the three, but is hindered by low rates of transfection, limited protein generation in tissue of interest, and lack of a predictable dose response. Liposome and viral delivery on the other hand should theoretically induce greater levels of transfection than naked DNA delivery alone. Not only is the gene of interest encapsulated and protected,

but genes can be tagged and imaged *in vivo*, and also directed to their target of interest using tissue specific vectors. However, viral vectors may induce an immunogenic response in the host and may also produce only a short-term response. New generations of viral vectors aim to be less immunogenic and demonstrate longer tissue-specific expression [145].

Gene transfer therapy in clinical trials have shown mixed results. Phase I clinical trials have demonstrated that VEGF gene therapy is safe in humans in both myocardial and peripheral ischemia [146], but its efficacy is controversial. Naked delivery of $VEGF_{165}$ in patients with critical limb ischemia will improve wound healing, perfusion and increase limb salvage rates [147]. Similarly, adenoviral- and plasmid-$VEGF_{165}$ delivery by intravascular catheter demonstrates significant improvement in patients experiencing peripheral vascular disease [147]. Also, transthoracic intramyocardial injection of adenoviral VEGF-2 delivery resulted in some clinical improvement in angina patients [148]. Interestingly the latter study was not associated with any evidence of myocardial angiogenesis which suggests that VEGF may have alternative beneficial effects outside of simple neovascularization. However, the NORTHERN trial, which assessed the intramyocardial delivery of adeno$VEGF_{165}$, demonstrates that this provided no overall benefits in any of the end points measured [149]. In addition, the 'Euroinject One' phase II clinical trial, which also measured the efficacy the intramyocardial delivery of plasmid-$VEGF_{165}$ similarly did not achieve any of its clinical end points [150].

Human clinical trials investigating the therapeutic role of FGF gene therapy remain as mixed as VEGF data. In phase II clinical trials, the intramuscular injection of adenoFGF-1 to patients with critical limb ischemia reduces amputation rates by 39% versus placebo alone [151]. In prospective, blinded studies, intramyocardial delivery of sustained-release adenoFGF-2 in non-revascularizable myocardium (i.e. myocardium that cannot be revascularized) at the time of coronary artery bypass grafting (CABG) demonstrates a significant improvement in angina and reduction in residual ischemic myocardium [152]. Furthermore, phase II, randomized clinical trials assessing the efficacy of intra-coronary infusion of plasmid-FGF-2 (FIRST [122]) and adenoFGF-4 (AGENT [153]) demonstrate symptomatic angina relief in patients but failed to show a statistically significant increase in either exercise tolerance or myocardial perfusion.

Most recently, porcine models with significant endothelial dysfunction show dramatically decreased cardiac angiogenesis in response to FGF, suggesting that coronary endothelial dysfunction is limiting clinically effective angiogenesis [152]. *Voisine et al.* have demonstrated that L-arginine supplementation can partially restore the myocardial angiogenic response to FGF [154]. These findings suggest that the endothelial dysfunction present in clinical settings may limit efficacious therapy with FGF and other pro-angiogenics, and also highlights the importance of utilizing animal models with common cardiac co-morbidities. This may explain the marginal, and mixed, results that have been witnessed thus far in phase II myocardial clinical trials. Further study of synergistic cytokine delivery

utilizing vasodilatory adjuncts, such as L-arginine, may potentiate both myocardial angiogenesis and function in future clinical trials.

3.3.3 Cell therapy

Much research has been undertaken to more fully understand the reparative and regenerative potential of stem/progenitor cells in ischemic heart disease. The advantage of this approach is that not only will exogenous cells replace and/or supplement native cells, but they can also secrete paracrine factors to support those cells, leading to improvement in their function. Transplanted cells also secrete exosomes containing proteins, RNA and microRNAs which stimulate both receptor-mediated and genetic mechanisms that contribute significantly toward paracrine support of native cells [155]. The paracrine effect of stem/progenitor cells inhibits cell death, enhances cell proliferation, activates resident stem/progenitor cells in the ischemic tissue, and recruits additional stem/progenitor cells to the ischemic site [156]. The cells furthest along in clinical development so far are adult stem cells – namely endothelial progenitor cells (EPCs). EPCs constitute a mixed population of progenitor cells of different lineages. Within this population are true endothelial cells that can incorporate into the vascular network, and haematopoietic progenitors, which may instead contribute to vascular remodelling by secreting pro-angiogenic cytokines. It is thought that EPCs can be divided into two categories: H-EPCs and non-H-EPCs. Non-H-EPCs are the minority of EPCs. They are derived from non-canonical cell sources, including adipose tissue, blood vessel walls, spleen, kidney and the liver. They are defined as being CD34/CD31^{-} but despite this can differentiate into endothelial cells and

promote angiogenesis. H-EPCs on the other hand fall into the canonical, and most well characterized EPC population [157]. They express classic CD34/CD133^{+} markers and are probably maintained in the bone marrow. Studies show H-EPCs are likely derived from haemangioblasts, and they will circulate in the blood at very low levels. Their prevalence in the blood can change according to a variety of stimuli including ischemia and shear stress, which alone are sufficient to mobilize EPCs to leave the vascular niche. Key endogenous mobilization factors include HIF, NO, VEGF (ischemia) and NF-kB (shear stress). It is important to note that the exogenous mobilization of EPCs is usually achieved using techniques such as granulocyte colony stimulating factor (G-CSF) or granulocyte-macrophage colony stimulating factor (GM-CSF), meaning that EPCs throughout may be described by both their method of mobilization (e.g. G-CSF) and where they were mobilized from (e.g. bone marrow). Regardless, after mobilization EPCs will enter the vasculature and hone to the site of ischemia, where they will either: a) incorporate into the pre-existing vascular plexus and form endothelial cells, pericytes, or smooth muscle cells or b) potentiate local angiogenesis by releasing paracrine factors into their surroundings [158].

One attractive feature of EPCs is that numerous studies show that they can be harvested, expanded and then re-administered to the same person they were isolated from [159]. Autologous transfer should in theory induce significantly less immunogenicity than in allogeneic implants. Since EPCs are isolated from adult tissues and are not derived from foetal tissues, they also face no major ethical concerns. Furthermore, as adult stem cells, their differentiation potential is limited

down a particular developmental lineage, meaning there is much lower risk for aberrant tissue formation and tumorigenesis. On the other hand, cell-based therapies still face several limitations. Upon isolation, the cell population can be very heterogeneous, which is worsened by the fact that there is not yet a strict protocol for the cell isolation of EPCs. This can lead to adverse effects, including: microvascular embolism, pathological neovascularization and malignancy. In addition, to obtain the large cell numbers needed for transplantation, *ex vivo* cell expansion is often required, which leads to regulatory concerns and increased cost and time, thereby increasing the barriers for clinical translation. This not only means that there is a delay in treatment due to the time needed to collect and expand cells, but 'old' EPCs demonstrate reduced proliferation (both *ex vivo* and *in vitro*), and also reduced capacity to integrate into existing capillary networks [160]. The patients that often require EPC therapy the most are usually older individuals, meaning that it is often difficult to expand their cells to the required amount. They often also present with multiple co-morbidities including diabetes (and old age itself), which itself impairs angiogenic functionality and induces EPC dysfunction. Interestingly, chronic insulin therapy may increase circulating levels of EPCs in diabetic patients [161], which suggests we may be able to enhance EPC therapy in these patients with synergistic co-factors. Furthermore, the cell engraftment efficiency is typically very low upon transplantation and may vary greatly between patients. Not only might this induce a supraphysiological (or inflammatory) response, but it also makes it very difficult for clinicians to predict a physiological response for a given 'dose' of cells.

Pre-clinical studies in animal models illustrate a wealth of data demonstrating the effectiveness of EPC transplantation after ischemic injury. In one seminal study *Kocher et al.* show that the intravenous injection of labelled human $CD34^+$ bone marrow-derived cells into rats after MI surgery (LAD-ligation) significantly enhanced neoangiogenesis in the infarct zone and estimates that around 25-30% of new vessels were composed of labelled cells. Therapy led to a 3-fold improvement in left ventricular ejection fraction versus controls [162]. Similarly, *Orlic et al.* observed that pre-treatment of mice with bone marrow progenitor cells will enhance survival from 20%-90% four weeks post-MI, with evidence that all components of the injured myocardium were restored, including blood vessels and even cardiomyocytes [163]. In parallel, multiple studies also observe that EPCs are able to repair large vessels after injury or atherosclerosis. Here, EPCs will engraft onto balloon damaged carotid arteries and rapidly re-endothelialise denuded areas, leading to salient improvements in vessel morphology and function [164]. Furthermore, lacZ labelled EPCs colonize vein grafts in the carotid arteries of 'healthy' mice. Interestingly the levels of engraftment were lower in atherosclerotic ($ApoE^{-/-}$), hyperlipidaemic mice, which coincides with lower circulating levels of EPCs in those same mice [165]. Chronic treatment of elderly atherosclerotic mice ($ApoE^{-/-}$) with young, (but not 'old') non-atherosclerotic bone marrow derived progenitor cells halts the progression of atherosclerosis despite persistent hypercholesteremia [166]. Following on from these early findings it was shown that by engineering the longevity of transplanted cells we can drastically

enhance their reparative capacity. *Mangi et al.* show that engineering rat mesenchymal stem cells to overexpress pro-survival Akt will regenerate ischemic myocardium up to four times more effectively than in controls [167]. Other groups report similar findings [168] [169]. This raises the question as to whether or not EPCs themselves can be modified to survive for longer, and if they can, will doing so enhance their revascularization ability over time?

These and other studies show that EPCs can be used to enhance therapeutic angiogenesis and repair vascular injury in a wide variety of experimental animal models. The exact mechanisms of this is still not entirely understood, but cell-therapy was quickly transferred into clinical trials after those early experiments described. In humans, vascular regeneration has so far been attempted using autologous bone marrow mononuclear cells (BMNCs), G-CSF-expanded peripheral blood mononuclear cells (PBMNCs), human umbilical derived adult stem cells and fractionated EPCs. Other cell-types have been utilized (including non-expanded PBMNCs, MSCs and adipose derived stem cells (ADSCs), but the primary purpose of these cell types is usually not to induce revascularization, so will be omitted from discussion. Table 2 includes a summary list of some of the clinical trials to date utilizing cell-therapy for revascularization in myocardial ischemia and PAD (adapted from [170] and [171]). Overall, meta-analysis of current clinical trial data indicates that cell-based therapy remains an encouraging treatment option but consensus dictates more extensive study is necessary before real world application [172] [173] [174] [175]. There remains a number of trials that failed to meet their hard-clinical end points and so optimisation of therapy is

certainly required. One interesting treatment modality that could improve cell-therapy efficacy is to combine cells with synergistic cell types, genes or growth factors. *Tang et al.* do exactly this by transfecting MSCs to overexpress VEGF and SDF-1α. Rats receiving those cells demonstrate significantly smaller infarct size, improved left ventricular function and increased capillary density after myocardial infarction versus either growth factor therapy, or cell-therapy alone [176].

Cell-type	Disease	Route of administration	Follow up duration	Outcomes	Trial author (including ref)
BM-MNC	PAD	IM	1m	Inc. ABI and $TcPO_2$	Arai et al. [177]
BM-MNC	PAD	IA	120d	Inc. Limb salvage	Prochazka et al. [178]
BM-MNC	PAD	IA	6m	Inc. Ulcer healing, Red. Resting pain, No change ABI or limb salvage	Walter et al. [179]
BM-MNC	PAD	IM	6m	Red. Amputation rate	Benoit et al. [180]
BM-MNC	PAD	IM	6m	Red. Resting pain, Inc. Ucler healing and API	Li et al. [181]
BM-MNC	MI	IA	3m	Red. Infarct region, Inc. SV, LVESV, contractility and perfusion of infarct region	Strauer et al. [182]

BM-MNC	MI	IA	6m	Inc. LVEF and myocardial perfusion, Red. LVDd	Ge et al. [183]
BM-MNC	MI	IA	6m	Inc. LVEF, Red. Infarct area, No change LVEDV	Huang et al. [184]
BM-MNC	MI	IA	4m	Inc. LVEF, Red. Infarct area, No change myocardial perfusion	Janssens et al. [185]
BM-MNC	MI	IA	6m	Inc. LVEF, No change Infarct area or LVEDV	Lunde et al. [186]
G-CSF PBSC	MI	IA	6m	Inc. LVEF, LVEDV	Kang et al. [187]
G-CSF PBSC	MI	IA	6m	Inc. LVEF, LVEDV	Li et al. [188]
G-CSF PBSC	PAD	IM	3m	Inc. ABI, blood perfusion, ulcer healing and angio score	Huang et al. [189]
G-CSF PBSC	PAD	IM	12w	Inc. ABI, $TcPO_2$, walking distance and ulcer healing. Red. Fontaine's stage and resting pain	Ozturk et al. [190]

G-CSF PBSC	PAD	IM	12m	Inc. Maximal walking distance and rest pain	Tateno et al. [191]
G-CSF $CD34^+$	PAD	IM	12m	Red. Amputation rate	Losordo et al. [192]
G-CSF $CD34^+$	PAD	IM	52w	Inc. Efficacy score	Kawamoto et al. [193]
G-CSF $CD34^+$	PAD	IM	52w	Met all clinical end points	Fujita et al. [194]
G-CSF $CD34^+$	PAD	IM	6m	No change in any clinical measures	Perin et al. [195]

Table 14: Brief summary of cell-based revascularization therapy in early clinical trials for PAD and MI. Key: Inc. Is increased, Red. Is reduced, ABI is ankle-brachial reflex, TcPO2 is transcutaneous oxygen, SV is stroke volume, LVEF is left ventricular ejection fraction, LVEDV left ventricular end diastolic volume, LVESV left ventricular end systolic volume, Left ventricular diastolic diameter.

Aside from delivering exogenous EPCs, mobilizing endogenous EPCs using techniques such as granulocyte colony stimulating factor (G-CSF) and granulocyte-macrophage colony stimulating factor (GM-CSF) can also increase endogenous circulating EPC concentration, and consequently contribute toward myocardial revascularization. As such, G-CSF and GM-CSF will improve myocardial regeneration and accelerate cardiac healing in a number of rodent myocardial infarction models [163] [196]. In addition, GM-CSF displays strong pro-angiogenic efficacy in other models of ischemia. *Buschmann et al.* demonstrate that the continuous infusion of GM-CSF for 7 days into the proximal stump of the acutely occluded femoral artery of rabbits produced a 2-fold increase in the number and size of collateral arteries and increased the maximal blood flow during

vasodilation 5-fold [197]. When GM-CSF and MCP-1 were simultaneously infused the effects on arteriogenesis were additive, and even more significant – 80% of normal maximal conductance of the occluded artery was restored versus 40% in GM-CSF alone [197]. Clinically, G-CSF and GM-CSF have been utilized in relatively few trials. In PAD, G-CSF and conventional therapy combined improved a patient's subjective symptoms, ankle brachial pressure index (ABI), and transcutaneous partial oxygen pressure ($TcPO_2$) to the same degree as with bone marrow mononuclear cell transplantation and conventional therapy combined. Such improvements were not seen in conventional therapy alone [177]. GM-CSF in the 'stimulation of arteriogenesis' (START) study however, did not improve walking distance (i.e. primary endpoint) in the setting of intermittent claudication in both small, and large-scale randomized trials [198] [199].

Overall, there is no clear evidence that cell-based approaches are more preferable than angiogenic gene/protein therapies in clinical settings. However, theoretically, stem/progenitor cell therapies may be superior over protein or gene therapy due to not only direct vasculogenic properties but also paracrine action by secreting multiple growth factors besides a single angiogenic factor. It is likely that the two in tandem would yield the most effective therapy option.

3.4 Adhesion Molecules

3.4.1 Integrins

Integrins are a family of transmembrane heterodimeric cell surface glycoprotein

receptors which mediate cell-extracellular matrix (ECM) interactions. They are expressed ubiquitously in all cellular components (including those of the cardiovascular system) and are essential in normal development, as well as in disease [200]. Integrins are composed of non-covalently associated heterodimeric α and β subunits, and consist of a large extracellular domain, a single transmembrane domain, and a short cytoplasmic tail. It is through extracellular domains that integrins are able to bind ECM ligands, whilst cytoplasmic tails determine appropriate intracellular signalling potentiation. The ligand binding site of integrins is found within the head domains of the α and β subunits and will normally recognize short peptide motifs in their target ligands. α- subunit heads are characterized by a metal ion-dependent adhesion site (MIDAS), which binds cations such as magnesium and calcium, and is critical for integrin activation. The α chain is also central in determining ligand specificity, and the arginine-glycine-aspartic acid (RGD) sequence is the most common integrin-binding sequence here [201]. The cytoplasmic tails of integrins are generally short (20-60kDa) and serve as transmembrane adaptor links between extracellular contacts and the intracellular cytoskeleton, through proteins such as paxillin and tallin.

In mammals, 18α and 8β integrin subunits exist. Each associate in various combinations to form 24 integrins. The composition of specific heterodimers confers ligand specificity, and each cell type expresses a different repertoire of integrins. Most integrins recognize several ECM proteins, and in turn, most matrix proteins bind more than one integrin. There are four main groups of integrins, as outlined in figure 7. Of the greatest importance to my own work is the RGD-integrin

family, which recognizes and binds to an arginine-glycine-aspartate (RGD) recognition sequence on ECM ligands.

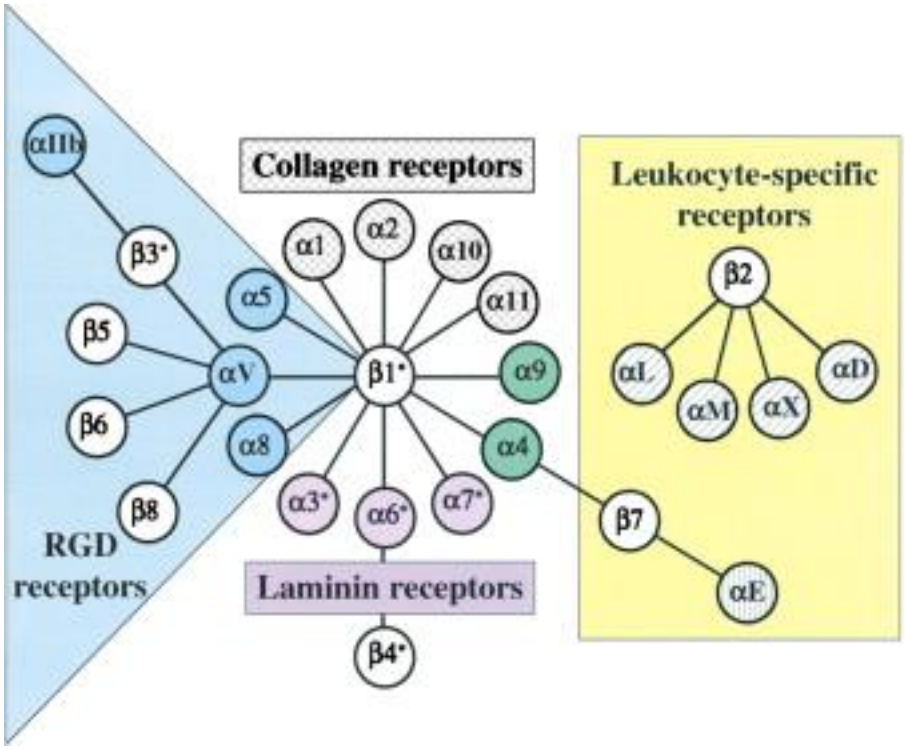

Figure 7: A combination of 18α and 8β integrin subunits form 24 functional integrins. These are divided into arginine-glycine-aspartic acid (RGD) recognition receptors, collagen receptors, leukocyte-specific receptors and laminin receptors. The α4 and α9 subunits in green are restricted to chordates. Taken from [202].

3.4.2 Integrins and growth factor signalling

Integrins potentiate a variety of essential signal transduction pathways involved in the regulation of many diverse processes, including: cell proliferation, adhesion, migration, survival and differentiation [203]. As part of this, integrins are

bidirectional signalling molecules that are able to transduce signals either ‘inside out’ or ‘outside in’ [204]. Both extracellular and intracellular portions of the integrin heterodimer are capable of binding to ligands. It is this ability that allows them to signal in both directions across the membrane. In ‘outside in signalling’, ligand binding to the extracellular integrin domain results in integrin clustering at the plasma membrane, and this leads to signal transduction to the interior of the cell. By contrast, ‘inside out signalling’ results from activation signals from within the cell and induces changes to integrin conformation. This includes straightening of extracellular domains from an inactive bent conformation, which exposes its external ligand binding site and therefore increases the affinity for extracellular ligands. In many cases an integrin will preferentially bind its primary ligand, however some integrins can also recognize other extracellular matrix components and bind multiple with differing affinities.

Integrin activation results in clustering and recruitment of a wide variety of proteins at specialised sites named focal contacts or focal adhesions. Focal contacts establish a link between the ECM and the actin cytoskeleton. They are composed of integrins associating with a number of molecules, including: adaptor proteins (e.g. talin and viniculin), kinases (e.g. FAK), protein kinase C (PKC), phosphatidylinositol 3-kinase (PI3K), integrin linked kinase (ILK), Src-family kinases (e.g. Src and Fyn) and finally small GTPases (e.g. Rho and Rac). All these molecules work together to generate a whole signalling cascade. For example, integrin activation leads to the recruitment of FAK and Src-family kinases to focal contacts, which subsequently activates PI3K. Downstream signalling pathways of

PI3K in turn activates Akt and small GTPases, including Rac and Rho, which will regulate cytoskeletal changes, resulting in e.g. changes to cell migration, invasion and cell contractility.

3.4.3 Endothelial integrins

Endothelial cells are greatly influenced by the expression and activation of cell-surface adhesion molecules like integrins. Integrin binding, and consequent changes in cytoskeletal organisation and thus cell shape, determine vital endothelial processes including migration, proliferation, differentiation, angiogenesis and apoptosis. As such, endothelial cells express several integrins that mediate interactions with a wide spectrum of ECM components and cell types, including collagen receptors ($\alpha1\beta1$ and $\alpha2\beta1$), laminin receptors ($\alpha3\beta1$, $\alpha6\beta1$ and $\alpha6\beta4$), fibronectin receptor ($\alpha4\beta1$and $\alpha5\beta1$) and vitronectin receptors ($\alpha v\beta3$ and $\alpha v\beta5$). Different combinations of integrin subunits on the endothelial cell surface allow them to recognize and respond to a number of different extracellular matrix proteins under different physiological conditions. Accordingly, the expression level of integrins can also change depending upon the activity status, age and location of the endothelium [205]. In this way, endothelial cells are able to adapt to local changes in their microenvironment and respond accordingly.

The next subsections in this chapter will discuss αv- and β- integrin subunits and whole $\alpha v\beta3$- $\alpha v\beta5$- integrins themselves in the context of the endothelium and their respective contribution toward angiogenesis.

3.4.4 αv-integrin subunit

αv-integrin subunits are widely expressed on multiple cell types, including the endothelium. They have a wide range of potential ligands and will readily associate with β-integrin subunits, which themselves show distinct patterns of expression and activity, particularly during development or in the 'active' endothelium [206] [207]. This together implies diverse functions for αv-containing integrins, potentially including neovascularization. αv-null mice develop normally up until E9.5, with normal organogenesis, vasculogenesis and angiogenesis. Thereafter 80% die mid-gestation, probably due to placental defects, 20% survive up until birth and all of those live-born die within the first day. Live-born mice exhibit intracerebral haemorrhage due to defective interactions between blood vessels and brain parenchymal cells [208]. This implies that αv-integrin subunits are not absolutely necessary for normal neovascularization during development but may be important for mature cerebral blood vessel formation. Interestingly however, selective genetic ablation of αv-integrin subunit expression in the vascular endothelium has no detectable effect on cerebral blood vessel development, and at birth, mutant mice display no phenotypic defects. Instead, glial-specific αv-knockout leads to embryonic and neonatal cerebral haemorrhage [209]. This demonstrates that endothelial αv-integrin expression in the vascular endothelium was not responsible for cerebral haemorrhage in whole αv-null mice, perhaps indicating its overall redundancy toward developmental blood vessel formation. More recently, αv subunits have been selectively ablated in the endothelium in tandem to α5 integrin subunits. *Van der Flier et al.* show that α5 conditional

knockout mice were viable and lacked any immediately obvious phenotype [210]. Further characterization showed that this was due to compensation by αv-containing integrin subunits, which highlights their overlapping and converging function. Thus, αv-α5 selective combined knockout mice develop normal vasculature initially, but most die mid-gestation (E11.5 onward) due to vascular remodelling defects in the great vessels and the heart [210]. Once again, this study provides salient evidence that αv (or in fact α5) is not absolutely essential for normal blood vessel formation during development but highlights a very important contribution of the two toward 'late' neovascularization, particularly in the heart.

3.4.5 β-integrin subunit

Unlike the αv knockout mouse, β3- and β5- null mice (and double null mice) are all viable and fertile and produce a vascular network without any obvious defects during developmental angiogenesis [211] [212] [36]. In later development however, those mice display enhanced tumour growth and pathological angiogenesis [36]. This shows that β3 and β5 integrin subunits are differentially involved in adult and developmental angiogenesis. Their involvement was further delineated by studying mutant β3 integrin receptors. Here, mutant mice (DiYF) (i.e. where β3 integrin subunits cannot be phosphorylated) are viable and fertile with normal developmental angiogenesis, but in contrast to null mice, display reduced pathological angiogenesis and reduced tumour growth [213]. In theory a dominant negative mutant integrin could be physically occupied by a ligand, but not functionally active, whereas a null integrin can be neither active nor occupied.

Thus, this difference demonstrates that β3 can differentially regulate angiogenesis according to these principles. This will be discussed in further detail later. Elsewhere, studies have also shown that β3-null mice display enhanced inflammatory and wound healing responses [214] [215], the latter of which is due to increased fibroblast infiltration and increased TGF-β1expression [215]. Collectively this indicates that β3-containing integrins are an active component of the host vasculature.

β3 may be specifically important during cardiac vascular development. *Weis at al.* show that in the developing heart the mRNA expression of β3 integrin subunits decreases significantly as vessel maturation progresses, which was concurrent with the cessation of physiological angiogenesis [216]. Additionally, male, but not female, β3-null mice display immature coronary capillaries characterized by irregular endothelial thickness, endothelial protrusions into the lumen, and expanded cytoplasmic vacuoles [216]. The phenotype could be resolved by inhibiting VEGF and was recapitulated by the intravenous injection of VEGF into the hearts of adult wild-type mice [216]. This probably indicates that β3 containing integrins represents some sort of endogenous VEGF biosensor *in vivo* which will act as a 'brake' to dampen excessive VEGF activity and allow vessels to mature properly. In this model VEGF initiates angiogenesis but is 'turned off' by β3. Indeed, there is evidence *in vitro* that αvβ3 and VEGFR-2 will bind to one another and directly interact [217], and previous studies also reinforce a similar notion *in vivo* [37].

In the adult, β3 is not expressed on endothelial cells of the heart or elsewhere, although it may be expressed in microvessels of the lung [218]. As will be discussed, it is however expressed in heterodimer complexes with αv- integrin subunits in tumours and during inflammation. Taken together this points to the fact that β3 is downregulated in quiescent endothelium but upregulated during active proliferation. To support this, endothelial cells that are grown in culture will often actively express β3 (own observations) and β3 mRNA has also been detected in cardiac vascular structures in animal models of myocardial infarction [219]. Interestingly, VEGF-A expression is actually relatively short lived in the adult myocardium after infarction [220], which might be a product of upregulated and transdominant β3-containing integrin expression. In this fashion, VEGF-A would initiate early myocardial angiogenesis post MI but is then downregulated by β3 to ensure vessels mature appropriately, as was postulated in the previously described *Weis et al.* study [216].

The related integrin subunit, β5, is also present in cardiac endothelial cells. *Le Gat et al.* show that early in development, β5 gene expression was observed within embryonic sites of haematopoiesis and was documented in angiogenic endothelial cells of the lung, heart and kidneys at postnatal time points [221]. This study did not appear to differentiate between angiogenic or quiescent endothelial cells so it is unclear whether there is a difference in β5 expression between these states.

3.4.6 Targeting αvβ5 and αvβ3-integrins for angiogenesis control

Of the 24 vertebrate integrin heterodimers, the expression of 9 have been implicated in blood vessel formation: α1β1, α2β1, α4β1, α5β1, α6β4, αvβ1, αvβ3, αvβ5 and αvβ8. Of these, αvβ3 was the first endothelial cell αv- integrin to be shown to regulate angiogenesis. αvβ3 is most abundantly expressed on angiogenic endothelial cells in remodelling and pathology and is not expressed on quiescent endothelium [222] [223]. Antagonists of αvβ3 will block pathological angiogenesis in several pre-clinical animal models with little impact on pre-existing blood vessels, making it an attractive target for therapeutic intervention. Indeed, some of these inhibitors have reached human clinical trials as angiogenic inhibitors including Vitaxin and Cilengitide, although both of these failed to meet their hard-clinical end points {Stupp, 2014 #199} {Gutheil, 2000 #533}. The reason for this failure is still open to debate, but one conceivable theory explains that genetic ablation experiments do not fully summarize the function of αvβ3 integrin because of overlapping of functions or compensation by other integrin, or non-integrin, partners. Integrins are well known to regulate the activation state of other integrin and non-integrin membrane receptors within the same cell – a phenomenon referred to as integrin crosstalk (or transdominance) – which is believed to play a role in determining how they regulate overall cell behaviour [224]. Thus, it is conceivable that the loss of αvβ3 integrin could result in the relief of inhibitory transdominance of other integrins (or non-integrins) and enhance their respective pro- or anti-angiogenic functions accordingly. Numerous examples detail events like this in the literature. With regards to non-integrins for example, the most well-

established compensatory partnership is crosstalk between αvβ3 and VEGFR-2. Previous work has shown that if the expression of αvβ3 integrin is lost, both tumour and VEGF-induced angiogenesis is increased. This was not due to enhanced expression or activity of other cell-integrins but is instead a consequence of elevated VEGFR-2 endothelial cell expression [36]. Furthermore, β3 deficiency alone in β3-null mice increases the sensitivity of endothelial cells to VEGF-A by elevating VEGFR-2 expression, and consequently enhances VEGF-A-mediated endothelial permeability [225]. Both mutational and phosphorylation studies demonstrate that altering the cytoplasmic tail of β3 integrin subunits can prevent VEGFR-2-αvβ3 cross-activation, and therefore prevent successful angiogenesis through transdominant interaction [33] [226] [213].

Elsewhere, other studies reveal that integrins certainly overlap in function but may not strictly compensate for one another, however the potential for compensation remains. For example, the expression of α5β1 integrin in cells inhibits αvβ3 mediated adhesion and migration but constitutively active β3 is resistant to this inhibitory effect [227]. Similarly, simultaneous inhibition of both αvβ3 and α5β1 may be required for potent anti-angiogenic effects whereas the inhibition of either alone may not be sufficient in specific cases [228]. Finally, *Gonzalez et al.* have shown that *in vitro* there exists a crosstalk in endothelial cells between β1 and β3 integrin subunits, such that when αvβ3 integrin is blocked there is a concomitant inhibition in ligand binding of α3β1 and α6β1 integrin. Similarly, a combination of blocking antibodies in those same cells against α3 and α6 integrin prevent ligand binding of αvβ3 integrin [229]. Collectively this illustrates the importance of the

compensatory/overlapping involvement of other integrins (and non-integrins), and also indicates the potential importance of targeting multiple integrins at once to inhibit angiogenesis, as oppose to functionally blocking a single target as with e.g. Vitaxin.

Aside from extracellular matrix molecules like vitronectin and fibronectin, αvβ3 can bind to any ECM molecule with an RGD motif to differentially regulate angiogenesis, as well as a multitude of growth factors. This means that αvβ3 can be both pro- or anti-angiogenic according to its current binding partner. Indeed, αvβ3 can bind a plethora of factors – a few of which are detailed in **table 15**. It is still unclear how αvβ3 integrin makes the decision to bind either stimulatory or inhibitory angiogenic factors, but an understanding of this may help us determine why Cilengitide and Vitaxin did not achieve their expected clinical outcome.

Binding partner	Pro- or anti- angiogenic?	Reference
Del-1	Pro-angiogenic	[230]
Bone sialoprotein	Pro-angiogenic	[231]
Proteolytically cleaved collagen type IV	Pro-angiogenic	[232]
Thrombin	Pro-angiogenic	[233]
ANGPTL3	Pro-angiogenic	[234]
CYR61	Pro-angiogenic	[235]
Growth factor receptors	Pro-angiogenic	[236]
Thrombospondin	Anti-angiogenic	[237] [238]
MMP2	Anti-angiogenic	[239] [240]
Angiostatin	Anti-angiogenic	[241]
Endostatin	Anti-angiogenic	[242]
Tumstatin	Anti-angiogenic	[243]

Table 15: Summary of pro- and anti-angiogenic binding partners of αvβ3 integrin.

Another explanation for the differences in the genetic ablation, mutation, inhibitor and clinical-trial data is due to the fact that integrins can regulate endothelial apoptosis according to their own ligation state, in a process termed integrin-mediated death (IMD). *Stupack et al.* show that unligated αvβ3 negatively regulates cell survival and promotes apoptosis by recruiting caspase-8 to the plasma membrane, whereas ligated integrins do not [244]. Accordingly, decreasing αvβ3 integrin levels increases survival of endothelial cells, whilst αvβ3-bearing cells undergo apoptosis [244]. This phenomenon is not specific to αvβ3, but also occurs with α5β1 [245], which is another important integrin regulator of angiogenesis [246]. Interestingly, this mechanism can be 'hijacked' to block tumorigenesis and metastasis. *Hood et al.* demonstrate this by using nanoparticles

coupled to αvβ3-targetting ligands to induce apoptosis of tumour-associated endothelium, which lead to tumour cell apoptosis and regression in Raf mutant mice [247]. In this fashion αvβ3 (or α5β1 for that matter) may function as a biosensor, promoting angiogenesis when ligated but preventing it by initiating endothelial cell apoptosis when ligands are absent or when the ligand binding site is antagonized. This mechanism may have developed to ensure the precise special regulation of vascular growth, in which endothelial cells will die if they spread to inappropriate environments but be left to migrate if properly coupled. It is plausible that genetic ablation of β3 integrin could enhance endothelial cell survival and thus enhance angiogenesis according to this theory, as wild-type mice would present with more overall unligated αvβ3 integrin, and thus see more endothelial apoptosis than mutant mice. This however, is unlikely as it is hard to believe that αvβ3 would exist primarily in its unligated form *in vivo* given its large amounts of potential binding partners. More likely is that differential endothelial cell apoptosis can explain the differences in phenotype between the β3 null and DiYF mice. Here, genetic ablation of β3 integrin could enhance endothelial cell survival and thus increase angiogenesis, whereas the DiFY functional mutation in β3 integrin would have the opposite effect and thus reduce angiogenesis.

A third reason to explain both the poor clinical-trial studies and the unreconciled inhibitor and genetic ablation data may involve the regulation of VEGFR-2 at the protein level. Given that both αvβ3 integrin and VEGFR-2 are well known to be internalized at the cell membrane into the endocytic pathway, from which they can be either degraded or recycled back to the cell surface, it is plausible that αvβ3

may regulate VEGFR-2 recycling or vice-versa [248]. *Reynolds et a*l. show that αvβ3 RGD-inhibitors can enhance the cell-surface recycling rates of αvβ3, αvβ5 and VEGFR-2 in endothelial cells. By doing so, the degradation of VEGFR-2 was prevented and αvβ3 recruitment to focal adhesions at the cell periphery was enhanced. This effect was mediated by the Rab4 recycling pathway as suppression of this clearly prevents the observed effects [4]. Collectively, this means that αvβ3 inhibition actually *enhanced* tumour growth and tumour angiogenesis *in vivo*, and also enhanced VEGF-mediated angiogenesis *ex vivo*, all of which was abrogated by inhibiting VEGFR-2 [4]. What was most interesting about this study was that the dose of αvβ3 RGD-inhibitor used for all assays was significantly lower than the effective dose used to inhibit angiogenesis in mouse and human studies, which means αvβ3/αvβ5 integrin inhibitors like Cilengitide may differentially regulate angiogenesis according to its own concentration. *Reynolds et al.* go on to say that utilizing RGD inhibitors at intermediate doses (neither high nor low) in an *ex vivo* angiogenic assay yields no overall angiogenesis – i.e. the expected anti-angiogenic effects (or pro-angiogenic effects for that matter) were compromised [4]. Based on this there are huge consequences for the design of clinical trials utilizing RGD-mimetic anti-angiogenic therapies like Cilengitide in tumours. Pharmacokinetic analysis of Cilengitide in those studies predicts that, based on its half-life and maximal plasma drug concentration (C_{max}), 30 hours after delivery the plasma concentration of Cilengitide would be at angiogenesis-promoting levels (0.2-20nM). According to this same study these plasma levels can persist in the plasma for several hours [4], so combining all this means that

Cilengitide probably exists in patients as an intermediate of ‘high’ and ‘low’ dose, thus achieving no overall angiogenic effect, which will compromise its efficacy in tumours. Theoretically you could chronically infuse patients with Cilengitide (or other RGD mimetics) to avoid this and ensure Cilengitide is kept at ‘high’ doses *in vivo*. Indeed, a similar method has undergone phase I clinical trials [249], but was unsuccessful and did not meet its primary end point. Several other groups also provide similar evidence that low doses of RGD-peptides yield agonistic effects, including *Legler et al.* who show enhanced adhesive function of αvβ3 to vitronectin after treatment [251].

Taken together this section demonstrates that, regardless of the apparently conflicting data at times, αvβ3, although not required, is absolutely involved in angiogenesis and likely plays both pro- and anti-angiogenic roles.

The related integrin αvβ5 similarly regulates angiogenesis, whereby its inhibitors (including Cilengitide) will block pathological angiogenesis. Interestingly, integrin blocking antibodies and genetic models have revealed that αvβ3 and αvβ5 integrin utilize two functionally distinct cytokine-dependent angiogenesis pathways. Integrin αvβ5-mediated angiogenesis is specifically VEGF- or transforming growth factor α (TGF-α)- dependent, whereas integrin αvβ3-mediated angiogenesis is FGF- or tumour necrosis factor α (TNF-α)- dependent [252]. The distinction between the two is due to the fact that β3 and β5 integrin will differentially activate the Ras/Raf/MEK/Erk pathway in blood vessels. Specifically, the αvβ5 integrin pathway downstream of VEGF leads to activation of FAK and Src kinase, whereas

the αvβ3 pathway potentiates p21-activated kinase (PAK) [253] [254]. In addition, VEGF/αvβ5 and FGF/αvβ3 differentially activate Raf, which results in differential endothelial protection from distinct pathways of apoptosis. The αvβ5 pathway activates Raf on serines 338/339 which protects against cell intrinsic-apoptosis, whilst αvβ3 signalling activates Raf on tyrosines 340/341 which protects from cell extrinsic-apoptosis [255]. These differences illustrate how local expression of integrins and extracellular matrix ligands can confer specificity and drive distinct cellular behaviours.

More recently, αvβ5 has been shown to guide pathological angiogenesis together with Angiopoeitin-1 in an ischemic retinopathy model [256], and will also prevent vascular lung permeability if blocked either genetically or with inhibitory antibodies [257]. In addition, stimulating αvβ5 with low dose Cilengitide will enhance vascular promotion, which in turn will reduce tumour growth and metastasis [5]. On balance there are significantly fewer studies examining αvβ5 than αvβ3, but it is probably a pivotal, if dispensable, player in angiogenesis.

3.4.7 Integrins in cardiomyocytes

Integrins participate in multiple critical cellular processes including adhesion, extracellular matrix organization, survival, proliferation and signalling. Particularly important for a contracting muscle cell is the fact that integrins are mechanotransducers, which translate mechanical to biochemical information. Integrin function in the cardiomyocyte covers ubiquitous tasks such as adhesion, signalling and formation of cytoskeletal-ECM junctions, and also cell-specific

activities like modulating ion channel function, stem cell differentiation, ischemic protection and modification of the hypertrophic growth response.

In the cardiomyocyte the most abundantly expressed integrin heterodimers are α1β1, α5β1 and α7β1, which are collagen, fibronectin and laminin binding receptors respectively. β1 is the dominant integrin subunit present, but β3 and β5 also appear to be functional [258] [259] [221]. In general, integrins are most concentrated within cells at focal adhesion points and cell-cell borders. As such, within the cardiomyocyte integrins are basally expressed at those equivalent cell specific sites – i.e. the costameres and z-lines, respectfully [260] [261]. During cell-signalling integrins will translocate to more specific sites. For example, β1 integrin will translocate to the intercalated disc in damaged areas of the myocardium after injury [262], whilst β3 is upregulated to the cell surface in RGD-stimulated adult cardiomyocytes [263]. In addition, cell-specific integrins vary temporally and during disease, meaning that foetal, adult, healthy and unhealthy cardiomyocytes will represent a very specific integrin profile. Interestingly however, adult cardiomyocytes can assume a foetal expression pattern when stressed and during disease. For instance, α5 and α7 subunits have been shown to be significantly increased by ischemia or post-MI and aortic constriction can increase α1, α5, α7 and β1D subunit expression [264] [265]. Finally, all of this is further made complex by the fact that alternative splice forms of integrins can exist within the cardiomyocyte. The most common example of this are the splice variants β1A and β1D, which are predominantly expressed in either the embryo or the adult, respectfully [266].

Most integrin subunits have been examined in the mouse, a few of which demonstrate myocardium defects. Global deletion of α5 show abnormalities in outflow tract formation, and others lack left-right heart symmetry [267] [268]. Gain of function α5 in the cardiomyocyte sees mice develop a rapid deterioration of ventricular function, rhythm abnormalities and increased expression of calreticulin [269]. Elsewhere, overexpression of α7 integrin will have a protective effect in cardiac myocytes during ischemia/reperfusion injury and will also reduce rates of cardiomyopathy [270] [271]. The most well studied cardiomyocyte integrin in mice is β1. Global β1 knockout is embryonic lethal, so cell-specific transgenic tools are used here. Cardiomyocyte-specific ablation of β1 early in cardiogenesis reduced myocyte proliferation, and whole heart development was progressively abnormal [272]. Deleting β1 immediately after birth in those same cells lead to progressive myocardial fibrosis and development of dilated cardiomyopathy [273]. Finally, deleting β1 in the adult leads to a blunted hypertrophic response and defective hypertrophic stress signalling [273] [274].

β3 is less well studied in murine models than other more abundant integrins, but there are a number of studies that implicate β3 as a pivotal member of cardiomyocyte signalling, particularly during disease. The first indicator of this was that cell culture models show that β3 is highly concentrated at focal adhesion sites in the cardiomyocyte, meaning that β3 is probably involved in cell mechanotransduction [275]. Next, it was determined that β3 null mice exhibit increased apoptosis during pressure overload, associated with a decreased ventricular mass. This was due to a reduced activity of the Ubiquitin-NF-kB

pathway, meaning cells undergo programmed cell death [276]. Soon after, those same β3 null mice were used to show that the specific loss of β3 in the cardiomyocyte will also lead to calpain-mediated myocyte death after pressure overload, which further corroborating the fundamental role of β3 during cardioprotection [259]. In parallel, the same lab demonstrates that β3 null mice are also deficient producers of interstitial fibronectin and collagen in the heart. This was associated with reduced levels of cardiac fibroblast proliferation, fibroblast function and synthesis of fibroblast-specific protein [258]. Cardiac fibrosis is a vital protective mechanism during cardiac disease, although if in excess it can lead to pathogenesis of a number of cardiac pathologies. Together with evidence showing that αvβ3 can control myofibroblast differentiation [277], this implicates β3 as an effector of multiple cardiac cell types.

Collectively this demonstrates that integrins clearly play a vital role in overall heart health. They provide a structural, chemical and mechanical network that allows tissue to adapt to both physiological and pathological stimulus. Indeed, recent RNA-seq and microarray data of whole human hearts have identified that cellular adhesion-related pathway elements are upregulated pathway elements during disease [6].

3.5 Aims of the study

My own study builds upon the findings of *Reynolds et al*. [4] and *Wong et al.* [5] and investigates the clinical efficacy of a pro-angiogenic low dose Cilengitide treatment regimen in a murine model of heart failure. It is my hypothesis that treatment with Cilengitide may not only increase the levels of cardiac angiogenesis, if given in nanomolar doses, but also have a direct effect upon other cardiac cell types such as cardiac fibroblasts and the cardiomyocytes themselves. It is likely that αvβ3/αvβ5 integrin heterodimers exist within many cell types of the heart, including cardiac fibroblasts [277], which offers multiple avenues for potential sites of action. Furthermore, Cilengitide appears to very safe in human clinical trials, which is in contrast to other pro-angiogenic based therapies such as VEGF, where side effects may be a cause for concern. To achieve all of this we have the following aims:

1) Establish and optimise a model of murine heart failure.
2) Examine the expression of αvβ3 and αvβ5 integrin heterodimers within human and mouse hearts, both diseased and healthy.
3) Carry out detailed analysis of the effect of Cilengitide in murine heart failure.
4) Investigate the molecular mechanisms underpinning these effects.

CHAPTER 4.0: RESULTS

VASCULAR PROMOTION IN HEART FAILURE

4.1 Optimisation of a murine model of heart failure

Heart failure is a common, complex condition with a poor prognosis and increasing incidence. The syndrome of heart failure comprises changes in myocardial electrophysiology, contraction and energy metabolism, leading to an inability of the heart to meet circulatory demands [278]. This complexity, and the interaction of the clinical syndrome with frequently concurrent medical conditions like diabetes, means that animal modelling of heart failure is difficult [279]. As such, many commonly used animal models of heart failure do not entirely recapitulate many of the important clinical features of heart failure, but instead offer a simplified, indispensable tool to monitor multiple features of cardiac physiology within a relevant disease setting.

Here we assessed the physiological and clinical features of two commonly utilised murine models of heart failure to deduce which model would enable me to most pertinently address – 'Vascular promotion in heart failure'.

4.1a Isoprenaline-induced heart failure mouse model

The first model we chose to investigate was chronic isoprenaline infusion, delivered via a minipump sewn into the scruff of a mouse's neck. Isoprenaline is a synthetic catecholamine that stimulates beta-adrenoreceptors in the heart resulting in a marked elevation of heart rate and cardiac contractility. Chronic administration of isoprenaline in experimental models causes cardiac hypertrophy, ECG abnormalities, myocardial apoptosis and myocardial fibrosis [279]. Chronically, this can lead to heart failure. These effects are both time and concentration dependent. In addition, minipump implantation surgeries are technically very easy, and the physiological outcome of isoprenaline infusion is very reproducible between mice [280].

In order to first find a suitable dose for the induction of murine heart failure via chronic isoprenaline infusion, we assessed several different isoprenaline doses (20, 30 and 40 mg/kg/day) in wild-type C57BL6 mice, and quantified end-point fractional shortening and cardiac hypertrophy. Isoprenaline administration increased cardiac fractional shortening to higher than normal physiological levels across doses within 1 week, and this was followed by a reduction in fractional shortening to baseline levels by the second week of infusion (**figure 8a-b**). The extent of change in end-point fractional shortening was relatively similar between isoprenaline doses and any apparent differences proved to be insignificant.

All measured isoprenaline concentrations also proved to significantly increase left ventricle plus septum/body weight (a measure of cardiac hypertrophy) in mice

versus controls after 2 weeks (**figure 8c**). This effect was not associated with any significant changes to lung weight (data not shown). As previously, there was little difference in the extent of cardiac hypertrophy between doses. This led me to the conclusion that 20mg/kg was the most appropriate isoprenaline concentration *in vivo*, as higher doses did not especially induce further deleterious effects to the myocardium.

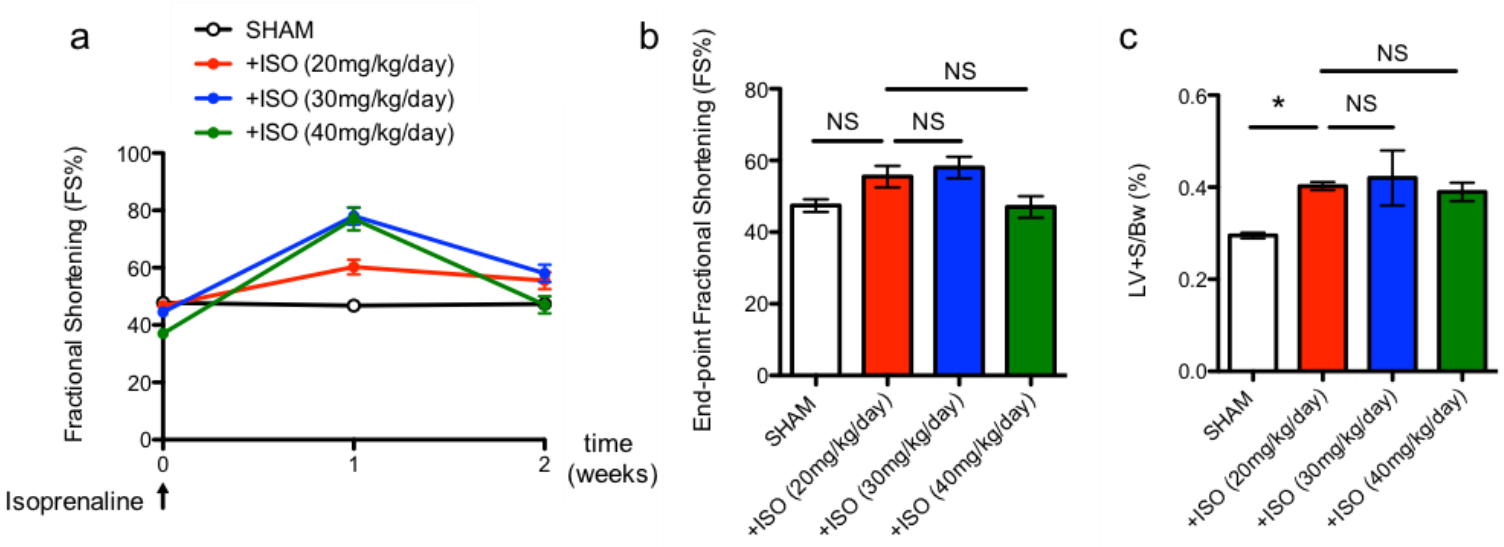

Figure 8: Chronic isoprenaline infusion in mice causes cardiac hypertrophy and an overall, time dependent change in fractional shortening. (**a**) Summary fractional shortening analysis, (**b**) end-point (2 week) fractional shortening and (**c**) Left ventricle + septum/body weight ratio in SHAM controls (n=12), and mice receiving 20 (n=8 hearts), 30 (n=2 hearts) or 40 (n=2 hearts) mg/kg/day isoprenaline infusion. Data are shown as mean ± SEM. Statistical analysis by 1-way ANOVA with Bonferoni's multiple comparison test post hoc; *P<0.05 versus SHAM vehicle control. NS is not significant.

4.1b Transverse-aortic constriction (TAC) model of murine heart failure

Transverse-aortic constriction (TAC) is a well-established surgical technique for inducing LV chronic pressure overload induced heart failure in rodents within 3-6 weeks [281]. Moderate TAC imposed at an early age triggers concentric LV hypertrophy with compensated chamber performance, and prominent diastolic filling abnormalities. The transition from compensated hypertrophy to early failure is time-dependent and heralded by LV dilation and the impairment of systolic function [281]. The pathophysiology observed here may be both strain [282], and gender specific [283], and so all my surgeries were conducted on age-matched C57BL6 male mice.

TAC (**figure 9a**) resulted in a sustained archetypal heart failure phenotype as expected, comprising reduced cardiac contractility (**figure 9b**) and increased cardiac hypertrophy (**figure 9c-d**) after 6 weeks. In addition, TAC hearts exhibited significant myocardial fibrosis after 6 weeks, as indicated by an increase in picrosirius red positive area in myocardial sections versus SHAM controls (**figure 9e-f**). SHAM controls, where aortic banding was not completed, exhibit normal fractional shortening, normal heart weight, and no deleterious fibrosis, and so were used as controls to TAC-surgeries in all experiments (**figure 9**).

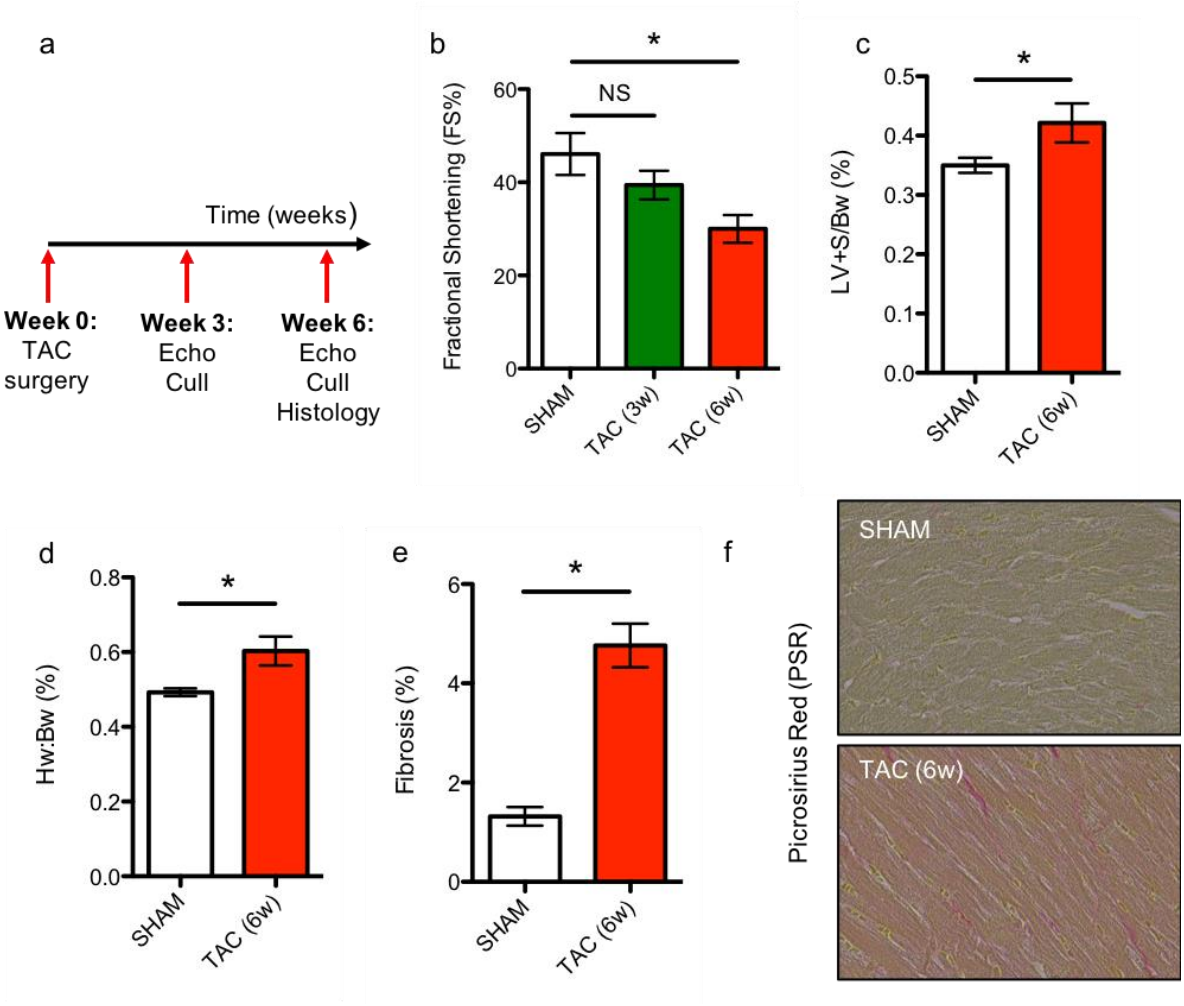

Figure 9: Transverse aortic constriction (TAC) surgery in mice causes cardiac hypertrophy, a reduction in cardiac contractility and an increase in myocardial fibrosis. (**a**) Schematic outline of TAC experiment, (**b**) End-point fractional shortening (%), (**c**) left ventricle + septum/body weight ratio, (**d**) heart weight: body weight (%), (**e**) fibrosis area of whole heart (%), (**f**) representative picrosirius red staining in SHAM control (n=8) and TAC (n=8) mice. Data are shown as mean ± SEM. Statistical analysis by 1-way ANOVA with Bonferoni's multiple comparison test post hoc or student's t-test if below 3 groups; *P<0.05 versus SHAM control.

Based on this data it is appears that chronic isoprenaline infusion results in cardiac hypertrophy without deleterious changes in cardiac inotropy (**figure 8**), whereas TAC surgery leads to deleterious changes to cardiac hypertrophy, inotropy, and fibrosis (**figure 9**). The two models chosen here therefore, can be broadly classified into two distinct heart failure categories: heart failure with preserved ejection fraction (ISO), and heart failure with reduced ejection fraction (TAC). Whilst the investigation of a murine model of heart failure with a preserved ejection fraction (HFpEF) would be a useful avenue of study, we believe it would be more beneficial for my thesis to instead study a murine model that models heart failure with reduced ejection fraction (HFrEF). This is due to the fact that HFpEF is relatively less well understood within mouse models and its mechanisms are poorly understood [284]. Furthermore, HFrEF offers more avenues for studying therapeutic intervention, like ejection fraction and fractional shortening. Aortic banding surgery has previously been linked to result in changes to myocardial angiogenesis [119], has a relatively well understood pathogenesis within the available literature [279], and yields consistent physiological outcomes in my own hands. In addition, aortic banding is also more physiologically relevant to human heart failure versus chronic isoprenaline infusion. Thus, for the rest of my PhD we decided to use the TAC model to study the control of angiogenesis in a pathological heart condition.

4.2 Integrins β3 and β5 are expressed in human cardiac endothelial cells and cardiomyocytes

αvβ3 is expressed at low levels by quiescent endothelium but is significantly upregulated during angiogenesis, especially within the myocardium after infarction [285] [286]. As such, it has been postulated that αvβ3 is an important determinant of myocardial recovery in the endothelium, and an indispensable regulator of pathological myocardial angiogenesis overall. Indeed, αvβ3 is increased at sites of recent myocardial infarction and its expression correlates with recovering regions [287]. Similarly, αvβ5 is an important regulator of endothelial cell function and angiogenesis, although these features have not been investigated specifically in the cardiac endothelial cell to date [257] [256]. In the cardiomyocyte αvβ3 has relatively low expression, but this may also be elevated after infarction [219]. αvβ5 on the other hand has not had its expression evaluated within the cardiomyocyte to my knowledge. Collectively this demonstrates that αvβ3 is an important regulator of cardiac endothelial cell and cardiomyocyte function, especially during disease. Additionally, there is sufficient evidence to postulate that αvβ5 will also play a role here, too. All things considered, we set out to establish the expression patterns and relative cell-specific levels of αvβ3 and αvβ5 integrins within the heart. To do this we gathered relevant human LV biopsies and stained for β3 and β5 integrin in tandem with endothelial (CD31), mural cell (alpha-smooth muscle actin) or cardiomyocyte (cardiac troponin) cell-specific markers. Both β3 and β5 integrins were present in human cardiomyocytes (**figure 10**), cardiac endothelial cells

(**figure 11**) and cardiac mural cells (**figure 12**) as assessed by co-localisation with their respective cell-specific markers.

Across cells, integrins are most concentrated at focal adhesions and cell-cell borders. Within the cardiomyocyte these equivalent sites are the costamere and z-line, respectively [288]. In longitudinal myocardium sections, β5 integrin subunits especially were clearly concentrated in 'individual lines' that represent the cardiac costamere (**figure 10l**). β3 integrin subunits were expressed in a more diffuse pattern across the cardiomyocyte, and at much lower levels than β5. In transverse myocardial sections β5- was expressed similarly diffused, probably because defined costamere structures are not easily visible within these regions (**figure 10m**). The negative controls within myocardial sections confirm that β3 and β5 staining was specific (**figure 10n-o**). Controls are particularly important for this sort of analysis as the myocardium is classically a very auto-fluorescent tissue-type.

In contrast to this, β3 integrin subunits were more concentrated within the endothelium, rather than the surrounding cardiomyocytes (**figure 11c**). Both β3 and β5 co-localise with the endothelium-specific marker CD31 in the vast majority of samples. This was seen across multiple vessel types, including:

1) Artery, or arteriole-like structures with a clearly defined vascular smooth muscle and collagen layer (**figure 11e and j**).

2) Vein or venule-like structures without any clearly defined surrounding layers (**figure 11k and m-n**).

3) Relatively ‘small’ undefined vessel subtypes (**figure 11l and o**).

Both β3 and β5 demonstrate co-localisation with alpha-smooth muscle actin (α-SMA) in vessels, and so are probably present in human pericytes (**figure 12d-e and i-j**). We cannot say with absolute certainty that the cells outlined here are indeed mural cells as fibroblasts may also transiently express α-SMA [39].

These experiments together constitute important preliminary evidence that demonstrates the presence of αvβ3 and αvβ5 integrins in cells of the myocardium. It is my hypothesis that not only will these integrins be differentially expressed across the course of human, or murine, heart disease, but that they can be therapeutically modulated (by e.g. Cilengitide) to reduce disease severity. Proving their expression in human heart cells was an important first step toward this overarching goal.

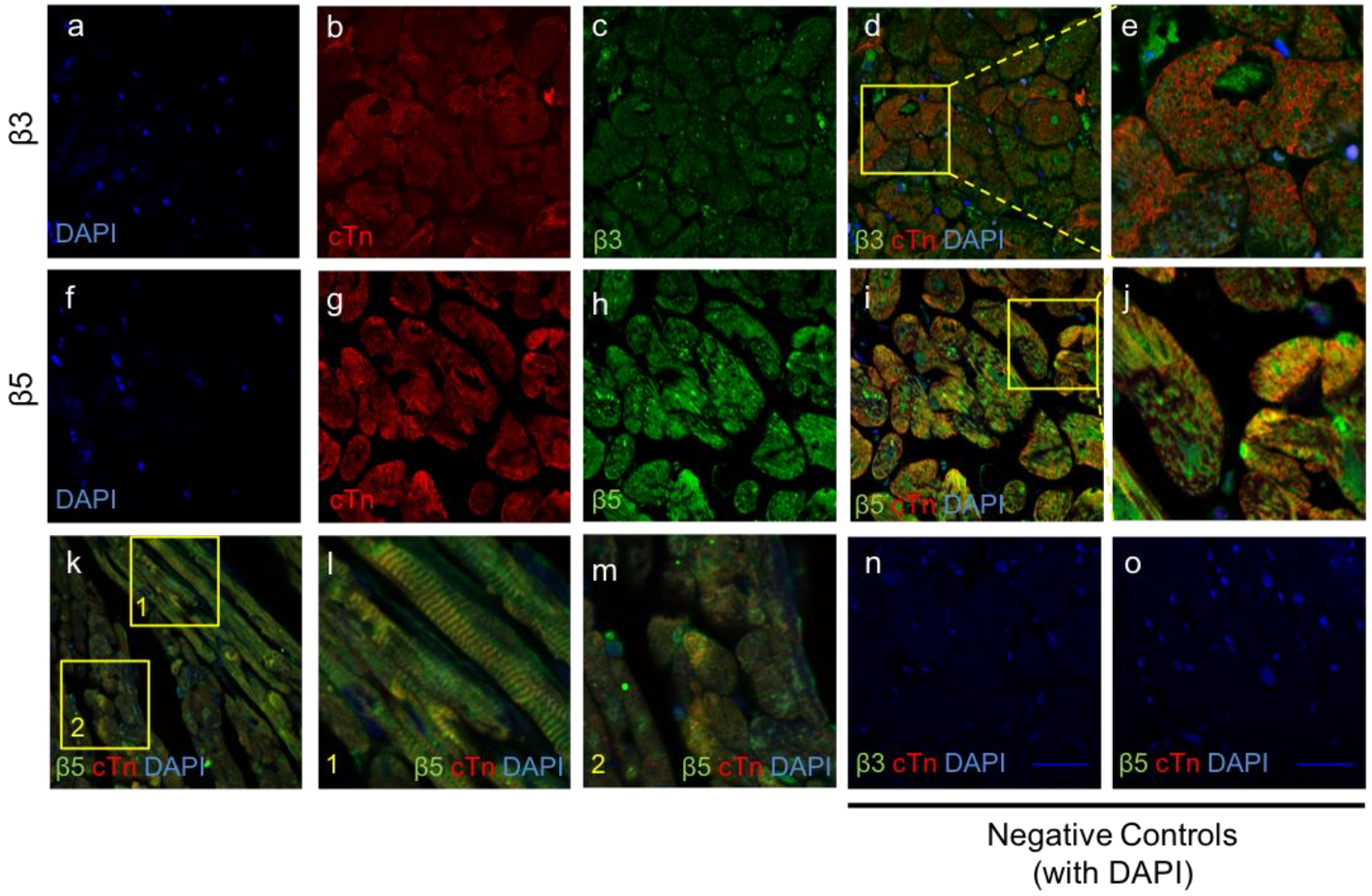

Figure 10: β3 and β5 integrin subunits are expressed in human cardiomyocytes in human heart sections. Immunofluorescence of human myocardial tissue demonstrating co-localisation between the cardiomyocyte-specific marker, cardiac troponin, and β3 and β5 integrin subunits. (**a**) DAPI, (**b**) cardiac troponin, (**c**) β3 integrin subunit and (**d-e**) cardiac troponin, β3 integrin subunit and DAPI merged. (**f**) DAPI, (**g**) cardiac troponin, (**h**) β5 integrin subunit, and (**i-j**) cardiac troponin, β5 integrin subunit and DAPI merged. (**k-m**) β5 integrin subunit and cardiac troponin. (**n-o**) Immunofluorescent negative control stain using secondary antibodies only for cardiac troponin and β3 (**n**) and β5 (**o**) integrin subunit (and DAPI) (scale bar 50μm). Note: Images a-m taken at same scale as n-o.

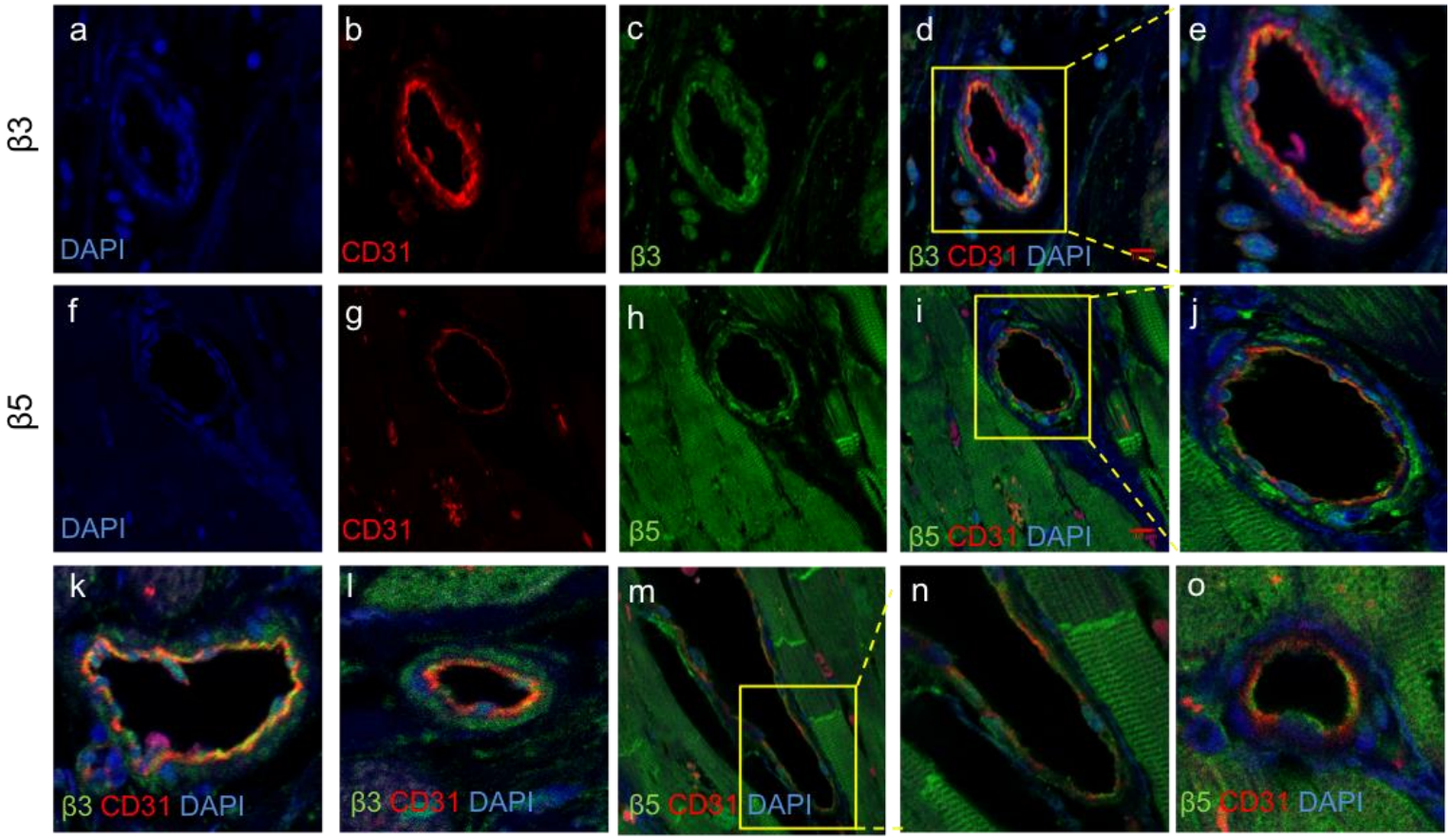

Figure 11: β3 and β5 integrin subunits are expressed in human cardiac endothelial cells in human heart sections. Immunofluorescence of human myocardial tissue demonstrating β3 and β5 integrin subunits in CD31+ endothelial cells. (**a**) DAPI, (**b**) CD31, (**c**) β3 integrin subunit, (**d-e**) CD31, β3 integrin subunit and DAPI merged. (**f**) DAPI, (**g**) CD31, (**h**) β5 integrin subunit, (**i-j**) β5 integrin subunit, CD31 and DAPI merged. (**k-l**) DAPI, CD31 and β3 integrin subunit merged. (**m-o**) β5 integrin subunit, CD31 and DAPI merged. Scale bars 10μm.

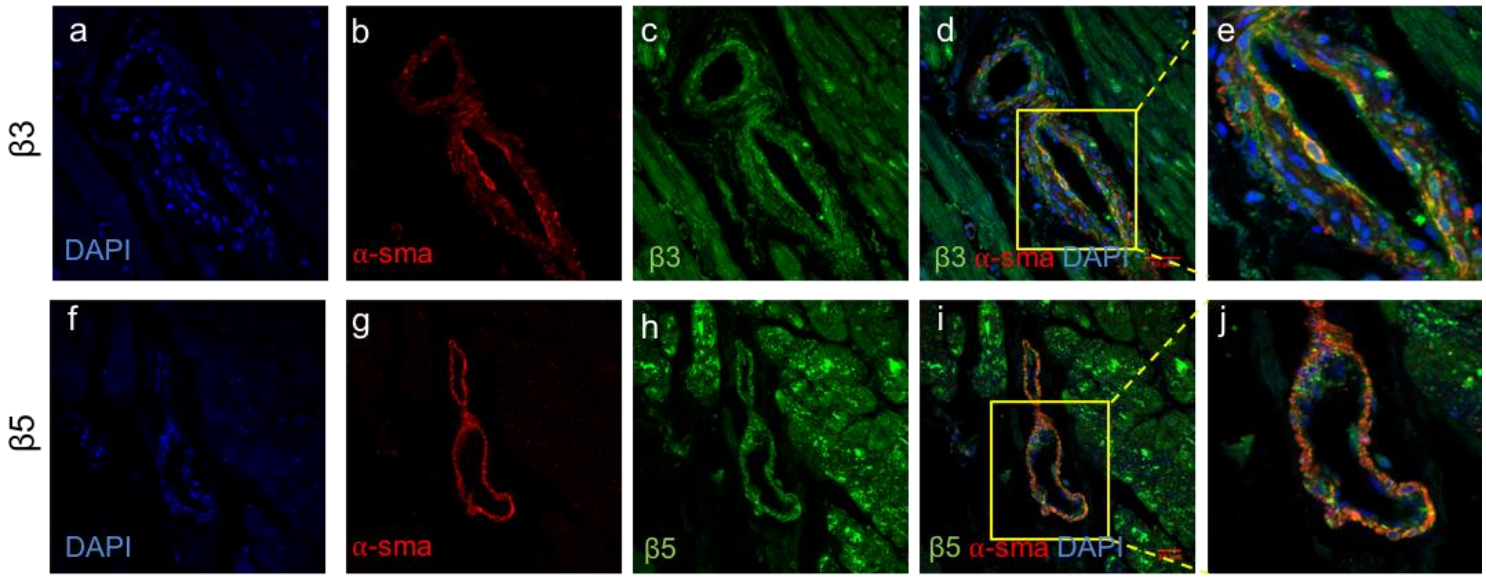

Figure 12: β3 and β5 integrin subunits are expressed in human mural cells in human heart sections. Immunofluorescence of human myocardial tissue demonstrating co-localization between the mural cell marker, α-SMA, and β3 and β5 integrin subunits. (**a**) DAPI, (**b**) α-SMA, (**c**) β3 integrin subunit, (**d-e**) α-SMA, β3 integrin subunit and DAPI merged. (**f**) DAPI, (**g**) α-SMA, (**h**) β5 integrin subunit, (**i-j**) α-SMA, β5 integrin subunit, and DAPI merged. Scale bars 30μm.

4.3 β3 and β5 integrin subunit receptor expression does not change in human cardiac disease

Trans-membrane receptors such as integrins are important for the dynamic interaction between intracellular processes and the extracellular environment. They are critical to cellular form and function and are essential in regulating cellular processes such as differentiation, proliferation and cell death [203].

In the adult heart, cellular-ECM interactions provide a structural, chemical, and mechanical substrate that is essential for normal homeostasis and adaptations to pathophysiologic signals. Because integrins are the principal receptors for the ECM, their appropriate expression and function is likely to be necessary for normal cardiovascular function in the adult [289]. To investigate the relative expression of β3 and β5 in the heart, both in healthy and diseased tissue, we gathered 4 different human cardiac biopsy variants (non-failing (NF), non-failing with hypertrophy (NH), dilated (Dil.), and ischemic (Isc.)) and quantified β3 and β5 expression across samples.

β3 protein expression did not change amongst the hearts of heart failure patients (dilated or ischemic groups) or healthy controls (non-failing and non-failing with hypertrophy groups), as shown by immunoblot (**figure 13a-b**) and immunofluorescent assays (**figure 14a-d** and **k**). β3 expression did not change at the RNA level between samples (**figure 13d**).

Similarly, β5 protein expression did not change amongst the hearts of heart failure patients (dilated or ischemic groups) or healthy controls (non-failing and non-failing with hypertrophy groups), as shown by immunoblot (**figure 13a-b**) and

immunofluorescent assays (**figure 14a-d** and **k**). β5 expression did not change at the RNA level between samples (**figure 13d**).

It has been noted that GAPDH may not be an appropriate control for the western blots in this instance, as GAPDH may actually increase in heart failure. If I had more time therefore, I would repeat these studies with other controls like actin or hsc-70. However, it is worth noting that other similar studies have used GAPDH as a control like Lee *et al* [403], which is why these studies were constructed in such a manner.

Overall, these data were important to show that the targets of Cilengitide is expressed in the diseased heart.

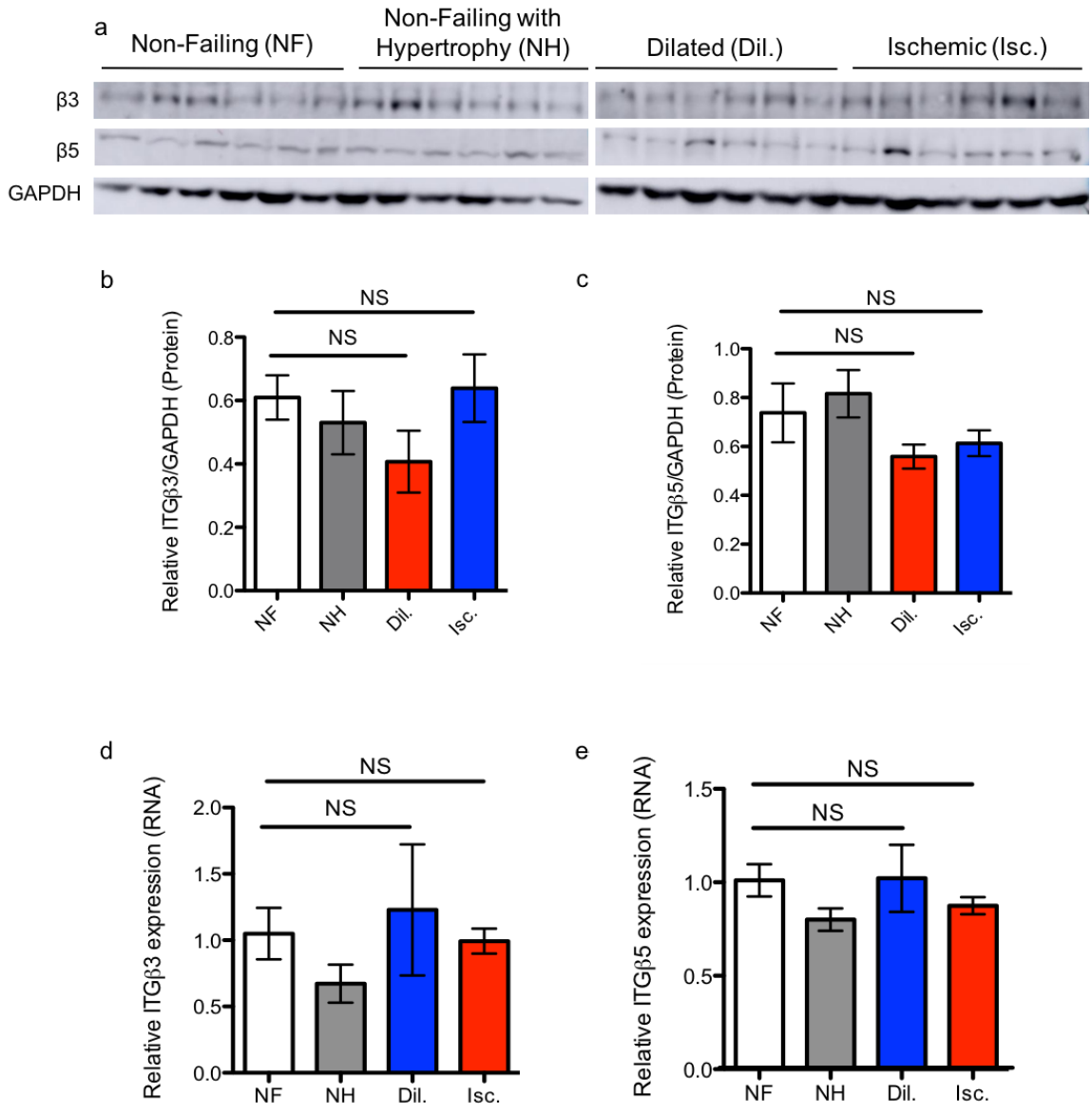

Figure 13: β3 and β5 integrin subunit protein and mRNA levels do not change in human heart disease. (**a**) β3 and β5 integrin subunit western blots of human non-failing (NF), non-failing with hypertrophy (NH), Dilated (Dil.) and Ischemic (Isc.) whole heart tissue lysates with (**b-c**) associated densitometry analysis (n=6 separate hearts per group). (**d-e**) β3 and β5 integrin RT-qPCR of human NF, NH, Dilated and Ischemic hearts (n=3 separate hearts per group). Data are shown as mean ± SEM. Statistical analysis by 1-way ANOVA with Tukey's multiple comparison test post hoc; NS is not statistically significant.

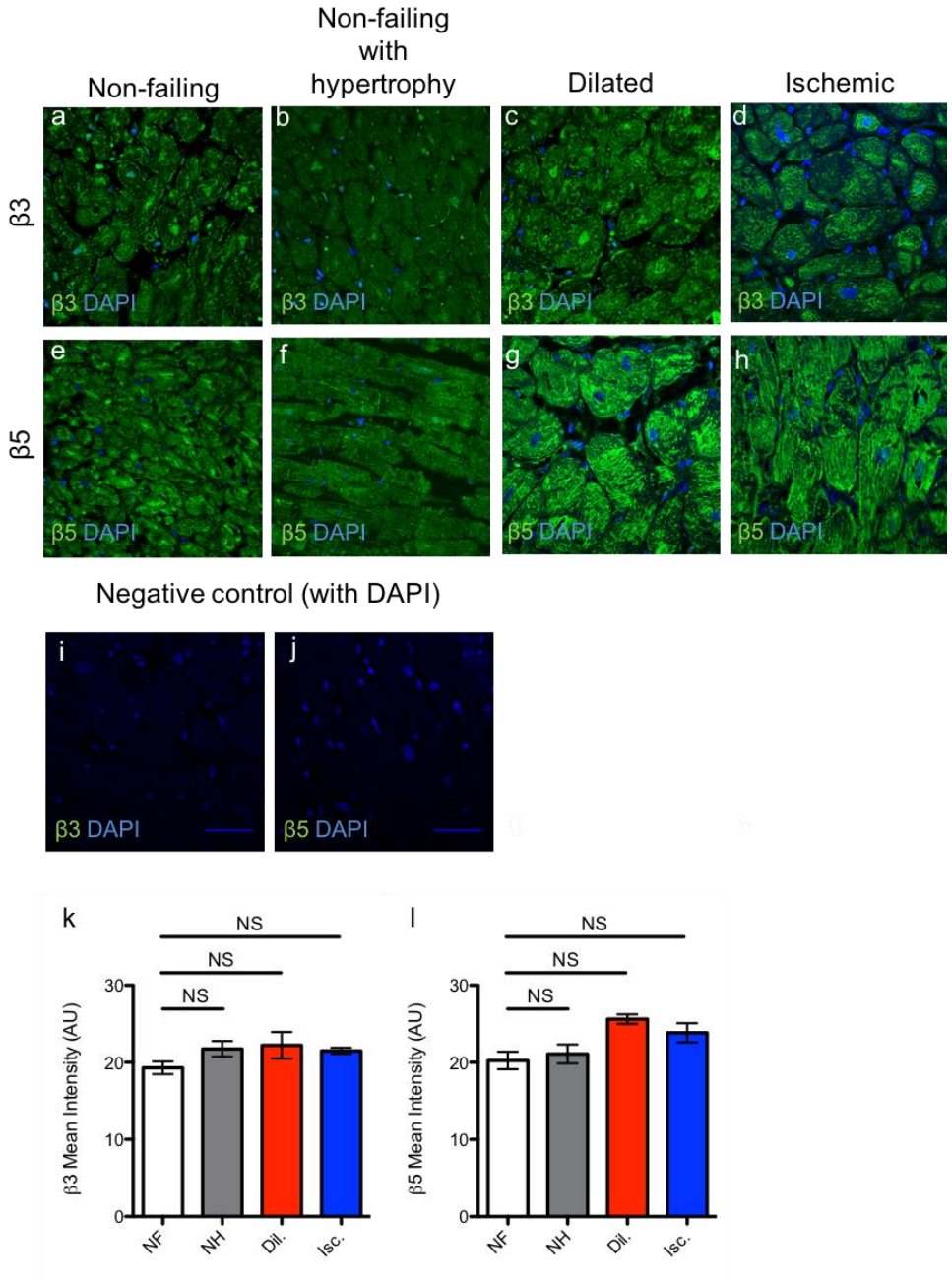

Figure 14: Integrin β3 and β5 cardiac expression does not change in human heart disease. Immunofluorescence of human heart tissue across four different cardiac phenotypes demonstrating relative β3 and β5 integrin subunit expression. (**a**) non-failing (NF), (**b**) non-failing with hypertrophy (NH), (**c**) Dilated (Dil.) and (**d**) Ischemic (Isc.) hearts stained with DAPI and β3 integrin. (**e**) NF, (**f**) NH, (**g**) Dilated and (**h**) Ischemic hearts stained with DAPI and β5 integrin. (**i-j**) Immunofluorescent negative control stain using secondary antibodies only for cardiac troponin and β3 (**i**) and β5 (**j**) integrin (and DAPI). Scale bars 50μm – note: images a-h taken at same scale. (**k-l**) Mean intensity of β3 and β5 immunofluorescence (assessed via image J) (n=4 heart samples per group). Data are shown as mean ± SEM. Statistical analysis by 1-way ANOVA with Tukey's multiple comparison test post hoc; NS is not significant.

4.4 β3 and β5 integrin subunit receptor cardiac protein expression is not differentially expressed after TAC surgery

Now we have established that β3 and β5 integrin subunit expression is present within human heart failure samples, but their expression does not change with disease, we sought to investigate whether those same integrins were differentially expressed in a TAC model of heart failure after 6 weeks. Neither β3 nor β5 was significantly upregulated in the myocardium of TAC surgical mice versus SHAM controls as assessed by immunofluorescence (**figure 15a-h**). However, although immunofluorescence signals were greater than that of the negative antibody controls, we are not convinced that this is bonafide integrin staining, partially because it is very different to that in the human heart. Similarly, both β3 and β5 integrin subunit protein levels did not change after TAC surgery as assessed by western blot (**figure 15i-k**). Interestingly, β3 RNA was upregulated in the whole hearts of mice that had undergone TAC surgery (**figure 15l**). This could indicate that the rate of β3 protein breakdown is higher in those mice, or its translation is slower.

Collectively these results demonstrate that β3 and β5 integrin expression does not change in 'late-stage' stage heart failure tissue (in humans or murine models). This is perhaps unsurprising and may reflect the fact that the tissue sampled here has already undergone cardiac remodelling, and so the molecules involved during this process are now mostly downregulated to normal levels. Several studies previously have implicated integrin β3 especially as an important mediator of cardiac remodelling. The majority also show that its levels return to normal after

cardiac remodelling is over [219] [286] [285]. With that said, we do not actually have any evidence to say that my human heart tissue actually represents ‘late-stage’ disease, nor can we ascertain that the tissue itself was taken after recovery from e.g. ischemic insult.

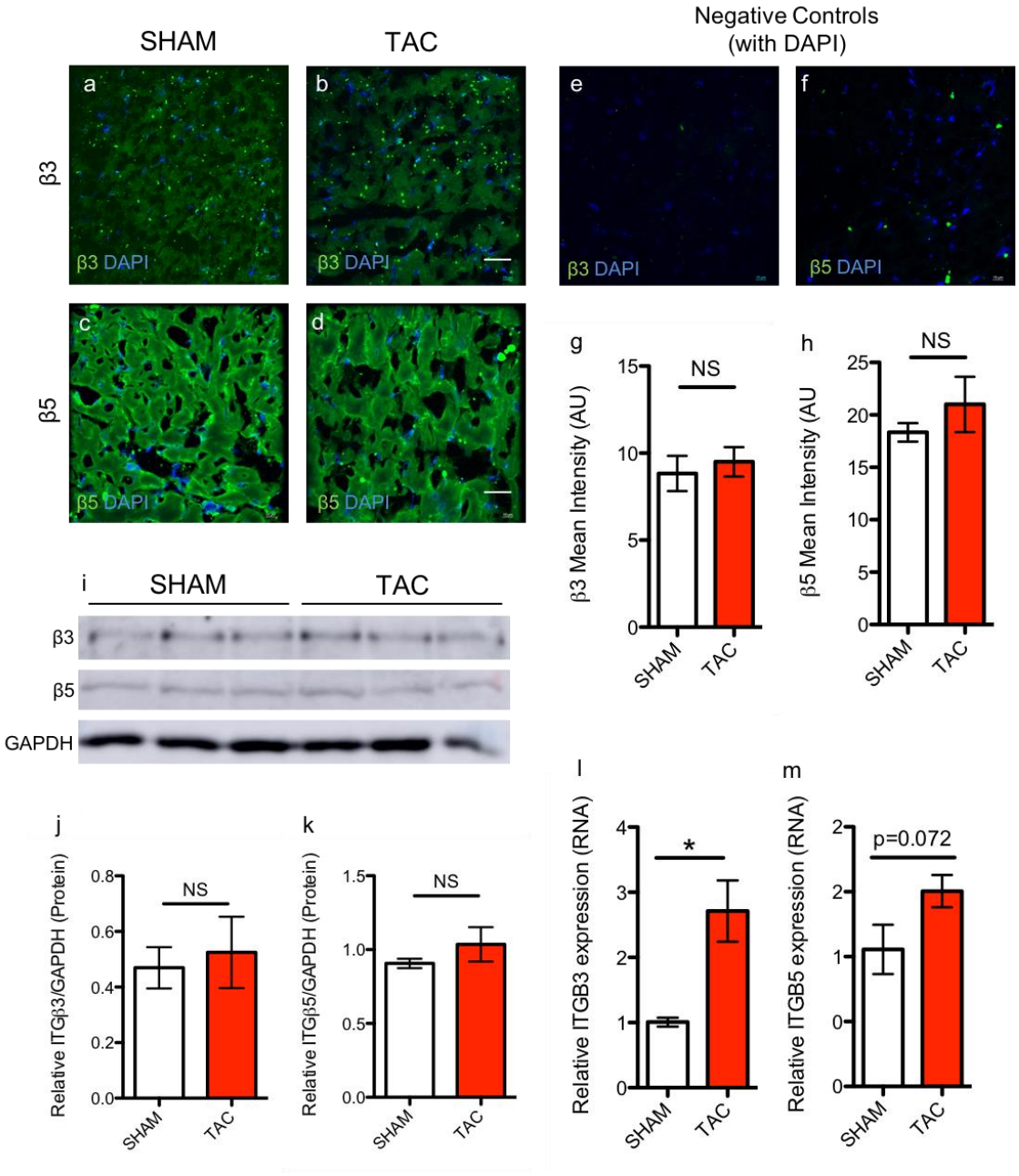

Figure 15: β3 and β5 integrin subunit protein is not differentially expressed in whole mouse heart tissue after TAC surgery. Immunofluorescence, immunoblot and RT-qPCR demonstrating β3 and β5 integrin expression and mRNA levels in whole heart tissue of 6-week TAC mice versus SHAM controls. (**a**) SHAM and (**b**) TAC heart tissue stained with β3 integrin and DAPI antibodies. (**c**) SHAM and (**d**) TAC heart tissue stained with β5 integrin and DAPI antibodies. (**e-f**) Immunofluorescent negative control stain using secondary antibodies for β3 (**e**) and β5 (**f**) integrin (and DAPI). (**g-h**) Mean intensity of β3 and β5 immunofluorescence (assessed via image J) (n=3 heart samples per group). (**i-k**) Western blot assessing β3 and β5 protein expression (n=3 hearts per group). (**l**) β3 and (**m**) β5 whole heart RNA expression in mice undergoing either SHAM or TAC surgery (age-matched) (n=4 hearts per group). Data are shown as mean ± SEM. Statistical analysis by student's t-test; *P<0.05 versus control. NS is not significant. Scale bars 20μm.

4.5 Cilengitide functions as a dose dependent regulator of cardiac inotropy in pressure-overload-induced heart failure

Now we have established the expression of αvβ3 and αvβ5 integrin in both a murine model of heart failure, and human heart failure itself, we sought to investigate the utility of Cilengitide in the TAC model of heart failure. Cilengitide is an αvβ3/αvβ5 integrin-specific RGD-peptidomimetic (i.e. antagonist) developed initially as an anti-angiogenic therapy. *In vivo*, high dose Cilengitide acts as a highly potent inhibitor of angiogenesis, and will also induce the apoptosis of growing endothelial cells [290] [291]. Cilengitide has entered multiple clinical trials as an anti-cancer therapy, but has been withdrawn from many, including a phase III clinical trial for the treatment of glioblastoma, mostly due to failure to meet its clinical endpoints [250]. Most recently, Cilengitide has been discontinued as an anti-cancer therapeutic. In a bid to repurpose this drug the Hodivala-Dilke lab has shown that, in contrast to a high dose Cilengitide treatment regimen, low dose Cilengitide paradoxically exerts a VEGF-mediated pro-angiogenic effect on the tumour vasculature, most likely through altered vascular endothelial growth factor receptor-2 trafficking and recycling [4]. My own study builds upon this finding and investigates the clinical efficacy of a pro-angiogenic low dose Cilengitide treatment regimen in a murine model of heart failure. Efficient blood supply to cardiomyocytes is necessary to meet their high metabolic demand and oxygen requirements. Pathological cardiac stressors such as hypertension or myocardial ischemia can upset the balance between the volume of myocardial tissue mass and adequate blood supply, leading to a relative impairment in local tissue

oxygenation [292] [293]. Thus, revascularizing and reperfusing damaged, or non-functional heart tissue, may potentially restore cardiac function, vastly improve the symptoms of heart failure, and/or halt the progression of heart failure entirely [294] [295].

It is my hypothesis that treatment with Cilengitide may not only increase levels of cardiac angiogenesis (and therefore myocardial perfusion) if given in nanomolar doses, but also have a direct effect upon other cardiac cell types, such as cardiomyocytes. To this end, Cilengitide was administered to mice either in tandem to, or after TAC surgery and the clinical outcome measured. As this was a preliminary experiment only one indices of disease severity was measured – cardiac contractility, which was quantified by fractional shortening.

Cilengitide was administered intraperitoneally 3 times per week in tandem to the onset of surgery as a 'low dose' (50μg/kg), or 'high dose' (500μg/kg) therapy. As expected, TAC surgery itself brought about a sustained decline in fractional shortening across the 7-week period, which as mentioned, is an archetypal feature of heart failure (**figure 16a-d**). In contrast, SHAM-surgery control mice exhibit normal fractional shortening across the 7 weeks (**figure 16a-d**). Of the Cilengitide doses used, 50μg/kg (i.e. 'low dose Cilengitide') proved to be cardioprotective against TAC surgery, whilst 500μg/kg Cilengitide (i.e. 'high dose Cilengitide') was ineffective as a cardioprotectant. Here, administration of 'low dose Cilengitide' prevented measured aspects of deleterious cardiac remodelling, and so the fractional shortening of those mice receiving this therapy regime remained normal (46.5%) (i.e. similar to SHAM controls – 47.4%), and did not decline, as in

untreated TAC-surgery mice (29.8%) (**figure 16a-d**). In contrast, the fractional shortening of those mice receiving 'high dose Cilengitide' in tandem with TAC surgery fell to 34% within 7 weeks, which was significantly lower than SHAM controls (47.4%) and low dose Cilengitide treated TAC surgery-mice (46.5%) (**figure 16a-d**).

Henceforth, we classify a Cilengitide dose of 50μg/kg to be 'low dose Cilengitide' (LdCil). Perhaps fortuitously, this is the same concentration that was demonstrated to exhibit tumour angiogenic properties by previous lab members [4] [5].

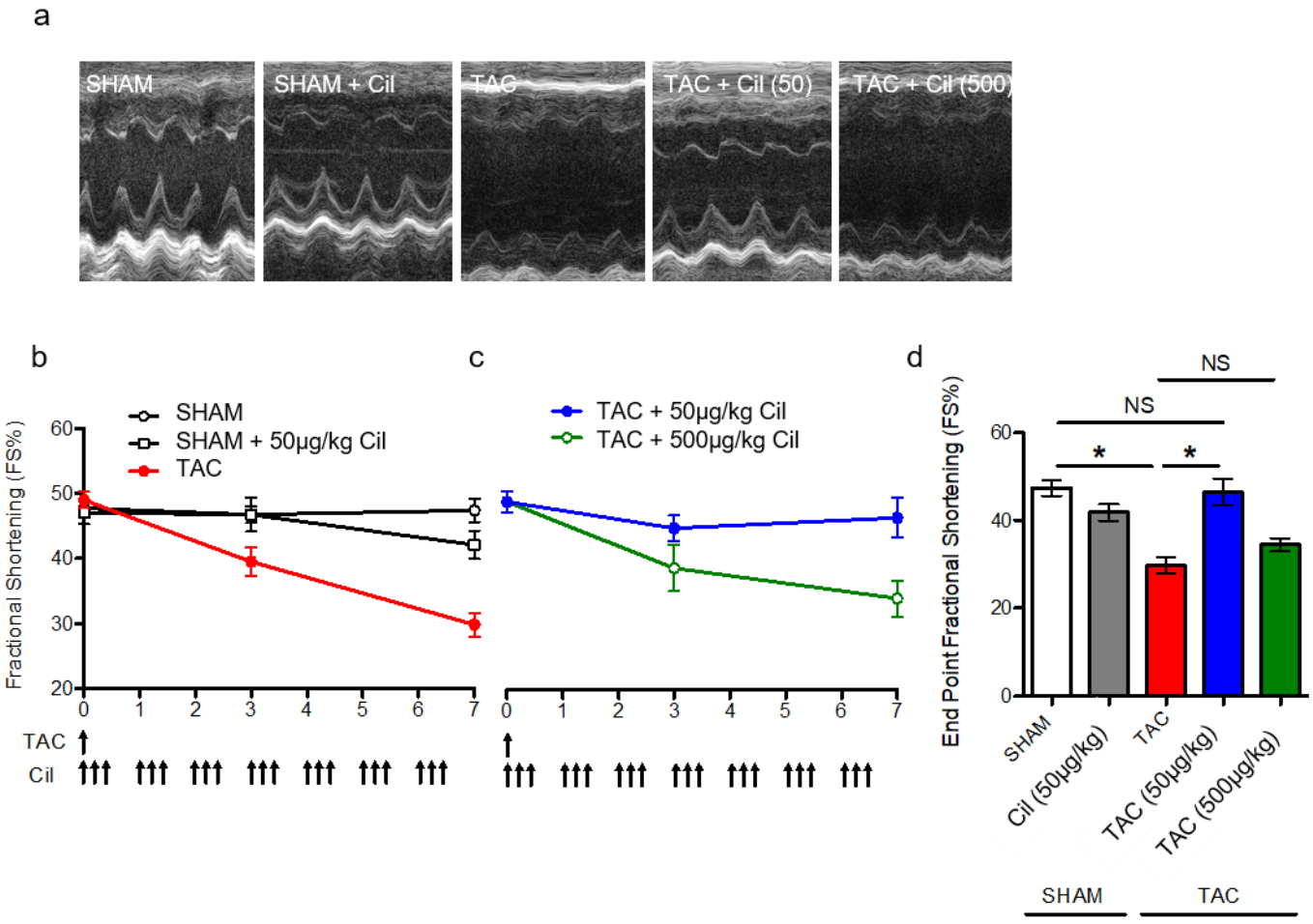

Figure 16: Cilengitide functions as a dose dependent regulator of cardiac inotropy in pressure-overload-induced heart failure. Wild-type, male, C57BL6 mice underwent either SHAM, or TAC surgery and were treated with prophylactic Cilengitide or used as vehicle controls. (**a**) Representative echocardiographic images in SHAM (n=10), TAC (n=6) and Cilengitide treated (SHAM n=8, TAC 50 n=9, TAC 500 n=7) mice. (**b-c**) Summary fractional shortening (%FS) analysis and (**d**) End point fractional shortening analysis. Statistical analysis by 1-way ANOVA with Tukey's multiple comparison test post hoc; *P<0.05 versus control. NS is not statistically significant.

4.6 Pressure-overload-induced cardiac pathobiology is suppressed with delayed low dose Cilengitide treatment

Since human heart failure patients will not report symptoms until after cardiovascular disease has already developed, it would be remiss of us to solely report beneficial data from a treatment that was given in tandem with TAC surgery. Thus, in order to recapitulate the circumstances seen in the clinic mice were left to develop cardiac dysfunction after TAC surgery before commencing low dose Cilengitide treatment.

Based upon previous observations we chose to investigate whether or not cardiac dysfunction had developed by 3 weeks post-TAC surgery. This constitutes a time-point that was early enough in the TAC-experimental protocol to allow for therapy with Cilengitide, but also late enough that cardiac dysfunction should be established. By 3 weeks post-surgery those mice that had undergone TAC displayed significantly lower fractional shortening and ejection fraction than at baseline, and also their hearts were hypertrophied, and the left ventricle displayed some minor dilatation (**figure 17a-d**). Together this shows that some cardiac dysfunction had already been established, and for this reason we classified 3 weeks post-TAC surgery as the time point by which heart failure had been established, and so treatment could begin here. Thus, after 3 weeks low dose Cilengitide (LDCIL) was administered 3 times per week for a further 3 weeks.

TAC surgery without associated treatment brought about an archetypal heart failure phenotype as previously shown, which comprised of significantly reduced

cardiac contractility (as measured by fractional shortening and ejection fraction), and also LV dilatation, which here was quantified by measuring LV internal diameter at systole (LVID;s) and diastole (LVID;d) (**figure 18a-f**). Within 3 weeks of LDCIL treatment, there was a significant reversal in each of the measured indices of disease severity, including cardiac contractility and LV dilatation. Indeed, the fractional shortening and ejection fraction of mice that had undergone TAC surgery improved significantly after low dose Cilengitide treatment, and their LVID;s was also reduced versus untreated controls (TAC) (**figure 18b-f**). These effects were independent to changes in mean arterial blood pressure (MABP) (**figure 18h**), which excludes the possibility that low dose Cilengitide may lead to peripheral dilatation and a reduction in the cardiac overload, which could in theory indirectly dampen any heart failure phenotype.

Low dose Cilengitide also prevented maladaptive changes in cardiac hypertrophy, which is another salient feature of heart failure. Indeed, mice that have undergone TAC surgery exhibit significantly 'heavier' hearts (relative to body weight), which is due to extensive cardiomyocyte hypertrophy (**figure 19a-c**). Treatment with low dose Cilengitide 3 weeks after TAC surgery will ostensibly return cardiomyocytes back to normal size, which manifests as significantly lower heart weight (relative to body weight) (**figure 19a**) and smaller myocytes (**figure 19b-c**) versus untreated surgical controls (TAC) (as assessed by wheat germ agglutinin staining (WGA)).

A hallmark feature of the heart during pathophysiological situations is the suppression of the post-natal gene program and return to a predominant foetal-like gene program [296]. This is an adaptive mechanism which facilitates extensive cardiac remodelling and includes: a decrease in the rate of aerobic metabolism, an increased in cell survivability, increased cardiomyocyte size and also a change in cardiac contractility, amongst others [297]. Overall, these features exist to maintain overall cardiac output whilst also increasing the rate of cardiac efficiency during the pathogenesis of disease. As part of this foetal-like gene program, the pathological hypertrophy markers Myh7, Myh6, ANP and BNP will be re-expressed. Multiple investigators have demonstrated that many of these genes will be upregulated after TAC surgery in murine models [298] [299] [300] [301], and so we sought to investigate whether or not low dose Cilengitide treatment could prevent the deleterious cardiac transition which is heralded by the re-expression of fetal-like genes.

Across the markers sampled (Myh7, Myh6, ANP and BNP), TAC surgery surprisingly did not induce a significant increase in Myh7, ANP and BNP or Myh6, although the results did tend toward an increase (**figure 20a-d**). The administration of Cilengitide 3 weeks after TAC surgery did appear to reduce the expression of those ANP, BNP and MYH7 markers, although this was insignificant (**figure 20a-d**).

Collectively this indicates that the salutary effects of low dose Cilengitide are sufficient to significantly reverse many of the disease features of pressure-overload

induced heart failure, including: reduced cardiac contractility, LV dilatation, deleterious cardiac hypertrophy, and finally a return to a foetal-like gene expression pattern (**figure 18-20**). We have previously been able to assess cardiac fibrosis in my TAC models of heart failure, but unfortunately was not able to do this in any of the studies we conducted with low dose Cilengitide. This was because the majority of the hearts from experimental mice were snap-frozen for further investigation. We found it impossible to properly stain frozen myocardium sections with picrosirius red, as the stain itself is optimised for paraffin-embedded sections. We attempted multiple other stains for cardiac fibrosis, including Masson's trichrome and Collagen type 1 (data not shown) (Collagen type 1 has specifically been shown to be the primary collagen type within cardiac fibrosis [302] [303]), but these did not capture extensive fibrosis following TAC surgery, as was seen with picrosirius red stains. *Sarrazy et al.* show that integrins αvβ5 and αvβ3 are upregulated in myofibroblast-enriched fibrotic lesions, and will together activate latent TGF-β1 activation, which will itself trigger myofibroblast differentiation [277]. They show that by blocking those integrins you could theoretically block the progression of fibrosis in the heart, and so modulating their expression with Cilengitide could be either detrimental or beneficial. Perhaps Cilengitide worked so well in these experiments precisely because there was so little fibrosis in mouse models of TAC. By contrast, fibrosis is itself an early adaptive mechanism to cardiac injury, and so by potentiating early fibrosis αvβ5 and αvβ3 may actually facilitate repair.

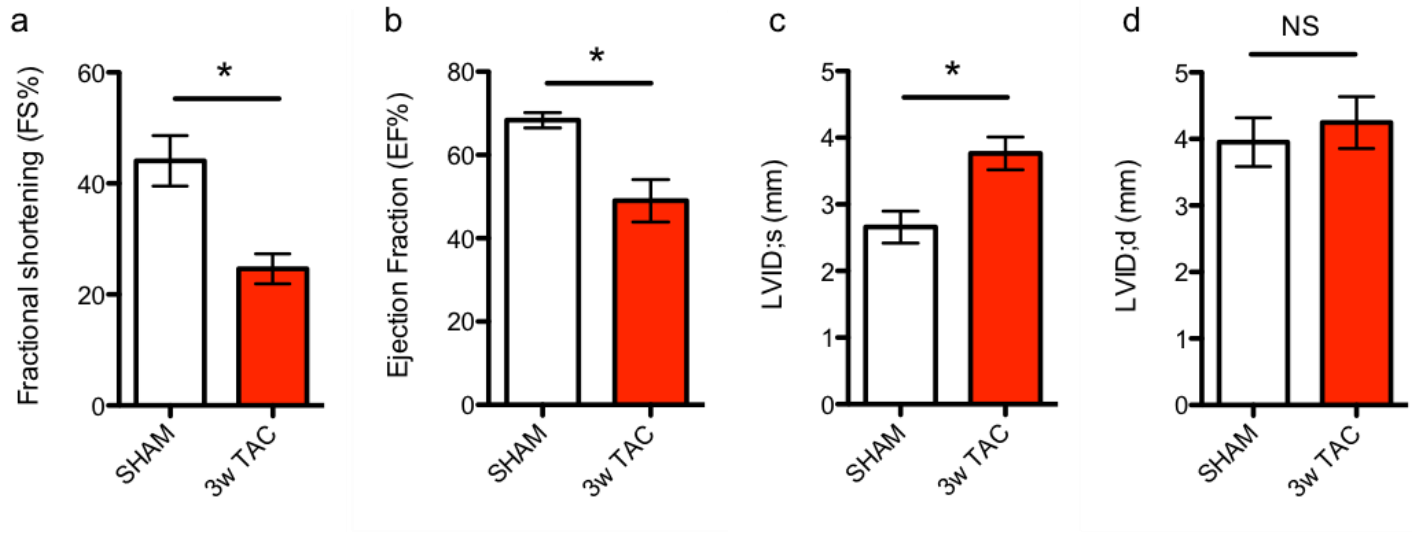

Figure 17: Transverse aortic constriction (TAC) surgery in mice causes a reduction in cardiac contractility and an increase in left ventricular dilatation by 3 weeks. (**a**) Fractional shortening (FS%), (**b**) ejection fraction (EF%), (**c**) left ventricle internal diameter (at systole) (LVID;s) and (**d**) left ventricle internal diameter (at diastole) (LVID;d) for SHAM (n=3) and 3w TAC (n=3) surgical mice. Data are shown as mean ± SEM. Statistical analysis by student's t-test; *P<0.05 versus control.

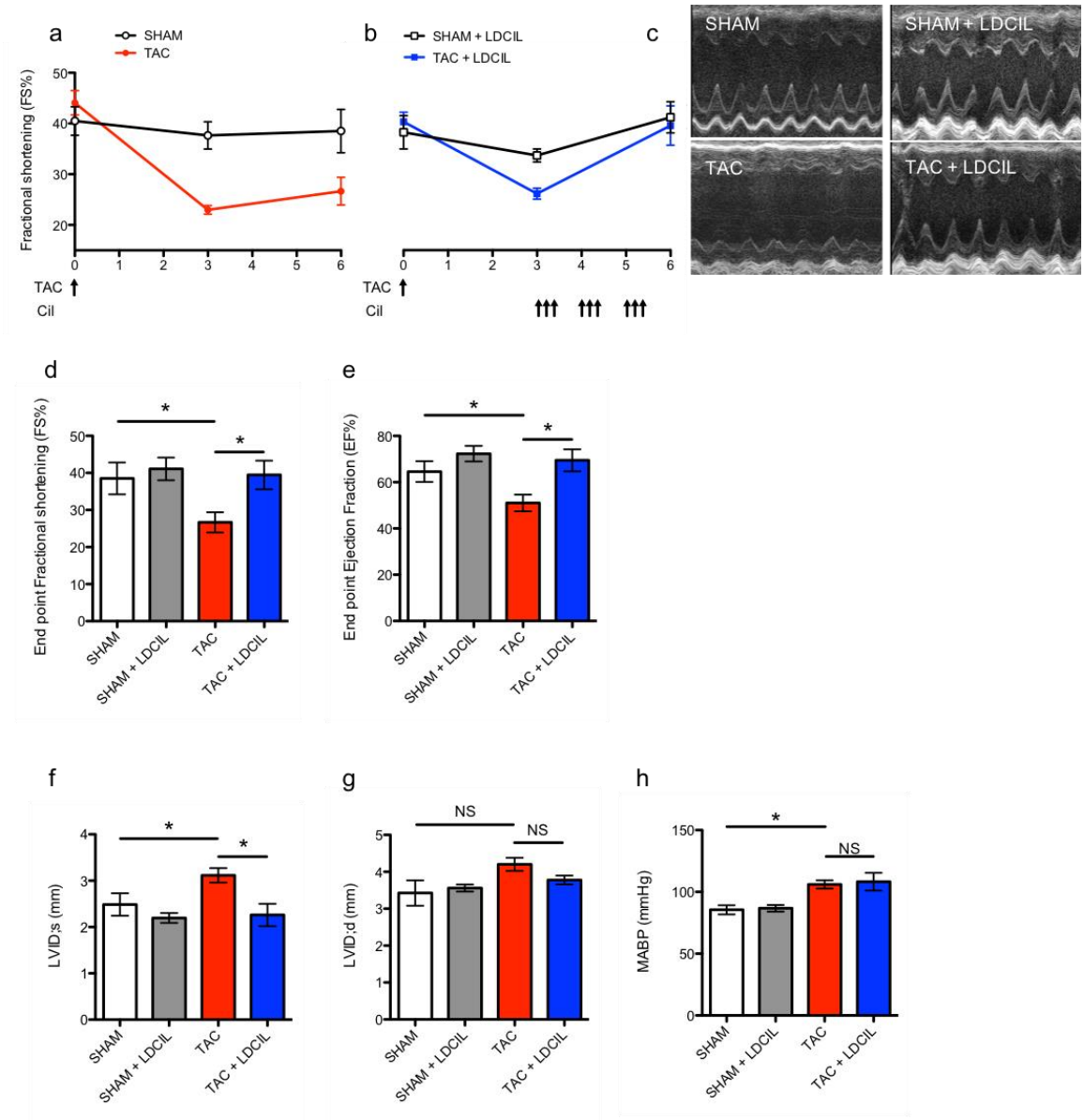

Figure 18: Pressure overload induced cardiac pathobiology is suppressed with delayed low dose Cilengitide treatment. Wild type, male, C57BL6 mice underwent either SHAM, or TAC surgery and were treated with 'low dose Cilengitide' (LDCIL) 3 weeks after surgery or used as vehicle controls. (**a-b**) Summary fractional shortening (%FS) analysis and (**c**) representative echocardiographic images in SHAM (n=6), TAC (n=7) and delayed low dose Cilengitide treatment (SHAM LD n=7) (TAC LD n=7) mice. (**d**) End point fractional shortening, (**e**) ejection fraction (%EF), (**f**) left ventricular internal diameter (during systole) (LVID;s), (**g**) left ventricular internal diameter (during diastole) (LVID;d), (**h**) and mean arterial blood pressure (MABP) across treatment groups. Data are shown as mean ± SEM. Statistical analysis by 1-way ANOVA with Tukey's multiple comparison test post hoc; *P<0.05 versus control. NS is not statistically significant.

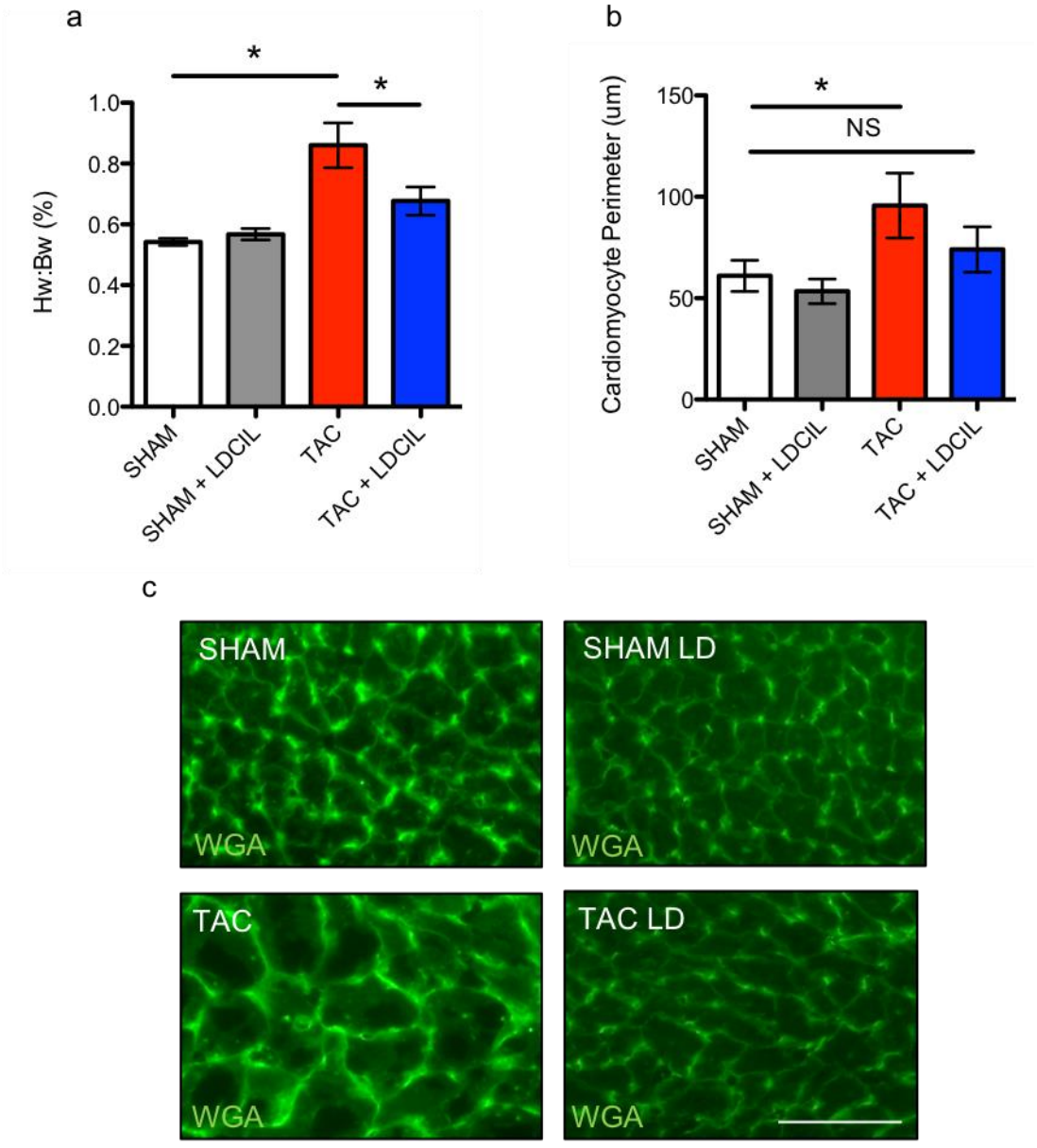

Figure 19: Pressure overload induced cardiac hypertrophy is ameliorated with delayed low dose Cilengitide treatment. Wild type, male, C57BL6 mice underwent either SHAM, or TAC surgery and were treated with 'low dose Cilengitide' (LDCIL) 3 weeks after surgery or used as vehicle controls. (**a**) Heart weight normalized to body weight (Hw:Bw %) in SHAM (n=6), TAC (n=7) and delayed low dose Cilengitide treatment (SHAM LD n=7) (TAC LD n=7) mice. (**b**) Quantitation of wheat germ agglutinin stained myocardium, with (**c**) representative image (n=3 hearts per group). Data are shown as mean ± SEM. Statistical analysis by 1-way ANOVA with Tukey's multiple comparison test post hoc; *P<0.05 versus controls. Scale bar 20µm.

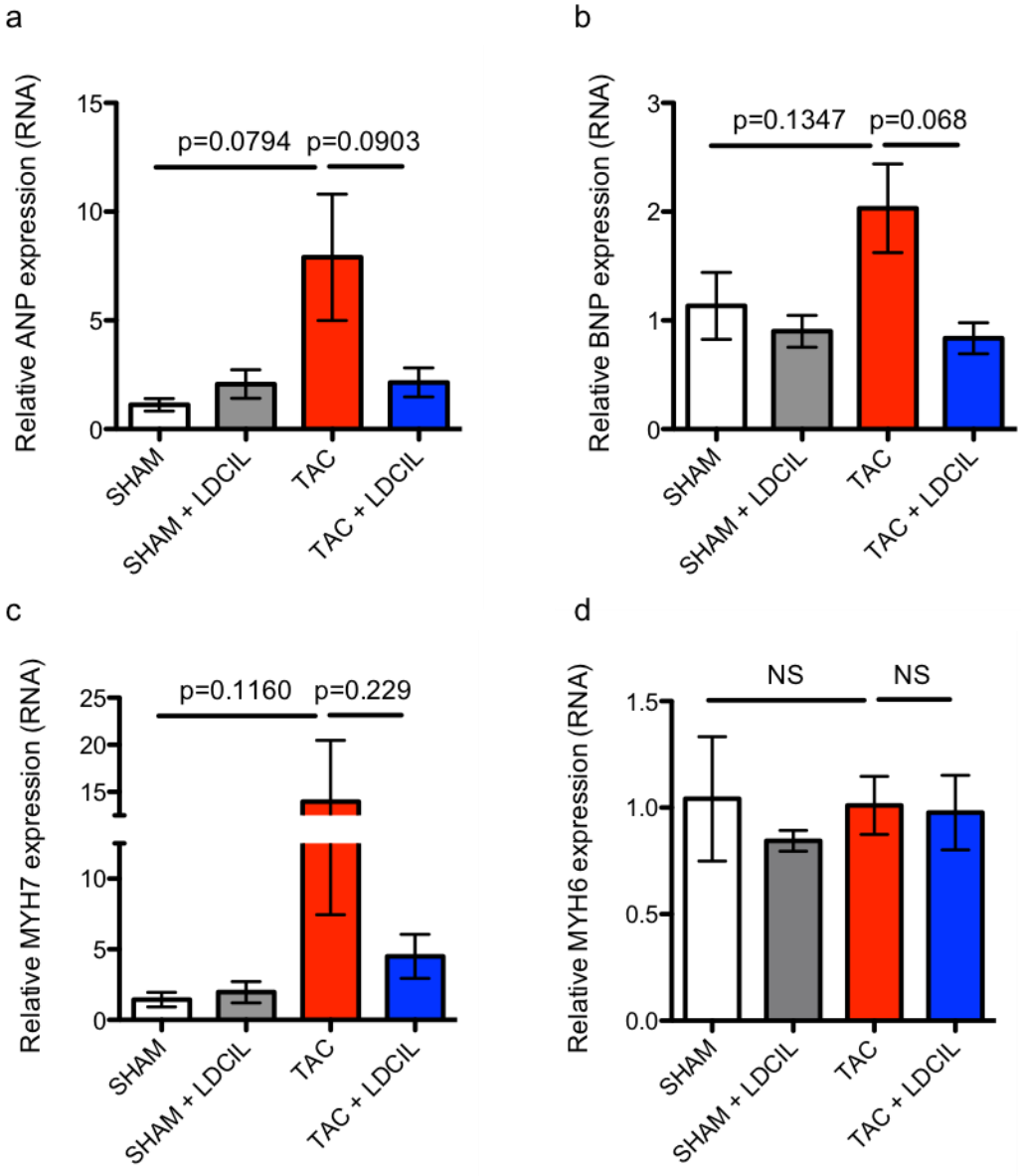

Figure 20: Pressure overload induced cardiac gene changes are ameliorated with delayed low dose Cilengitide treatment. Wild type, male, C57BL6 mice underwent either SHAM, or TAC surgery and were treated with 'low dose Cilengitide' (LDCIL) 3 weeks after surgery or used as vehicle controls. (**a-d**) ANP, BNP, MYH7 and MYH6 whole heart RNA expression levels (normalised to GAPDH) (n=6 hearts per group). Data are shown as mean ± SEM. Statistical analysis by 1-way ANOVA with Tukey's multiple comparison test post hoc; NS is not significant.

4.7 Low dose Cilengitide's cardioprotective effects continue, even after cessation of treatment

It has been reported that the beneficial effects of Cilengitide may continue even after its cessation [5]. For this reason, we performed TAC surgery, allowed heart failure to develop for 3 weeks, and then treated mice with low dose Cilengitide for 3 weeks. At 6 weeks, treatment with Cilengitide was stopped, and mice were left for a further 6 weeks before culling and post-mortem analysis.

Abdominal TAC surgery here brought about a significant change in fractional shortening within 3 weeks (average 25 FS%) (**figure 21a**) but did not induce any further deleterious changes beyond 3 weeks (average 27 FS%) (**figure 21a**). By 12 weeks the majority of the indices of disease severity, including: cardiac contractility (fractional shortening and ejection fraction), LV dilatation (LVID;s and LVID;d) and cardiac hypertrophy (heart weight relative to body weight) were not significantly different from SHAM controls (**figure 21a-g**). It is likely that cardiac contractility did not change beyond 3 weeks because by this time point it was already as low as 25% on average, which reflects a value whereby abdominal TAC surgery will rarely induce further deleterious change. In addition, by 6 weeks post-surgery one mouse from a cohort of 6 total had already died (probably due to heart failure – Hw:Bw % = 1.3, FS% = 12%), and by 12 weeks post-surgery 2 more had died (also probably due to heart failure – Hw:Bw % = 1.23, 1.18, FS% Unknown), which left only 3 mice alive from a total cohort of 6 by 12 weeks (**figure 21h**). It is thought that TAC surgery produces a variable cardiac phenotype in which only a subset of mice will develop heart failure 'proper', and others will develop

compensated LV hypertrophy, or no deleterious phenotype whatsoever [304]. Thus, it is my hypothesis that the 3 mice (from 6) that had died over the course of the experiment constituted the majority, if not all, of the heart failure developing group within the cohort. The other 3 mice will represent either those mice with compensated LV hypertrophy or those mice where TAC-surgery was relatively ineffective. **Figures 21c-g** contain only data from mice that had survived the entire 12 weeks as they represent 'end point data', meaning that within the TAC surgery group this only contains the sample of 3 that do not represent models of heart failure. A sample of 3 itself is difficult to draw meaningful conclusions from, especially considering these circumstances, and so this may be why all indices of severity within TAC-surgical groups prove to be non-significant whereas previously they have been significantly different from SHAM-surgical controls. Overall this does constitute a major caveat to the model we have chosen to use, and we will discuss this in later sections.

Despite all this, we can draw meaningful conclusion from mice undergoing TAC surgery that were treated with low dose Cilengitide. As previously, low dose Cilengitide will reverse the decline in cardiac contractility observed 3 weeks after TAC surgery (**figure 21b**). Interestingly, once treatment with Cilengitide has been stopped (i.e. at 6 weeks post-TAC), both fractional shortening and ejection fraction do not decline by the 12-week measured end-point (**figure 21b-d**). Furthermore, LV dilatation and cardiac size were 'normal' (i.e. not significantly different from control groups) in those same mice (**figure 21e-g**). Finally, treatment with low dose Cilengitide improved the survival of those mice undergoing TAC surgery – 3

‘naïve’, or untreated, mice that had undergone surgery died across the 12-week experiment from a total of 6, whereas only 1 mouse from a cohort of 6 died within the low dose Cilengitide treated surgical group (**figure 21h**). Whilst this experiment clearly had its setbacks, we think it represents some interesting preliminary evidence that low dose Cilengitide confers benefits even after its cessation in the TAC model of murine heart failure.

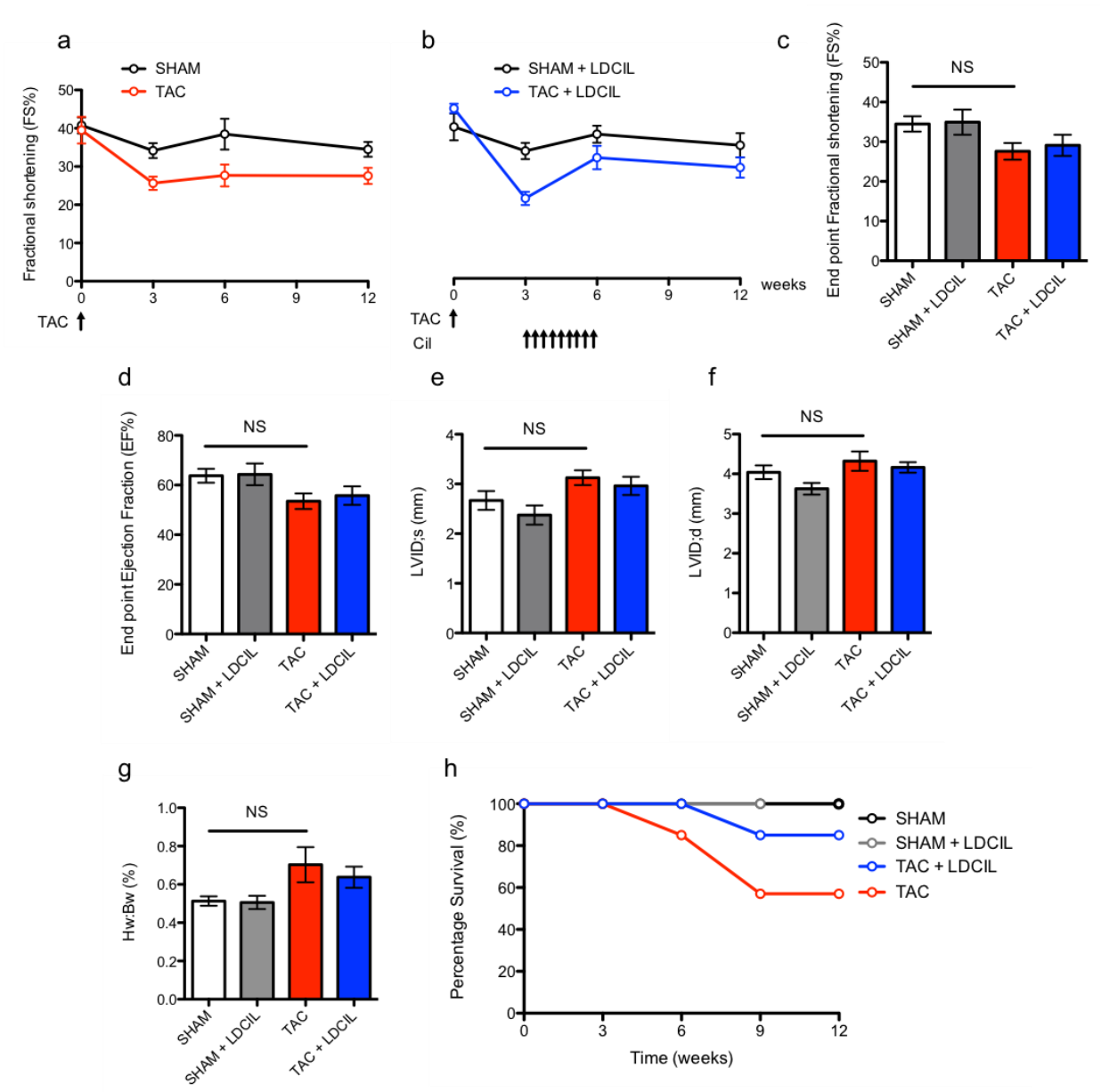

Figure 21: Low dose Cilengitide's cardioprotective effects may continue, even after cessation of treatment. Wild type, male, C57BL6 mice underwent either SHAM (n=6), or TAC (n=3) surgery and were treated with 'low dose Cilengitide' (LDCIL) 3 weeks after surgery or used as vehicle controls (SHAM treated n=6, TAC treated n=5). After 3 weeks treatment was stopped, and mice were monitored for a further 6 weeks. (**a-b**) Summary fractional shortening (%FS) analysis, (**c**) end point fractional shortening, (**d**) end point ejection fraction (EF%) and end point left ventricular internal diameter at (**e**) systole (LVID;s) and (**f**) diastole (LVID;d). (**g**) Heart weight normalized to body weight and (**h**) percentage survival. Data are shown as mean ± SEM. NS is not significant.

4.8 Treatment with low dose Cilengitide enhances cardiac angiogenesis *in vivo*

Pressure-overload induced heart failure (TAC) will modulate cardiac angiogenesis in the heart by modifying both the capillary density itself and the total number of pericytes present overall [119]. *Souders et al.* used a thoracic TAC model to detail these observations, so first we sought to investigate whether not abdominal TAC, which is a milder and slower onset model of heart failure, would yield similar results. To this end, we performed TAC surgery and culled mice at either 2, 3 or 6-weeks post-surgery and measured their blood vessel number against age-matched hearts from SHAM-surgical control mice. In order to count blood vessel number, we took 5 fields of view at 40x magnification per heart and counted the number of CD31+ blood vessels. From 2-6 weeks post-TAC surgery the number of blood vessels within the heart did not change significantly (**figure 22a-b**). However, TAC surgery will induce cardiac hypertrophy by 6 weeks, which means that the blood vessel density, or the number of blood vessels per cardiomyocyte, may actually be higher between controls and those hearts 6 weeks post-TAC surgery. To measure this, we stained serial sections of myocardium with CD31 and then WGA and counted both the number of CD31+ blood vessels and the number of WGA+ cells across 5 fields of view at 40x magnification per heart. CD31 is a marker of endothelial cells, and thus blood vessels, whilst WGA will mark cell borders but has previously been used by myself and other lab members to also determine cardiomyocyte size [298]. The number of CD31+ blood vessels per WGA+ cell was not significantly increased between those mice receiving SHAM,

or TAC surgery after 6 weeks, but the result did tend toward significance (**figure 22c**). Potentially a reduction in capillary density in those mice undergoing TAC surgery may generate an imbalance in the amount of oxygen delivered to cardiomyocytes, and thus potentiate a relative local ischemia, which in turn could lead toward the transition from compensated to uncompensated heart failure. A higher sample size may yield more powerful observations in this study and is worth pursuing, especially considering the data generated by *Souders et al* [119]. Furthermore, we did not assess the number of vessels relative to cell size in mice 2 or 3-weeks post-TAC surgery. This time point may represent a view of when hearts initially develop failure in the TAC model, and so is worthy of study. Because the hearts of those mice do not display an increase in actual vessel number, and it is unlikely that the cardiomyocytes of those mice are any larger than at 6 weeks post-TAC surgery, it is unlikely we would receive more positive data if we were to analyse it as blood vessel number per cardiomyocyte as previously. However, the structure of vessels may change at this time point, or their association with pericytes and other mural cells, so this is worth investigating.

Low dose Cilengitide increases angiogenesis across various murine tumour models [4]. It is my hypothesis that any functional improvements observed in cardiac disease indices following treatment with low dose Cilengitide may be partly due to an increase in cardiac angiogenesis. In order to study this, we double stained myocardium for CD31 and α-smooth muscle actin (α-SMA), which has been used by lab members to successfully mark mural cells in the past [305, 306].

CD31 will identify most, if not all, vessels in the heart, including much of the small capillary microvasculature. α-SMA on the other hand will label only those vessels supported by mural cells, which constitutes most vessels larger than capillaries.

The number of blood vessels in the hearts of those mice 6 weeks post-TAC surgery increased modestly (but not significantly) versus SHAM controls (**figure 23a-b**), which is in line with previous observations made in **figure 22**. Interestingly, low dose Cilengitide increased cardiac angiogenesis significantly in those mice that underwent TAC surgery, but not in those mice that underwent SHAM-surgical control (**figure 23a-b**).

In order to determine whether or not the number of 'mature', or mural cell covered, vessels changed between groups we analysed data from α-SMA and CD31 stained myocardium. In general, α-SMA+ vessels constitute a very small fraction of overall vessels in the heart. For a given 40x field of view they represent around 1-4% of total vessels (**figure 23c-d**). This did not change between samples, and the total number of α-SMA+ vessels totalled across 10 fields of view was the same across groups (**figure 23c-d**). In order to more accurately sample the number of α-SMA+ vessels in the myocardium between hearts, we attempted to measure this figure in the entire heart and then match this against the overall size of the heart itself, but we were not able to do this within the available time.

Overall this shows that low dose Cilengitide will enhance cardiac angiogenesis in a murine model of heart failure. The exact disposition and physiology of these vessels is unknown but would be a useful avenue of study if we had more time.

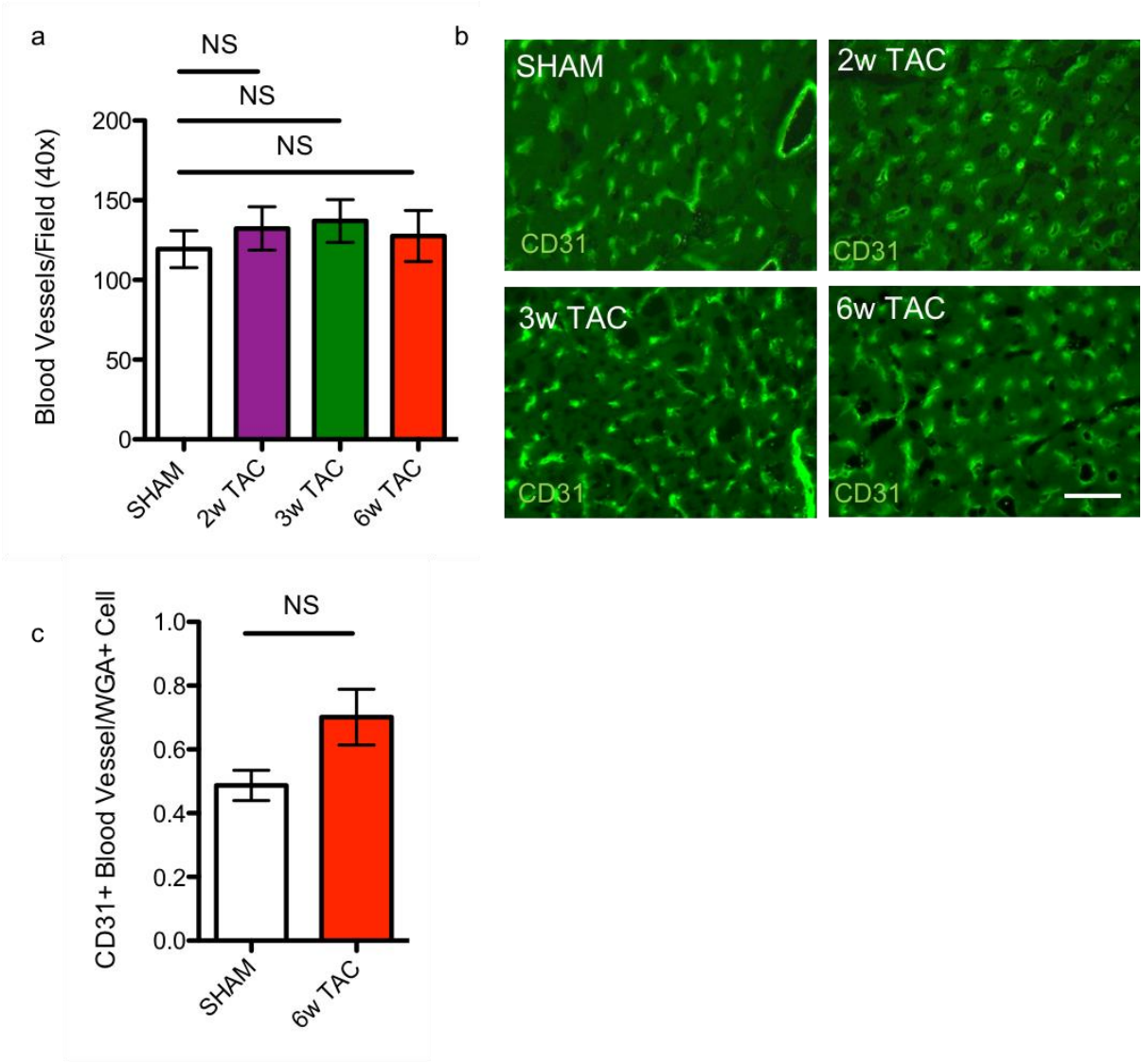

Figure 22: Cardiac blood vessel number does not differ temporally after TAC surgery. (**a**) CD31+ blood vessel number per field of view (at 40x magnification) with (**b**) representative CD31 stained mouse myocardium. (**c**) CD31+ blood vessel number per wheat germ agglutinin positive (WGA +) cell number. Data are shown as mean ± SEM. Statistical analysis by 1-way ANOVA with Tukey's multiple comparison post hoc (if greater than 2 groups) or student's t-test (if less than 3); NS is not significant. Scale bars 20μm.

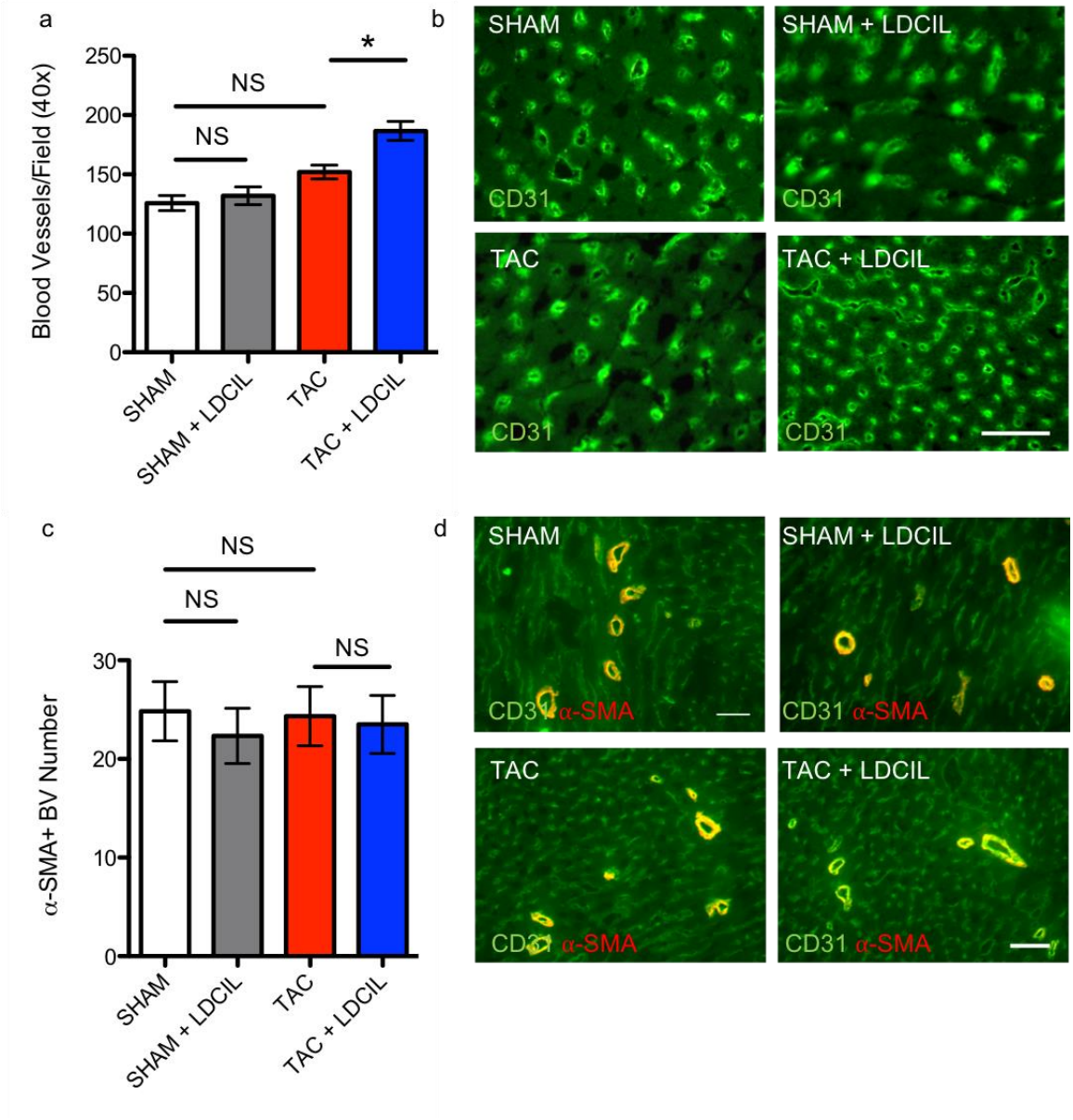

Figure 23: Treatment with low dose Cilengitide enhances cardiac angiogenesis *in vivo.* Wild type, male, C57BL6 mice underwent either SHAM, or TAC surgery and were treated with 'low dose Cilengitide' (LDCIL) 3 weeks after surgery or used as vehicle controls. (**a**) CD31+ blood vessel number per field of view (at 40x magnification) with (**b**) representative CD31 stained mouse myocardium. (**c**) α-smooth muscle actin (SMA) positive blood vessel number across 10 fields of view (at 40x magnification) with (**d**) representative images of α-SMA and CD31 stained myocardium. Data are shown as mean ± SEM. Statistical analysis by 1-way ANOVA with Tukey's multiple comparison test post hoc; *P<0.05 versus control, NS is not significant. Scale bars 30μm.

4.9 Low dose Cilengitide as a dual function therapy for the treatment of heart failure (effect on cardiac endothelial cells)

The next question we sought to investigate was whether or not mouse cardiac endothelial cells and cardiomyocytes will express β3 and β5 integrin receptor subunits, and if so in what relative quantities. This serves the dual purpose of corroborating the evidence we have already accumulated in human hearts, whilst also being the first in a set of experiments that aims to uncover why low dose Cilengitide demonstrates efficacy in a murine model of heart failure. To this end, we isolated cardiac endothelial cells and cardiomyocytes from mouse hearts, cultured cells for a period of time and then quantified the relative β3 and β5 mRNA and protein expression levels within isolates by RT-qPCR and western blot analysis. At the RNA level, endothelial cells express significantly more β3- integrin than corresponding cardiomyocytes, whereas cardiomyocytes express significantly more β5- integrin (**figure 24a-d**). Both integrins are expressed relatively abundantly in cells despite overall apparent differences (qPCR threshold cycle 22-28 – **figure 24c-d**). Western blot analysis reveals diverging results. Here, β3- integrin is upregulated in endothelial cells, as is β5- integrin versus cardiomyocytes. This may indicate that there is less overall translation in the cardiomyocytes of β5- integrin than endothelial cells, despite their being relatively more transcription of β5- integrin in those same cardiomyocytes. Interestingly, we have observed in both human and mouse myocardium sections that β5- integrin appears to be relatively more present in the cardiomyocytes and β3- integrin in the endothelial cells. These results may reflect the fact that we are using isolated foetal

cardiomyocytes to assess β5- integrin in **figure 24**, which may not perfectly recapitulate the same protein expression pattern that is observed in adult cardiomyocytes. In addition, cardiomyocytes will certainly behave differently in culture than *in vivo,* and so may differentially express integrins according to their culture period and strategy.

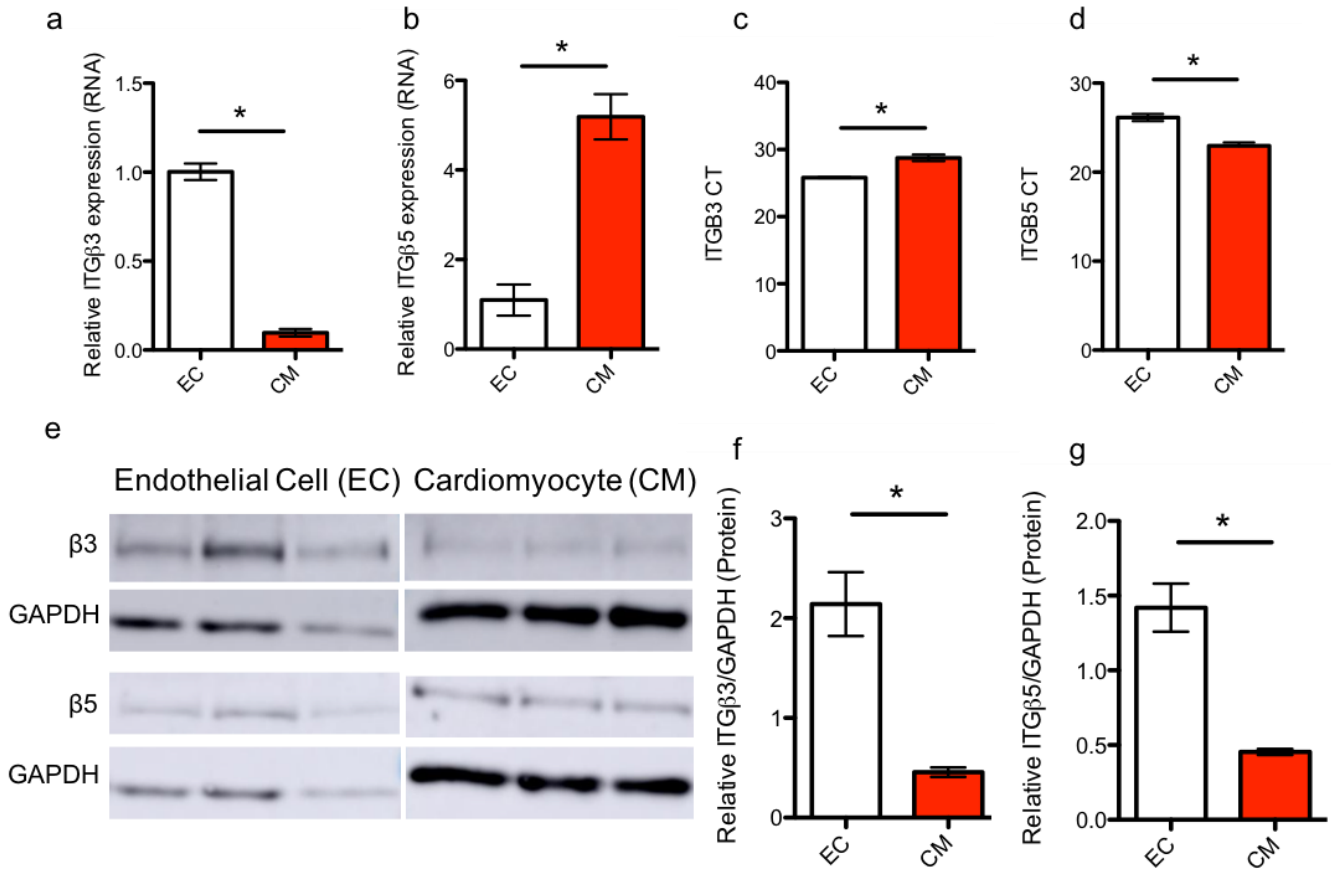

Figure 24: Isolated cardiomyocytes and cardiac endothelial cells express β3 and β5 integrin receptor subunits in differing relative quantities. Mouse cardiac endothelial cells and cardiomyocytes were isolated as described and β3 and β5 integrin expression quantified using (**a-d**) RT-qPCR or (**e-g**) western blots. Data are shown as mean ± SEM. Statistical analysis by student's t-test; *P<0.05 versus control.

After having established that mouse cardiomyocytes and cardiac endothelial cells did in fact express β3- and β5- integrin, we next investigated the mechanism of action underpinning Cilengitide's cardioprotective effects *in vivo*. To do this we isolated cardiac endothelial cells and cardiomyocytes *in vitro* and extracted RNA for RNA-Seq analysis. This allowed me to sample the entire genome for potential genetic targets of interest in cells both treated and untreated.

500,000 endothelial cells were seeded in a T25 flask, serum starved for 24 hours, treated with either vehicle or low dose Cilengitide for 24 or 48 hours and then lysed for RNA-seq analysis. Briefly, raw reads were first aligned to the reference genome GRCm38/mm10 using HISAT2, at which point the number of uniquely aligned reads (q>10) which aligned to the exonic region of each gene was counted using HTseq. Only those genes that achieved at least one read per million reads (CPM) in at least 2 samples were kept, which gave us 13,459 filtered genes in total. Reads were further normalised using the 'cqn' method, accounting for gene length and GC content. Those filtered genes were analysed using initial principle component analysis (PCA), which revealed that between samples of the same group, the differential gene profile was wholly similar, indicating that within treatment groups different samples display an overall similar response to either vehicle or Cilengitide (**figure 25a**). As the separation was clear between groups, this means that differentially expressed genes in the future section were identified based upon FDR $q < 0.05$ and an absolution value of $\log2FC > 1$. Differential expression (DE) analysis was performed using the 'limma' R package.

Under the microscope low dose Cilengitide treated endothelial cells appeared modestly more confluent than vehicle controls within 48 hours, and similarly elongated within the available flask space. Morphologically they were very similar, and if allowed to reach confluence, both treated and untreated cardiac endothelial cells exhibit a classic endothelial cobblestone morphology. After 24-hours of low dose Cilengitide treatment cardiac endothelial cells exhibit 146 differentially expressed genes versus vehicle controls (FDR $q < 0.05$ and absolute log2FC >1) of a total 13,459 filtered genes sampled. Of these, 36 transcripts are upregulated and 116 downregulated. For the top 10 most differentially regulated genes see **table 16**. Genes of interest which have previously been implicated as important or novel players during angiogenesis are highlighted and will be discussed later. These include: Mt2, Csf2rb, Nov, and Bcl6.

At a whole pathway level, the most upregulated pathways include: cell-cycle mitosis, DNA-replication, cell-cycle transition and DNA-strand elongation (**figure 26a**). Angiogenesis relies upon a complex balance of stimuli which will balance and modulate endothelial cell migration and proliferation [38]. In theory, active DNA-replication, mitosis and cell-cycle transition could point to the fact that cells are in an ‘active’ state of turnover or proliferation. Thus, for perhaps the first time these pathways combined appear to point to the fact that low dose Cilengitide will promote cardiac endothelial cell proliferation *in vitro*, which is a major driving force underpinning angiogenesis [307]. However, this conclusion needs to be tested

and/or verified with e.g. a cell-counting *in vitro* assay. In addition, the small sample size used in these preparations may have had an impact on results and need to be increased in future.

After 48-hour treatment, many of those genes differentially expressed were similar to that which were differentially expressed after 24 hours of treatment. Versus vehicle controls, 107 genes are differentially expressed, of which 30 are upregulated and 77 downregulated, (FDR $q < 0.05$ and absolute log2FC >1) (of a total 13,459 filtered genes sampled). For the most differentially regulated genes see **table 17**. At a pathway level, the most enriched pathways correlate to: cell cycle mitosis reactome, cell cycle transition and DNA-replication (**figure 27a**). Between 24 and 48-hour treatments, only 54 genes were differentially expressed between groups, but none of these genes passed an FDR $q < 0.05$ threshold, indicating the two group's overall similarity.

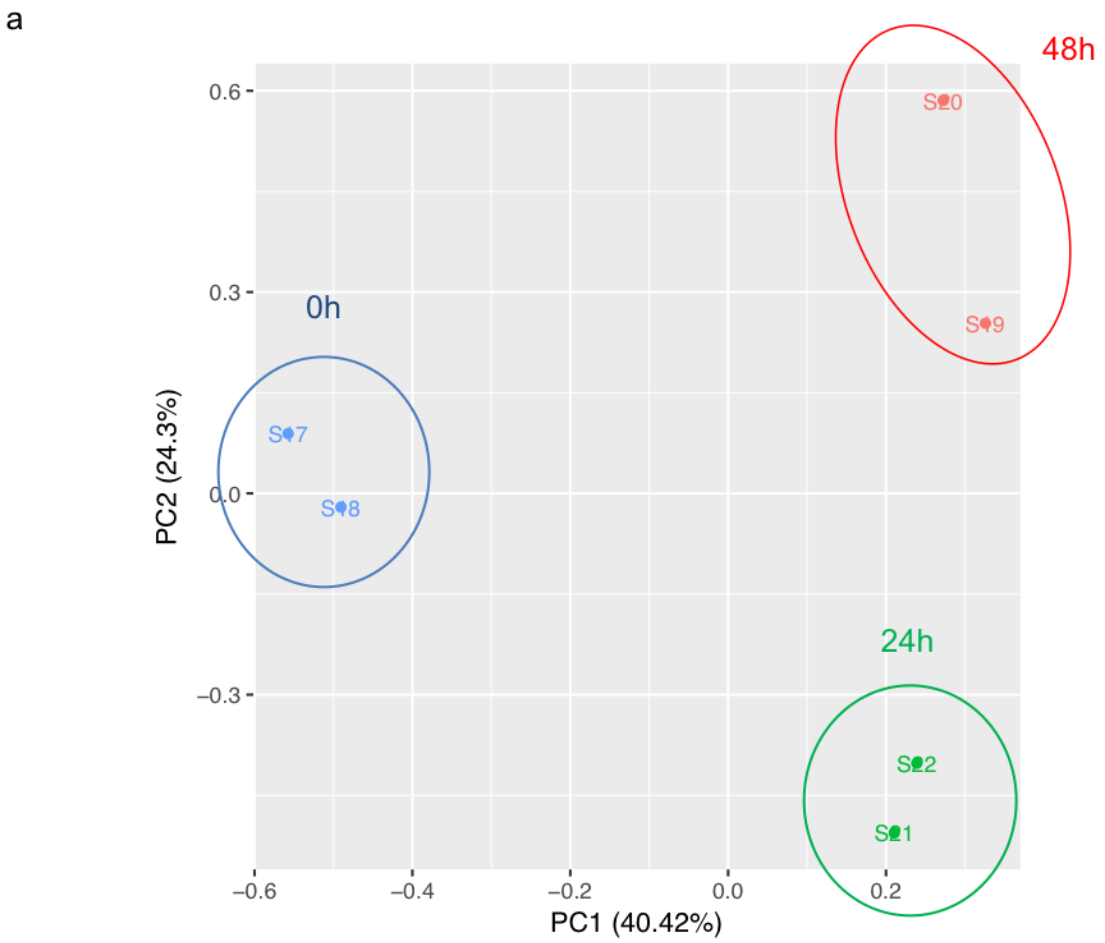

Figure 25: Principle component analysis (PCA) demonstrates good clustering between cardiac endothelial cells treated with low dose Cilengitide. Cardiac endothelial cells were plated, treated for 0, 24 or 48 hours with low dose Cilengitide (n=2 per group) and then isolated, sequenced via RNA-Seq, and clustered with PCA analysis. (**a**) Principle component analysis of treated cells.

Gene Name	Log Fold Change (FC) 24h LDCIL vs Control	Description
Mt2	4.60717235	metallothionein 2 [Source:MGI Symbol;Acc:MGI:97172]
Fgf23	4.3769134	fibroblast growth factor 23 [Source:MGI Symbol;Acc:MGI:1891427]
Mt1	2.88623252	metallothionein 1 [Source:MGI Symbol;Acc:MGI:97171]
Csf2rb	1.93229863	colony stimulating factor 2 receptor, beta, low-affinity (granulocyte-macrophage) [Source:MGI Symbol;Acc:MGI:1339759]
Nov	1.90298234	nephroblastoma overexpressed gene [Source:MGI Symbol;Acc:MGI:109185]
Hey2	-2.1800461	hairy/enhancer-of-split related with YRPW motif 2 [Source:MGI Symbol;Acc:MGI:1341884]
Lmntd2	-2.1884053	lamin tail domain containing 2 [Source:MGI Symbol;Acc:MGI:1919250]
Bcl6	-2.7046606	B cell leukemia/lymphoma 6 [Source:MGI Symbol;Acc:MGI:107187]
Mpl	-2.9459403	myeloproliferative leukemia virus oncogene [Source:MGI Symbol;Acc:MGI:97076]
Ankrd55	-3.1127775	ankyrin repeat domain 55 [Source:MGI Symbol;Acc:MGI:1924568]

Table 16: Top 10 most differentially expressed genes in cardiac endothelial cells after 24-hour low dose Cilengitide treatment. Bold denotes angiogenesis-related genes that will be discussed later.

Gene Name	Log Fold Change (FC) 48h LDCIL vs Control	Description
Mt2	5.37494602	metallothionein 2 [Source:MGI Symbol;Acc:MGI:97172]
Fgf23	4.71331743	fibroblast growth factor 23 [Source:MGI Symbol;Acc:MGI:1891427]
Mt1	3.182225	metallothionein 1 [Source:MGI Symbol;Acc:MGI:97171]
Csf2rb	2.88230495	colony stimulating factor 2 receptor, beta, low-affinity (granulocyte-macrophage) [Source:MGI Symbol;Acc:MGI:1339759]
Csf2rb2	2.59823504	colony stimulating factor 2 receptor, beta 2, low-affinity (granulocyte-macrophage) [Source:MGI Symbol;Acc:MGI:1339760]
Nov	2.49984628	nephroblastoma overexpressed gene [Source:MGI Symbol;Acc:MGI:109185]
Ankrd55	-2.4914517	ankyrin repeat domain 55 [Source:MGI Symbol;Acc:MGI:1924568]
Bcl6	-2.5118543	B cell leukemia/lymphoma 6 [Source:MGI Symbol;Acc:MGI:107187]
Gm567	-2.5485162	predicted gene 567 [Source:MGI Symbol;Acc:MGI:2685413]
Mpl	-2.7282001	myeloproliferative leukemia virus oncogene [Source:MGI Symbol;Acc:MGI:97076]

Table 17: Top 10 most differentially expressed genes in cardiac endothelial cells after 48-hour low dose Cilengitide treatment.

a

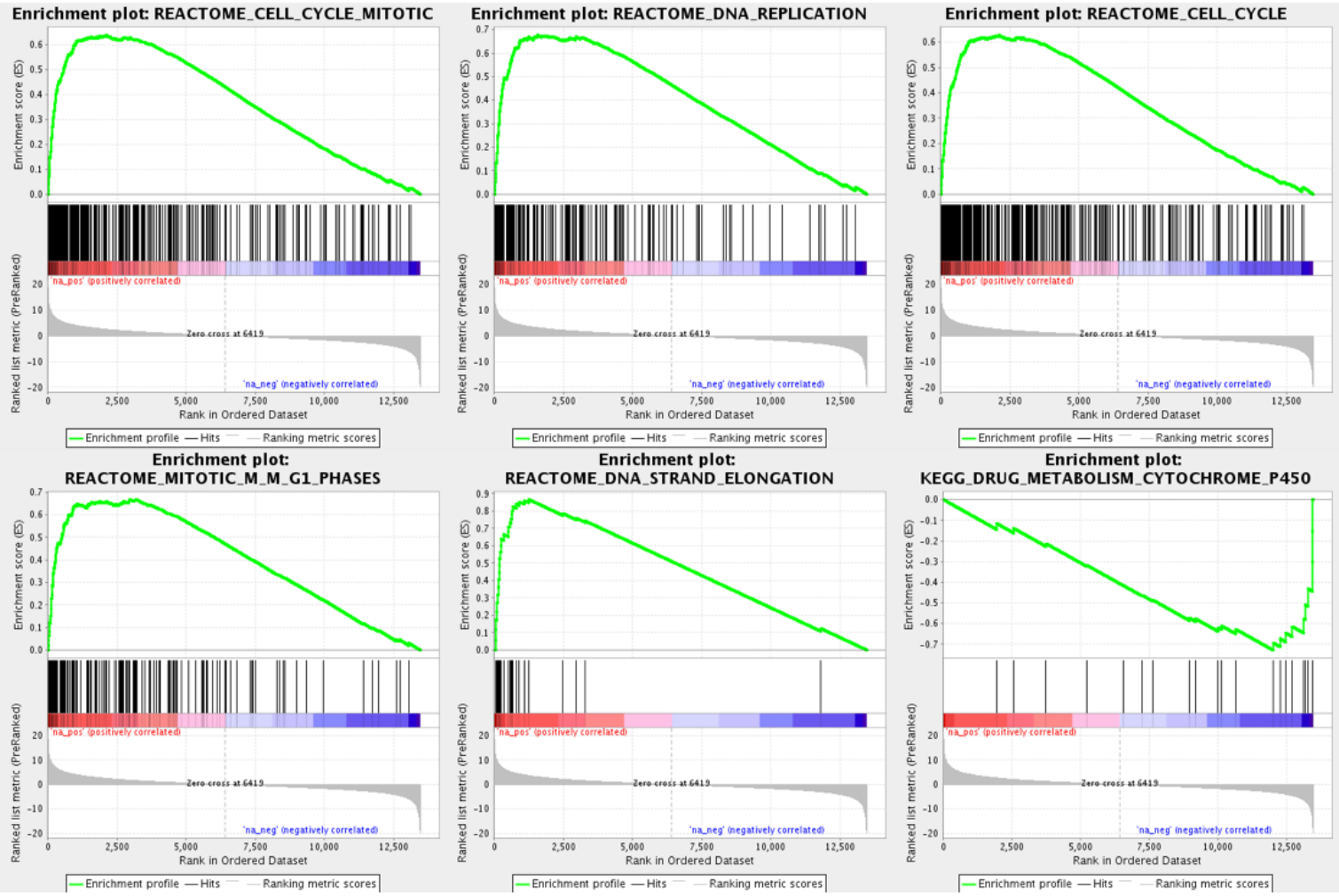

Figure 26: Low dose Cilengitide stimulates DNA-replication, mitosis and cell-cycle transition in cardiac endothelial cells *in vitro* within 24 hours. (**a**) Enrichment plot analysis for those whole pathways enriched in 24 hour treated cells (n=2), versus untreated controls (n=2).

a

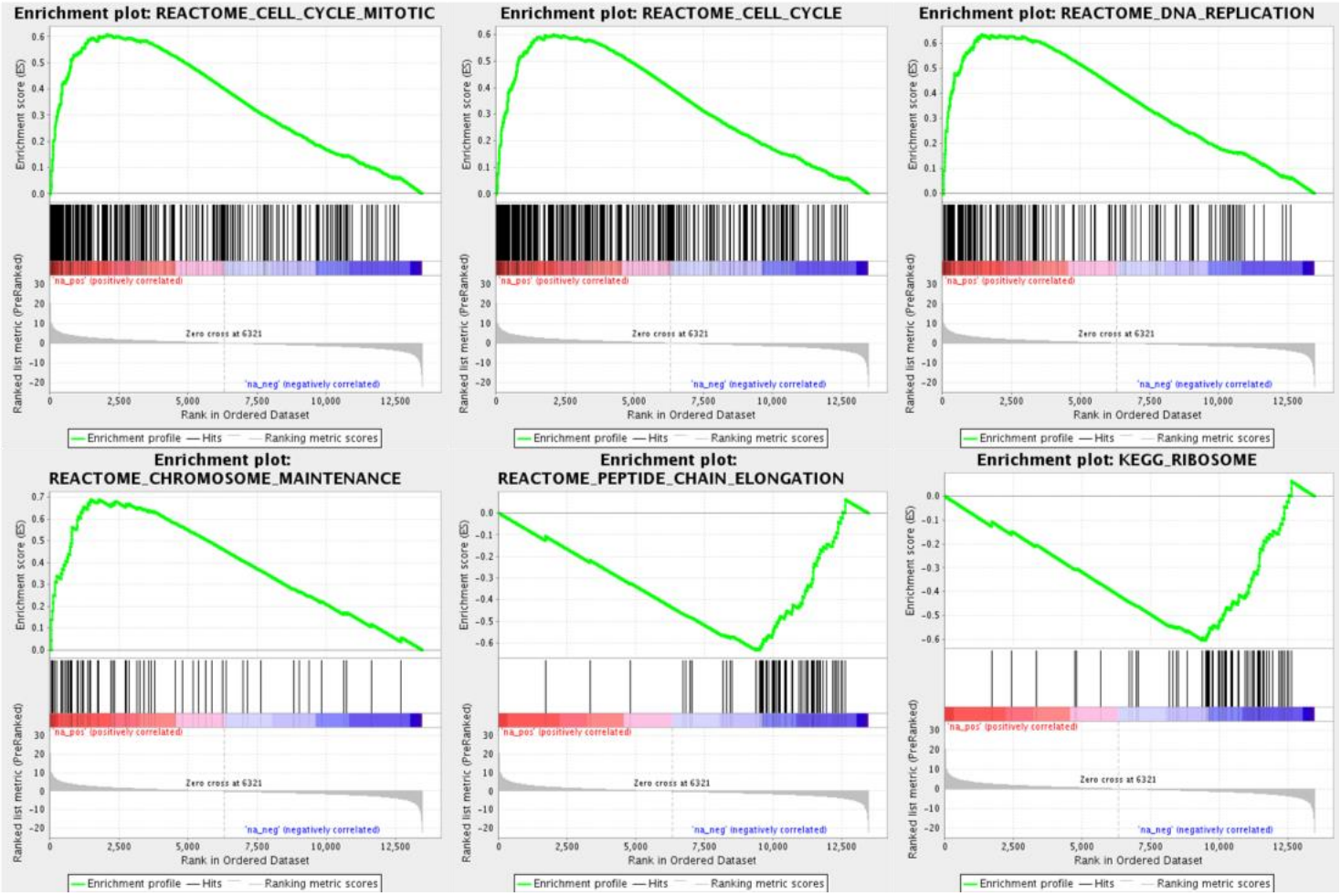

Figure 27: Low dose Cilengitide stimulates DNA-replication, mitosis and cell-cycle transition in cardiac endothelial cells *in vitro* within 48 hours. (**a**) Enrichment plot analysis for those whole pathways enriched in 48 hour treated cells (n=2), versus untreated controls (n=2).

4.10 Low dose Cilengitide as a dual function therapy for the treatment of heart failure (effect on cardiomyocytes)

We have previously shown that both mouse and human cardiomyocytes express β3 and β5 integrin receptor subunits. This means that low dose Cilengitide could potentially be an effector of these cells to modify their underlying behaviour. Indeed, integrin-based modulation by external reagents can play a pivotal role in determining the health and biological activity of cardiomyocytes [308], but is not currently a well understood area of research. Because of this, we believe it is reasonable to postulate that Cilengitide may serve a dual purpose by potentiating effects in both cardiac endothelial cells and cardiomyocytes after administration. To study the mechanism underpinning the function, if any, of low dose Cilengitide in cardiomyocytes, we isolated cells from 1-3-day old pups, seeded cells at a density of 1 million cells per 6 well dish, and left them for 3 days before performing assays. The extraction of cardiomyocytes from pups did not involve any cell-specific isolation techniques, and so cells must be left for 3 days (if not longer) to ensure media selection and enrichment of a cardiomyocyte population. Cultured cardiomyocytes proved to be very difficult to assay – they are not proliferative, begin to die within 6-7 days and the overall yield between preparations can vary drastically. The assay we eventually decided to use was to add angiotensin II (1µm for 48 hours) to cardiomyocyte media, which will generate cardiomyocyte hypertrophy within 24 hours. This same phenotype could then be assessed with or without low dose Cilengitide. Angiotensin II induces cardiomyocyte hypertrophy *in vitro* through the activation of protein kinase cascades, initiation of a foetal-like

gene program, impairment of calcium handling, and increasing the production of reactive oxygen species [309] [310] [311] [312]. In my hands, angiotensin II induced significant cardiac hypertrophy in treated cells within 24-hours (**figure 28a-b**).

Having established that angiotensin II will induce hypertrophy amongst cardiomyocytes, we investigated the effects of low dose Cilengitide in the cardiomyocyte using RNA-seq analysis. Here, we investigated vehicle control cardiomyocytes (n=3), angiotensin II (n=4), low dose Cilengitide (n=4) and angiotensin II and low dose Cilengitide combined treated cardiomyocytes (n=4). The analysis of these samples was made difficult due to the fact that low dose Cilengitide and low dose Cilengitide-angiotensin II treated cells exhibit large intra-sample variation, as demonstrated by poor sample clustering in PCA (**figure 29a**). It was evident that, especially in low dose Cilengitide (alone) treated samples, that there were 2 samples that were similar to control cardiomyocytes, and two samples similar to angiotensin II treated cells (**figure 29a**). The method we used to isolate cardiomyocytes does not guarantee that preparations will be 100% ‘pure’ (i.e. consist of solely cardiomyocytes). Indeed, we estimate that a single well will consist of an average of 70% cardiomyocytes, with the rest appearing to be a mixture of endothelial cells and fibroblasts. This estimate is based upon the ratio of ‘beating’ to ‘non-beating’ cell-types. Between samples, and certainly between different preparations, there can be a large amount of variation in the purity of

cardiomyocytes, and this may explain the large intra-sample variation exhibited by some groups.

To examine whether or not low dose Cilengitide will ameliorate the deleterious effects of angiotensin II in cardiomyocytes we compared RNA-seq pathway and gene analysis data from vehicle control, angiotensin II treated and angiotensin II-low dose Cilengitide treated cells. This allowed us to highlight first specific genes, and next whole pathways, that were enriched in cardiomyocytes after the addition of Cilengitide. **Table 18** shows those genes that are most enriched concordantly between control samples and angiotensin II-low dose Cilengitide treated cardiomyocytes, that have already been published in the cardiovascular field. Comparing control to Cilengitide-angiotensin II treated cardiomyocytes allowed us to establish a 'healthy' genetic baseline profile. For instance, both Irs2 and Glul are upregulated within control and angiotensin II-low dose Cilengitide treated cardiomyocytes, whilst they are downregulated in samples treated only with angiotensin II. Thus, they represent genes that may restore cardiomyocytes to a 'healthier' phenotype after the addition of Cilengitide. In addition, we identified several whole signalling pathways that became differentially regulated by treating cardiomyocytes with Cilengitide in tandem to angiotensin II (**figure 30a**). Of these, the most interesting was the fact that that angiotensin II alone will downregulate the PI3K-Akt pathway, but this pathway is moderately upregulated in those same cardiomyocytes also treated low dose Cilengitide (**figure 30a**). This may suggest

that low dose Cilengitide may upregulated PI3k-Akt signalling in cardiomyocytes. This will be discussed in further detail later.

Next, we aimed to add human relevance to the *in vitro* observations and data we had already accumulated. To do this, we took available human microarray and RNA-seq data from *Liu et al.* [313] and compared this to my own *in vitro* RNA-Seq data. The human dataset included data from 6 RNA-seq and 313 microarray data sets - and included information from two subsets of heart failure: ischemic heart disease and dilated cardiomyopathy. The first question we asked was whether treating cardiomyocytes with angiotensin II results in changes to similar genes, or whole pathways, to that which were differentially expressed amongst heart failure patients. Interestingly, angiotensin II treated cardiomyocytes expressed a surprisingly similar number of differentially expressed whole pathways to that of ischemic and idiopathic dilated heart failure (**figure 31a-b**). Indeed, many of these enriched pathways were concordantly dysregulated between angiotensin II treated cardiomyocytes and human heart failure patients (**figure 31c-d**). This analysis provides novel evidence that angiotensin II will recapitulate many of the whole pathway features of human heart failure, which adds increasing validity to the model we have chosen to use. Having taken this into account, we sought to measure what whole pathways were most enriched across control cardiomyocytes, non-failing human heart patients and angiotensin II-low dose Cilengitide treated cardiomyocytes (**figure 32 and 33**). This was used to establish a ‘normal’ or ‘healthy’ pathway expression signature, which can point to a pathway

which underpins the effect of low dose Cilengitide in cardiomyocytes. Between pathways we found that a commonly upregulated ‘healthy’ signalling effector was PI3K-Akt, and a downregulated ‘healthy’ signalling effector was the TCA cycle. PI3K-Akt is relatively upregulated with low dose Cilengitide treatment, whereas TCA cycle metabolism is downregulated across all pathway analysis. The PI3K-Akt pathway will be discussed in more detail later.

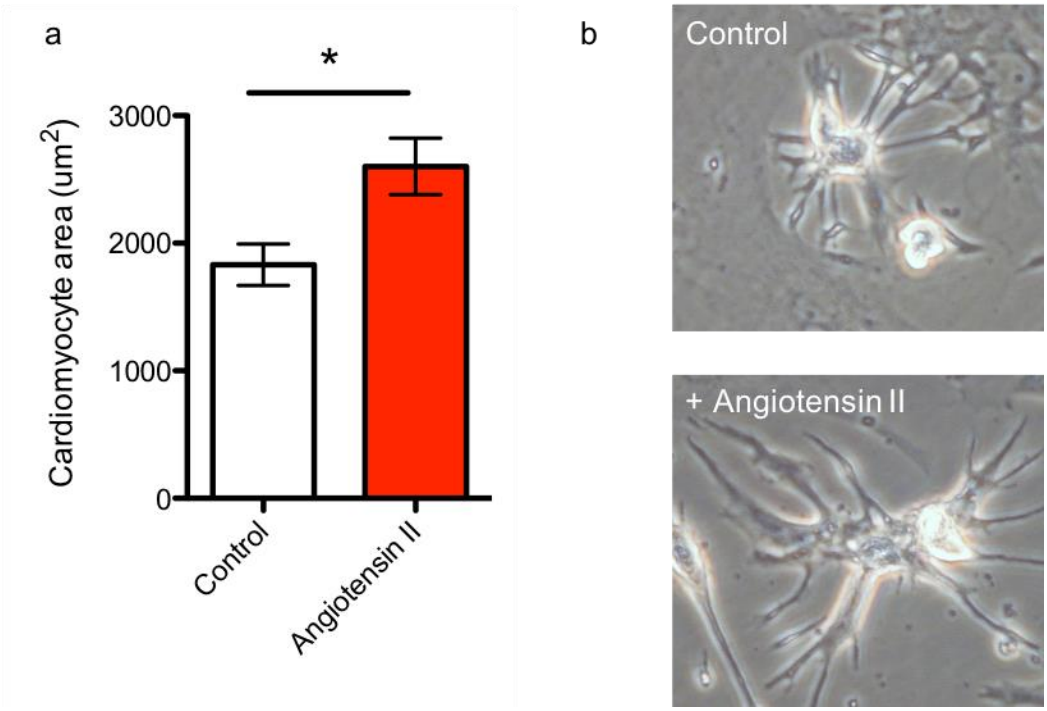

Figure 28: Angiotensin II induces cardiac hypertrophy *in vitro*. (**a**) Cardiomyocyte area in control and angiotensin II treated cardiomyocytes (n=50 cells) and (**b**) representative images. Data are shown as mean ± SEM. Statistical analysis by student's t-test; *P<0.05 versus control.

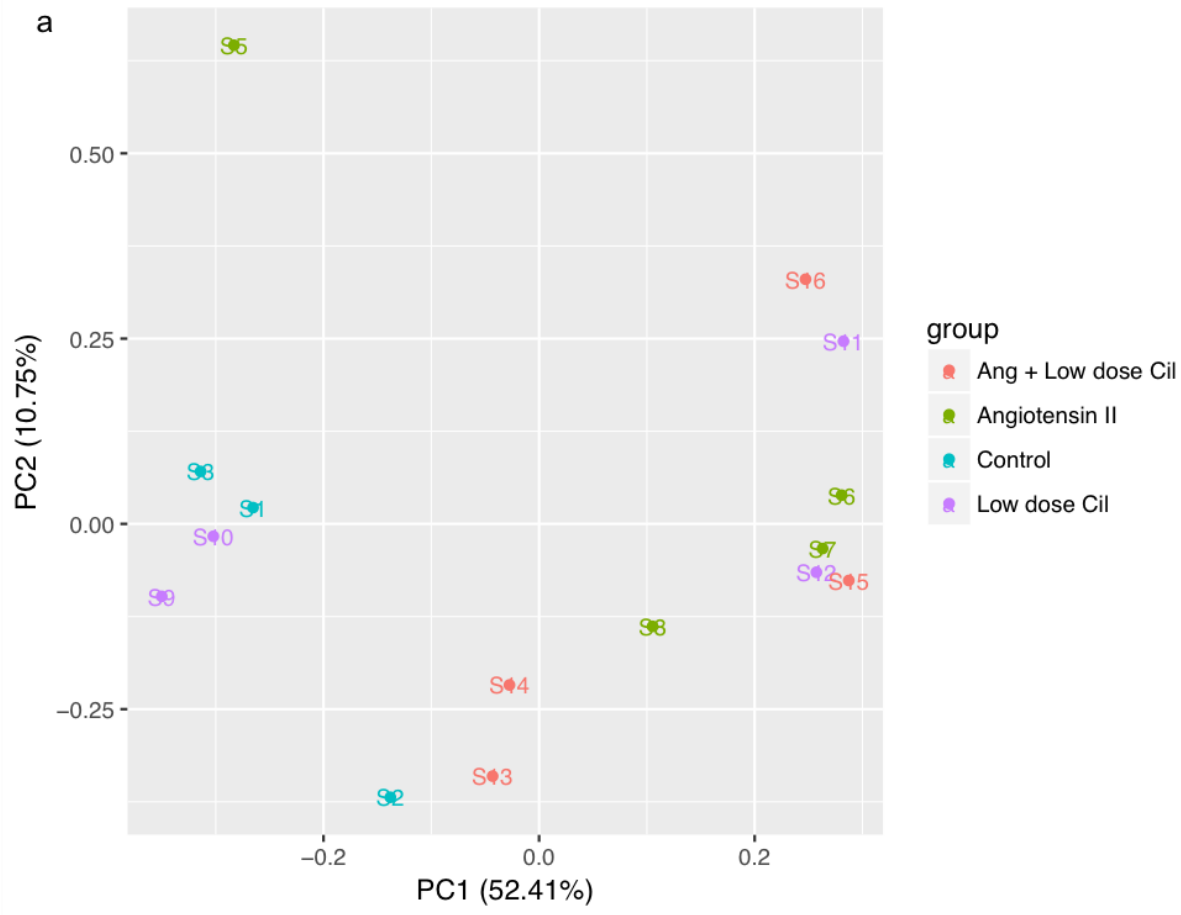

Figure 29: Principle component analysis (PCA) demonstrates poor clustering between cardiomyocytes treated with vehicle, low dose Cilengitide, angiotensin II or angiotensin II-low dose Cilengitide combined. Cardiomyocytes were plated and left to expand for 3 days, before being serum starved for 24 hours and then treated with vehicle (n=3), low dose Cilengitide (n=4), angiotensin II (n=4) or angiotensin II-low dose Cilengitide (n=4) combined for 48 hours. Samples were sequenced via RNA-seq and clustered with PCA analysis. (**a**) Principle component analysis of treated cells.

Gene	Log Fold Change (FC) AngII-LDCIL vs AngII	Log Fold Change (FC) Control vs Ang II	Log Fold Change (FC) Ang II vs Control	Reference
Sprr1a	-1.7651457	-1.51252528	+1.51252528	[314]
Irs2	0.65326632	0.4872927	-0.4872927	[315]
Akap6	0.60451254	0.4761421	-0.4761421	[316]
Lrrc10	0.69439078	0.6152291	-0.6152291	[317]
Glul	0.98877967	0.8555815	-0.8555815	[318]

Table 18: Candidate genes have previously been published as important factors in the heart. All represent a 'healthy' gene expression pattern – i.e. are concordantly enriched between control and angiotensin II-low dose Cilengitide treated cardiomyocytes.

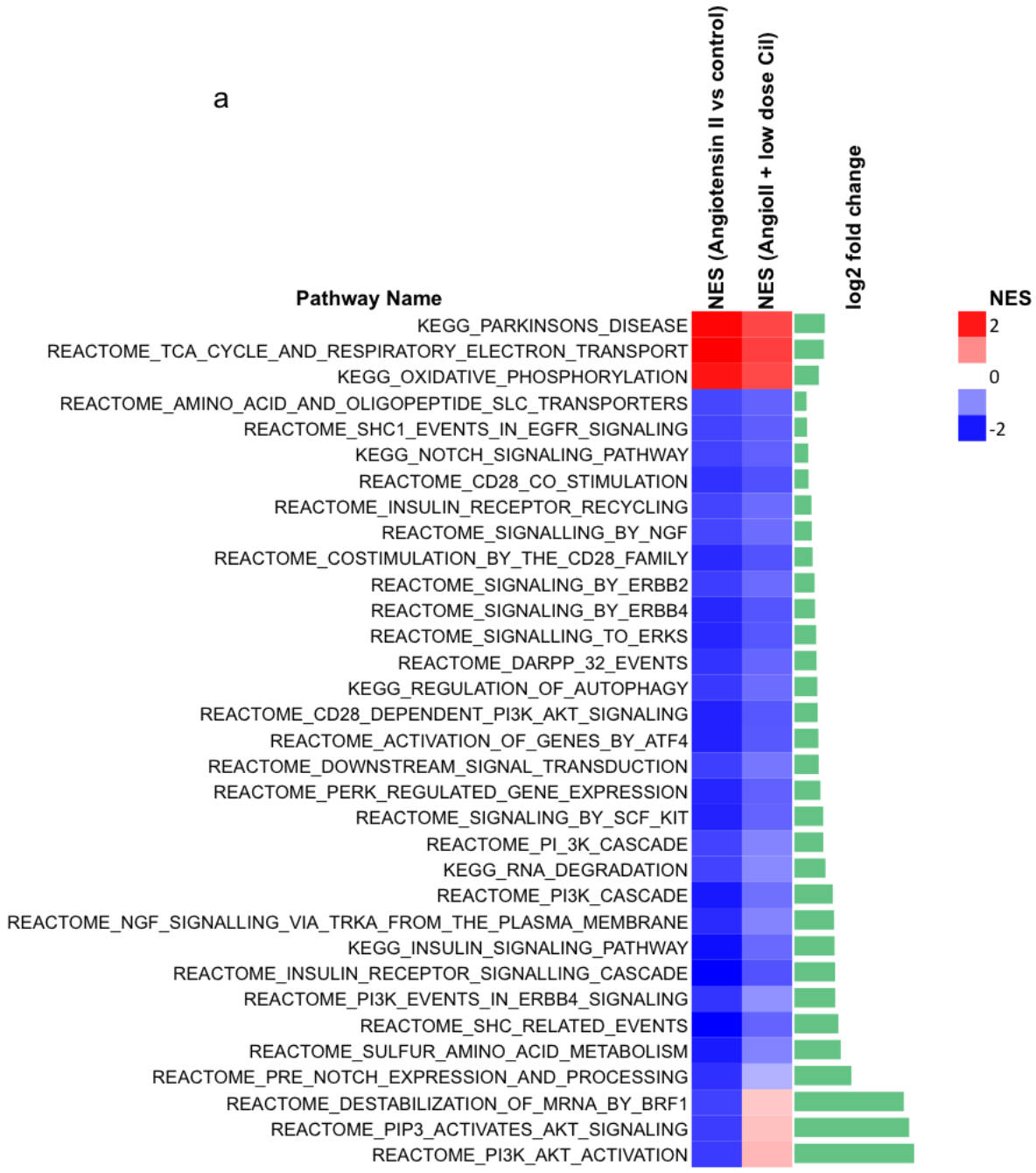

Figure 30: Low dose Cilengitide dysregulates several enriched pathways in angiotensin II treated cardiomyocytes. (**a**) Whole pathway analysis of differentially expressed pathways between angiotensin II and angiotensin II-low dose Cilengitide treated cells. All those pathways selected P<0.05.

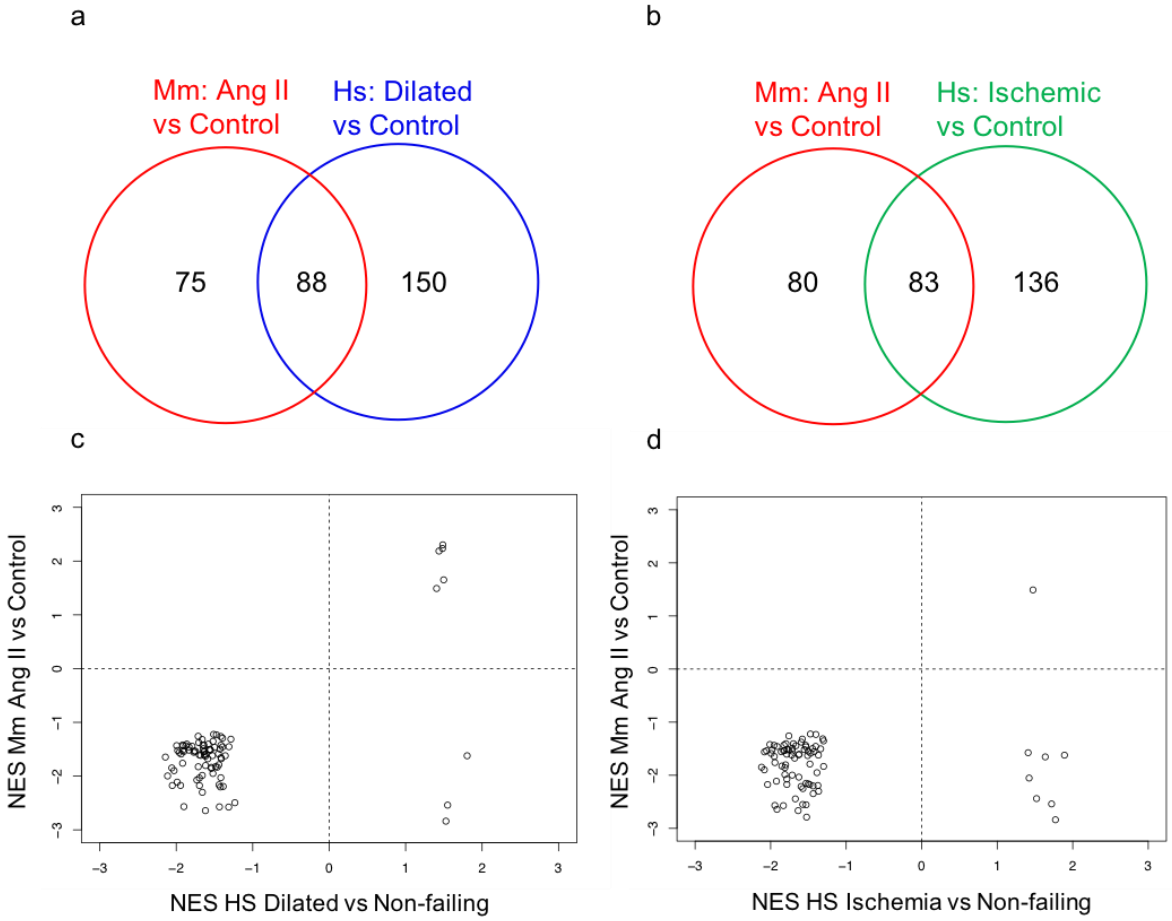

Figure 31: Gene set enrichment analysis (GSEA) reveals that there is a high concordance between those pathways enriched in angiotensin II treated cardiomyocytes and human heart failure. (**a**) Venn diagram illustrating overlap of GSEA pathways between angiotensin II treated cardiomyocytes and dilated human heart failure. (**b**) Venn diagram illustrating overlap of GSEA pathways between angiotensin II treated cardiomyocytes and ischemic human heart failure. (**c**) Scatterplot of the normalised enrichment scores (NES) of the 88 overlapping pathways identified by GSEA between angiotensin II treated cardiomyocytes and dilated cardiomyopathic heart failure patients. (**d**) Scatterplot of the normalised enrichment scores (NES) of the 83 overlapping pathways identified by GSEA between angiotensin II treated cardiomyocytes and ischemic heart failure patients. Only those pathways selected P<0.05.

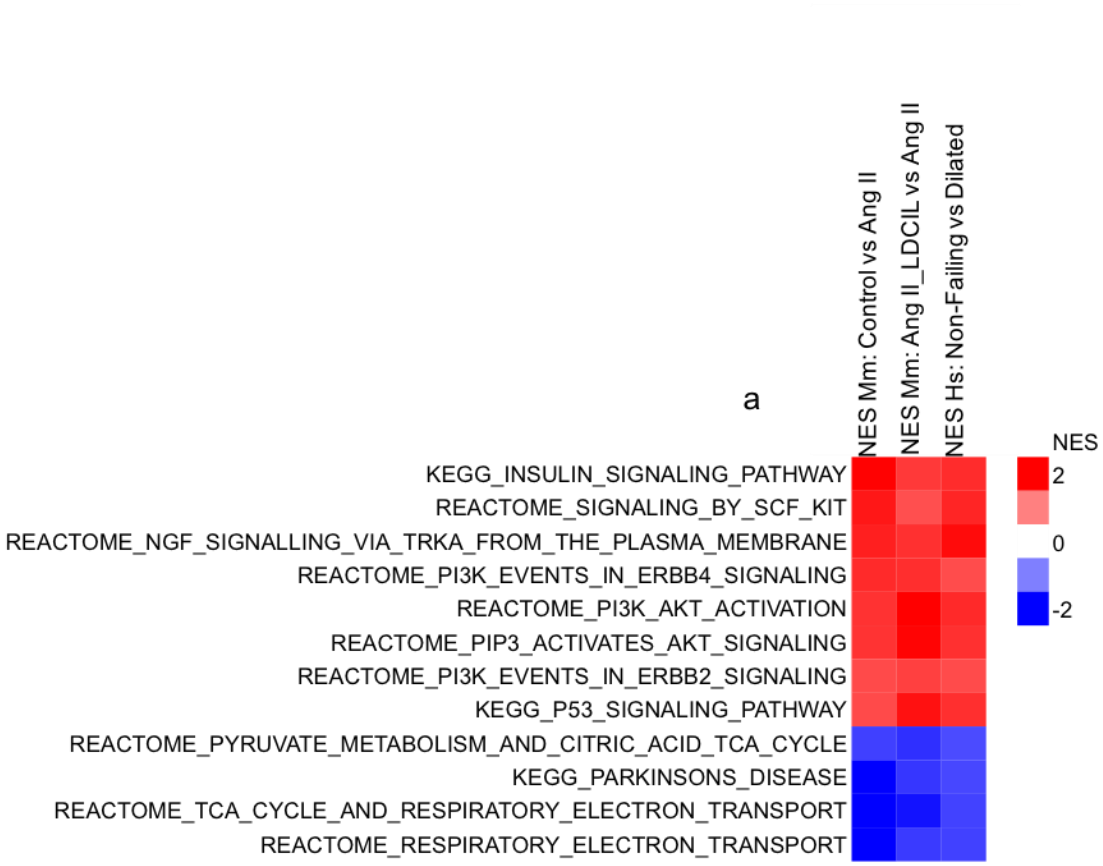

Figure 32: Low dose Cilengitide will restore several enriched pathways back to 'heathy' levels in angiotensin II treated cells. (**a**) Heat map illustrating concordant gene expression pathways between vehicle and angiotensin II-low dose Cilengitide treated cardiomyocytes, and non-failing human tissue (versus dilated). Only those pathways selected P<0.05.

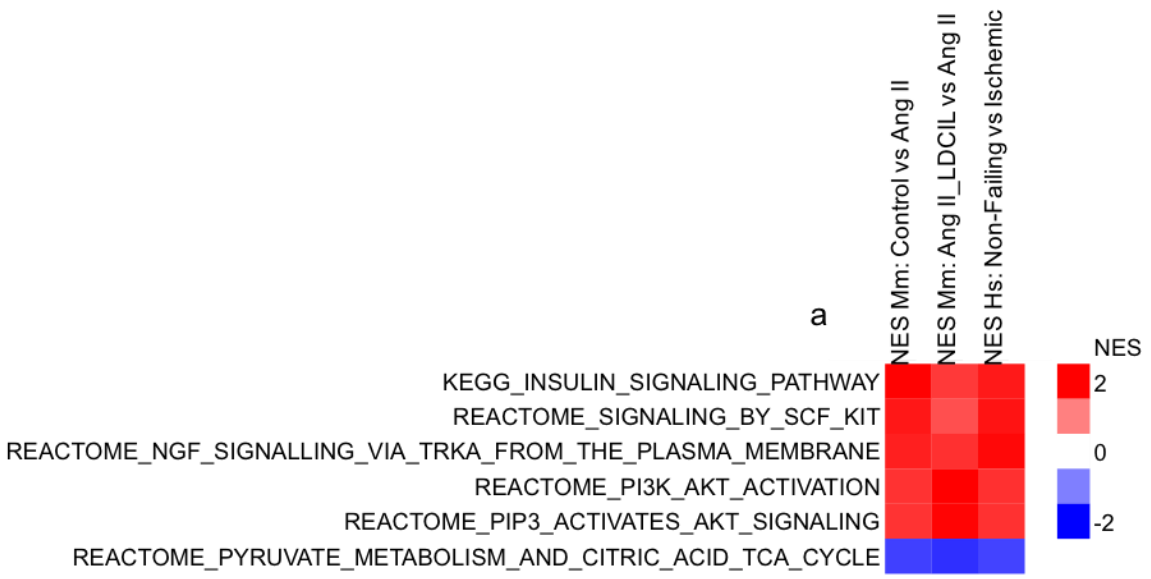

Figure 33: Low dose Cilengitide will restore several enriched pathways back to 'heathy' levels in angiotensin II treated cells. (**a**) Heat map illustrating concordant gene expression pathways between vehicle and angiotensin II-low dose Cilengitide treated cardiomyocytes, and non-failing human tissue (versus ischemia). Only those pathways selected P<0.05.

By this point we have established common pathways and genes that may indicate that low dose Cilengitide is a dual effector of cardiomyocytes and endothelial cells. My next priority was to functionally validate the information we had received from RNA-seq. RNA-seq appears to indicate that low dose Cilengitide will have some effect on isolated cardiomyocytes, and so we investigated whether Cilengitide will ameliorate cardiac hypertrophy in angiotensin II treated cardiomyocytes. As a readout of cardiomyocyte hypertrophy, we examined the RNA expression of 3 hypertrophy-related genes used previously, that are also re-expressed as part of a deleterious cardiac foetal-like gene pattern: Myh7, ANP and BNP. Here, the addition of angiotensin II alone modestly increased the expression of Myh7, ANP and BNP, and this was somewhat reversed, especially for Myh7 (significantly), after the concordant addition of low dose Cilengitide (**figure 34a**). In contrast, low dose Cilengitide alone had no effect on cardiomyocyte hypertrophy (**figure 34a**). This provides tentative proof of principle evidence that low dose Cilengitide will restore a healthy phenotype within disease cardiomyocytes, although much more work needs to be done here.

To functionally validate the pathways teased out by RNA-seq we performed preliminary westerns in cardiomyocytes treated with either: vehicle control (n=1), angiotensin II (n=1) and angiotensin II-low dose Cilengitide combined (n=1). This was a small sample size (n=1), but we saw no significant difference between groups (data not shown).

Finally, because endothelial cells are important paracrine regulators of cell behaviour [306] (i.e. angiocrine signalling) we attempted to study the effect of

endothelial cell conditioned media on cardiomyocytes. Unfortunately, cardiomyocytes did not survive for an extended period of time in this media, and so we were unable to conduct the experiments we had hoped.

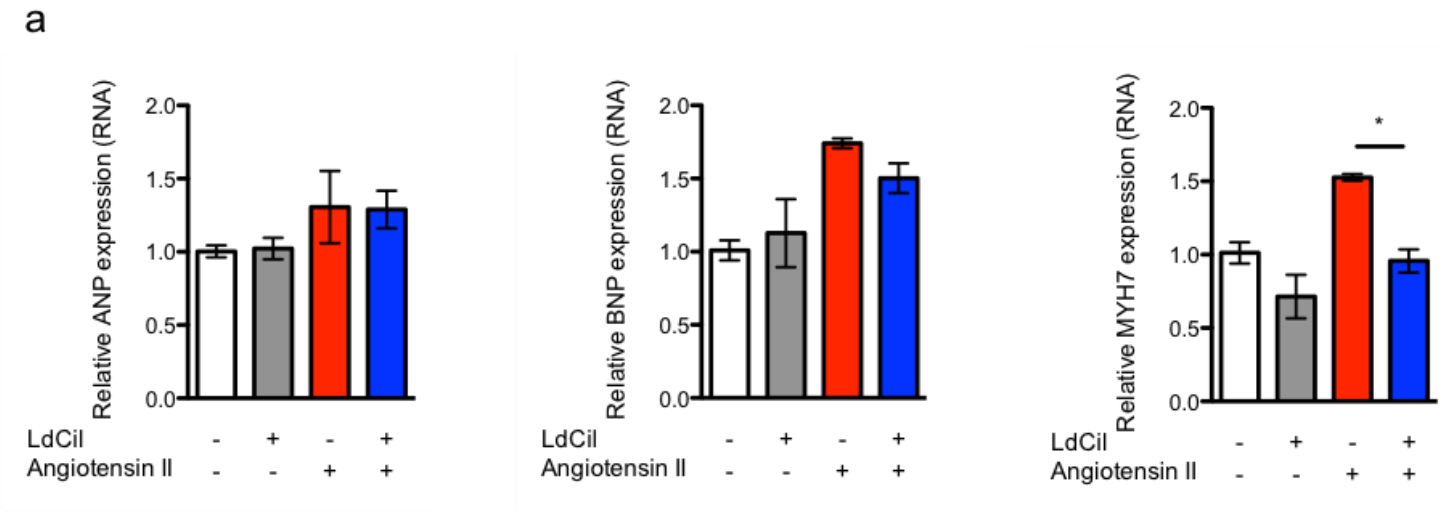

Figure 34: Low dose Cilengitide may reverse cardiac hypertrophy in cardiomyocytes. (**a**) Relative ANP, BNP and Myh7 expression in cardiomyocytes treated with: vehicle control, low dose Cilengitide, angiotensin II and low dose Cilengitide-angiotensin II combined (n=1 preparation).

4.11 Summary of chapter results

The results presented during this chapter show that:

1) Both human cardiac endothelial cells and cardiomyocytes express β3 and β5 integrin receptor subunits.
2) The relative expression of β3 and β5 integrin receptor subunits does not differ in heart failure in both humans and mice.
3) Treatment with low dose Cilengitide will reduce or even reverse disease severity in a murine model of pressure-overload induce heart failure.
4) Low dose Cilengitide will enhance cardiac angiogenesis.
5) Low dose Cilengitide may enhance endothelial cell proliferation *in vitro*.
6) Low dose Cilengitide may potentiate a number of cellular signaling cascades within cardiomyocytes *in vitro*, which themselves may restore a healthy cardiomyocyte phenotype after injury.
7) Low dose Cilengitide may be an effector of cardiomyocytes *in vitro* to ameliorate cardiac hypertrophy.

CHAPTER 5.0: DISCUSSION

VASCULAR PROMOTION IN HEART FAILURE

In the previous chapter we optimised a murine model of heart failure (TAC) and used it to determine the utility of low dose Cilengitide in a murine model of heart failure. To this end, we first establish that the targets of Cilengitide, $\alpha v\beta 3$ and $\alpha v\beta 5$ integrin, are expressed in cardiac endothelial cells and cardiomyocytes in both mice and humans. The relative whole expression levels of those $\beta 3$ and $\beta 5$ integrin receptor subunits are not differentially expressed, either in two subtypes of human heart failure, or in a pressure-overload induced murine model of heart failure, as compared to controls. Both prevention and intervention studies show that treatment with low dose Cilengitide will suppress many of the deleterious features of cardiac pathobiology which are induced following pressure-overload induced heart failure, including: cardiac contractility, LV dilatation, cardiac hypertrophy and foetal-gene expression pathways. Those improvements in cardiac disease severity are concordant to an increase in myocardial angiogenesis. Specifically, low dose Cilengitide will significantly increase the number of microvessels in the left ventricles of 'diseased' hearts, but has no effect on the number of mature, α-SMA covered vessels in those same sections. Finally, we include preliminary evidence that show low dose Cilengitide will potentiate a number of intracellular signalling cascades *in vitro* to propagate cardiac endothelial cell proliferation, and which may also restore cardiomyocytes to a healthier phenotype after their injury. These

results together provide rudimentary proof of principle evidence that low dose Cilengitide may function as a dual function effector of both cardiac endothelial cells and cardiomyocytes to modify their underlying behaviour, which may be effective in the treatment of heart failure.

5.1 Caveats to the TAC model of murine heart failure

Heart failure is a common, complex condition that is often concurrently associated with multiple secondary conditions, like diabetes and pulmonary disease. This ensures that the animal modelling of heart failure is very difficult. The majority, if not all, of the models available to us will not recapitulate many of the features of human heart failure, but instead offer us a reductionist setting to model more specific features. The TAC model herein offers an excellent system to model pressure-overload induce heart failure but is attached to a few caveats. The most major of these is the fact that TAC may be variably characterized as a model of either pressure overload induced hypertrophy of pressure overload induced heart failure. *Mohammed et al.* [304] show that TAC surgery will only induce heart failure in a subset (28% of mice). Importantly, their classification of heart failure was that mice develop pulmonary congestion. Those mice that did not develop pulmonary congestion, which itself was classified according to lung weight, were instead categorized as mice with compensated LV hypertrophy. The mean ejection fraction of the mice within these groups differed significantly. We did not measure lung weight in my own study, and instead classified heart failure according to more fundamental cardiac parameters, like cardiac hypertrophy, contractility and LV

dilatation. We do see some variability amongst cardiac contractility changes in my own study, but this itself has not been an overt issue, as the vast majority of those mice develop at least modest cardiac pathobiology. Variability amongst mice undergoing TAC surgery most obviously manifested as a problem during the 12-week study in **figure 21**. Here, only 50% of mice developed significantly reduced cardiac contractility, and those that did had to be culled by the experimental end point due to their symptoms (ejection fraction less than 10% in one measured case). This left me with 3 mice that clearly did not develop significant heart failure, which made it more difficult to properly interpret the results of this study as we have previously. If we were to use the TAC model in future, we would put more stringent roadblocks in place to minimize the variability amongst mice and to maximise the efficacy of the surgery. The first of these would be to assess the dimensions of the aorta before surgery. Mice would then be stratified not by their weight, but by their aortic size. This should ensure that the pressure gradient generated by the aortic band is more similar between mice, which should in turn generate cardiac pathobiology with less variability. In addition, it may be necessary to stratify mice according to their LV ejection fraction by 3 weeks and remove those mice did not meet a specific criterion. This could further ensure that we only choose those mice that have absolutely developed heart failure with reduced ejection fraction for later study. Of course, minimizing groups according to these selection criteria generates its own problems, in that any future conclusions we draw from those groups will only reflect a very small subset of heart failure cases, whereas previously we may have been utilizing models that more accurately reflect a wider group of patients.

Aside from also classifying heart failure differently, *Mohammed et al.* also used a subtly different model than my own to generate their data. Investigators modelled aortic constriction at the thoracic level in the aortic arc, whereas we used a model of abdominal aortic constriction. Thoracic TAC will generate a significantly higher early mortality rate (32% survival by 3 weeks) as compared to our own study (90% survival by 3 weeks) and will also induce more significant cardiac hypertrophy and inotropy changes [304]. The fact that thoracic TAC induces higher early mortality may mean that there is actually a significantly higher subset of mice that actually develop heart failure within this study, but they were not accurately depicted because they were not sufficiently investigated before their death. This may explain why most studies choose to only investigate thoracic TAC across a 2-week period [319]. Overall, we think it is reasonable to suggest that the variability amongst TAC surgeries is a caveat to the model, but we think they can certainly be minimized with effective checks in place and probably did not overtly influence my own study negatively.

5.2 αvβ3 and αvβ5 integrins are not differentially expressed during cardiac disease

β3 and β5 integrin receptor subunits are not differentially expressed in either a mouse model of heart failure or subtypes of human heart failure itself. This may be due to the type of hearts we investigated, or rather the stage of disease that they reflect. The tissue used here could represents ‘late-stage’ disease, although as discussed earlier we do not have the evidence to ascertain this, especially in the

human myocardium. We use this term to describe myocardium that has already transitioned from compensated to uncompensated heart failure, and so manifests as deleterious, symptomatic, cardiac pathobiology. Increasing evidence suggests that integrins play a pivotal role in cardiovascular remodelling [320] [321]; and so, by strictly investigating late-stage heart failure tissue, we may have missed significant integrin expression changes that occur during acute cardiac remodelling. The integrins involved may then be downregulated to normal levels after this phase has ended, to be replaced by other proteins (including integrins) whose function instead serves to potentiate chronic remodelling. Cardiac remodelling constitutes changes in the size, shape, structure and function of the heart. Those changes are characterized by rearrangement of the architecture of the cardiac ventricular wall, which involves (among others) myocyte hypertrophy, fibroblast proliferation, increased deposition of ECM proteins and altered expression of miRNAs [322] [323] [324].

Because integrins are the principle anchoring proteins of myocardial cells to one another and to the ECM, it is probable that their expression will change temporally as the structures they anchor themselves change. Indeed, a variety of integrin heterodimers are altered concomitantly with the initiation of both acute and chronic cardiac remodelling. In rodents, increased expression of β1A, β1D, α1, α3 and α5 (among others) have been detected after aortic constriction, whilst α1, α3 and α5 integrin subunits will also change temporally after MI [325] [265] [264]. MI involves both an acute healing phase and also a chronic remodelling phase. Work has been performed to evaluate the changes in several integrin subunits across these

stages. Early work saw that by 7 days post MI α1 was expressed in both the normal myocytes of the peri-infarct zone and also the myocytes of the remodelled tissue within the infarct zone itself. The peri-infarct expression of α1 remained elevated at 6 weeks post MI, but its expression within remodelled tissue was downregulated. By contrast, α5 integrin expression was increased in peri-infarct regions by day 7 but returned to normal levels within 2 weeks [264].

More recently, myocardial αvβ3 integrin expression was shown to be upregulated within 2 weeks of MI in infarct regions [287]. Interestingly its expression here is thought to activate latent myofibroblast differentiation and also induce myocardial salvage by increasing angiogenesis [277] [287]. By 10 weeks post-MI αvβ3 integrin expression persisted in infarct regions but was reduced in comparison with 2 week-assessment [287]. In addition, multiple other studies have also demonstrated that αvβ3 integrin will accumulate at early sites of infarction. Those same studies collectively demonstrate its levels will peak between 1 and 3 weeks, and will then begin to decline [285] [326] [327].

Furthermore, the subcellular localisation of integrins may also change during remodelling. For instance, pulmonary artery banding will result in mobilization of β3 integrin to the cytoskeleton of lysed myocardial fractions within 4 hours, but by 48 hours its expression was found in both cytoskeletal and membrane-bound fractions. Thereafter its levels returned to baseline within 1 week [328]. We saw that αvβ5 especially was concentrated within focal contact costameres of the cardiomyocytes (as expected) but did not analyse its subcellular localisation or

concentration within costameres, and so did not observe any changes in its localisation after disease.

Certainly, these studies together demonstrate the importance of αvβ3 integrin especially during cardiac remodelling. Indeed, other studies reinforce the notion that β3 integrin subunits play an important role in the stressed myocardium [276] [275] [259]. For example, *Johnston et al.* show that when aortic constriction is performed on β3-null mice they will exhibit reduced compensatory hypertrophy and depressed ventricular function, which results in increased mortality [276]. Similarly, β3-null mice in a secondary study show increased myocardial cell death after pressure-overload, demonstrating that β3 integrin contributes toward cardioprotective signalling [259].

Collectively this indicates that the expression of β3 and β5 integrins may only be differentially expressed early on in the cardiac remodelling process, which is why we didn't see any expression changes in late disease tissue. In order to more accurately reflect their localisation, expression and function we may need to in future analyse tissue taken from hearts early after surgery, such as within 1-2 weeks of TAC. With that said, it is important to note that the studies discussed here will often use different imaging modalities to quantify temporal integrin changes. Those techniques may differ in sensitivity, and so two different imaging modalities for the same event may yield different results. we have used immunofluorescence, western blotting and RT-qPCR to investigate the expression changes of β3 and β5-integrin receptor subunits, and so a different imaging modality may give different quantitative results.

5.3 Cilengitide functions as a dose dependent regulator of cardiac pathobiology in pressure-overload-induced heart failure

In this present report we show that low dose Cilengitide will ameliorate many of the cardiac disease features of pressure overload induced murine heart failure. These effects are dose-dependent and may even be continued after Cilengitide's cessation. To my knowledge this is the first time Cilengitide has been used for this treatment purpose. Cilengitide has previously undergone clinical study trialling its anti-tumour efficacy but has not achieved its expected clinical outcome [250]. Considering the wealth of clinical data available, and the fact that chemotherapy may often induce concomitant cardiotoxicity in patients [329], one might expect that there is human data available that might indicate that Cilengitide will improve cardiac function if my findings were to be true. Unfortunately, we have not been able to find any data supporting this theory however, probably because patients with serious heart disease are often excluded from clinical trials, and also because the dose of Cilengitide used in human trials does not constitute sustained 'low dose' therapy.

Despite displaying efficacy in the model used here, it is important that the utility of Cilengitide is studied in other murine heart failure models. These investigations could also be extended to models of peripheral artery disease (PAD) and cerebral ischemia, where Cilengitide also may yield benefit.

5.4 Low dose Cilengitide enhances cardiac angiogenesis

Low dose Cilengitide enhanced myocardial angiogenesis in a murine model of heart failure, but not in SHAM surgical controls. This suggests that Cilengitide will only potentiate angiogenesis in challenged but not quiescent or unchallenged organs. It would be interesting to investigate whether angiogenesis was upregulated in other organs, such as the skin or in the eye, as this would give us a readout of how Cilengitide will affect 'unchallenged' organs. However, previous work from our lab indicates low dose Cilengitide has no effect on blood vessels density in non-stressed or non-damaged tissue {Reynolds, 2009 #78}. Overall, Cilengitide probably had no, or only minimal angiogenic effects in 'offsite' tissue. We saw no deleterious side effects of therapy, as might be seen if there was excessive angiogenesis in the retina, for example. In this fashion, we expect that tissue needs to be 'primed' before low dose Cilengitide will enhance angiogenesis. *Reynolds et al.* demonstrate that low dose Cilengitide will enhance angiogenesis in tumour models [4], which themselves are tissues that are already undergoing extensive vascular remodelling once a specific volume is reached. Similarly, the TAC model used here will undergo changes in capillary density without the administration of pro-angiogenic therapy, and so the tissue may be equally 'primed' for Cilengitide function [119]. This raises the question of what primes a tissue-type for later Cilengitide activity. In this case it may be endogenous pro-angiogenic factors like VEGF, or even an upregulation of $\alpha v\beta 3$ itself. Both factors are notably upregulated in the early phases of myocardial angiogenesis, and also in tumours [220] [287] [330] [331].

The mechanism underlying the pro-angiogenic effects of low dose Cilengitide are that therapy will promote recycling of both αvβ3 and VEGFR-2, which in turn will attenuate the degradation of VEGFR-2 and also enhance the recruitment of αvβ3 to focal contacts [4]. Indeed, there is evidence elsewhere that αvβ3 and VEGFR-2 are able to directly interact, which reinforces the notion that the two are able to modulate one another's function [217].

VEGFR-2 appears to mediate almost all known cellular responses to VEGF [332], so conceivably almost all subtypes of VEGF could be responsible for increasing myocardial angiogenesis after low dose Cilengitide. The most obvious candidate for enhancing myocardial angiogenesis is VEGF-A, but this might not necessarily be the case. VEGF-A is persistently downregulated in the infarcted myocardium post MI. Its expression was only significantly increased at the border zone 1 day after MI, but not in later stages, which may indicate that VEGF-A may initiate angiogenesis but is not necessary for its later stages [220]. In contrast to this, VEGF-A isoforms have been detected in myocardial infarct regions at points as late as 40 days post MI in other MI models, which seems to suggest its continual angiogenic involvement [333]. This may reflect the fact that the two studies used different methods to evaluate the expression of VEGF-A.

It may be that VEGF-A is downregulated at later time points to ensure proper vascular stabilization. Indeed, the transgenic over expression of VEGF in cardiomyocytes will result in the production of abnormal vascular trees, which consist of irregular, sac-like vessels, which ultimately lead to 'leakiness', and a highly disruptive oedema in the adult heart [334]. This highlights the fact that VEGF

must be downregulated to facilitate vascular maturation. Indeed, recent studies have shown that αvβ3 can exert phosphorylation dependent transdominant effects over VEGFR-2 [226]. In this fashion, αvβ3 may potentiate or dysregulate VEGF signalling according to its own phosphorylation status.

If Cilengitide does indeed potentiate VEGFR-2 activity, and VEGF must be downregulated to achieve vascular maturity, then Cilengitide may actually generate immature, 'leaky' blood vessels. We saw no obvious vascular oedema, and the microvessel morphology in low dose Cilengitide treated myocardium appeared to be similar to that of controls. Unfortunately, we were unable to properly assess the maturity of the microvessels however, as, unlike in tumours, α-SMA did not mark pericytes that associate with myocardial capillaries. Instead α-SMA only appeared to mark vessels that were much larger than what we have classified as microvessel capillaries. Overall the number of α-SMA positive vessels were similar between all groups, which is unsurprising given the type of vessels that α-SMA marks in my samples. More work certainly needs to be conducted to investigate the type of vessels generated after the administration of Cilengitide. One possible method could be to intravenously inject PE (phycoerythrin) labelled CD31 into mice before culling, which will then mark 'active' vasculature. These could then be measured against unlabelled CD31+ (488) vessels in sections to determine the ratio of inactive to active microvessels.

5.5 Low dose Cilengitide as a dual action therapy

Herein we provide preliminary evidence that low dose Cilengitide may potentiate cardiac endothelial cell proliferation, as well as restore cardiomyocytes to a healthier phenotype after their injury. Thus, Cilengitide at nanomolar concentrations will function as a dual function effector of both cardiac endothelial and cardiomyocyte cell types *in vitro*. Furthermore, we show that both cardiac endothelial cells and cardiomyocytes express the necessary $\alpha v\beta 3$ and $\alpha v\beta 5$ receptors for Cilengitide function, which reinforces this notion.

Notably, we show that low dose Cilengitide will upregulate the expression of Mt2, Csf2rb and Nov, and also downregulate Bcl6 in isolated cardiac endothelial cells. All have been shown to be pivotal players during angiogenesis.

Mt1 and 2 are more classically categorized as regulators of metal detoxification as part of cellular homeostasis. However, more recently Mt2 is demonstrably required for endothelial cell migration, proliferation and angiogenic sprouting upstream of VEGF-C in zebrafish [335]. Similarly, CCN3 (Nov) will support endothelial adhesion, migration and survival. It will bind directly to $\alpha v\beta 3$, which will determine CCN3-induced endothelial cell migration. In addition, CCN3 will induce neovascularization in rat corneas and its expression is also altered in a variety of tumours, whereby it may be a novel mediator of tumour angiogenesis [336]. Finally, the inhibition of Bcl6 will induce endothelial sprouting, and will also control Notch target genes like Hey2, which is another downregulated protein highlighted by RNA-seq analysis in treated endothelial cells [337]. We need to functionally validate these targets with proteomic analysis to be certain that their expression is

differentially regulated. In addition, we also need to perform function assays to demonstrate that low dose Cilengitide will indeed induce cardiac endothelial cell proliferation. Low dose Cilengitide will induce migration, but not proliferation, in lung endothelial cells [4], so it is perhaps surprising that RNA-seq seems to point to the fact that low dose Cilengitide will potentiate proliferation in the cardiac endothelium. However, cardiac endothelial cells do exhibit a distinct gene expression profile when compared to pulmonary endothelial cells so there is certainly evidence to indicate it is feasible for the two cell types to differentially respond to a given therapy [120].

The major pathway that was highlighted as an important feature of cardiomyocyte signalling after low dose Cilengitide administration was the PI3K-Akt pathway. This signalling cascade was ostensibly highlighted as a signature of cardiomyocyte health, in that it was upregulated in low dose Cilengitide and vehicle treated cardiomyocytes and also in non-failing human hearts. The PI3K-Akt pathway will promote cardiomyocyte proliferation, survival and physiological hypertrophy, and so low dose Cilengitide may perpetuate those functions in the cardiomyocyte [338]. RGD stimulation in adult cardiomyocytes will activate β3 integrin, which is accompanied by c-Src sarcolemmal localisation, and also p130Cas binding and FAK phosphorylation [275]. FAK is thought to be upstream of NF-kB in cardiomyocytes and will regulate their survival following ischemia reperfusion injury through NF-kB [339]. The NF-kB survival pathway also has the ability to crosstalk with PI3k-Akt pathways in some cell types [340], so this same interaction

may be present in the cardiomyocytes also. Similarly, studies show that RGD stimulation will activate pro-survival ubiquitination and NF-kB pathways in cardiomyocytes *in vitro* [276]. Finally, the *in vivo* ablation of β3 can lead to calpain mediated myocardial cell loss [259]. Importantly, calpain activation will inhibit Akt signalling in rat diaphragm muscle [341], highlighting that αvβ3 could indeed potentiate Akt signalling by downregulating calpain activity. Collectively these studies show that RGD mimetics can regulate cardiomyocyte behaviour, possibly through modulation of the NF-kB and PI3K-Akt signalling. We certainly need to functionally validate those same pathways in my own cardiomyocyte preparations after treatment with low dose Cilengitide to ascertain the data we obtained by RNA-seq.

5.6 Future work

The main objective of any future work should first aim to clarify the mechanism of low dose Cilengitide function *in vitro*. To do so, we would continue to perform western blot analysis for phosphorylated Akt in Cilengitide and angiotensin II treated cardiomyocytes. We have isolated the PI3K-Akt pathway as a potentially important target signalling target of low dose Cilengitide, and we require functional validation of the RNA-seq data that initially highlighted this. In parallel we would perform MTT and cell counting assays on low dose Cilengitide treated cardiac endothelial cells to functionally validate the hypothesis that low dose Cilengitide will induce proliferation in those cells. In addition, we would investigate how conditioned media from low dose Cilengitide treated and untreated cardiac endothelial cells effects cardiomyocyte viability, hypertrophy and survival after their injury with angiotensin II.

In the long term, we think it would be interesting to examine functional and genetic differences between cardiac endothelial cells isolated from mice that had undergone TAC surgery, and those that had undergone TAC surgery, both untreated and treated with low dose Cilengitide. The experiments themselves here would be tricky, as the initial isolation of cardiac endothelial cells yields a very small number of cells which may be insufficient for investigation but plating them to expand colonies for assessment could minimize any differences in phenotype between the cells. Similarly, we would have liked to focus on isolating adult cardiomyocytes, and in an ideal would examine them over the foetal cardiomyocytes we have used previously. Adult and foetal cardiomyocytes display

significantly different functional features, including cell morphology, electrophysiological characteristics, sarcomere organization and contractile force, which means that the two cell-types may yield different results under investigation [342] [343]. Examining cardiomyocytes from adult mice would also mean that we could determine the functional effects of TAC surgery on those myocytes, both with and without Cilengitide. we would have liked to perform functional siRNA knockouts of targets on those mice, to more properly ascertain the functional mechanism of low dose Cilengitide on those cells.

Furthermore, it would be interesting to observe the effects of low dose Cilengitide therapy in other mouse models, including after myocardial infarction. Pro-angiogenic therapy appears to be a promising strategy to treat MI, as the formation of microvessels could salvage ischemic myocytes, especially in its early stages [295].

In addition, we would have liked to further delineate how low dose Cilengitide will enhance cardiac angiogenesis. We have so far been able to postulate using RNA-seq data and the information from the *Reynolds et al.* paper, but this is no substitute for actually measuring the activity of e.g. VEGFR/VEGF activity within those treated hearts. Similarly, it would have been interesting to observe how $\alpha v\beta 3$ and $\alpha v\beta 5$ expression and activity changes a) temporally after TAC surgery and b) temporally after low dose Cilengitide therapy. To do this we could sacrifice mice at various time points and examine protein/RNA levels with western blots and RT-qPCR respectively. It may be that those integrin expression does not change

temporally within the whole heart itself, and so we may more specifically need to classify changes within particular areas, such as the wall of the LV itself.

CHAPTER 6.0: INTRODUCTION

FOCAL ADHESION KINASE AND ANGIOCRINE SIGNALLING IN CANCER

6.1 Focal adhesion kinase (FAK)

Focal adhesion kinase (FAK) is a cytoplasmic, non-receptor tyrosine kinase that plays a vital role in integrin and growth factor mediated signalling, extending to functions in a variety of cellular processes including: motility, focal adhesion turnover, survival, growth and invasion [344]. FAK is ubiquitously expressed across most cell types and is overexpressed within many types of solid and non-solid tumours [345] [346]. FAK is concentrated within specialized intracellular structures called focal contacts. Focal contacts are the interface site between integrins and the cytoskeleton, which together mediate adhesion to the extracellular matrix (ECM). In general, they are composed of dynamic groups of structural, adaptor and regulatory proteins which transduce both extracellular, and intracellular, activity [347]. The subsequent sections will outline FAK expression, function, structure and activity, with particular emphasis upon its pivotal role in the endothelium.

6.1.1 FAK domains, associated proteins and downstream signalling pathways

Structurally, FAK is composed of a central catalytic kinase domain, a carboxyl-terminal focal adhesion targeting (FAT) domain and an N-terminal regulatory FERM domain (see figure 1). Historically, FAK function has more generally been attributed to its central kinase domain kinase activity, but this has more recently been challenged by its interrelated scaffold function [345]. The FAT domain of FAK is necessary and sufficient to direct FAK to focal adhesion complexes. Its integrity is absolutely vital for FAK signalling as cells displaying FAK isoforms with a truncated FAT domain do not spread or migrate as normal [348]. Structural studies reveal that the FAT domain of FAK is composed of a four-helix bundle that resembles alpha-catenin and vinculin, two other cellular adhesion proteins [349]. Paxillin binding to the FAT domain requires the integrity of the four helical bundle, but binding to other proteins, like talin for instance, does not [349]. Together, paxillin and talin appear to mediate focal adhesion targeting [350] [351].

The C-terminal of FAK also contains FRNK (FAK-related non-kinase) in certain cells. FRNK is thought to be a negative regulatory of kinase activity [352]. FRNK is upregulated in vascular smooth muscle cells and may be upregulated in vascular injury [353]. The forced overexpression of FRNK in FAK inhibits cell spreading, cell migration and growth factor-mediated signals to MAP kinase [353] [354] [355].

The FERM domain of FAK on the other hand is thought to be the majority binding site linking the plasma membrane to cytoskeletal structures at specific cellular locations [356]. To this end, integrins, PDGF receptors and c-Met will bind to the

FERM domain, amongst others [357] [358]. The FERM domain also contains a nuclear localisation signal (NLS) which indicates that FAK can shuffle between the nucleus and membrane. Indeed, in the nucleus FAK promotes cell survival and proliferation whilst at the membrane FAK regulates integrin-dependent cell interactions with the ECM [356]. In addition, the FERM domain has also been implicated in FAK auto-inhibition. We know this because deleting the first 375 amino acids of FAK at its N-terminal will increase its catalytic activity and also directly inhibit cell-cycle progression in CHO cells *in vitro* [359] [360]. In addition, the analysis of several point mutations in the FERM domain of FAK revealed that some of those mutations increased FAK phosphorylation whilst others decreased it, which reinforces the notion that the FERM domain is an important regulator of FAK activity [361]. The precise molecular and structural basis for FERM auto-inhibition describes a model whereby the FERM domain will bind directly to the kinase C-lobe, which impedes access to the active cleft that contains Tyr 397 and the Src recognition site [362].

The central portion of FAK is thought to be the catalytic, or kinase, domain (**figure 35**). The activation of FAK and its downstream signalling via this domain is a complex process [363]. A model has been proposed to describe this from accumulating from crystallography studies [359] [361] [364]. Briefly, prior to activation FAK is maintained in an inactive conformation in which the FERM domain impedes access to the active site of the FAK kinase domain. This prevents phosphorylation of the Tyr 397 residue of FAK, which leads to FAK auto-inhibition. Integrin clustering at focal contacts of the cell membrane initiates a signal that

releases the auto-inhibitory interaction between the FERM and kinase domains, leading to kinase activation and subsequent autophosphorylation of Tyr 397. There is evidence that Tyr 397 can also be transphosphorylated to activate FAK signalling, but it is unclear how much non-canonical activity like this contributes to overall FAK function [365]. Phosphorylation of Tyr 397 provides a high-affinity SH2-binding site which allows Src, or other SH2-binding proteins like phospholipase Cγ (PLCγ), to functionally interact with FAK. Next, Src transphosphorylates FAK on a number of key tyrosine residues, including Tyr 576, Tyr 577, Tyr 861 and Tyr 925. It is thought that Tyr 576 and Tyr 577 in particular are required for maximal catalytic activity [366]. The phosphorylation of Tyr 861and Tyr 925 together increases the binding of proteins like p130Cas, paxillin and GRB2 to FAK. In this instance, p130Cas binding will go on to potentiate the PI3-kinase signalling pathway, GRB2 will activate the MAPK signalling pathway. Both are thought to differentially mediate focal adhesion dynamics, proliferation and survival [367]. On top of all this, Tyr 861 phosphorylation may itself result in further auto-phosphorylation of Tyr 397, which adds multiple layers of complexity to FAK signalling [368].

FAK also contains four serine residues that can be phosphorylated: serines 722, 732, 843 and 910. Serine phosphorylation is thought to modulate binding and stability of downstream signalling proteins [369]. *Ma et al.* show that of these, Ser 722 may play a role in regulating FAK binding to the SH3 domain of p130Cas. This did not manifest as any functional changes in this study during mitosis however. Instead, Ser 843 and 91 exhibit increased phosphorylation during mitosis [370]. In

addition, it was shown that the phosphorylation of Ser 843 inhibits Tyr 397 phosphorylation, which inhibited cell migration and spreading [371].

Aside from phosphorylation there are other events governing FAK kinase activity. Perhaps the most well studied mechanism of this demonstrates that autophosphorylation of Tyr 397 will differ significantly between FAK isoforms. The functional effects of this were not established in this particular study however [365].

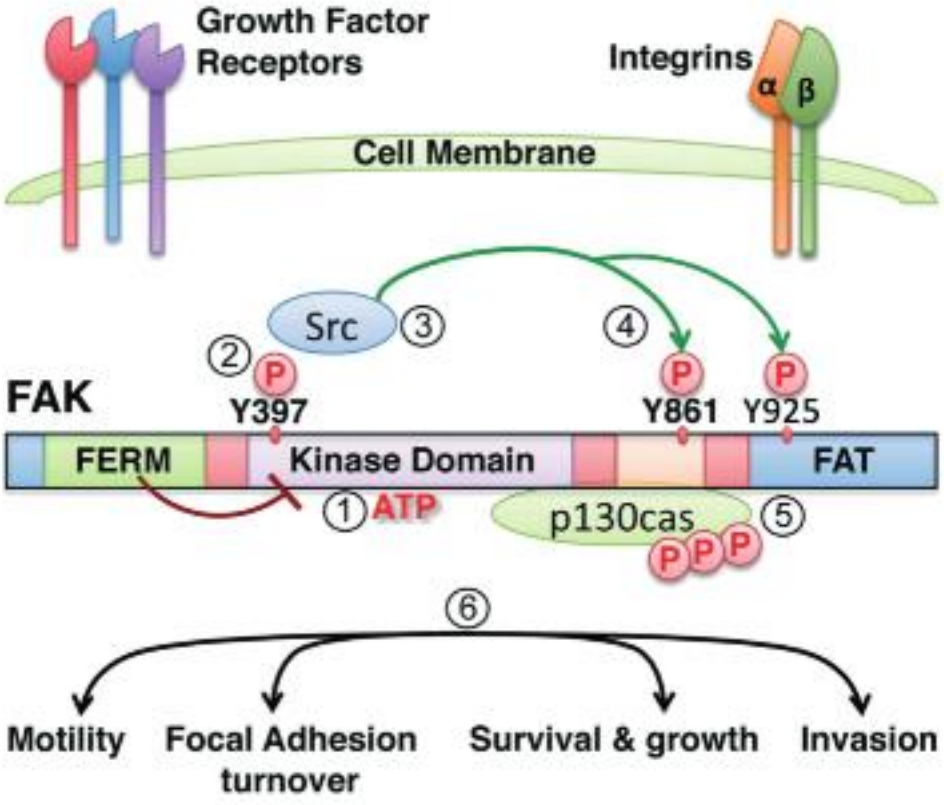

Figure 35: FAK structure and function. Canonical FAK signalling involves a number of events: (1) ligand-bound growth factors or clustered integrins initiate signals that release the auto-inhibitory interaction between the FERM and kinase domains, leading to FAK kinase activation by facilitating ATP binding. (2) FAK autophosphorylates Tyr 397. (3) phosphorylation creates a high affinity binding site for Src. (4) Src transphosphorylates FAK at key FAK residues including Tyr 861 and 925. (5) p130cas binds proline-rich domains of phosphorylated FAK and is phosphorylated itself. (6) downstream signalling of activated FAK elicits changes in cellular morphology and behaviour, including changes in motility, focal adhesion turnover, survival, growth and invasion. Taken from [344].

6.1.2 FAK in tumour cells

FAK lies at the intersection between several important signalling pathways in cancer growth and metastasis, including cell motility, invasion and epithelial-mesenchymal-transition (EMT) [372]. Conditional tissue-specific mouse models and chemical FAK inhibitors combined with the study of human cancers have together allowed investigators to delineate the involvement of FAK in several solid and non-solid cancers. Early examples of this include *Weiner et al.* who saw that FAK mRNA was upregulated in a number of human cancer tissue samples which covered a range of neoplasms and malignancies [373]. Similar findings were seen across colon and breast tumour samples [374], and more recently thyroid, prostate, cervix, colon, rectum, oral epithelium and ovary cancers [375]. Indeed, increased FAK expression and activity frequently correlates with poor prognosis, malignancy or metastasis which could indicate that FAK protein levels are a valuable prognosis indicator [376] [377] [378]. The mechanisms that underpin the fact that FAK is increased in tumour cells are not well understood, but one study postulates that the amplification of FAK gene copy numbers may be a contributing factor, especially in head and neck cancer [379].

More direct involvement for the involvement of FAK in both tumour formation and malignancy progression comes from an early mouse skin carcinogen model. Here *Quintanilla et al.* show that FAK expression was increased in a stepwise fashion in cell lines derived from progressive stages of the mouse skin cancer [380]. When global FAK heterozygote knockouts are analysed in this same skin assay 'half FAK' is sufficient impair papilloma formation [381]. In addition, the conditional

deletion of FAK in epidermal cells substantially reduces both the formation and progression of skin carcinomas in mouse models, probably through enhanced apoptosis of those cells harbouring deletion [381].

The success of these observations has led to FAK kinase inhibitors progressing to clinical trial. As is often the case, the initial positive results observed in mice with these same inhibitors have not yet translated to efficacy in humans however. This may be due to the fact that FAK inhibitors will not only affect tumour cells, but also other cells of the tumour microenvironment, including pericytes, endothelial cells and fibroblasts. For example, PF-573,228 produces a defect in platelet aggregation *in vitro* so could consequently induce similar, if not deleterious, aggregation defects *in vivo* [382].

Additionally, tumour growth and malignancy may not strictly be characterized by an overexpression of FAK protein. It has been reported that in some cancers, such as cervical or liver metastasis, low FAK expression actually correlates to a much poorer prognosis [383] [384]. Furthermore, inhibiting FAK correlates with increases in tumour cell migration, invasion and metastasis in some human carcinoma lines [385]. Together this implies regulating global FAK may not strictly yield the most effective anti-cancer efficacy across all variants. In fact, recent evidence from colleagues indicates that the endothelial cells themselves may be a promising FAK-related target in the fight against cancer [305, 306].

6.1.3 Endothelial cell FAK - Angiogenesis

Tumours, like any other organs, require a system of blood vessels to ensure that their oxygen and nutrient requirements are met. This is achieved primarily through angiogenesis. Early stage, pre-malignant tumours will typically display little or no intra-tumour vascularization. In contrast, malignant tumours exhibit robust intra-tumoural angiogenesis. The progression of tumours from a benign to a malignant state involves the activation of the so-called ‘angiogenic switch’ [386]. It is this switch that triggers the development of a vascular network that will facilitate the active growth and invasiveness of tumours. Hypoxia is a key instigator of this tumour angiogenesis. Hypoxic cancer cells secrete VEGFA, which stimulates tumour angiogenesis by activating VEGFR2, expressed on neighbouring endothelial cells. Gradients of soluble VEGFA induce the formation of motile endothelium, called tip cells, which break down the surrounding extracellular matrix (ECM) and lead the growth of new vascular sprouts towards VEGFA [387].

FAK is an important regulator of endothelial cell (EC) function, especially during angiogenesis [305]. Indeed, VEGF stimulation increases endothelial FAK kinase activity, FAK Tyr 397 is phosphorylated in tumour endothelium (which will in turn potentiates EC migration and cell-cycle inhibition) and finally, FAK inhibits p53 mediated apoptosis and controls EC survival [388] [389] [390] [391] [392]. Furthermore, FAK is thought to be essential during Angiopoietin-1 mediated porcine pulmonary EC migration and also differentially regulates EC

proliferation/cell-cycle transition in culture dependent upon their particular growth strategy [393] [394].

EC migration and proliferation are essential aspects of angiogenesis so extrapolating this evidence certainly implicates FAK as a vital mediator of angiogenesis. To this end, mouse models have been employed to further address this hypothesis. In general, global FAK ablation results in embryonic death at E8.5 due to multiple defects, including those in the cardiovascular system [395]. Deleting specific domains of FAK yields similar results, as knock-in mutations which impede FAK catalytic domain activity lead to embryonic death at E9.5, associated with haemorrhage and disruption of the blood vascular network [396]. More specifically, targeted deletion of Tyr 397 within the FAK kinase domain causes mice to develop an abnormal vasculature by E12.5, which is later than in kinase dead global knockouts, indicating that the role of FAK in early development is independent of its autophosphorylation [397]. On further investigation it was noted that the vascular defects exhibited in FAK-null mice were due to defects in endothelial migration, and not the impairment of EC differentiation [398]. The relatively early embryonic death of global FAK knockouts limits their use in analysing FAK's role in angiogenesis, so tissue specific, conditional models have been employed to circumvent this.

In endothelial cells FAK has been both over and under expressed. FAK overexpression was achieved in mouse models using a Tie2 promoter and enhancer to overexpress wild-type chicken FAK. As might be expected, FAK overexpression did not induce any defects in vascular development in those mice,

but instead increased wound healing angiogenesis and microvessel density in hindlimb ischemia models [399]. In contrast, the constitutive deletion of FAK in mouse ECs results in embryonic lethality by E11.5, associated with severe vascular defects [400] [401]. Of the two groups that measured this, they each reached differing conclusions regarding why FAK ablation lead to vascular dysfunction. *Shen at al.* [400] showed that deleting FAK will reduce EC migration and proliferation in response to VEGF or fibronectin, whilst *Braren et al.* [401] reveal that ECs exhibit spreading and lamellipodia defects. Surprisingly, the deletion of FAK in adult endothelial cells has no effect on angiogenesis. It has been shown that this is due to compensation by PYK2 [402]. PYK2 will not however compensate for global or developmental EC FAK deletion, as described above. It remains unclear why this is the case but may indicate that PYK2 is dispensable during embryonic development but is required post-development. As such, it may be necessary to inhibit both FAK and PYK2 in the adult to achieve maximal efficacy. Indeed, *Weis et al.* show in the same study that the FAK inhibitor PF-573,228 will not decrease sprout length in aortic ring assays alone, but the synergistic inhibition of FAK and PYK2 will decrease sprout length [402].

Studies also demonstrate that there are elevated levels of FAK (and phosphorylated FAK) in ECs isolated from astrocytomas, which specifically demonstrates the potential importance of EC-FAK in cancer progression and/or growth [390]. In contrast to the previous report by *Weis et al.* it is thought that this may be due to the involvement of adult EC-FAK in angiogenesis. *Tavora et al.*

show that the deletion of FAK in the endothelium will inhibit tumour growth and reduce tumour angiogenesis. Furthermore, FAK deletion will significantly impair both FGF and VEGF-induced neovascularization in aortic ring assays [305]. Similarly, Lee et al. demonstrate that EC-FAK deletion will reduce the volume of gliomas and reduce the diameter of the associated vasculature. Interestingly, there were actually more tumour-related blood vessels in these gliomas, and the vessels were less permeable and more 'normalized' (i.e. less tortuous and branched) than controls [403]. In both studies there was no compensation by PYK2 which may reflect the fact that the studies used different promoter sets, which may target different subpopulations of the endothelium.

In addition, global FAK heterozygote mice actually display enhanced tumour angiogenesis [404]. Interestingly, low doses of FAK inhibitor will phenocopy this as it will also enhance angiogenesis *ex vivo* and tumour growth *in vivo* [404]. This same study showed that FAK-heterozygous endothelial cells demonstrate increased proliferation and microvessel sprouting, but not migration. PYK2 levels did not change across assays, however ECs did display increased Akt expression [404]. Sustained Akt expression in ECs results in enhanced blood vessel size and permeability [405], so increased Akt in ECs may be the causative molecule behind these results. Collectively these data indicate the importance of FAK in both developmental and tumour angiogenesis, and also indicates that PYK2 will not always compensate for the loss of FAK. Furthermore, the latter studies show that FAK may be a non-linear, dose-dependent regulator of angiogenesis.

More recent studies have sought to establish the relative contribution of kinase-

dependent and kinase-independent FAK function. The most recent study by *Sun et al.* used a kinase dead FAK mutant to explore the role of FAK kinase activity in the endothelium of adult mice during angiogenesis. They show here that the inactivation of the FAK kinase domain results in suppressed angiogenesis during wound healing and in the retina. Consistent with this, they also show that loss of FAK kinase activity decreased endothelial cell proliferation and migration, which suggests that kinase-dependent function is vital for this. Central to this was the fact that FAK kinase activity, and its movement to the nucleus, is an essential regulator of VEGFR2, which is crucially involved in angiogenesis, as described later [406]. In addition, colleagues show similar findings indicating that the loss of FAK kinase in the endothelium will reduce tumour size, associated with reduced tumour blood vessel density, increased tumour hypoxia, and also reduced vascular leakage [7]. Together this indicates the probable predominant role of FAK kinase activity over its non-kinase (e.g. scaffolding function) in tumour angiogenesis and also adult pathogenesis. During developmental angiogenesis the relative contribution of FAK kinase-independent and dependent function may differ. *Zhao et al.* show that the majority of endothelial FAK-null mice will die during development by E13.5, whereas knock-in models displaying defective FAK kinase activity were relatively normal here. Those mice lacking FAK kinase activity display reduced EC apoptosis versus total FAK null mice but exhibit similar levels of dysregulated angiogenesis and vessel dilation. Furthermore, both groups exhibit similar vascular permeability, VE-cadherin expression abnormalities and reduced VE-cadherin Tyr 658 phosphorylation [407]. In contrast to adult data this shows that FAK kinase activity

is dispensable during early vascular development (prior to E13.5), but kinase-independent activity alone is insufficient to maintain EC function to allow for completion of embryogenesis. More specifically, they show that FAK non-kinase activity alone can modulate EC survival but not other aspects of EC behaviour during development [407].

6.1.4 Endothelial cell FAK - Chemosensitivity and angiocrine signalling

Chemotherapy is often used as a main stead of therapy in the overall treatment of most cancers. However, despite encouraging initial responses to DNA-damaging chemotherapies, many tumours become resistant to treatment (chemoresistance), which presents a major hurdle in cancer therapy. Therefore, there is an urgent need to identify a strategy that can overcome chemoresistance and sensitize tumour cells to chemotherapeutic agents. Previous work has concentrated on understanding resistance by focusing on mechanisms within tumour cells. More recently, colleagues have identified endothelial cells as an important regulator of chemoresistance [306].

Endothelial cells are now known to secrete organ-specific sets of molecules, known as angiocrine factors, which will actively modify whole organ patterning, regeneration and repair by e.g. progenitor cells [2]. There are increasing lines of evidence that show factors within the endothelium can determine their angiocrine signalling profile and thus differentially regulate both the efficacy of existing

chemotherapy treatments, and also the basal invasiveness and malignancy of tumours. For example, endothelial-derived IL6 will help to generate a 'chemo-resistant niche' in lymphoma mouse models that moderately protects a subset of tumour cells from senescence after DNA damage [408]. In addition, tumour ECs will upregulate Jag1 in response to FGFR1 activation by B cell lymphoma cells, which induces a crosstalk between cells which manifests as a more aggressive lymphoma cell phenotype. Consequently, deleting FGFR1 or Jag1 in ECs diminishes the aggressiveness of lymphomas and prolongs mouse survival [409]. In line with this, EC-FAK may also play a pivotal role in establishing chemoresistance. *Tavora et al.* first show that the genetic ablation of EC-FAK will not reduce tumour angiogenesis or tumour growth if FAK is conditionally deleted after tumour growth has already begun. Next, they treated EC-FAK null mice with various DNA damaging therapies and showed that this is sufficient to sensitize malignant cells to these therapies, which resulted in significant tumour growth control without affecting tumour angiogenesis. The survival of EC-FAK knockout mice was significantly extended in doxorubicin-treated melanoma and lymphoma models, and their perivascular niches show increased apoptosis and reduced tumour cell proliferation. Mechanistically, FAK deficiency inhibited the NF-kB-dependent production of tumour protective endothelial cell-derived cytokines [306]. It is unclear whether or not EC-FAK can regulate other molecules previously implicated in tumour-related angiocrine signalling or whether we can therapeutically harness angiocrine signalling to modify chemoresistance itself. We do however know that EC Akt deletion will lead to the gradual loss of Jag1/Notch

signalling within vascular smooth muscle cells [410], and FAK heterozygote mice exhibit increased EC FAK [404], so it is a logical step to assume that EC FAK can a) regulate EC Akt levels, and b) Akt in turn can modify Notch signalling within the EC compartment, and thus could modify the angiocrine output of the endothelium.

6.2 Aims of the study

My own study builds upon the findings of *Tavora et al.* [306] and investigates whether the kinase domain of EC-FAK is required for EC-FAK mediated chemosensitisation. It is my hypothesis that the FAK kinase domain is an important mediator of this process, and that it is likely that the mechanism underlying this is the same as previously described [306]. To achieve this, we have the following aims:

1) Follow on from the work of previous lab members to assess tumour growth rate in a melanoma model of cancer in EC-FAK Kinase Dead (EC FAK^{KD}) mice.
2) Should there prove to be chemosensitisation in EC FAK^{KD} mice, what is the mechanism underlying tumour cell sensitisation to DNA damaging therapy?

CHAPTER 7.0: RESULTS

FOCAL ADHESION KINASE AND ANGIOCRINE SIGNALLING IN CANCER

7.1 The kinase domain of endothelial cell FAK is a pivotal mediator of FAK-dependent tumour cell sensitisation

Chemotherapy is often used as a main stead of therapy in the overall treatment of most cancers. However, despite encouraging initial responses to DNA-damaging chemotherapies, many tumours become resistant to treatment (chemoresistance), which presents a major hurdle in successful cancer therapy. Therefore, there is an urgent need to identify a strategy that can overcome chemoresistance and sensitise tumour cells to chemotherapeutic agents. Previous work has concentrated on understanding resistance by focusing on mechanisms within tumour cells. More recently, colleagues have identified endothelial cells as an important regulator of chemoresistance [306]. *Tavora et al.* show that targeting endothelial-cell FAK in established tumours is sufficient to sensitise tumour cells to DNA-damaging therapies. They go on to show that deletion of FAK in endothelial cells has no apparent effect on blood vessel function *per se* but induces increased apoptosis and decreased proliferation within perivascular tumour-cell compartments of doxorubicin- and radiotherapy-treated mice. In addition, they demonstrate that the mechanism underlying this phenomenon is that DNA-damage will induce NF-kB activation, which leads to the production of cytoprotective cytokines from the endothelium. Loss of endothelial-cell FAK will reduce DNA-damage-induced cytokine production, and so enhance

chemosensitisation of tumour cells to DNA-damaging therapies *in vitro* and *in vivo* [306].

FAK is a cytoplasmic, non-receptor tyrosine kinase that plays a vital role in integrin and growth factor mediated signalling, extending to functions in a variety of cellular processes including: motility, focal adhesion turnover, survival, growth and invasion [344]. FAK is ubiquitously expressed across most cell types and is overexpressed within many types of solid and non-sold tumours [345] [346]. More recently, FAK activity in the endothelium has been shown to govern tumour angiogenesis [404] [305] and chemosensitisation [306]. Historically, FAK function has more generally been attributed to its central kinase domain kinase activity, but this has more recently been challenged by its interrelated scaffold function.

Herein, we follow on work from previous lab members to investigate tumour growth in mice whose FAK kinase function has been abrogated specifically in the endothelium. These mice are engineered using a knockout/knockin cre-recombinase system to simultaneously knockout mouse FAK and knockin chicken FAK (with a disabled kinase domain) specifically in the endothelium. The kinase domain is disabled in constructs by mutating the ATP binding site in lysine (AAA) position 454 to arginine (AGA) (K454R) {Tavora, 2014 #430}.

Pdgfb-iCre^{ER};R26FAK$^{KD/KD}$;FAK$^{fl/fl}$ (Cre+) mice were injected subcutaneously with mouse melanoma (B16F0) cell line. 11 days after tumour-cell inoculation endothelial-cell FAK was deleted and the kinase dead mutation (K454R) was

introduced with three consecutive IP tamoxifen injections, to generate EC-FAK^{KD} mice. Mice were then treated with doxorubicin on days 13, 15 and 17 post tumour-cell inoculation. Similarly treated Pdgfb-iCre^{ER};R26FAK$^{KD/KD}$;FAK$^{fl/fl}$ (Cre-) were used as controls (EC-FAK^{WT}). The loss of kinase activity in endothelial FAK did not affect B16 tumour growth in placebo-treated mice (**figure 36a**). Similarly, the abrogation of kinase activity in endothelial FAK did not affect B16F0 tumour growth in doxorubicin-treated mice (**figure 36b**). In comparison to tumour growth assays that had been conducted previously in the lab, we saw that B16F0 tumours grew faster than they had in other studies, and so potentially there was not enough time after the last dose of doxorubicin for there to be a differential response to chemotherapy. The data from *Tavora et al.* show that it took 3-4 days for the tumours from EC-FAK^{KO} mice to be differentially sensitised to doxorubicin, and we were forced to cull mice 1-2 days after doxorubicin was administered in my own study. The experiment here took place in C57BL6/129SVJ mice of a 'mixed' background. Prior lab members had observed that B16F0 tumours may grow at different rates amongst mice of different backgrounds, and so we investigated B16F0 tumour growth in mice of a C57BL6 'pure' background as compared to mice of a C57BL6/129SVJ 'mixed' background.

Pdgfb-iCre^{ER};R26FAK$^{KD/KD}$;FAK$^{fl/fl}$ ('pure') and Pdgfb-iCre^{ER};R26FAK$^{KD/KD}$;FAK$^{fl/fl}$ (C57BL6/129SVJ) background mice were injected subcutaneously with 1 million B16F0 cells. The time taken for the average tumour to reach the legal limit of 1500mm^3 was investigated. It took 18 days for those tumours in mice of a mixed background to reach 1500mm^3, whereas it took 23 days in mice of a 'pure'

background (**figure 37**). On average, tumours in 'mixed' background mice took 12 days to reach a volume of 100mm^3 and 13 days in tumours on a 'pure' background. Ideally, 100mm^3 is the size when we aim to begin tamoxifen treatment. Activating cre recombinase with tamoxifen in tumours smaller than this volume will potentially affect their size by differentially regulating tumour angiogenesis [305]. Thus, investigating tumours on a 'pure' background could extend the time over which we can observe tumour growth. Of course, this is a preliminary experiment and tumour growth rates in general can vary dramatically between mice, even those of the same background. This did however give us some rudimentary early evidence to indicate that we might have more success in this particular experiment by observing mice on a 'pure' background.

Having established that B16 tumours may grow more slowly on a 'pure' background, we performed the same study as in **figure 36**, but on Pdgfb-iCre^{ER};R26FAK$^{KD/KD}$;FAK$^{fl/fl}$ from a 'pure' C57BL6 background. To this end, Pdgfb-iCre^{ER};R26FAK$^{KD/KD}$;FAK$^{fl/fl}$ (Cre+) mice were injected subcutaneously with 1 million B16F0 mouse melanoma cells. At 11 days after tumour-cell inoculation, the kinase domain of endothelial-cell FAK was deleted with three consecutive intraperitoneal tamoxifen injections, to generate EC-FAK^{KD} mice. Mice were then treated with doxorubicin on days 13, 15 and 17 post tumour-cell inoculation. Similarly treated Pdgfb-iCre^{ER};R26FAK$^{KD/KD}$;FAK$^{fl/fl}$ (Cre-) mice were used as controls (EC-FAK^{WT}). Herein, the loss of kinase activity in endothelial FAK did not affect B16F0 tumour growth in placebo-treated mice (**figure 38a**). However, the

loss of kinase activity in endothelial FAK may affect B16 tumour growth in doxorubicin-treated mice (**figure 38b**). The difference in tumour volume between doxorubicin treated EC-FAK^{WT} and EC-FAK^{KD} mice was not significant but did tend toward significance.

Previous reports suggest that chemotherapy may generate chemoresistant niches in the perivascular space that will protect tumour cells from apoptosis [306] [408] [411]. In addition, EC FAK has also been shown to regulate tumour angiogenesis accompanied by changes in tumour growth [305]. 48 hours after doxorubicin treatment cessation, the number of endomucin positive blood vessels did not increase in either untreated or treated mice (**figure 39a-b**). This indicates that any potential changes in tumour volume between EC FAK^{WT} and EC FAK^{KD} doxorubicin treated mice were independent to changes in tumour angiogenesis. The number of blood vessels within apoptotic perivascular tumour-cell niches, detected by cleaved caspase 3 staining, was enhanced significantly in doxorubicin-treated ECFAK^{KD} mice when compared with similarly treated ECFAK^{WT} or placebo-treated control mice (**figure 39c**). This suggests that, upon doxorubicin treatment, endothelial cells will secrete factors that will protect tumour cells from apoptosis. The kinase domain of FAK is a pivotal element upstream of these factors, as when it is abrogated in the endothelium, the peri-vascular tumour cell niche in doxorubicin treated EC FAK^{KD} mice is itself is significantly more apoptotic.

Together these experiments constitute preliminary evidence that demonstrate the kinase domain of EC FAK is required during tumour-cell sensitisation to

doxorubicin therapy. Certainly more *in vivo* work needs to be done to ascertain this however.

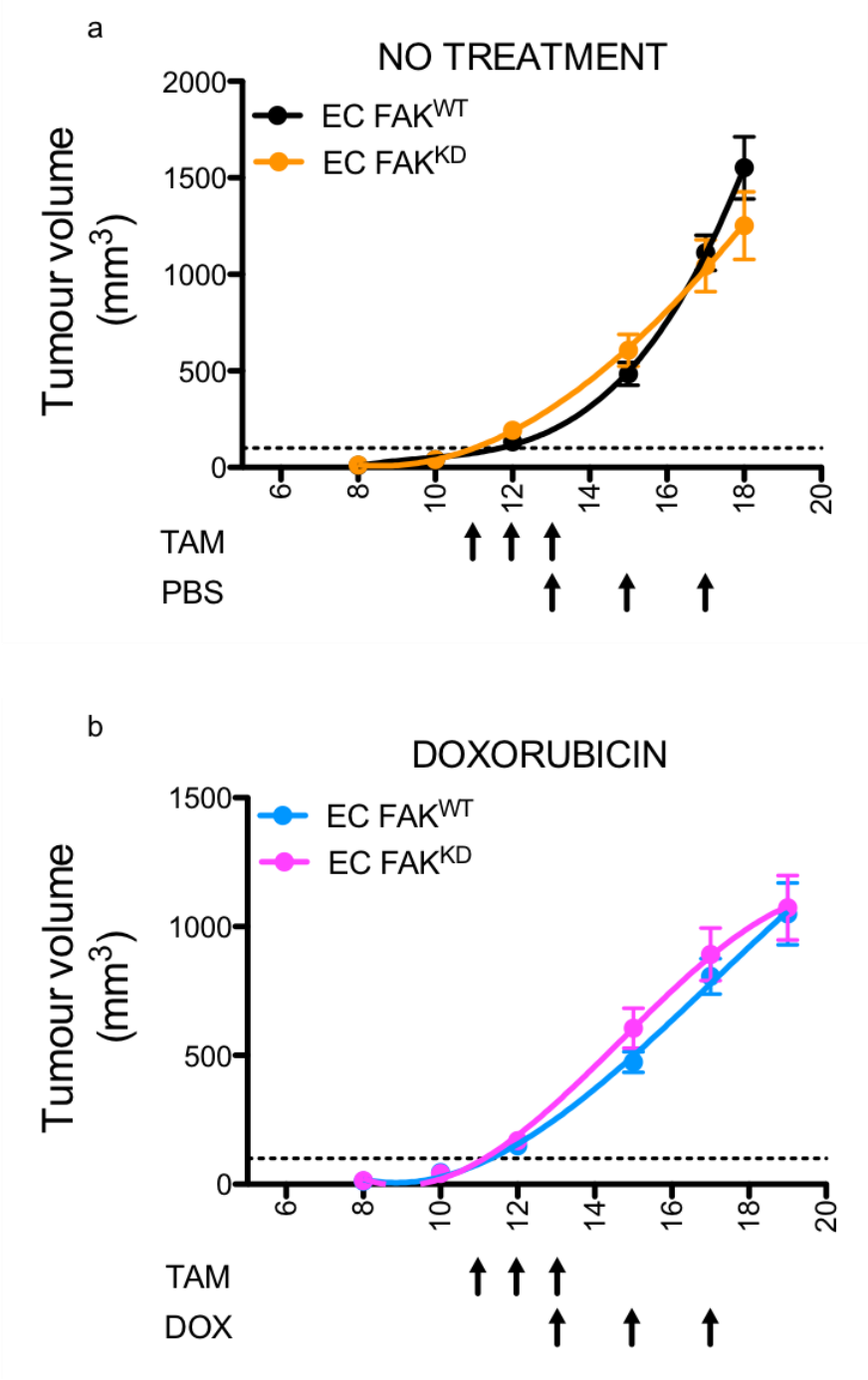

Figure 36: Deleting the kinase domain of endothelial cell FAK (EC FAK^{KD}) will not sensitise cancer cells to doxorubicin *in vivo* in mice from a 'mixed' C57BL6/129SVJ background. Pdgfb-iCre^{ER};R26FAK$^{KD/KD}$;FAK$^{fl/fl}$ (n=12) and control mice (n=12) were injected subcutaneously with B16 tumour cells (day 0), given tamoxifen (Tam.; from day 11 for 3 consecutive days) to generate EC FAK^{KD} and EC FAK^{WT} mice, respectively, and subsequently treated with either doxorubicin or PBS (Dox/PBS; day 13,15 and 17). (**a**) B16 tumour volume in PBS treated and (**b**) doxorubicin treated EC FAK^{KD} and EC FAK^{WT} mice (C57BL6/129SVJ). Data are shown as mean ± SEM.

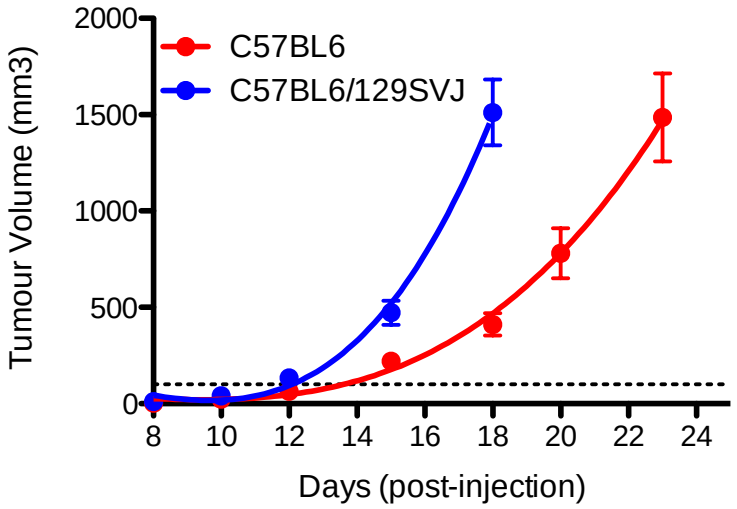

Figure 37: The background of C57BL6 mice can determine B16 tumour growth rate. 1 million B16 tumour cells were injected subcutaneously into mice from either a pure C57BL6 or C57BL6/129SVJ background (n=10 mice per group). The time taken to reach a tumour volume of 1500mm^3 was investigated. Data are shown as mean ± SEM.

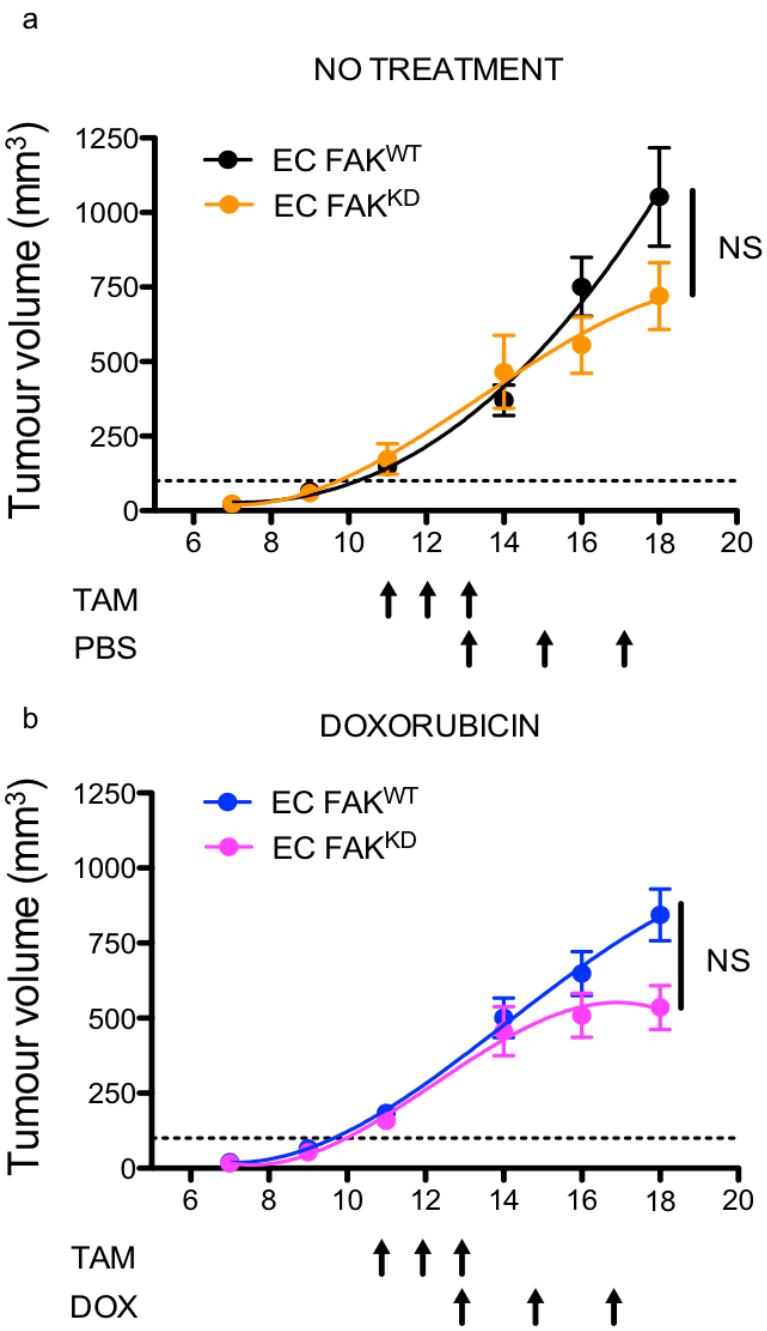

Figure 38: Deleting the kinase domain of endothelial cell FAK (EC FAK^{KD}) will potentially sensitise cancer cells to doxorubicin *in vivo*. *Pdgfb-iCre^{ER};R26FAK$^{KD/KD}$;FAK$^{fl/fl}$* (n=12) and control mice (n=12) were injected subcutaneously with B16 tumour cells (day 0), given tamoxifen (Tam; from day 11 for 3 consecutive days) to generate EC FAK^{KD} and EC FAK^{WT} mice, respectively, and subsequently treated with either doxorubicin or PBS (Dox/PBS; day 13,15 and 17). (**a**) B16 tumour volume in PBS treated and (**b**) doxorubicin treated EC FAK^{KD} and EC FAK^{WT} mice (C57BL6 pure background) **(p=0.1138).** Data are shown as mean ± SEM. Statistical analysis by 1-way ANOVA with Tukey's multiple comparison test post hoc; NS is not significant.

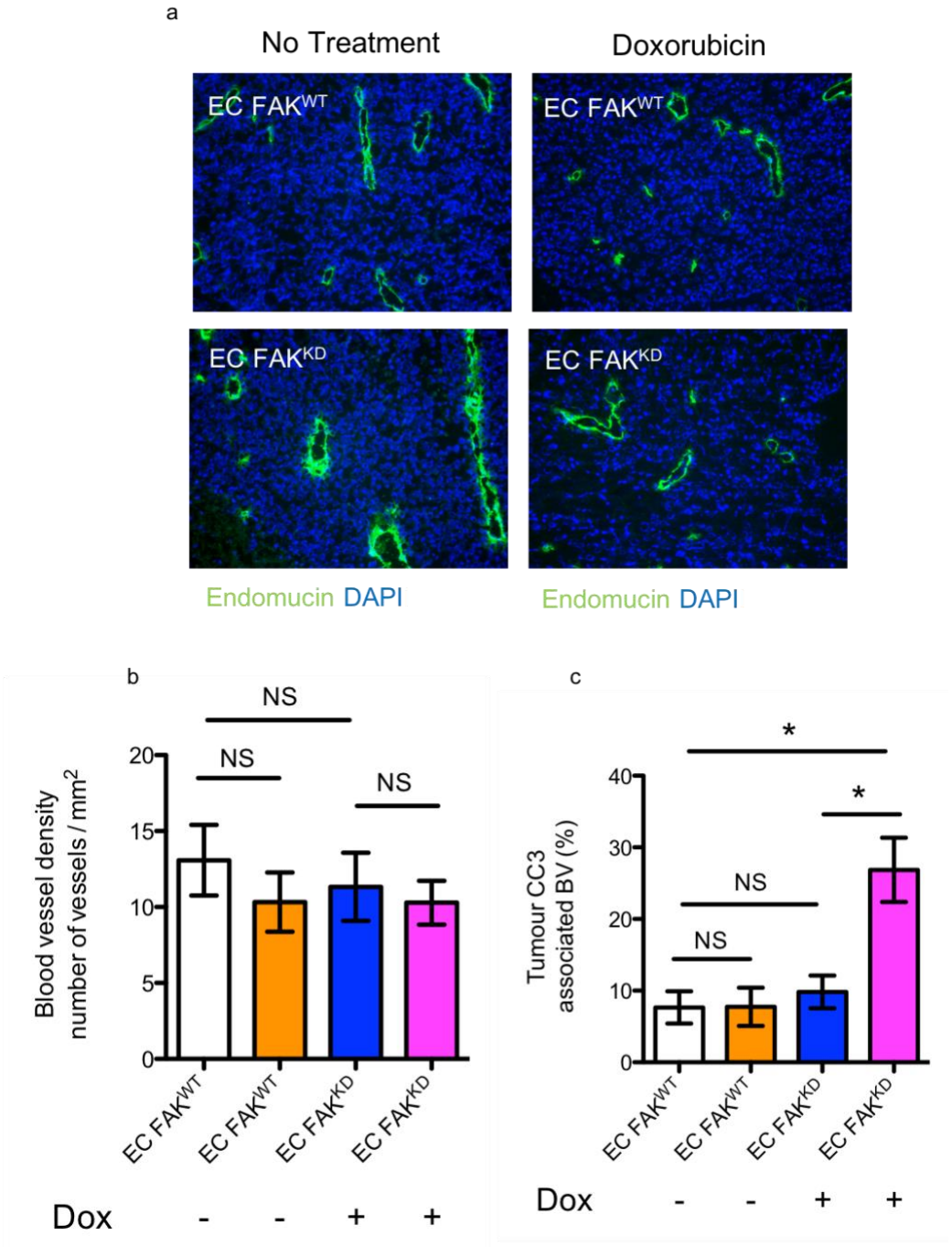

Figure 39: Loss of the kinase domain of endothelial-cell FAK (EC FAK^{KD}) sensitizes tumour cells to doxorubicin but will not affect tumour blood vessel density. Tumour sections from mice treated with either doxorubicin or PBS were stained for the endothelial cell marker (**a-b**) endomucin or the apoptotic marker (**b**) cleaved caspase 3 (CC3). Data are shown as mean ± SEM. Statistical analysis by 1-way ANOVA with Tukey's multiple comparison test post hoc; NS is not significant, *P<0.05. Work done in tandem with Dr. Delphine Lees.

7.2 Abrogating the kinase domain of endothelial cell FAK can modify the angiocrine output of endothelial cells after doxorubicin therapy

Endothelial cells are now known to secrete organ-specific sets of molecules, known as angiocrine factors, which will actively modify whole organ patterning, regeneration and repair by e.g. progenitor cells [2]. There are increasing lines of evidence that show factors within the endothelium can determine their angiocrine signalling profile and thus differentially regulate both the efficacy of existing chemotherapy treatments, and also the basal invasiveness and malignancy of tumours. To confirm that the production of cytoprotective factors from the endothelium is dependent on the kinase domain of FAK after doxorubicin therapy, we performed conditioned media assays and cytokine arrays.

To first validate the cell lines that we will use in subsequent assays, we performed RT-qPCR and western blot analysis to confirm the knockout of mouse FAK and the re-expression of chicken FAK in those EC FAK^{KD} cells. Control cells (EC FAK^{WT}) do not express Cre, and so will express normal mouse FAK and no chicken FAK (**figure 40**).

To determine whether endothelial cells will continue to secrete protective paracrine factors after the kinase domain of FAK is abrogated, we performed MTT assays to investigate B16F0 survival in conditioned media. Here, conditioned media from untreated EC FAK^{KD} or wild type control endothelial cells did not affect B16F0 tumour cell survival (**figure 41a-b**). Similarly, conditioned media from doxorubicin

treated EC FAK^{KD} or wild type control endothelial cells will not protect B16F0 tumour cells from doxorubicin therapy (**figure 41c-d**). Since doxorubicin therapy alone will significantly decrease the survival of tumour cells, we chose to investigate whether using a suboptimal dose of doxorubicin would achieve a differential experimental outcome. To this end, we investigated the effects of varying doses of doxorubicin on B16 tumour cell survival (**figure 42**). We used 125nM doxorubicin in the previous MTT assay, which based on this evidence, will almost entirely kill my tumour cell population. It may therefore be more appropriate to use a suboptimal dose like 40-50nM in future experiments.

We next examined whether abrogating kinase activity in EC FAK will affect doxorubicin-induced cytokine production. Cytokine protein array analysis revealed that doxorubicin stimulation induced an increase in production of several cytokines in wild-type endothelial cells (EC FAK^{WT}) as compared with untreated controls (**figure 43**). In contrast, doxorubicin did not induce an increase in cytokine production with EC FAK^{KD} endothelial cells (**figure 43**). This data shows that abrogating the kinase domain of EC FAK will reduce cytokine secretion by the endothelium after doxorubicin induction.

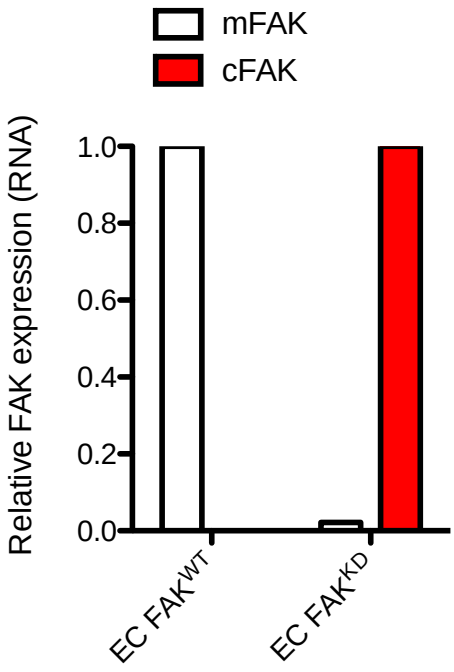

Figure 40: Confirmation of kinase deletion in endothelial-cell FAK. RT-qPCR demonstrating effective knockout of mouse FAK and re-expression of kinase dead chicken FAK in EC FAK^{KD} immortalised endothelial cells.

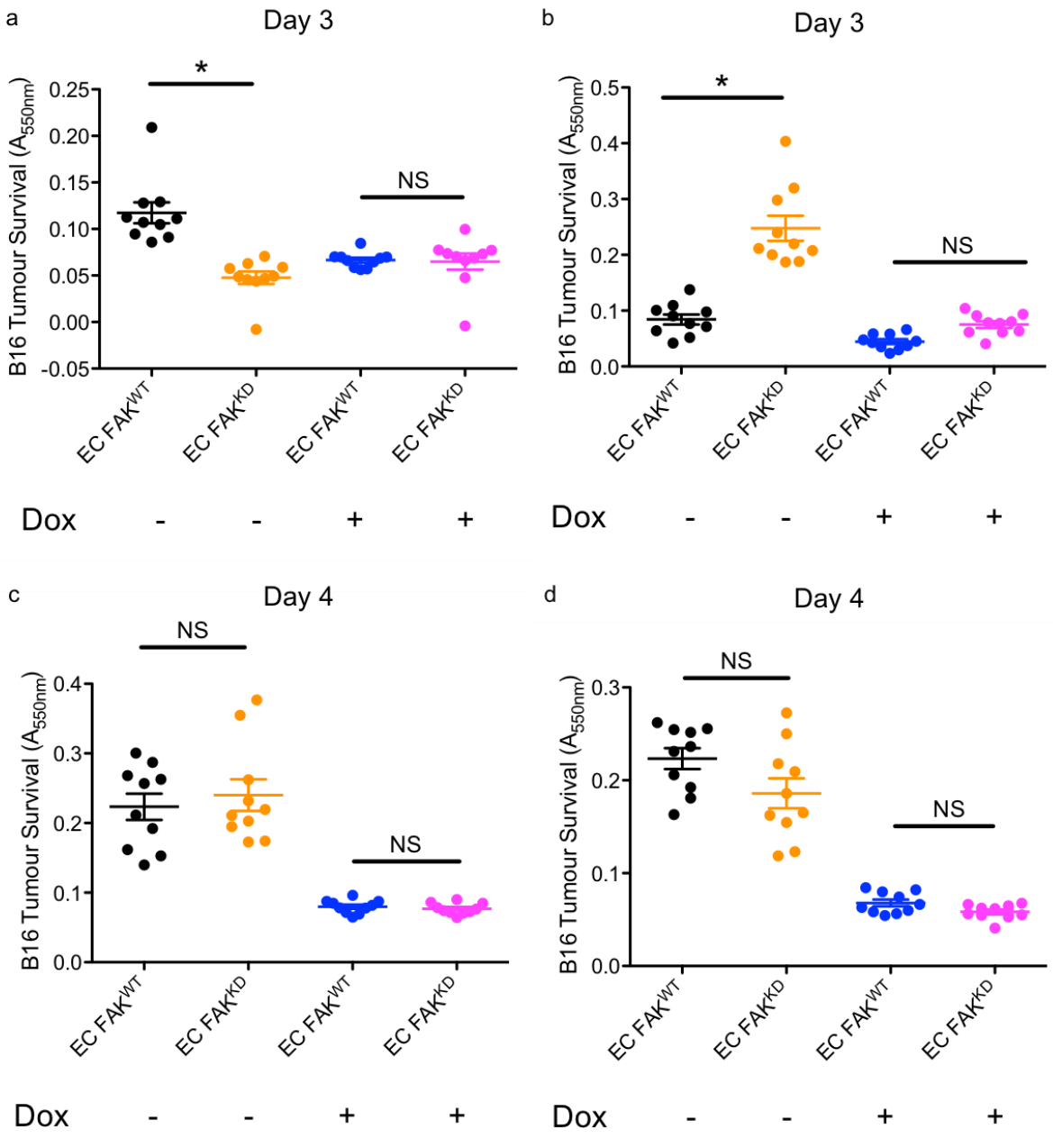

Figure 41: Conditioned media from endothelial cells will not protect B16F0 tumour cells from doxorubicin. (**a-d**) Conditioned media from untreated (−) and doxorubicin-treated (+) endothelial cells were applied to B16 cell cultures 3 (**a-b**) or 4 (**c-d**) days after seeding, and tumour-cell survival was measured (A_{550nm}). n = 2 technical repeats. Data are shown as mean ± SEM. Statistical analysis by 1-way ANOVA with Tukey's multiple comparison test post hoc; NS is not significant.

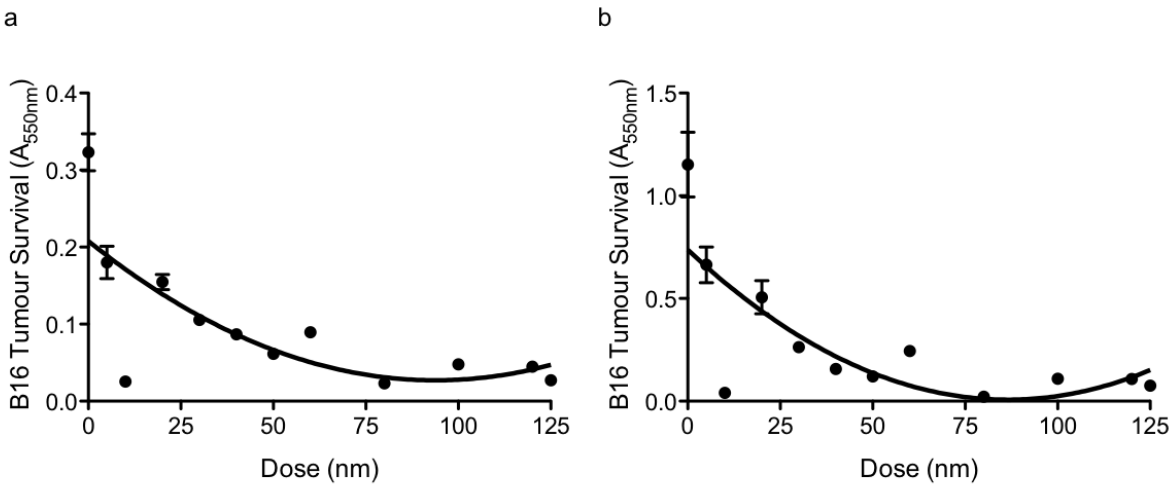

Figure 42: A suboptimal dose of doxorubicin may allow us to more accurately examine tumour-cell survival in MTT assays. (**a-b**) Conditioned media from range of doxorubicin-treated endothelial cells were applied to B16 cell cultures 3 (**a**) or 4 (**b**) days after seeding, and tumour-cell survival was measured (A_{550nm}).

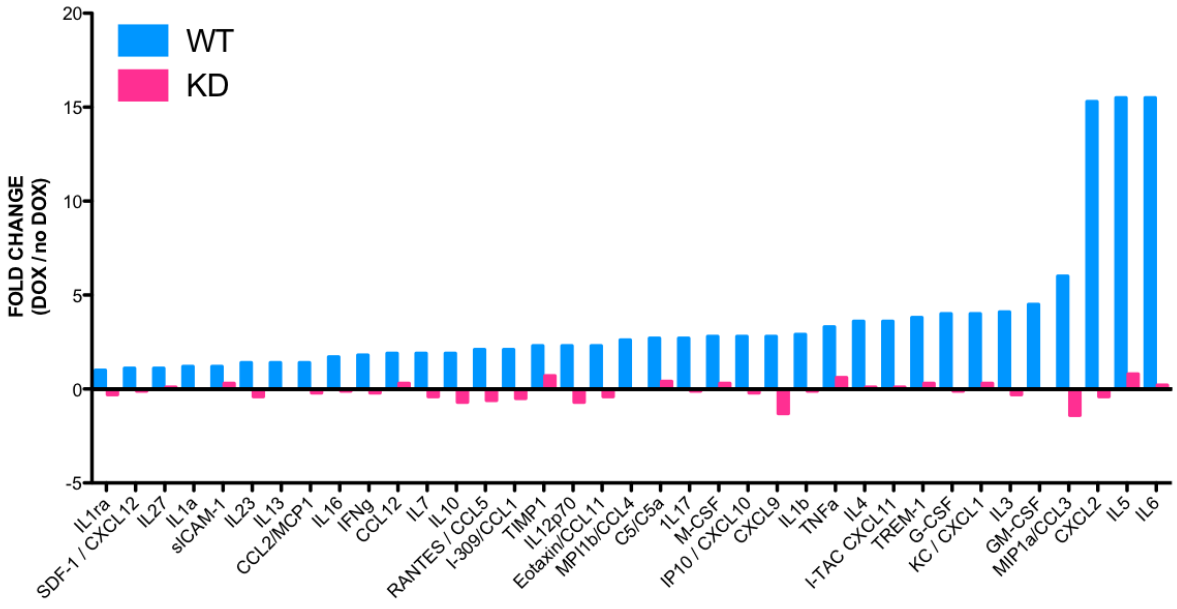

Figure 43: Loss of the kinase domain of endothelial-cell FAK inhibits doxorubicin-induced production of endothelial cytokines. Quantitation of fold difference in cytokine expression between doxorubicin-treated and non-treated wild-type (WT) and kinase dead (KD) FAK endothelial cells. *n* = 1 experimental array. Work done in tandem with Dr. Delphine Lees.

7.3 Summary of chapter results

We have previously shown that specific deletion of focal adhesion kinase (FAK) in endothelial cells is sufficient to induce tumour-cell sensitization to DNA-damaging therapies and thus significantly inhibit tumour growth in mouse models. Here we present novel in vitro and in vivo evidence that indicates FAK kinase activity may be crucial for tumour cell sensitization to the DNA-damaging therapy Doxorubicin. Mechanistically, we demonstrate that the kinase domain of endothelial FAK is required for doxorubicin induced cytokine production – a so called 'angiocrine response' – leading to enhanced chemosensitisation. We anticipate that this data will be useful in determining new chemotherapy strategies, particularly with the clinical availability of FAK kinase domain inhibitors for this purpose.

CHAPTER 8.0: DISCUSSION

FOCAL ADHESION KINASE AND ANGIOCRINE SIGNALLING IN CANCER

The primary objective of this chapter was to determine whether the kinase domain of FAK is an essential feature of endothelial-cell mediated tumour-cell chemosensitisation to DNA-damaging doxorubicin therapy. Indeed, we show preliminary data that indicates that abrogating the kinase domain of FAK (EC FAK^{KD}) in the endothelium will sensitise B16F0 tumour-cells to doxorubicin therapy, versus controls (EC FAK^{WT}). These effects may be mouse background specific, as deleting kinase activity in mice of a C57BL6/129SVJ background will not generate differences in tumour responsiveness. In parallel, we show that tumour angiogenesis within EC FAK^{KD} mice is not different from controls, and instead the perivascular apoptosis of tumour cells within doxorubicin-treated EC FAK^{KD} tumours is significantly upregulated. The mechanism underlying these effects may potentially be that endothelial cells which lack the kinase domain of FAK will secrete significantly fewer cytokines after doxorubicin treatment, as compared to controls. MTT assays could provide functional evidence that the angiocrine factors of endothelial cells could either protect or sensitise B16F0 tumour cells to doxorubicin therapy, but those that we attempted here were unsuccessful, possibly because the dose of doxorubicin used was too high. We propose that with a suboptimal dose of doxorubicin we may see a different experimental outcome.

8.1 The effect of genetic background on tumour-growth rate assays

Genetically engineered mouse models of tumourigenesis have significantly improved our understanding of the molecular mechanisms which propagate cancer. However, this comes with a caveat. The models themselves may display strain-specific phenotypic variation for a given cancer, which will arise due to the influence of their genetic background [412] [413]. This phenomenon has been observed in a variety of strains, across multiple tumour-types. For example, the tumour susceptibility of p53-null and Atm-null mice was increased in mice on a 129SVJ background as compared to mice that were backcrossed onto a C57BL6 background [414] [415]. Consistent with these observations, B16F0 tumours grew at different rates on mice on a C57BL6/129SVJ background as compared to a 'pure' C57BL6 background. In addition, the chemosensitivity of tumours within these mice also differed for a given targeted mutagenesis strategy. In all experiments, mice were kept in the same conditions, treated with the same drugs and to the same diet, and were injected in the same position with the same number of tumour cells, so we can assume that differences in environmental factors did not influence these phenotypic characteristics.

Phenotypic changes in mice of different strains and genetic backgrounds arise due to the differential activity and expression of modifier genes [416]. Modifier genes are genes that have small qualitative effects on the level of expression of another gene [416]. This may manifest for instance, in the coat colour of mice, where instead of a particular gene masking the effects of another gene, it will instead modify its phenotypic expression. It is thought that the background that will present

with the widest variety of phenotypic differences is a ‘mixed’ ground [413]. In theory then, using mice of a ‘pure’ background could limit the inherent variation between models for a given assay that exists for a particular set of experimental mice. ‘Mixed’ mice may give a result that is less consistent, and more variable, than ‘pure’ mice therefore. On the basis of this it could be important to conduct all future experiments on mice of a pure background to reduce phenotypic variability amongst different experimental sets. Of course, this itself presents problems in that mice of a ‘pure’ background are probably less representative of wider human populations, which themselves are an amalgamation of many different genetic heritages.

Aside from this we have also found that the B16F0 tumour cells that we have used will themselves grow at very different rates, both *in vitro* and *in vivo*. This has meant that some experiments have had to be finished much earlier than others since tumour volumes have reached their legal limit before we could properly begin therapy. To minimise these events, we propose that B16F0 tumours should be used from a particular known ‘stock’ vial. The act of culturing cells multiple times, re-freezing those cells, and then recycling this same process can introduce intra-sample genetic drift and selection pressures, which could manifest as differences in e.g. proliferation, amongst other cellular behaviours [417], which may contribute to different tumour growth rates *in vivo*.

8.2 Targeting the kinase domain of FAK is a valuable anti-cancer strategy

Targeting FAK is a promising cancer therapy because it is highly expressed amongst cancer cells and is associated with promoting oncogenic signals and inactivating tumour suppressive signals [418]. The vast majority of FAK-based therapeutics focus on inhibiting the kinase's catalytic function and not the large scaffold it creates that includes may oncogenic and tumour-suppressant proteins [418]. Amongst these, is PF-562,271, which demonstrates robust antitumor activity *in vivo* in tumour models [419]. Preliminary clinical trial data shows that FAK inhibitors may be best used as combination therapy [420]. The reason for this may be to the fact that FAK-inhibition will enhance or synergize with either immunotherapy or chemotherapy [421] [422] [423]. FAK is a known regulator of chemokine transcription [345], and so it is perhaps unsurprising that in both dual-therapy strategies, beneficial effects are thought to be, at least in part, chemokine-dependent [423] [306]. In immunotherapy for instance, small molecular inhibitors of FAK alter tumour-cell production of pro-inflammatory and immunosuppressive cytokines, which improves the responsiveness of pancreatic cancers to checkpoint immunotherapy [423]. Similarly, we show that deleting the kinase domain of FAK in the endothelium will reduce their secreting of a number of chemokines after induced by doxorubicin.

8.3 Future work

In the short term we would certainly repeat the tumour model experiments we have previously completed under different conditions. Primarily, we would ensure that

the mice modelled were specifically injected with Tamoxifen only once their tumours had reached a volume of 100mm^3. We have previously seen that abrogating the kinase domain of FAK in the endothelium will reduce B16F0 tumour volume without any doxorubicin therapy (appendix 1.0 **figure 44**). This could be due to the fact that there is reduced tumour angiogenesis in those EC-FAK^{KD} mice. Similarly, EC-FAK null mice, where tamoxifen was given in tandem to B16F0 tumour inoculation, resulted in reduced tumour angiogenesis, which led to reduced tumour volume itself [305].

In addition, we would perform further mechanistic assays to determine the effects of kinase abrogation with kinase inhibitors on cytokine secretion. In parallel, we would perform further MTT-conditioned media (as in **figure 41**) assays with a suboptimal doxorubicin dose, to investigate whether we would see different experimental outcomes.

CHAPTER 9.0: FINAL STATEMENT

The specific objectives of my PhD were to (a) determine the utility of low dose Cilengitide in a pressure-overload induced murine model of heart failure and (b) investigate whether the kinase domain of FAK is an essential feature of endothelial-cell mediated tumour-cell chemosensitisation to DNA-damaging doxorubicin therapy. In summary of the work presented in this thesis, I consider that I have completed the objectives of the former and have laid some of the foundation work that will help complete the latter. In addition, I have established a useful connection between two previously unrelated labs that have already began to benefit the two.

The information gathered during my PhD could be useful to direct further therapy in the observed fields. Low dose Cilengitide is a novel dual effector of RGD-integrins in both the cardiac endothelial cells and the cardiomyocytes, whilst targeting the kinase domain of FAK in the endothelium with available therapeutics may improve the efficacy of existing chemotherapies.

APPENDIX 1.0: SUPPLEMENTARY DATA

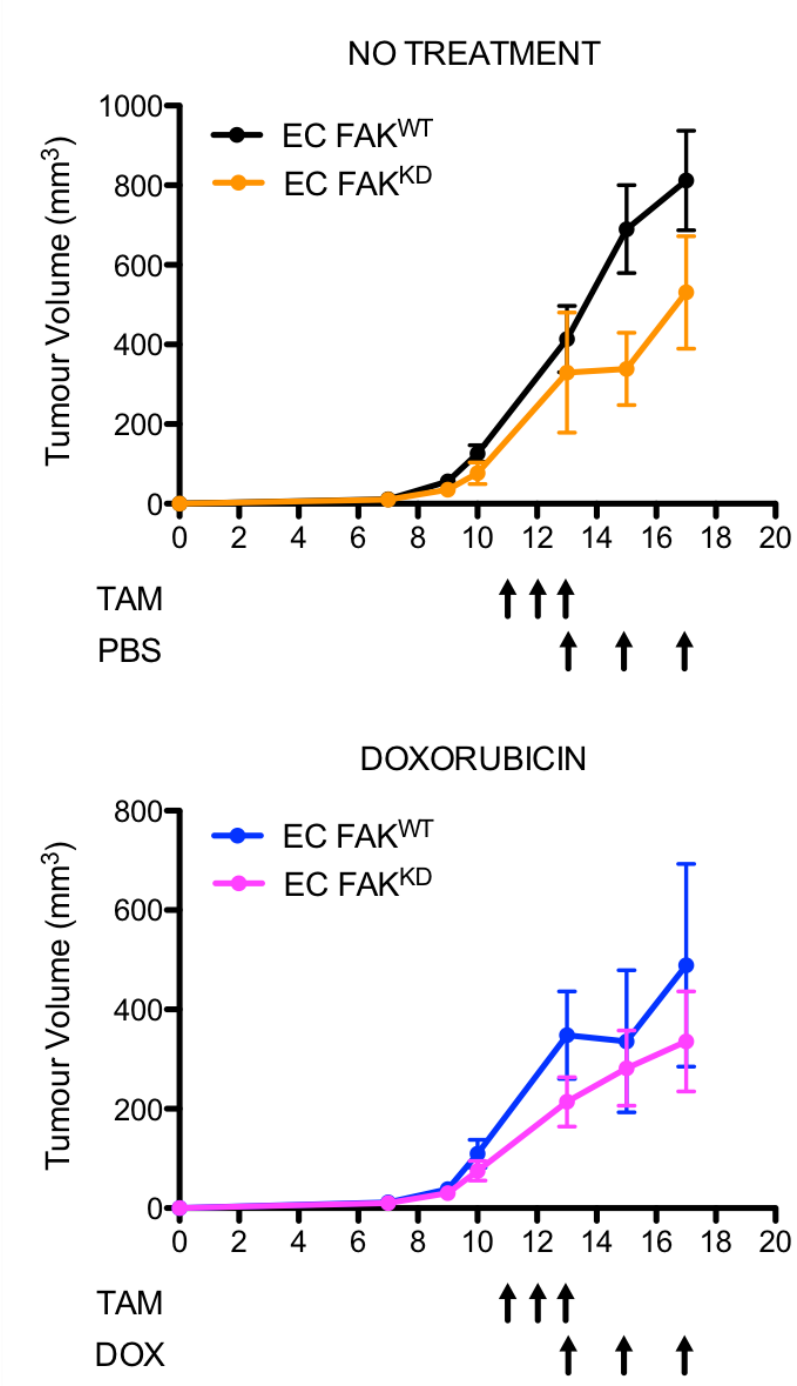

Figure 44: B16F0 tumour survival in EC FAK^{KD} doxorubicin treated and untreated mice as compared to EC FAK^{WT} controls. *Pdgfb-iCre^{ER};R26FAK$^{KD/KD}$;FAK$^{fl/fl}$* (n=12) and control mice (n=12) were injected subcutaneously with B16 tumour cells (day 0), given tamoxifen (Tam; from day 11 for 3 consecutive days) to generate EC FAK^{KD} and EC FAK^{WT} mice, respectively, and subsequently treated with either doxorubicin or PBS (Dox/PBS; day 13,15 and 17). Repeat experiment – no effect of doxorubicin between genotypes in a 'pure' C57BL6 background.

BIBLIOGRAPHY

1. Rajendran, P., et al., *The Vascular Endothelium and Human Diseases*, in *Int J Biol Sci*. 2013. p. 1057-69.
2. Rafii, S., J.M. Butler, and B.S. Ding, *Angiocrine functions of organ-specific endothelial cells.* Nature, 2016. **529**(7586): p. 316-25.
3. Hohimer, A.R., L.E. Davis, and D.C. Hatton, *Repeated daily injections and osmotic pump infusion of isoproterenol cause similar increases in cardiac mass but have different effects on blood pressure.* Can J Physiol Pharmacol, 2005. **83**(2): p. 191-7.
4. Reynolds, A.R., et al., *Stimulation of tumor growth and angiogenesis by low concentrations of RGD-mimetic integrin inhibitors.* Nat Med, 2009. **15**(4): p. 392-400.
5. Wong, P.P., et al., *Dual-action combination therapy enhances angiogenesis while reducing tumor growth and spread.* Cancer Cell, 2015. **27**(1): p. 123-37.
6. Liu, Y., et al., *RNA-Seq identifies novel myocardial gene expression signatures of heart failure.* Genomics, 2015. **105**(2): p. 83-9.
7. Alexopoulou, A.N., et al., *Focal Adhesion Kinase (FAK) tyrosine 397E mutation restores the vascular leakage defect in endothelium-specific FAK-kinase dead mice*, in *J Pathol*. 2017. p. 358-70.
8. Tavora, B., et al., *Generation of point-mutant FAK knockin mice.* Genesis, 2014. **52**(11): p. 907-15.
9. Monahan-Earley, R., A.M. Dvorak, and W.C. Aird, *Evolutionary origins of the blood vascular system and endothelium.* J Thromb Haemost, 2013. **11**(Suppl 1): p. 46-66.
10. Udan, R.S., J.C. Culver, and M.E. Dickinson, *Understanding vascular development: WIRE Developmental Biology (2012).* Wiley Interdiscip Rev Dev Biol, 2013. **2**(3): p. 327-46.
11. Moorman, A., et al., *DEVELOPMENT OF THE HEART: (1) FORMATION OF THE CARDIAC CHAMBERS AND ARTERIAL TRUNKS*, in *Heart*. 2003. p. 806-14.
12. Savolainen, S.M., J.F. Foley, and S.A. Elmore, *Histology atlas of the developing mouse heart with emphasis on E11.5 to E18.5.* Toxicol Pathol, 2009. **37**(4): p. 395-414.
13. Krishnan, A., et al., *A detailed comparison of mouse and human cardiac development.* Pediatr Res, 2014. **76**(6): p. 500-7.
14. Goldie, L.C., M.K. Nix, and K.K. Hirschi, *Embryonic vasculogenesis and hematopoietic specification*, in *Organogenesis*. 2008. p. 257-63.
15. Balasubramanian, R. and X. Zhang, *Mechanisms of FGF gradient formation during embryogenesis.* Semin Cell Dev Biol, 2016. **53**: p. 94-100.
16. Czirok, A., et al., *Multicellular sprouting during vasculogenesis.* Curr Top Dev Biol, 2008. **81**: p. 269-89.

17. Potente, M., H. Gerhardt, and P. Carmeliet, *Basic and therapeutic aspects of angiogenesis.* Cell, 2011. **146**(6): p. 873-87.
18. Duran, C.L., et al., *Molecular Regulation of Sprouting Angiogenesis.* Compr Physiol, 2017. **8**(1): p. 153-235.
19. Marcelo, K.L., L.C. Goldie, and K.K. Hirschi, *Regulation of endothelial cell differentiation and specification.* Circ Res, 2013. **112**(9): p. 1272-87.
20. Blanco, R. and H. Gerhardt, *VEGF and Notch in Tip and Stalk Cell Selection*, in *Cold Spring Harb Perspect Med*. 2013.
21. Gerhardt, H., et al., *VEGF guides angiogenic sprouting utilizing endothelial tip cell filopodia.* J Cell Biol, 2003. **161**(6): p. 1163-77.
22. Herbert, S.P. and D.Y. Stainier, *Molecular control of endothelial cell behaviour during blood vessel morphogenesis.* Nat Rev Mol Cell Biol. **12**(9): p. 551-64.
23. Mack, J.J. and M.L. Iruela-Arispe, *NOTCH regulation of the endothelial cell phenotype*, in *Curr Opin Hematol*. 2018. p. 212-8.
24. Hellstrom, M., et al., *Dll4 signalling through Notch1 regulates formation of tip cells during angiogenesis.* Nature, 2007. **445**(7129): p. 776-80.
25. Lobov, I.B., et al., *Delta-like ligand 4 (Dll4) is induced by VEGF as a negative regulator of angiogenic sprouting.* Proc Natl Acad Sci U S A, 2007. **104**(9): p. 3219-24.
26. Suchting, S., et al., *The Notch ligand Delta-like 4 negatively regulates endothelial tip cell formation and vessel branching.* Proc Natl Acad Sci U S A, 2007. **104**(9): p. 3225-30.
27. Rundhaug, J.E., *Matrix metalloproteinases and angiogenesis.* J Cell Mol Med, 2005. **9**(2): p. 267-85.
28. Herbert, S.P., et al., *Arterial-venous segregation by selective cell sprouting: an alternative mode of blood vessel formation.* Science, 2009. **326**(5950): p. 294-8.
29. Tvorogov, D., et al., *Effective suppression of vascular network formation by combination of antibodies blocking VEGFR ligand binding and receptor dimerization.* Cancer Cell, 2010. **18**(6): p. 630-40.
30. Barry, D.M., et al., *Cdc42 is required for cytoskeletal support of endothelial cell adhesion during blood vessel formation in mice.* Development, 2015. **142**(17): p. 3058-70.
31. Ananthakrishnan, R. and A. Ehrlicher, *The Forces Behind Cell Movement*, in *Int J Biol Sci*. 2007. p. 303-17.
32. Mui, K.L., C.S. Chen, and R.K. Assoian, *The mechanical regulation of integrin–cadherin crosstalk organizes cells, signaling and forces*, in *J Cell Sci*. 2016. p. 1093-100.
33. Mahabeleshwar, G.H., et al., *Mechanisms of integrin-vascular endothelial growth factor receptor cross-activation in angiogenesis.* Circ Res, 2007. **101**(6): p. 570-80.
34. Fassler, R. and M. Meyer, *Consequences of lack of beta 1 integrin gene expression in mice.* Genes Dev, 1995. **9**(15): p. 1896-908.

35. Carlson, T.R., et al., *Cell-autonomous requirement for β1 integrin in endothelial cell adhesion, migration, and survival during angiogenesis in mice.* Development, 2008. **135**(12): p. 2193-202.
36. Reynolds, L.E., et al., *Enhanced pathological angiogenesis in mice lacking beta3 integrin or beta3 and beta5 integrins.* Nat Med, 2002. **8**(1): p. 27-34.
37. Reynolds, A.R., et al., *Elevated Flk1 (vascular endothelial growth factor receptor 2) signaling mediates enhanced angiogenesis in beta3-integrin-deficient mice.* Cancer Res, 2004. **64**(23): p. 8643-50.
38. Carmeliet, P., *Angiogenesis in life, disease and medicine.* Nature, 2005. **438**(7070): p. 932-6.
39. Bergers, G. and S. Song, *The role of pericytes in blood-vessel formation and maintenance1*, in *Neuro Oncol*. 2005. p. 452-64.
40. McIlroy, M., et al., *Pericytes influence endothelial cell growth characteristics: role of plasminogen activator inhibitor type 1 (PAI-1).* Cardiovasc Res, 2006. **69**(1): p. 207-17.
41. Teichert, M., et al., *Pericyte-expressed Tie2 controls angiogenesis and vessel maturation.* Nat Commun, 2017. **8**: p. 16106.
42. Burri, P.H. and V. Djonov, *Intussusceptive angiogenesis--the alternative to capillary sprouting.* Mol Aspects Med, 2002. **23**(6s): p. S1-27.
43. Paku, S., et al., *A New Mechanism for Pillar Formation during Tumor-Induced Intussusceptive Angiogenesis: Inverse Sprouting*, in *Am J Pathol*. 2011. p. 1573-85.
44. Asahara, T., et al., *Isolation of putative progenitor endothelial cells for angiogenesis.* Science, 1997. **275**(5302): p. 964-7.
45. Lin, Y., et al., *Origins of circulating endothelial cells and endothelial outgrowth from blood.* J Clin Invest, 2000. **105**(1): p. 71-7.
46. Takahashi, T., et al., *Ischemia- and cytokine-induced mobilization of bone marrow-derived endothelial progenitor cells for neovascularization.* Nat Med, 1999. **5**(4): p. 434-8.
47. Murayama, T., et al., *Determination of bone marrow-derived endothelial progenitor cell significance in angiogenic growth factor-induced neovascularization in vivo.* Exp Hematol, 2002. **30**(8): p. 967-72.
48. Kalka, C., et al., *Transplantation of ex vivo expanded endothelial progenitor cells for therapeutic neovascularization.* Proc Natl Acad Sci U S A, 2000. **97**(7): p. 3422-7.
49. Tepper, O.M., et al., *Human endothelial progenitor cells from type II diabetics exhibit impaired proliferation, adhesion, and incorporation into vascular structures.* Circulation, 2002. **106**(22): p. 2781-6.
50. Ferrara, N., *VEGF-A: a critical regulator of blood vessel growth.* Eur Cytokine Netw, 2009. **20**(4): p. 158-63.
51. Guyot, M. and G. Pages, *VEGF Splicing and the Role of VEGF Splice Variants: From Physiological-Pathological Conditions to Specific Pre-mRNA Splicing.* Methods Mol Biol, 2015. **1332**: p. 3-23.
52. Ferrara, N., et al., *Heterozygous embryonic lethality induced by targeted inactivation of the VEGF gene.* Nature, 1996. **380**(6573): p. 439-42.

53. Carmeliet, P., et al., *Abnormal blood vessel development and lethality in embryos lacking a single VEGF allele.* Nature, 1996. **380**(6573): p. 435-9.
54. Holmes, D.I. and I. Zachary, *The vascular endothelial growth factor (VEGF) family: angiogenic factors in health and disease*, in *Genome Biol*. 2005. p. 209.
55. Giordano, F.J., et al., *A cardiac myocyte vascular endothelial growth factor paracrine pathway is required to maintain cardiac function.* Proc Natl Acad Sci U S A, 2001. **98**(10): p. 5780-5.
56. Maes, C., et al., *Impaired angiogenesis and endochondral bone formation in mice lacking the vascular endothelial growth factor isoforms VEGF164 and VEGF188.* Mech Dev, 2002. **111**(1-2): p. 61-73.
57. Carmeliet, P., et al., *Impaired myocardial angiogenesis and ischemic cardiomyopathy in mice lacking the vascular endothelial growth factor isoforms VEGF164 and VEGF188.* Nat Med, 1999. **5**(5): p. 495-502.
58. Pritchard-Jones, R.O., et al., *Expression of VEGF(xxx)b, the inhibitory isoforms of VEGF, in malignant melanoma.* Br J Cancer, 2007. **97**(2): p. 223-30.
59. Lee, S., et al., *Autocrine VEGF signaling is required for vascular homeostasis.* Cell, 2007. **130**(4): p. 691-703.
60. Aase, K., et al., *Vascular endothelial growth factor-B-deficient mice display an atrial conduction defect.* Circulation, 2001. **104**(3): p. 358-64.
61. Carmeliet, P., et al., *Synergism between vascular endothelial growth factor and placental growth factor contributes to angiogenesis and plasma extravasation in pathological conditions.* Nat Med, 2001. **7**(5): p. 575-83.
62. Li, G.H., et al., *Dual effects of VEGF-B on activating cardiomyocytes and cardiac stem cells to protect the heart against short- and long-term ischemia-reperfusion injury.* J Transl Med, 2016. **14**(1): p. 116.
63. Bellomo, D., et al., *Mice lacking the vascular endothelial growth factor-B gene (Vegfb) have smaller hearts, dysfunctional coronary vasculature, and impaired recovery from cardiac ischemia.* Circ Res, 2000. **86**(2): p. E29-35.
64. Silvestre, J.S., et al., *Vascular endothelial growth factor-B promotes in vivo angiogenesis.* Circ Res, 2003. **93**(2): p. 114-23.
65. Li, X., et al., *Reevaluation of the role of VEGF-B suggests a restricted role in the revascularization of the ischemic myocardium.* Arterioscler Thromb Vasc Biol, 2008. **28**(9): p. 1614-20.
66. Joukov, V., et al., *Proteolytic processing regulates receptor specificity and activity of VEGF-C.* EMBO J, 1997. **16**(13): p. 3898-911.
67. Stacker, S.A., et al., *Biosynthesis of vascular endothelial growth factor-D involves proteolytic processing which generates non-covalent homodimers.* J Biol Chem, 1999. **274**(45): p. 32127-36.
68. Leppänen, V.M., et al., *Structural and mechanistic insights into VEGF receptor 3 ligand binding and activation*, in *Proc Natl Acad Sci U S A*. 2013. p. 12960-5.
69. Alitalo, K. and P. Carmeliet, *Molecular mechanisms of lymphangiogenesis in health and disease.* Cancer Cell, 2002. **1**(3): p. 219-27.

70. Karkkainen, M.J., et al., *Vascular endothelial growth factor C is required for sprouting of the first lymphatic vessels from embryonic veins.* Nat Immunol, 2004. **5**(1): p. 74-80.
71. Baldwin, M.E., et al., *Vascular endothelial growth factor D is dispensable for development of the lymphatic system.* Mol Cell Biol, 2005. **25**(6): p. 2441-9.
72. Haiko, P., et al., *Deletion of vascular endothelial growth factor C (VEGF-C) and VEGF-D is not equivalent to VEGF receptor 3 deletion in mouse embryos.* Mol Cell Biol, 2008. **28**(15): p. 4843-50.
73. Stacker, S.A., et al., *VEGF-D promotes the metastatic spread of tumor cells via the lymphatics.* Nat Med, 2001. **7**(2): p. 186-91.
74. Kopfstein, L., et al., *Distinct roles of vascular endothelial growth factor-D in lymphangiogenesis and metastasis.* Am J Pathol, 2007. **170**(4): p. 1348-61.
75. Shibuya, M., *Role of VEGF-flt receptor system in normal and tumor angiogenesis.* Adv Cancer Res, 1995. **67**: p. 281-316.
76. Shibuya, M. and L. Claesson-Welsh, *Signal transduction by VEGF receptors in regulation of angiogenesis and lymphangiogenesis.* Exp Cell Res, 2006. **312**(5): p. 549-60.
77. Kliche, S. and J. Waltenberger, *VEGF receptor signaling and endothelial function.* IUBMB Life, 2001. **52**(1-2): p. 61-6.
78. Witmer, A.N., et al., *Expression of vascular endothelial growth factor receptors 1, 2, and 3 in quiescent endothelia.* J Histochem Cytochem, 2002. **50**(6): p. 767-77.
79. Shalaby, F., et al., *Failure of blood-island formation and vasculogenesis in Flk-1-deficient mice.* Nature, 1995. **376**(6535): p. 62-6.
80. Hiratsuka, S., et al., *Flt-1 lacking the tyrosine kinase domain is sufficient for normal development and angiogenesis in mice.* Proc Natl Acad Sci U S A, 1998. **95**(16): p. 9349-54.
81. Laakkonen, P., et al., *Vascular endothelial growth factor receptor 3 is involved in tumor angiogenesis and growth.* Cancer Res, 2007. **67**(2): p. 593-9.
82. Alitalo, K., *The lymphatic vasculature in disease.* Nat Med, 2011. **17**(11): p. 1371-80.
83. Koch, S., et al., *Signal transduction by vascular endothelial growth factor receptors.* Biochem J, 2011. **437**(2): p. 169-83.
84. Dumont, D.J., et al., *Cardiovascular failure in mouse embryos deficient in VEGF receptor-3.* Science, 1998. **282**(5390): p. 946-9.
85. Van Vliet, P., et al., *Early cardiac development: a view from stem cells to embryos.* Cardiovasc Res, 2012. **96**(3): p. 352-62.
86. Katz, T.C., et al., *Distinct Compartments of the Proepicardial Organ Give Rise to Coronary Vascular Endothelial Cells.* Dev Cell, 2012. **22**(3): p. 639-50.
87. Krainock, M., et al., *Epicardial Epithelial-to-Mesenchymal Transition in Heart Development and Disease*, in *J Clin Med*. 2016.
88. Brand, T., *Heart development: molecular insights into cardiac specification and early morphogenesis.* Dev Biol, 2003. **258**(1): p. 1-19.

89. Paradis, A.N., M.S. Gay, and L. Zhang, *Binucleation of cardiomyocytes: the transition from a proliferative to a terminally differentiated state.* Drug Discov Today, 2014. **19**(5): p. 602-9.
90. Ali, S.R., et al., *Existing cardiomyocytes generate cardiomyocytes at a low rate after birth in mice.* Proc Natl Acad Sci U S A, 2014. **111**(24): p. 8850-5.
91. Luttun, A. and P. Carmeliet, *De novo vasculogenesis in the heart.* Cardiovasc Res, 2003. **58**(2): p. 378-89.
92. Tirziu, D., et al., *Myocardial hypertrophy in the absence of external stimuli is induced by angiogenesis in mice.* J Clin Invest, 2007. **117**(11): p. 3188-97.
93. Markkanen, J.E., et al., *Growth factor-induced therapeutic angiogenesis and arteriogenesis in the heart--gene therapy.* Cardiovasc Res, 2005. **65**(3): p. 656-64.
94. Seiler, C., et al., *The human coronary collateral circulation: development and clinical importance.* Eur Heart J, 2013. **34**(34): p. 2674-82.
95. Meier, P., et al., *The collateral circulation of the heart.* BMC Med, 2013. **11**: p. 143.
96. Talman, V. and H. Ruskoaho, *Cardiac fibrosis in myocardial infarction-from repair and remodeling to regeneration.* Cell Tissue Res, 2016. **365**(3): p. 563-81.
97. Watt, A.J., et al., *GATA4 is essential for formation of the proepicardium and regulates cardiogenesis.* Proc Natl Acad Sci U S A, 2004. **101**(34): p. 12573-8.
98. Tevosian, S.G., et al., *FOG-2, a cofactor for GATA transcription factors, is essential for heart morphogenesis and development of coronary vessels from epicardium.* Cell, 2000. **101**(7): p. 729-39.
99. Yang, J.T., H. Rayburn, and R.O. Hynes, *Cell adhesion events mediated by alpha 4 integrins are essential in placental and cardiac development.* Development, 1995. **121**(2): p. 549-60.
100. Kwee, L., et al., *Defective development of the embryonic and extraembryonic circulatory systems in vascular cell adhesion molecule (VCAM-1) deficient mice.* Development, 1995. **121**(2): p. 489-503.
101. Carmeliet, P., *Mechanisms of angiogenesis and arteriogenesis.* Nat Med, 2000. **6**(4): p. 389-95.
102. Lal, N., K. Puri, and B. Rodrigues, *Vascular Endothelial Growth Factor B and Its Signaling*, in *Front Cardiovasc Med*. 2018.
103. Aase, K., et al., *Localization of VEGF-B in the mouse embryo suggests a paracrine role of the growth factor in the developing vasculature.* Dev Dyn, 1999. **215**(1): p. 12-25.
104. Schultz, J.E., et al., *Fibroblast growth factor-2 mediates pressure-induced hypertrophic response.* J Clin Invest, 1999. **104**(6): p. 709-19.
105. Virag, J.A., et al., *Fibroblast growth factor-2 regulates myocardial infarct repair: effects on cell proliferation, scar contraction, and ventricular function.* Am J Pathol, 2007. **171**(5): p. 1431-40.

106. Zhao, T., et al., *Acidic and Basic Fibroblast Growth Factors Involved in Cardiac Angiogenesis following Infarction.* Int J Cardiol, 2011. **152**(3): p. 307-13.
107. Fernandez, B., et al., *Transgenic myocardial overexpression of fibroblast growth factor-1 increases coronary artery density and branching.* Circ Res, 2000. **87**(3): p. 207-13.
108. Tomanek, R.J., et al., *Vascular endothelial growth factor and basic fibroblast growth factor differentially modulate early postnatal coronary angiogenesis.* Circ Res, 2001. **88**(11): p. 1135-41.
109. Karch, R., et al., *The spatial pattern of coronary capillaries in patients with dilated, ischemic, or inflammatory cardiomyopathy.* Cardiovasc Pathol, 2005. **14**(3): p. 135-44.
110. Izumiya, Y., et al., *Vascular endothelial growth factor blockade promotes the transition from compensatory cardiac hypertrophy to failure in response to pressure overload.* Hypertension, 2006. **47**(5): p. 887-93.
111. Jesmin, S., et al., *Age-related changes in cardiac expression of VEGF and its angiogenic receptor KDR in stroke-prone spontaneously hypertensive rats.* Mol Cell Biochem, 2005. **272**(1-2): p. 63-73.
112. Muhlhauser, J., et al., *VEGF165 expressed by a replication-deficient recombinant adenovirus vector induces angiogenesis in vivo.* Circ Res, 1995. **77**(6): p. 1077-86.
113. Xie, X., et al., *Genetic modification of embryonic stem cells with VEGF enhances cell survival and improves cardiac function.* Cloning Stem Cells, 2007. **9**(4): p. 549-63.
114. Sano, M., et al., *p53-induced inhibition of Hif-1 causes cardiac dysfunction during pressure overload.* Nature, 2007. **446**(7134): p. 444-8.
115. Ravi, R., et al., *Regulation of tumor angiogenesis by p53-induced degradation of hypoxia-inducible factor 1alpha.* Genes Dev, 2000. **14**(1): p. 34-44.
116. Shiojima, I., et al., *Disruption of coordinated cardiac hypertrophy and angiogenesis contributes to the transition to heart failure.* J Clin Invest, 2005. **115**(8): p. 2108-18.
117. Gkontra, P., et al., *Deciphering microvascular changes after myocardial infarction through 3D fully automated image analysis.* Sci Rep, 2018. **8**(1): p. 1854.
118. Benjamin, L.E., I. Hemo, and E. Keshet, *A plasticity window for blood vessel remodelling is defined by pericyte coverage of the preformed endothelial network and is regulated by PDGF-B and VEGF.* Development, 1998. **125**(9): p. 1591-8.
119. Souders, C.A., et al., *Pressure Overload Induces Early Morphological Changes in the Heart*, in *Am J Pathol*. 2012. p. 1226-35.
120. Lother, A., et al., *Cardiac Endothelial Cell Transcriptome.* Arterioscler Thromb Vasc Biol, 2018. **38**(3): p. 566-574.
121. Henry, T.D., et al., *The VIVA trial: Vascular endothelial growth factor in Ischemia for Vascular Angiogenesis.* Circulation, 2003. **107**(10): p. 1359-65.

122. Simons, M., et al., *Pharmacological treatment of coronary artery disease with recombinant fibroblast growth factor-2: double-blind, randomized, controlled clinical trial.* Circulation, 2002. **105**(7): p. 788-93.
123. Dor, Y., et al., *Conditional switching of VEGF provides new insights into adult neovascularization and pro-angiogenic therapy.* EMBO J, 2002. **21**(8): p. 1939-47.
124. Tao, Z., et al., *Coexpression of VEGF and angiopoietin-1 promotes angiogenesis and cardiomyocyte proliferation reduces apoptosis in porcine myocardial infarction (MI) heart.* Proc Natl Acad Sci U S A, 2011. **108**(5): p. 2064-9.
125. Richardson, T.P., et al., *Polymeric system for dual growth factor delivery.* Nat Biotechnol, 2001. **19**(11): p. 1029-34.
126. Zheng, Y., et al., *Chimeric VEGF-E(NZ7)/PlGF promotes angiogenesis via VEGFR-2 without significant enhancement of vascular permeability and inflammation.* Arterioscler Thromb Vasc Biol, 2006. **26**(9): p. 2019-26.
127. Taimeh, Z., et al., *Vascular endothelial growth factor in heart failure.* Nat Rev Cardiol, 2013. **10**(9): p. 519-30.
128. Testa, U., G. Pannitteri, and G.L. Condorelli, *Vascular endothelial growth factors in cardiovascular medicine.* J Cardiovasc Med (Hagerstown), 2008. **9**(12): p. 1190-221.
129. Atluri, P. and Y.J. Woo, *Pro-angiogenic cytokines as cardiovascular therapeutics: assessing the potential.* BioDrugs, 2008. **22**(4): p. 209-22.
130. Unger, E.F., et al., *Effects of a single intracoronary injection of basic fibroblast growth factor in stable angina pectoris.* Am J Cardiol, 2000. **85**(12): p. 1414-9.
131. Nakamura, T., et al., *Myocardial protection from ischemia/reperfusion injury by endogenous and exogenous HGF.* J Clin Invest, 2000. **106**(12): p. 1511-9.
132. Madonna, R., et al., *Hepatocyte growth factor: molecular biomarker and player in cardioprotection and cardiovascular regeneration.* Thromb Haemost, 2012. **107**(4): p. 656-61.
133. Shao, S., et al., *Role of SDF-1 and Wnt signaling pathway in the myocardial fibrosis of hypertensive rats.* Am J Transl Res, 2015. **7**(8): p. 1345-56.
134. Dai, W. and R.A. Kloner, *Cardioprotection of insulin-like growth factor-1 during reperfusion therapy: what is the underlying mechanism or mechanisms?*, in *Circ Cardiovasc Interv*. 2011: United States. p. 311-3.
135. Hsieh, P.C., et al., *Controlled delivery of PDGF-BB for myocardial protection using injectable self-assembling peptide nanofibers.* J Clin Invest, 2006. **116**(1): p. 237-48.
136. Huber, B.C., et al., *Attenuation of cardiac hypertrophy by G-CSF is associated with enhanced migration of bone marrow-derived cells.* J Cell Mol Med, 2015. **19**(5): p. 1033-41.
137. Chong, A.Y., G.J. Caine, and G.Y. Lip, *Angiopoietin/tie-2 as mediators of angiogenesis: a role in congestive heart failure?* Eur J Clin Invest, 2004. **34**(1): p. 9-13.

138. Bersell, K., et al., *Neuregulin1/ErbB4 signaling induces cardiomyocyte proliferation and repair of heart injury.* Cell, 2009. **138**(2): p. 257-70.
139. Calvillo, L., et al., *Recombinant human erythropoietin protects the myocardium from ischemia-reperfusion injury and promotes beneficial remodeling.* Proc Natl Acad Sci U S A, 2003. **100**(8): p. 4802-6.
140. Makinen, K., et al., *Increased vascularity detected by digital subtraction angiography after VEGF gene transfer to human lower limb artery: a randomized, placebo-controlled, double-blinded phase II study.* Mol Ther, 2002. **6**(1): p. 127-33.
141. Lederman, R.J., et al., *Therapeutic angiogenesis with recombinant fibroblast growth factor-2 for intermittent claudication (the TRAFFIC study): a randomised trial.* Lancet, 2002. **359**(9323): p. 2053-8.
142. Rajagopalan, S., et al., *Regional angiogenesis with vascular endothelial growth factor in peripheral arterial disease: a phase II randomized, double-blind, controlled study of adenoviral delivery of vascular endothelial growth factor 121 in patients with disabling intermittent claudication.* Circulation, 2003. **108**(16): p. 1933-8.
143. Naim, C., A. Yerevanian, and R.J. Hajjar, *Gene Therapy for Heart Failure: Where Do We Stand?* Curr Cardiol Rep, 2013. **15**(2): p. 333.
144. Hajjar, R.J., *Potential of gene therapy as a treatment for heart failure*, in *J Clin Invest*. 2013. p. 53-61.
145. Gonçalves, G.A.R. and M.A. Paiva Rde, *Gene therapy: advances, challenges and perspectives*, in *Einstein (Sao Paulo)*. 2017. p. 369-75.
146. Muona, K., et al., *10-year safety follow-up in patients with local VEGF gene transfer to ischemic lower limb.* Gene Ther, 2012. **19**(4): p. 392-5.
147. Iyer, S.R. and B.H. Annex, *Therapeutic Angiogenesis for Peripheral Artery Disease: Lessons Learned in Translational Science*, in *JACC Basic Transl Sci*. 2017. p. 503-12.
148. Fortuin, F.D., et al., *One-year follow-up of direct myocardial gene transfer of vascular endothelial growth factor-2 using naked plasmid deoxyribonucleic acid by way of thoracotomy in no-option patients.* Am J Cardiol, 2003. **92**(4): p. 436-9.
149. Stewart, D.J., et al., *VEGF Gene Therapy Fails to Improve Perfusion of Ischemic Myocardium in Patients With Advanced Coronary Disease: Results of the NORTHERN Trial.* Mol Ther, 2009. **17**(6): p. 1109-1115.
150. Kastrup, J., et al., *Direct intramyocardial plasmid vascular endothelial growth factor-A165 gene therapy in patients with stable severe angina pectoris A randomized double-blind placebo-controlled study: the Euroinject One trial.* J Am Coll Cardiol, 2005. **45**(7): p. 982-8.
151. Nikol, S., et al., *Therapeutic angiogenesis with intramuscular NV1FGF improves amputation-free survival in patients with critical limb ischemia.* Mol Ther, 2008. **16**(5): p. 972-8.
152. Ruel, M., et al., *Long-term effects of surgical angiogenic therapy with fibroblast growth factor 2 protein.* J Thorac Cardiovasc Surg, 2002. **124**(1): p. 28-34.

153. Grines, C., et al., *Angiogenic gene therapy with adenovirus 5 fibroblast growth factor-4 (Ad5FGF-4): a new option for the treatment of coronary artery disease.* Am J Cardiol, 2003. **92**(9b): p. 24n-31n.
154. Voisine, P., et al., *Effects of L-arginine on fibroblast growth factor 2-induced angiogenesis in a model of endothelial dysfunction.* Circulation, 2005. **112**(9 Suppl): p. I202-7.
155. Kahlon, A., G. Vaidya, and R. Bolli, *Cell therapy for heart disease: current status and future directions.* Minerva Cardioangiol, 2018. **66**(3): p. 273-291.
156. Tsilimigras, D.I., et al., *Stem Cell Therapy for Congenital Heart Disease: A Systematic Review.* Circulation, 2017. **136**(24): p. 2373-2385.
157. Chong, M.S., W.K. Ng, and J.K. Chan, *Concise Review: Endothelial Progenitor Cells in Regenerative Medicine: Applications and Challenges.* Stem Cells Transl Med, 2016. **5**(4): p. 530-8.
158. Tilling, L., P. Chowienczyk, and B. Clapp, *Progenitors in motion: mechanisms of mobilization of endothelial progenitor cells.* Br J Clin Pharmacol, 2009. **68**(4): p. 484-92.
159. Lam, C.F., et al., *Autologous transplantation of endothelial progenitor cells attenuates acute lung injury in rabbits.* Anesthesiology, 2008. **108**(3): p. 392-401.
160. Altabas, V., K. Altabas, and L. Kirigin, *Endothelial progenitor cells (EPCs) in ageing and age-related diseases: How currently available treatment modalities affect EPC biology, atherosclerosis, and cardiovascular outcomes.* Mech Ageing Dev, 2016. **159**: p. 49-62.
161. Antonio, N., et al., *Reduced levels of circulating endothelial progenitor cells in acute myocardial infarction patients with diabetes or pre-diabetes: accompanying the glycemic continuum.* Cardiovasc Diabetol, 2014. **13**: p. 101.
162. Kocher, A.A., et al., *Neovascularization of ischemic myocardium by human bone-marrow-derived angioblasts prevents cardiomyocyte apoptosis, reduces remodeling and improves cardiac function.* Nat Med, 2001. **7**(4): p. 430-6.
163. Orlic, D., et al., *Mobilized bone marrow cells repair the infarcted heart, improving function and survival.* Proc Natl Acad Sci U S A, 2001. **98**(18): p. 10344-9.
164. Griese, D.P., et al., *Isolation and transplantation of autologous circulating endothelial cells into denuded vessels and prosthetic grafts: implications for cell-based vascular therapy.* Circulation, 2003. **108**(21): p. 2710-5.
165. Xu, Q., et al., *Circulating progenitor cells regenerate endothelium of vein graft atherosclerosis, which is diminished in ApoE-deficient mice.* Circ Res, 2003. **93**(8): p. e76-86.
166. Rauscher, F.M., et al., *Aging, progenitor cell exhaustion, and atherosclerosis.* Circulation, 2003. **108**(4): p. 457-63.
167. Mangi, A.A., et al., *Mesenchymal stem cells modified with Akt prevent remodeling and restore performance of infarcted hearts.* Nat Med, 2003. **9**(9): p. 1195-201.

168. Gnecchi, M., et al., *Evidence supporting paracrine hypothesis for Akt-modified mesenchymal stem cell-mediated cardiac protection and functional improvement.* Faseb j, 2006. **20**(6): p. 661-9.
169. Li, W., et al., *Bcl-2 engineered MSCs inhibited apoptosis and improved heart function.* Stem Cells, 2007. **25**(8): p. 2118-27.
170. Fujita, Y. and A. Kawamoto, *Stem cell-based peripheral vascular regeneration.* Adv Drug Deliv Rev, 2017. **120**: p. 25-40.
171. Martin-Rendon, E., et al., *Autologous bone marrow stem cells to treat acute myocardial infarction: a systematic review.* Eur Heart J, 2008. **29**(15): p. 1807-18.
172. Xie, B., et al., *Autologous Stem Cell Therapy in Critical Limb Ischemia: A Meta-Analysis of Randomized Controlled Trials.* Stem Cells Int, 2018. **2018**.
173. Liew, A., et al., *Cell Therapy for Critical Limb Ischemia: A Meta-Analysis of Randomized Controlled Trials.* Angiology, 2016. **67**(5): p. 444-55.
174. Fisher, S.A., et al., *Meta-analysis of cell therapy trials for patients with heart failure.* Circ Res, 2015. **116**(8): p. 1361-77.
175. Gyongyosi, M., et al., *Meta-Analysis of Cell Therapy Studies in Heart Failure and Acute Myocardial Infarction.* Circ Res, 2018. **123**(2): p. 301-308.
176. Tang, J., et al., *Combination of chemokine and angiogenic factor genes and mesenchymal stem cells could enhance angiogenesis and improve cardiac function after acute myocardial infarction in rats.* Mol Cell Biochem, 2010. **339**(1-2): p. 107-18.
177. Arai, M., et al., *Granulocyte colony-stimulating factor: a noninvasive regeneration therapy for treating atherosclerotic peripheral artery disease.* Circ J, 2006. **70**(9): p. 1093-8.
178. Prochazka, V., et al., *Cell therapy, a new standard in management of chronic critical limb ischemia and foot ulcer.* Cell Transplant, 2010. **19**(11): p. 1413-24.
179. Walter, D.H., et al., *Intraarterial administration of bone marrow mononuclear cells in patients with critical limb ischemia: a randomized-start, placebo-controlled pilot trial (PROVASA).* Circ Cardiovasc Interv, 2011. **4**(1): p. 26-37.
180. Benoit, E., et al., *The role of amputation as an outcome measure in cellular therapy for critical limb ischemia: implications for clinical trial design*, in *J Transl Med*. 2011. p. 165.
181. Li, M., et al., *Autologous bone marrow mononuclear cells transplant in patients with critical leg ischemia: preliminary clinical results.* Exp Clin Transplant, 2013. **11**(5): p. 435-9.
182. Strauer, B.E., et al., *Repair of infarcted myocardium by autologous intracoronary mononuclear bone marrow cell transplantation in humans.* Circulation, 2002. **106**(15): p. 1913-8.
183. Ge, J., et al., *Efficacy of emergent transcatheter transplantation of stem cells for treatment of acute myocardial infarction (TCT-STAMI).* Heart, 2006. **92**(12): p. 1764-7.
184. Huang, R.C., et al., *[Long term follow-up on emergent intracoronary autologous bone marrow mononuclear cell transplantation for acute inferior-*

wall myocardial infarction]. Zhonghua Yi Xue Za Zhi, 2006. **86**(16): p. 1107-10.
185. Janssens, S., et al., *Autologous bone marrow-derived stem-cell transfer in patients with ST-segment elevation myocardial infarction: double-blind, randomised controlled trial.* Lancet, 2006. **367**(9505): p. 113-21.
186. Lunde, K., et al., *Intracoronary injection of mononuclear bone marrow cells in acute myocardial infarction.* N Engl J Med, 2006. **355**(12): p. 1199-209.
187. Kang, H.J., et al., *Differential effect of intracoronary infusion of mobilized peripheral blood stem cells by granulocyte colony-stimulating factor on left ventricular function and remodeling in patients with acute myocardial infarction versus old myocardial infarction: the MAGIC Cell-3-DES randomized, controlled trial.* Circulation, 2006. **114**(1 Suppl): p. I145-51.
188. Li, Z.Q., et al., *The clinical study of autologous peripheral blood stem cell transplantation by intracoronary infusion in patients with acute myocardial infarction (AMI).* Int J Cardiol, 2007. **115**(1): p. 52-6.
189. Huang, P., et al., *Autologous transplantation of granulocyte colony-stimulating factor-mobilized peripheral blood mononuclear cells improves critical limb ischemia in diabetes.* Diabetes Care, 2005. **28**(9): p. 2155-60.
190. Ozturk, A., et al., *Therapeutical potential of autologous peripheral blood mononuclear cell transplantation in patients with type 2 diabetic critical limb ischemia.* J Diabetes Complications, 2012. **26**(1): p. 29-33.
191. Tateno, K., et al., *Critical roles of muscle-secreted angiogenic factors in therapeutic neovascularization.* Circ Res, 2006. **98**(9): p. 1194-202.
192. Losordo, D.W., et al., *A randomized, controlled pilot study of autologous CD34+ cell therapy for critical limb ischemia.* Circ Cardiovasc Interv, 2012. **5**(6): p. 821-30.
193. Kawamoto, A., et al., *Intramuscular transplantation of G-CSF-mobilized CD34(+) cells in patients with critical limb ischemia: a phase I/IIa, multicenter, single-blinded, dose-escalation clinical trial.* Stem Cells, 2009. **27**(11): p. 2857-64.
194. Fujita, Y., et al., *Phase II clinical trial of CD34+ cell therapy to explore endpoint selection and timing in patients with critical limb ischemia.* Circ J, 2014. **78**(2): p. 490-501.
195. Perin, E.C., et al., *Evaluation of Cell Therapy on Exercise Performance and Limb Perfusion in Peripheral Artery Disease: The CCTRN PACE Trial (Patients With Intermittent Claudication Injected With ALDH Bright Cells).* Circulation, 2017. **135**(15): p. 1417-1428.
196. Minatoguchi, S., et al., *Acceleration of the healing process and myocardial regeneration may be important as a mechanism of improvement of cardiac function and remodeling by postinfarction granulocyte colony-stimulating factor treatment.* Circulation, 2004. **109**(21): p. 2572-80.
197. Buschmann, I.R., et al., *GM-CSF: a strong arteriogenic factor acting by amplification of monocyte function.* Atherosclerosis, 2001. **159**(2): p. 343-56.
198. van Royen, N., et al., *START Trial: a pilot study on STimulation of ARTeriogenesis using subcutaneous application of granulocyte-*

macrophage colony-stimulating factor as a new treatment for peripheral vascular disease. Circulation, 2005. **112**(7): p. 1040-6.
199. Poole, J., et al., *Effect of progenitor cell mobilization with granulocyte-macrophage colony-stimulating factor in patients with peripheral artery disease: a randomized clinical trial.* Jama, 2013. **310**(24): p. 2631-9.
200. Lal, H., et al., *Integrins: novel therapeutic targets for cardiovascular diseases.* Cardiovasc Hematol Agents Med Chem, 2007. **5**(2): p. 109-32.
201. Takagi, J., *Structural basis for ligand recognition by RGD (Arg-Gly-Asp)-dependent integrins.* Biochem Soc Trans, 2004. **32**(Pt3): p. 403-6.
202. Hynes, R.O., *Integrins: bidirectional, allosteric signaling machines.* Cell, 2002. **110**(6): p. 673-87.
203. Campbell, I.D. and M.J. Humphries, *Integrin structure, activation, and interactions.* Cold Spring Harb Perspect Biol, 2011. **3**(3).
204. Jones, J.L. and R.A. Walker, *Integrins: a role as cell signalling molecules.* Mol Pathol, 1999. **52**(4): p. 208-13.
205. Malinin, N.L., E. Pluskota, and T.V. Byzova, *Integrin signaling in vascular function.* Curr Opin Hematol, 2012. **19**(3): p. 206-11.
206. Sepp, N.T., et al., *Basic fibroblast growth factor increases expression of the alpha v beta 3 integrin complex on human microvascular endothelial cells.* J Invest Dermatol, 1994. **103**(3): p. 295-9.
207. Max, R., et al., *Immunohistochemical analysis of integrin alpha vbeta3 expression on tumor-associated vessels of human carcinomas.* Int J Cancer, 1997. **71**(3): p. 320-4.
208. Bader, B.L., et al., *Extensive vasculogenesis, angiogenesis, and organogenesis precede lethality in mice lacking all alpha v integrins.* Cell, 1998. **95**(4): p. 507-19.
209. McCarty, J.H., et al., *Selective ablation of alphav integrins in the central nervous system leads to cerebral hemorrhage, seizures, axonal degeneration and premature death.* Development, 2005. **132**(1): p. 165-76.
210. van der Flier, A., et al., *Endothelial α5 and αv integrins cooperate in remodeling of the vasculature during development.* Development, 2010. **137**(14): p. 2439-49.
211. Hodivala-Dilke, K.M., et al., *Beta3-integrin-deficient mice are a model for Glanzmann thrombasthenia showing placental defects and reduced survival.* J Clin Invest, 1999. **103**(2): p. 229-38.
212. Huang, X., et al., *Normal development, wound healing, and adenovirus susceptibility in beta5-deficient mice.* Mol Cell Biol, 2000. **20**(3): p. 755-9.
213. Mahabeleshwar, G.H., et al., *Integrin signaling is critical for pathological angiogenesis.* J Exp Med, 2006. **203**(11): p. 2495-507.
214. Weng, S., et al., *Beta3 integrin deficiency promotes atherosclerosis and pulmonary inflammation in high-fat-fed, hyperlipidemic mice.* Proc Natl Acad Sci U S A, 2003. **100**(11): p. 6730-5.
215. Reynolds, L.E., et al., *Accelerated re-epithelialization in beta3-integrin-deficient- mice is associated with enhanced TGF-beta1 signaling.* Nat Med, 2005. **11**(2): p. 167-74.

216. Weis, S.M., et al., *Cooperation between VEGF and beta3 integrin during cardiac vascular development.* Blood, 2007. **109**(5): p. 1962-70.
217. Borges, E., Y. Jan, and E. Ruoslahti, *Platelet-derived growth factor receptor beta and vascular endothelial growth factor receptor 2 bind to the beta 3 integrin through its extracellular domain.* J Biol Chem, 2000. **275**(51): p. 39867-73.
218. Singh, B., C. Fu, and J. Bhattacharya, *Vascular expression of the alpha(v)beta(3)-integrin in lung and other organs.* Am J Physiol Lung Cell Mol Physiol, 2000. **278**(1): p. L217-26.
219. Sun, M., et al., *Temporal response and localization of integrins beta1 and beta3 in the heart after myocardial infarction: regulation by cytokines.* Circulation, 2003. **107**(7): p. 1046-52.
220. Zhao, T., et al., *Vascular endothelial growth factor (VEGF)-A: role on cardiac angiogenesis following myocardial infarction.* Microvasc Res, 2010. **80**(2): p. 188-94.
221. Le Gat, L., et al., *Prominent beta-5 gene expression in the cardiovascular system and in the cartilaginous primordiae of the skeleton during mouse development.* Cell Commun Adhes, 2001. **8**(3): p. 99-112.
222. Brooks, P.C., R.A. Clark, and D.A. Cheresh, *Requirement of vascular integrin alpha v beta 3 for angiogenesis.* Science, 1994. **264**(5158): p. 569-71.
223. Storgard, C.M., et al., *Decreased angiogenesis and arthritic disease in rabbits treated with an alphavbeta3 antagonist.* J Clin Invest, 1999. **103**(1): p. 47-54.
224. Gonzalez, A.M., et al., *Transdominant Regulation of Integrin Function: Mechanisms of Crosstalk.* Cell Signal, 2010. **22**(4): p. 578.
225. Robinson, S.D., et al., *Beta3-integrin regulates vascular endothelial growth factor-A-dependent permeability.* Arterioscler Thromb Vasc Biol, 2004. **24**(11): p. 2108-14.
226. West, X.Z., et al., *Integrin beta3 crosstalk with VEGFR accommodating tyrosine phosphorylation as a regulatory switch.* PLoS One, 2012. **7**(2): p. e31071.
227. Ly, D.P., K.M. Zazzali, and S.A. Corbett, *De novo expression of the integrin alpha5beta1 regulates alphavbeta3-mediated adhesion and migration on fibrinogen.* J Biol Chem, 2003. **278**(24): p. 21878-85.
228. Laurens, N., et al., *Single and combined effects of alphavbeta3- and alpha5beta1-integrins on capillary tube formation in a human fibrinous matrix.* Angiogenesis, 2009. **12**(3): p. 275-85.
229. Gonzalez, A.M., et al., *Complex interactions between the laminin alpha 4 subunit and integrins regulate endothelial cell behavior in vitro and angiogenesis in vivo.* Proc Natl Acad Sci U S A, 2002. **99**(25): p. 16075-80.
230. Aoka, Y., et al., *The embryonic angiogenic factor Del1 accelerates tumor growth by enhancing vascular formation.* Microvasc Res, 2002. **64**(1): p. 148-61.

231. Bellahcene, A., et al., *Bone sialoprotein mediates human endothelial cell attachment and migration and promotes angiogenesis.* Circ Res, 2000. **86**(8): p. 885-91.
232. Xu, J., et al., *Proteolytic exposure of a cryptic site within collagen type IV is required for angiogenesis and tumor growth in vivo.* J Cell Biol, 2001. **154**(5): p. 1069-79.
233. Byzova, T.V. and E.F. Plow, *Activation of alphaVbeta3 on vascular cells controls recognition of prothrombin.* J Cell Biol, 1998. **143**(7): p. 2081-92.
234. Camenisch, G., et al., *ANGPTL3 stimulates endothelial cell adhesion and migration via integrin alpha vbeta 3 and induces blood vessel formation in vivo.* J Biol Chem, 2002. **277**(19): p. 17281-90.
235. Leu, S.J., S.C. Lam, and L.F. Lau, *Pro-angiogenic activities of CYR61 (CCN1) mediated through integrins alphavbeta3 and alpha6beta1 in human umbilical vein endothelial cells.* J Biol Chem, 2002. **277**(48): p. 46248-55.
236. Schneller, M., K. Vuori, and E. Ruoslahti, *Alphavbeta3 integrin associates with activated insulin and PDGFbeta receptors and potentiates the biological activity of PDGF.* Embo j, 1997. **16**(18): p. 5600-7.
237. Lawler, J., *The functions of thrombospondin-1 and-2.* Curr Opin Cell Biol, 2000. **12**(5): p. 634-40.
238. Adams, J.C., *Thrombospondins: multifunctional regulators of cell interactions.* Annu Rev Cell Dev Biol, 2001. **17**: p. 25-51.
239. Baker, A.H., D.R. Edwards, and G. Murphy, *Metalloproteinase inhibitors: biological actions and therapeutic opportunities.* J Cell Sci, 2002. **115**(Pt 19): p. 3719-27.
240. Lafleur, M.A., et al., *Endothelial tubulogenesis within fibrin gels specifically requires the activity of membrane-type-matrix metalloproteinases (MT-MMPs).* J Cell Sci, 2002. **115**(Pt 17): p. 3427-38.
241. Rehn, M., et al., *Interaction of endostatin with integrins implicated in angiogenesis.* Proc Natl Acad Sci U S A, 2001. **98**(3): p. 1024-9.
242. Tarui, T., L.A. Miles, and Y. Takada, *Specific interaction of angiostatin with integrin alpha(v)beta(3) in endothelial cells.* J Biol Chem, 2001. **276**(43): p. 39562-8.
243. Sudhakar, A., et al., *Human tumstatin and human endostatin exhibit distinct antiangiogenic activities mediated by alpha v beta 3 and alpha 5 beta 1 integrins.* Proc Natl Acad Sci U S A, 2003. **100**(8): p. 4766-71.
244. Stupack, D.G., et al., *Apoptosis of adherent cells by recruitment of caspase-8 to unligated integrins.* J Cell Biol, 2001. **155**(3): p. 459-70.
245. Kim, S., et al., *Inhibition of endothelial cell survival and angiogenesis by protein kinase A.* J Clin Invest, 2002. **110**(7): p. 933-41.
246. Kim, S., et al., *Regulation of Angiogenesis in Vivo by Ligation of Integrin α5β1 with the Central Cell-Binding Domain of Fibronectin*, in *Am J Pathol*. 2000. p. 1345-62.
247. Hood, J.D., et al., *Tumor regression by targeted gene delivery to the neovasculature.* Science, 2002. **296**(5577): p. 2404-7.

248. Jones, M.C., P.T. Caswell, and J.C. Norman, *Endocytic recycling pathways: emerging regulators of cell migration.* Curr Opin Cell Biol, 2006. **18**(5): p. 549-57.
249. O'Donnell, P.H., et al., *A phase I study of continuous infusion cilengitide in patients with solid tumors.* Invest New Drugs, 2012. **30**(2): p. 604-10.
250. Stupp, R., et al., *Cilengitide combined with standard treatment for patients with newly diagnosed glioblastoma with methylated MGMT promoter (CENTRIC EORTC 26071-22072 study): a multicentre, randomised, open-label, phase 3 trial.* Lancet Oncol, 2014. **15**(10): p. 1100-8.
251. Legler, D.F., et al., *Superactivation of integrin alphavbeta3 by low antagonist concentrations.* J Cell Sci, 2001. **114**(Pt 8): p. 1545-53.
252. Friedlander, M., et al., *Definition of two angiogenic pathways by distinct alpha v integrins.* Science, 1995. **270**(5241): p. 1500-2.
253. Eliceiri, B.P., et al., *Src-mediated coupling of focal adhesion kinase to integrin αvβ5 in vascular endothelial growth factor signaling*, in *J Cell Biol*. 2002. p. 149-60.
254. Hood, J.D., et al., *Differential alphav integrin-mediated Ras-ERK signaling during two pathways of angiogenesis.* J Cell Biol, 2003. **162**(5): p. 933-43.
255. Alavi, A., et al., *Role of Raf in vascular protection from distinct apoptotic stimuli.* Science, 2003. **301**(5629): p. 94-6.
256. Lee, J., et al., *Angiopoietin-1 guides directional angiogenesis through integrin alphavbeta5 signaling for recovery of ischemic retinopathy.* Sci Transl Med, 2013. **5**(203): p. 203ra127.
257. Su, G., et al., *Integrin αvβ5 Regulates Lung Vascular Permeability and Pulmonary Endothelial Barrier Function*, in *Am J Respir Cell Mol Biol*. 2007. p. 377-86.
258. Balasubramanian, S., et al., *beta3 integrin in cardiac fibroblast is critical for extracellular matrix accumulation during pressure overload hypertrophy in mouse.* PLoS One, 2012. **7**(9): p. e45076.
259. Suryakumar, G., et al., *Lack of beta3 integrin signaling contributes to calpain-mediated myocardial cell loss in pressure-overloaded myocardium.* J Cardiovasc Pharmacol, 2010. **55**(6): p. 567-73.
260. Borg, T.K., et al., *Specialization at the Z line of cardiac myocytes.* Cardiovasc Res, 2000. **46**(2): p. 277-85.
261. Zhang, J.Q., et al., *Ultrastructural and biochemical localization of N-RAP at the interface between myofibrils and intercalated disks in the mouse heart.* Biochemistry, 2001. **40**(49): p. 14898-906.
262. Matsushita, T., et al., *Remodeling of cell-cell and cell-extracellular matrix interactions at the border zone of rat myocardial infarcts.* Circ Res, 1999. **85**(11): p. 1046-55.
263. Laser, M., et al., *Integrin activation and focal complex formation in cardiac hypertrophy.* J Biol Chem, 2000. **275**(45): p. 35624-30.
264. Nawata, J., et al., *Differential expression of alpha 1, alpha 3 and alpha 5 integrin subunits in acute and chronic stages of myocardial infarction in rats.* Cardiovasc Res, 1999. **43**(2): p. 371-81.

265. Babbitt, C.J., et al., *Modulation of integrins and integrin signaling molecules in the pressure-loaded murine ventricle.* Histochem Cell Biol, 2002. **118**(6): p. 431-9.
266. Belkin, A.M., et al., *Beta 1D integrin displaces the beta 1A isoform in striated muscles: localization at junctional structures and signaling potential in nonmuscle cells.* J Cell Biol, 1996. **132**(1-2): p. 211-26.
267. Pulina, M.V., et al., *Essential roles of fibronectin in the development of the left-right embryonic body plan.* Dev Biol, 2011. **354**(2): p. 208-20.
268. Mittal, A., et al., *Fibronectin and integrin alpha 5 play requisite roles in cardiac morphogenesis.* Dev Biol, 2013. **381**(1): p. 73-82.
269. Valencik, M.L., et al., *Integrin activation in the heart: a link between electrical and contractile dysfunction?* Circ Res, 2006. **99**(12): p. 1403-10.
270. Burkin, D.J., et al., *Transgenic expression of {alpha}7{beta}1 integrin maintains muscle integrity, increases regenerative capacity, promotes hypertrophy, and reduces cardiomyopathy in dystrophic mice.* Am J Pathol, 2005. **166**(1): p. 253-63.
271. Liu, J., et al., *beta1D chain increases alpha7beta1 integrin and laminin and protects against sarcolemmal damage in mdx mice.* Hum Mol Genet, 2012. **21**(7): p. 1592-603.
272. Ieda, M., et al., *Cardiac fibroblasts regulate myocardial proliferation through beta1 integrin signaling.* Dev Cell, 2009. **16**(2): p. 233-44.
273. Shai, S.Y., et al., *Cardiac myocyte-specific excision of the beta1 integrin gene results in myocardial fibrosis and cardiac failure.* Circ Res, 2002. **90**(4): p. 458-64.
274. Okada, H., et al., *Integrins protect cardiomyocytes from ischemia/reperfusion injury.* J Clin Invest, 2013. **123**(10): p. 4294-308.
275. Willey, C.D., et al., *Focal complex formation in adult cardiomyocytes is accompanied by the activation of beta3 integrin and c-Src.* J Mol Cell Cardiol, 2003. **35**(6): p. 671-83.
276. Johnston, R.K., et al., *Beta3 integrin-mediated ubiquitination activates survival signaling during myocardial hypertrophy.* Faseb j, 2009. **23**(8): p. 2759-71.
277. Sarrazy, V., et al., *Integrins alphavbeta5 and alphavbeta3 promote latent TGF-beta1 activation by human cardiac fibroblast contraction.* Cardiovasc Res, 2014. **102**(3): p. 407-17.
278. Distefano, G. and P. Sciacca, *Molecular pathogenesis of myocardial remodeling and new potential therapeutic targets in chronic heart failure*, in *Ital J Pediatr*. 2012. p. 41.
279. Breckenridge, R., *Heart failure and mouse models.* 2010.
280. Brooks, W.W. and C.H. Conrad, *Isoproterenol-Induced Myocardial Injury and Diastolic Dysfunction in Mice: Structural and Functional Correlates*, in *Comp Med*. 2009. p. 339-43.
281. deAlmeida, A.C., R.J. van Oort, and X.H. Wehrens, *Transverse aortic constriction in mice.* J Vis Exp, 2010(38).

282. Garcia-Menendez, L., et al., *Substrain specific response to cardiac pressure overload in C57BL/6 mice*, in *Am J Physiol Heart Circ Physiol*. 2013. p. H397-402.
283. Witt, H., et al., *Sex-specific pathways in early cardiac response to pressure overload in mice*, in *J Mol Med*. 2008. p. 1013-24.
284. Valero-Muñoz, M., W. Backman, and F. Sam, *Murine Models of Heart Failure With Preserved Ejection Fraction: A "Fishing Expedition"*, in *JACC Basic Transl Sci*. 2017. p. 770-89.
285. Higuchi, T., et al., *Assessment of alphavbeta3 integrin expression after myocardial infarction by positron emission tomography.* Cardiovasc Res, 2008. **78**(2): p. 395-403.
286. Meoli, D.F., et al., *Noninvasive imaging of myocardial angiogenesis following experimental myocardial infarction.* J Clin Invest, 2004. **113**(12): p. 1684-91.
287. Jenkins, W.S.A., et al., *Cardiac αVβ3 integrin expression following acute myocardial infarction in humans.* 2017.
288. Brancaccio, M., et al., *Integrin signalling: the tug-of-war in heart hypertrophy.* Cardiovasc Res, 2006. **70**(3): p. 422-33.
289. Ross, R.S. and T.K. Borg, *Integrins and the myocardium.* Circ Res, 2001. **88**(11): p. 1112-9.
290. Oliveira-Ferrer, L., et al., *Cilengitide induces cellular detachment and apoptosis in endothelial and glioma cells mediated by inhibition of FAK/src/AKT pathway*, in *J Exp Clin Cancer Res*. 2008. p. 86.
291. Mas-Moruno, C., F. Rechenmacher, and H. Kessler, *Cilengitide: the first anti-angiogenic small molecule drug candidate design, synthesis and clinical evaluation.* Anticancer Agents Med Chem, 2010. **10**(10): p. 753-68.
292. Crossman, D.C., *The pathophysiology of myocardial ischaemia*, in *Heart*. 2004. p. 576-80.
293. Van Kerckhoven, R., et al., *Pharmacological therapy can increase capillary density in post-infarction remodeled rat hearts.* Cardiovascular Research, 2018. **61**(3): p. 620-629.
294. Robich, M.P., et al., *Myocardial Therapeutic Angiogenesis: A Review of the State of Development and Future Obstacles.* Expert Rev Cardiovasc Ther, 2011. **9**(11): p. 1469-79.
295. Cochain, C., K.M. Channon, and J.S. Silvestre, *Angiogenesis in the infarcted myocardium.* Antioxid Redox Signal, 2013. **18**(9): p. 1100-13.
296. Taegtmeyer, H., S. Sen, and D. Vela, *Return to the fetal gene program: A suggested metabolic link to gene expression in the heart.* Ann N Y Acad Sci, 2010. **1188**: p. 191-8.
297. Rajabi, M., et al., *Return to the fetal gene program protects the stressed heart: a strong hypothesis.* Heart Fail Rev, 2007. **12**(3-4): p. 331-43.
298. Baliga, R.S., et al., *Phosphodiesterase 2 inhibition preferentially promotes NO/guanylyl cyclase/cGMP signaling to reverse the development of heart failure.* 2018.

299. van den Bosch, B.J., et al., *Early and transient gene expression changes in pressure overload-induced cardiac hypertrophy in mice.* Genomics, 2006. **88**(4): p. 480-8.
300. Chien, K.R., et al., *Regulation of cardiac gene expression during myocardial growth and hypertrophy: molecular studies of an adaptive physiologic response.* Faseb j, 1991. **5**(15): p. 3037-46.
301. Komuro, I. and Y. Yazaki, *Control of cardiac gene expression by mechanical stress.* Annu Rev Physiol, 1993. **55**: p. 55-75.
302. Querejeta, R., et al., *Increased collagen type I synthesis in patients with heart failure of hypertensive origin: relation to myocardial fibrosis.* Circulation, 2004. **110**(10): p. 1263-8.
303. van Spreeuwel, A.C., et al., *Mimicking Cardiac Fibrosis in a Dish: Fibroblast Density Rather than Collagen Density Weakens Cardiomyocyte Function*, in *J Cardiovasc Transl Res*. 2017. p. 116-27.
304. Mohammed, S.F., et al., *Variable Phenotype in Murine Transverse Aortic Constriction (TAC).* Cardiovasc Pathol, 2012. **21**(3): p. 188-98.
305. Tavora, B., et al., *Endothelial FAK is required for tumour angiogenesis.* EMBO Mol Med, 2010. **2**(12): p. 516-28.
306. Tavora, B., et al., *Endothelial–cell FAK targeting sensitizes tumours to DNA–damaging therapy.* Nature, 2014. **514**(7520): p. 112-6.
307. Norton, K.A. and A.S. Popel, *Effects of endothelial cell proliferation and migration rates in a computational model of sprouting angiogenesis*, in *Sci Rep*. 2016.
308. Yun, J.S. and S.Y. Kim, *Antihistamines modulate the integrin signaling pathway in h9c2 rat cardiomyocytes: Possible association with cardiotoxicity.* Hum Exp Toxicol, 2015. **34**(8): p. 796-807.
309. Sadoshima, J. and S. Izumo, *Molecular characterization of angiotensin II--induced hypertrophy of cardiac myocytes and hyperplasia of cardiac fibroblasts. Critical role of the AT1 receptor subtype.* Circ Res, 1993. **73**(3): p. 413-23.
310. Paradis, P., et al., *Overexpression of angiotensin II type I receptor in cardiomyocytes induces cardiac hypertrophy and remodeling*, in *Proc Natl Acad Sci U S A*. 2000. p. 931-6.
311. Zhang, G.-X., et al., *Role of mitochondria in angiotensin II-induced reactive oxygen species and mitogen-activated protein kinase activation.* Cardiovascular Research, 2018. **76**(2): p. 204-212.
312. Zhang, M., et al., *Contractile Function During Angiotensin-II Activation: Increased Nox2 Activity Modulates Cardiac Calcium Handling via Phospholamban Phosphorylation*, in *J Am Coll Cardiol*. 2015. p. 261-72.
313. Liu, Y., et al., *RNA-Seq Identifies Novel Myocardial Gene Expression Signatures of Heart Failure.* Genomics, 2015. **105**(2): p. 83-9.
314. Pradervand, S., et al., *Small proline-rich protein 1A is a gp130 pathway- and stress-inducible cardioprotective protein*, in *EMBO J*. 2004. p. 4517-25.
315. Qi, Y., et al., *Myocardial Loss of IRS1 and IRS2 Causes Heart Failure and Is Controlled by p38α MAPK During Insulin Resistance*, in *Diabetes*. 2013. p. 3887-900.

316. Carnegie, G.K. and B.T. Burmeister, *A-Kinase Anchoring Proteins That Regulate Cardiac Remodeling.* J Cardiovasc Pharmacol, 2011. **58**(5): p. 451-8.
317. Brody, M.J., et al., *LRRC10 is required to maintain cardiac function in response to pressure overload.* Am J Physiol Heart Circ Physiol, 2016. **310**(2): p. H269-78.
318. *Prospective Association of GLUL rs10911021 With Cardiovascular Morbidity and Mortality Among Individuals With Type 2 Diabetes: The Look AHEAD Study.* Diabetes, 2016. **65**(1): p. 297-302.
319. Kuang, S.Q., et al., *Aortic remodeling after transverse aortic constriction in mice is attenuated with AT1 receptor blockade.* Arterioscler Thromb Vasc Biol, 2013. **33**(9): p. 2172-9.
320. Dullens, H.F., et al., *Integrin expression during reverse remodeling in the myocardium of heart failure patients.* Cardiovasc Pathol, 2012. **21**(4): p. 291-8.
321. Hsueh, W.A., R.E. Law, and Y.S. Do, *Integrins, adhesion, and cardiac remodeling.* Hypertension, 1998. **31**(1 Pt 2): p. 176-80.
322. Kapoun, A.M., et al., *B-type natriuretic peptide exerts broad functional opposition to transforming growth factor-beta in primary human cardiac fibroblasts: fibrosis, myofibroblast conversion, proliferation, and inflammation.* Circ Res, 2004. **94**(4): p. 453-61.
323. Brower, G.L., et al., *The relationship between myocardial extracellular matrix remodeling and ventricular function.* Eur J Cardiothorac Surg, 2006. **30**(4): p. 604-10.
324. Schipper, M.E., et al., *Changes in regulatory microRNA expression in myocardium of heart failure patients on left ventricular assist device support.* J Heart Lung Transplant, 2008. **27**(12): p. 1282-5.
325. Terracio, L., et al., *Expression of collagen binding integrins during cardiac development and hypertrophy.* Circ Res, 1991. **68**(3): p. 734-44.
326. Sun, Y., et al., *Application of (68)Ga-PRGD2 PET/CT for alphavbeta3-integrin imaging of myocardial infarction and stroke.* Theranostics, 2014. **4**(8): p. 778-86.
327. Sherif, H.M., et al., *Molecular imaging of early alphavbeta3 integrin expression predicts long-term left-ventricle remodeling after myocardial infarction in rats.* J Nucl Med, 2012. **53**(2): p. 318-23.
328. Kuppuswamy, D., et al., *Association of Tyrosine-phosphorylated c-Src with the Cytoskeleton of Hypertrophying Myocardium.* 1997.
329. Pai, V.B. and M.C. Nahata, *Cardiotoxicity of chemotherapeutic agents: incidence, treatment and prevention.* Drug Saf, 2000. **22**(4): p. 263-302.
330. Carmeliet, P., *VEGF as a key mediator of angiogenesis in cancer.* Oncology, 2005. **69 Suppl 3**: p. 4-10.
331. Robinson, S.D. and K.M. Hodivala-Dilke, *The role of beta3-integrins in tumor angiogenesis: context is everything.* Curr Opin Cell Biol, 2011. **23**(5): p. 630-7.

332. Holmes, K., et al., *Vascular endothelial growth factor receptor-2: structure, function, intracellular signalling and therapeutic inhibition.* Cell Signal, 2007. **19**(10): p. 2003-12.
333. Heba, G., et al., *Relation between expression of TNF alpha, iNOS, VEGF mRNA and development of heart failure after experimental myocardial infarction in rats.* J Physiol Pharmacol, 2001. **52**(1): p. 39-52.
334. Weis, S.M. and D.A. Cheresh, *Pathophysiological consequences of VEGF-induced vascular permeability.* Nature, 2005. **437**(7058): p. 497-504.
335. Schuermann, A., C.S. Helker, and W. Herzog, *Metallothionein 2 regulates endothelial cell migration through transcriptional regulation of vegfc expression.* Angiogenesis, 2015. **18**(4): p. 463-75.
336. Lin, C.G., et al., *CCN3 (NOV) is a novel angiogenic regulator of the CCN protein family.* J Biol Chem, 2003. **278**(26): p. 24200-8.
337. Buchberger, E., et al., *Inhibition of the transcriptional repressor complex Bcl-6/BCoR induces endothelial sprouting but does not promote tumor growth*, in *Oncotarget*. 2017. p. 552-64.
338. Lin, Z., et al., *Pi3kcb links Hippo-YAP and PI3K-AKT signaling pathways to promote cardiomyocyte proliferation and survival.* Circ Res, 2015. **116**(1): p. 35-45.
339. Hakim, Z.S., et al., *FAK regulates cardiomyocyte survival following ischemia/reperfusion.* J Mol Cell Cardiol, 2009. **46**(2): p. 241-8.
340. Hussain, A.R., et al., *Cross-Talk between NFkB and the PI3-Kinase/AKT Pathway Can Be Targeted in Primary Effusion Lymphoma (PEL) Cell Lines for Efficient Apoptosis*, in *PLoS One*. 2012.
341. Smith, I.J. and S.L. Dodd, *Calpain activation causes a proteasome-dependent increase in protein degradation and inhibits the Akt signalling pathway in rat diaphragm muscle.* Exp Physiol, 2007. **92**(3): p. 561-73.
342. Ehler, E., T. Moore-Morris, and S. Lange, *Isolation and Culture of Neonatal Mouse Cardiomyocytes*, in *J Vis Exp*. 2013.
343. Bird, S.D., et al., *The human adult cardiomyocyte phenotype.* Cardiovasc Res, 2003. **58**(2): p. 423-34.
344. Lechertier, T. and K. Hodivala-Dilke, *Focal adhesion kinase and tumour angiogenesis.* J Pathol, 2012. **226**(2): p. 404-12.
345. Sulzmaier, F.J., C. Jean, and D.D. Schlaepfer, *FAK in cancer: mechanistic findings and clinical applications.* Nat Rev Cancer, 2014. **14**(9): p. 598-610.
346. Golubovskaya, V.M., *Focal Adhesion Kinase as a Cancer Therapy Target.* Anticancer Agents Med Chem, 2010. **10**(10): p. 735-41.
347. Wu, C., *Focal Adhesion: A Focal Point in Current Cell Biology and Molecular Medicine*, in *Cell Adh Migr*. 2007. p. 13-8.
348. Parsons, J.T., et al., *Focal adhesion kinase: a regulator of focal adhesion dynamics and cell movement.* Oncogene, 2000. **19**(49): p. 5606-13.
349. Hayashi, I., K. Vuori, and R.C. Liddington, *The focal adhesion targeting (FAT) region of focal adhesion kinase is a four-helix bundle that binds paxillin.* Nat Struct Biol, 2002. **9**(2): p. 101-6.

350. Tachibana, K., et al., *Direct association of pp125FAK with paxillin, the focal adhesion-targeting mechanism of pp125FAK.* J Exp Med, 1995. **182**(4): p. 1089-99.
351. Chen, H.C., et al., *Interaction of focal adhesion kinase with cytoskeletal protein talin.* J Biol Chem, 1995. **270**(28): p. 16995-9.
352. Schaller, M.D., C.A. Borgman, and J.T. Parsons, *Autonomous expression of a noncatalytic domain of the focal adhesion-associated protein tyrosine kinase pp125FAK.* Mol Cell Biol, 1993. **13**(2): p. 785-91.
353. Taylor, J.M., et al., *Selective Expression of an Endogenous Inhibitor of FAK Regulates Proliferation and Migration of Vascular Smooth Muscle Cells*, in *Mol Cell Biol*. 2001. p. 1565-72.
354. Richardson, A., et al., *Inhibition of cell spreading by expression of the C-terminal domain of focal adhesion kinase (FAK) is rescued by coexpression of Src or catalytically inactive FAK: a role for paxillin tyrosine phosphorylation.* Mol Cell Biol, 1997. **17**(12): p. 6906-14.
355. Hauck, C.R., et al., *Inhibition of focal adhesion kinase expression or activity disrupts epidermal growth factor-stimulated signaling promoting the migration of invasive human carcinoma cells.* Cancer Res, 2001. **61**(19): p. 7079-90.
356. Frame, M.C., et al., *The FERM domain: organizing the structure and function of FAK.* Nat Rev Mol Cell Biol, 2010. **11**(11): p. 802-14.
357. Chen, S.Y. and H.C. Chen, *Direct interaction of focal adhesion kinase (FAK) with Met is required for FAK to promote hepatocyte growth factor-induced cell invasion.* Mol Cell Biol, 2006. **26**(13): p. 5155-67.
358. Sieg, D.J., et al., *FAK integrates growth-factor and integrin signals to promote cell migration.* Nat Cell Biol, 2000. **2**(5): p. 249-56.
359. Cooper, L.A., T.L. Shen, and J.L. Guan, *Regulation of focal adhesion kinase by its amino-terminal domain through an autoinhibitory interaction.* Mol Cell Biol, 2003. **23**(22): p. 8030-41.
360. Jacamo, R.O. and E. Rozengurt, *A truncated FAK lacking the FERM domain displays high catalytic activity but retains responsiveness to adhesion-mediated signals.* Biochem Biophys Res Commun, 2005. **334**(4): p. 1299-304.
361. Cohen, L.A. and J.L. Guan, *Residues within the first subdomain of the FERM-like domain in focal adhesion kinase are important in its regulation.* J Biol Chem, 2005. **280**(9): p. 8197-207.
362. Ceccarelli, D.F., et al., *Crystal structure of the FERM domain of focal adhesion kinase.* J Biol Chem, 2006. **281**(1): p. 252-9.
363. Mitra, S.K. and D.D. Schlaepfer, *Integrin-regulated FAK-Src signaling in normal and cancer cells.* Curr Opin Cell Biol, 2006. **18**(5): p. 516-23.
364. Dunty, J.M., et al., *FERM domain interaction promotes FAK signaling.* Mol Cell Biol, 2004. **24**(12): p. 5353-68.
365. Toutant, M., et al., *Alternative Splicing Controls the Mechanisms of FAK Autophosphorylation*, in *Mol Cell Biol*. 2002. p. 7731-43.

366. Calalb, M.B., T.R. Polte, and S.K. Hanks, *Tyrosine phosphorylation of focal adhesion kinase at sites in the catalytic domain regulates kinase activity: a role for Src family kinases.* Mol Cell Biol, 1995. **15**(2): p. 954-63.
367. Mitra, S.K., D.A. Hanson, and D.D. Schlaepfer, *Focal adhesion kinase: in command and control of cell motility.* Nat Rev Mol Cell Biol, 2005. **6**(1): p. 56-68.
368. Leu, T.H. and M.C. Maa, *Tyr-863 phosphorylation enhances focal adhesion kinase autophosphorylation at Tyr-397.* Oncogene, 2002. **21**(46): p. 6992-7000.
369. Parsons, J.T., *Focal adhesion kinase: the first ten years.* J Cell Sci, 2003. **116**(Pt 8): p. 1409-16.
370. Ma, A., et al., *Serine Phosphorylation of Focal Adhesion Kinase in Interphase and Mitosis: A Possible Role in Modulating Binding to p130Cas*, in *Mol Biol Cell*. 2001. p. 1-12.
371. Jacamo, R., et al., *FAK phosphorylation at Ser-843 inhibits Tyr-397 phosphorylation, cell spreading and migration.* J Cell Physiol, 2007. **210**(2): p. 436-44.
372. Roy-Luzarraga, M. and K. Hodivala-Dilke, *Molecular Pathways: Endothelial Cell FAK-A Target for Cancer Treatment.* Clin Cancer Res, 2016. **22**(15): p. 3718-24.
373. Weiner, T.M., et al., *Expression of focal adhesion kinase gene and invasive cancer.* Lancet, 1993. **342**(8878): p. 1024-5.
374. Owens, L.V., et al., *Overexpression of the focal adhesion kinase (p125FAK) in invasive human tumors.* Cancer Res, 1995. **55**(13): p. 2752-5.
375. McLean, G.W., et al., *The role of focal-adhesion kinase in cancer - a new therapeutic opportunity.* Nat Rev Cancer, 2005. **5**(7): p. 505-15.
376. Recher, C., et al., *Expression of focal adhesion kinase in acute myeloid leukemia is associated with enhanced blast migration, increased cellularity, and poor prognosis.* Cancer Res, 2004. **64**(9): p. 3191-7.
377. Schlaepfer, D.D., S.K. Mitra, and D. Ilic, *Control of motile and invasive cell phenotypes by focal adhesion kinase.* Biochim Biophys Acta, 2004. **1692**(2-3): p. 77-102.
378. Sood, A.K., et al., *Biological significance of focal adhesion kinase in ovarian cancer: role in migration and invasion.* Am J Pathol, 2004. **165**(4): p. 1087-95.
379. Agochiya, M., et al., *Increased dosage and amplification of the focal adhesion kinase gene in human cancer cells.* Oncogene, 1999. **18**(41): p. 5646-53.
380. Quintanilla, M., et al., *Carcinogen-specific mutation and amplification of Ha-ras during mouse skin carcinogenesis.* Nature, 1986. **322**(6074): p. 78-80.
381. McLean, G.W., et al., *Decreased focal adhesion kinase suppresses papilloma formation during experimental mouse skin carcinogenesis.* Cancer Res, 2001. **61**(23): p. 8385-9.
382. Jones, M.L., et al., *Characterization of a novel focal adhesion kinase inhibitor in human platelets.* Biochem Biophys Res Commun, 2009. **389**(1): p. 198-203.

383. Ayaki, M., et al., *Reduced Expression of Focal Adhesion Kinase in Liver Metastases Compared with Matched Primary Human Colorectal Adenocarcinomas.* 2001.
384. Gabriel, B., et al., *Weak expression of focal adhesion kinase (pp125FAK) in patients with cervical cancer is associated with poor disease outcome.* Clin Cancer Res, 2006. **12**(8): p. 2476-83.
385. Zheng, Y. and Z. Lu, *Paradoxical roles of FAK in tumor cell migration and metastasis.* Cell Cycle, 2009. **8**(21): p. 3474-9.
386. Bergers, G. and L.E. Benjamin, *Tumorigenesis and the angiogenic switch.* Nat Rev Cancer, 2003. **3**(6): p. 401-10.
387. Palma, M.D., D. Biziato, and T.V. Petrova, *Microenvironmental regulation of tumour angiogenesis.* Nature Reviews Cancer, 2017. **17**(8): p. 457.
388. Qi, J.H. and L. Claesson-Welsh, *VEGF-induced activation of phosphoinositide 3-kinase is dependent on focal adhesion kinase.* Exp Cell Res, 2001. **263**(1): p. 173-82.
389. Cary, L.A., J.F. Chang, and J.L. Guan, *Stimulation of cell migration by overexpression of focal adhesion kinase and its association with Src and Fyn.* J Cell Sci, 1996. **109 (Pt 7)**: p. 1787-94.
390. Haskell, H., et al., *Focal adhesion kinase is expressed in the angiogenic blood vessels of malignant astrocytic tumors in vivo and promotes capillary tube formation of brain microvascular endothelial cells.* Clin Cancer Res, 2003. **9**(6): p. 2157-65.
391. Ding, Q., et al., *p27Kip1 and cyclin D1 are necessary for focal adhesion kinase regulation of cell cycle progression in glioblastoma cells propagated in vitro and in vivo in the scid mouse brain.* J Biol Chem, 2005. **280**(8): p. 6802-15.
392. Golubovskaya, V.M., R. Finch, and W.G. Cance, *Direct interaction of the N-terminal domain of focal adhesion kinase with the N-terminal transactivation domain of p53.* J Biol Chem, 2005. **280**(26): p. 25008-21.
393. Kim, I., et al., *Angiopoietin-1 induces endothelial cell sprouting through the activation of focal adhesion kinase and plasmin secretion.* Circ Res, 2000. **86**(9): p. 952-9.
394. Pirone, D.M., et al., *An inhibitory role for FAK in regulating proliferation: a link between limited adhesion and RhoA-ROCK signaling.* J Cell Biol, 2006. **174**(2): p. 277-88.
395. Ilic, D., et al., *Reduced cell motility and enhanced focal adhesion contact formation in cells from FAK-deficient mice.* Nature, 1995. **377**(6549): p. 539-44.
396. Lim, S.T., et al., *Knock-in mutation reveals an essential role for focal adhesion kinase activity in blood vessel morphogenesis and cell motility-polarity but not cell proliferation.* J Biol Chem, 2010. **285**(28): p. 21526-36.
397. Zhao, X. and J.L. Guan, *Focal adhesion kinase and its signaling pathways in cell migration and angiogenesis.* Adv Drug Deliv Rev, 2011. **63**(8): p. 610-5.
398. Ilic, D., et al., *Focal adhesion kinase is required for blood vessel morphogenesis.* Circ Res, 2003. **92**(3): p. 300-7.

399. Peng, X., et al., *Overexpression of focal adhesion kinase in vascular endothelial cells promotes angiogenesis in transgenic mice.* Cardiovasc Res, 2004. **64**(3): p. 421-30.
400. Shen, T.L., et al., *Conditional knockout of focal adhesion kinase in endothelial cells reveals its role in angiogenesis and vascular development in late embryogenesis.* J Cell Biol, 2005. **169**(6): p. 941-52.
401. Braren, R., et al., *Endothelial FAK is essential for vascular network stability, cell survival, and lamellipodial formation.* J Cell Biol, 2006. **172**(1): p. 151-62.
402. Weis, S.M., et al., *Compensatory role for Pyk2 during angiogenesis in adult mice lacking endothelial cell FAK.* J Cell Biol, 2008. **181**(1): p. 43-50.
403. Lee, J., et al., *Conditional deletion of the focal adhesion kinase FAK alters remodeling of the blood-brain barrier in glioma.* Cancer Res, 2010. **70**(24): p. 10131-40.
404. Kostourou, V., et al., *FAK-heterozygous mice display enhanced tumour angiogenesis.* Nat Commun, 2013. **4**: p. 2020.
405. Phung, T.L., et al., *Pathological angiogenesis is induced by sustained Akt signaling and inhibited by rapamycin.* Cancer Cell, 2006. **10**(2): p. 159-70.
406. Sun, S., H.-J. Wu, and J.-L. Guan, *Nuclear FAK and its kinase activity regulate VEGFR2 transcription in angiogenesis of adult mice.* Scientific Reports, 2018. **8**(1): p. 2550.
407. Zhao, X., et al., *Role of kinase-independent and -dependent functions of FAK in endothelial cell survival and barrier function during embryonic development.* J Cell Biol, 2010. **189**(6): p. 955-65.
408. Gilbert, L.A. and M.T. Hemann, *DNA damage-mediated induction of a chemoresistant niche.* Cell, 2010. **143**(3): p. 355-66.
409. Cao, Z., et al., *Angiocrine factors deployed by tumor vascular niche induce B cell lymphoma invasiveness and chemoresistance.* Cancer Cell, 2014. **25**(3): p. 350-65.
410. Kerr, B.A., et al., *Stability and function of adult vasculature is sustained by Akt/Jagged1 signalling axis in endothelium.* Nature Communications, 2016. **7**: p. 10960.
411. Hambardzumyan, D., et al., *PI3K pathway regulates survival of cancer stem cells residing in the perivascular niche following radiation in medulloblastoma in vivo.* Genes Dev, 2008. **22**(4): p. 436-48.
412. Rivera, J. and L. Tessarollo, *Genetic background and the dilemma of translating mouse studies to humans.* Immunity, 2008. **28**(1): p. 1-4.
413. Doetschman, T., *Influence of Genetic Background on Genetically Engineered Mouse Phenotypes.* Methods Mol Biol, 2009. **530**: p. 423-33.
414. Donehower, L.A., et al., *Effects of genetic background on tumorigenesis in p53-deficient mice.* Mol Carcinog, 1995. **14**(1): p. 16-22.
415. Petiniot, L.K., et al., *RAG-mediated V(D)J recombination is not essential for tumorigenesis in Atm-deficient mice.* Mol Cell Biol, 2002. **22**(9): p. 3174-7.
416. Hamilton, B.A. and B.D. Yu, *Modifier Genes and the Plasticity of Genetic Networks in Mice*, in *PLoS Genet*. 2012.

417. Hughes, P., et al., *The costs of using unauthenticated, over-passaged cell lines: how much more data do we need?* Biotechniques, 2007. **43**(5): p. 575, 577-8, 581-2 passim.
418. Cance, W.G., et al., *Disrupting the Scaffold to Improve Focal Adhesion Kinase–Targeted Cancer Therapeutics.* Sci Signal. **6**(268): p. pe10.
419. Roberts, W.G., et al., *Antitumor activity and pharmacology of a selective focal adhesion kinase inhibitor, PF-562,271.* Cancer Res, 2008. **68**(6): p. 1935-44.
420. Ma, W.W., *Development of focal adhesion kinase inhibitors in cancer therapy.* Anticancer Agents Med Chem, 2011. **11**(7): p. 638-42.
421. Symeonides, S.N., S.M. Anderton, and A. Serrels, *FAK-inhibition opens the door to checkpoint immunotherapy in Pancreatic Cancer*, in *J Immunother Cancer*. 2017.
422. Lu, H., et al., *IGFBP2/FAK pathway is causally associated with dasatinib resistance in non-small cell lung cancer cells.* Mol Cancer Ther, 2013. **12**(12): p. 2864-73.
423. Jiang, H., et al., *Targeting focal adhesion kinase renders pancreatic cancers responsive to checkpoint immunotherapy.* Nat Med, 2016. **22**(8): p. 851-60.
424. Tucci, M., et al., Does cilengitide deserve another chance? The Lancet Oncology, 2014.
425. Dolgos., et al., In vitro and in vivo drug disposition of cilengitide in animals and human. Pharmacol Res Perspect, 2016.